Numerical Study for the Quantitative Assessment of Ground Displacements of Rock-Mass Slopes under Static and Seismic Conditions in the Landfall Areas of Offshore Pipelines

By

Stavroulakis Emmanouil

M.Sc., National Technical University of Athens, Greece, 2018

Dissertation Submitted in Partial Fulfillment of the
Requirements for the Degree of
Master of Science

in the
School of Naval Architecture &
Marine Engineering

NATIONAL TECHNICAL UNIVERSITY OF ATHENS

Winter 2018

Abstract

In the last decades, environmental considerations in coastal and offshore zones have shown a remarkable increase. In this sense, the integrity of coastal facilities, offshore oil & gas installations and facilities, and various pipeline networks both offshore and onshore play an important role due to their significant economic feasibility and environmental sustainability.

Because of the long, linear nature of pipeline corridors, they often cross areas that are highly susceptible to landslides. The landslide susceptibility that can translate into high or insignificant hazard to the pipeline depends on various factors. Landslide material ranging from bedrock with high intact compressive and shear strength to soil with low cohesion, and when a slope failure happens, rock falls and slide in soil flows can transmit damaging stresses to surface and buried pipelines. As the economic interested on coastal and offshore facilities increase, wider attention is focused on the problem of coastal rock slopes stability. The stability of rock slopes is significantly influenced by the geotechnical discontinuities in the rock, strength properties and its geometry.

This dissertation focus on the importance of the over mentioned parameters on the rock slope stability and on the influence of seismic loads on jointed rock slopes. The finite element method (FEM) have been used to simulate a jointed model as is a great tool to solve geotechnical problems due to its ability model nonlinear stress-strain behavior of materials. Six study cases carried out with static analysis for very good quality rock mass to observe how the geometry and main parameters of rock slopes affect their stability. Additionally, seismic forces imposed on the rock slope in order to note the influence of seismic loads on jointed rock slopes.

The results indicate that the bigger angle and unit weight of the slope are, the more unstable is the slope, and the bigger friction angle and cohesion of joint planes of the slope are, the more stable is the slope. Furthermore, it is observed that when the dip angle of joint planes is smaller than the slope angle, with its increase the equivalent plastic strain amplitude also increases and the slope become unstable. When it is sub parallel with slope angle plastic zones are reduced and the slope become more stable. Also, with the impose of seismic forces was noticed that all potential deformations of the jointed rock slope are larger than the static conditions and the rock slope is getting more unstable.

Finally, as this dissertation offers the displacements of the slope during seismic forces in critical points, a further study could be done examining the deformation of a pipe laid on studied rock mass slope.

Acknowledgements

The two years of my M.Sc. program at NTUA was full of great lessons. It has been a period of intense learning for me, not only in the scientific arena, but also on a personal level. I take this opportunity to thank all the people who have supported and helped me so much throughout this period.

At first, I would like to thank my supervisors Prodromos Psarropoulos and Michael Sakellariou for giving me the opportunity to do this dissertation and for all the great ideas that we shared all this time.

I would also like to thank my parents and my sister for their wise counsel and continuous encouragement. Finally, there are my friends that is always enjoyment to spent time with them.

Thank you very much, everyone!

Stavroulakis Emmanouil

Table of Contents

List of Tables

List of Figures

CHAPTER 1: INTRODUCTION

1.1 STATEMENT OF THE PROBLEM

In the last decades the development of computational methods and data acquisition techniques has contributed significantly in understanding of the behavior of rock slopes. Numerical modelling techniques have been widely used to solve complex slope problems, which otherwise, could not have been possible using conventional techniques. However, the application of these methods must be followed with such a manner, that the simulated models are reflected in situ circumstances as much as possible.

Rock slope stability as well as environmental considerations in coastal and offshore zones have shown remarkable increase. As the economic interested on coastal and offshore facilities increase, wider attention is focused on the problem of coastal rock slopes stability. The stability of rock slopes is significantly influenced by the geotechnical discontinuities in the rock, strength properties and its geometry. This dissertation make a brief to submarine and coastal geohazards and faces the importance of the over mentioned parameters on the rock slope stability. The finite element method (FEM) is used to simulate a jointed model as is a great tool to solve geotechnical problems due to its ability model nonlinear stress-strain behavior of materials.

1.2 RESEARCH OBJECTIVES

The principal objectives of this thesis are:

- to examine how the geometric and main parameters of the rock slopes with joint planes impact on the stability of rock slopes, and,
- to research the failure surface geometry and the range of plastic zones and displacements developed by the force of seismic actions.

1.3 THESIS STRUCTURE

This thesis consists of four chapters (Fig. 1.1). This chapter (chapter 1) presents the research problem, objectives and the structure of the thesis.

Chapter 2 presents literature reviews on submarine geohazards and geohazards in coastal rocky areas with a focus on the factors which accelerate and create these hazards. The mentioned hazards impose significant economic, social and environmental threats to society.

Chapter 3 considers geologic factors and other significant features that may intervene in slope stability and are responsible for the failure or the potential instability of a slope. A report is made for basic rock mass structures and for the main geological features which have a critical role to the behavior of the slope. Afterward, the type of slope failures analyzed and a special emphasis is given to the shear strength of discontinuities in a jointed slope. At the end of the chapter, limit equilibrium techniques and the finite element method (FEM) are introduced.

Chapter 4 studies the slope stability analysis using 2-D finite element method. A jointed material is presented and created to simulate the jointed rock mass. Two methods of analysis are used (a) static analysis with gravity loading and, b) pseudostatic analysis for seismic action) in order to examine the distribution or size of the plastic strain zones and displacements.

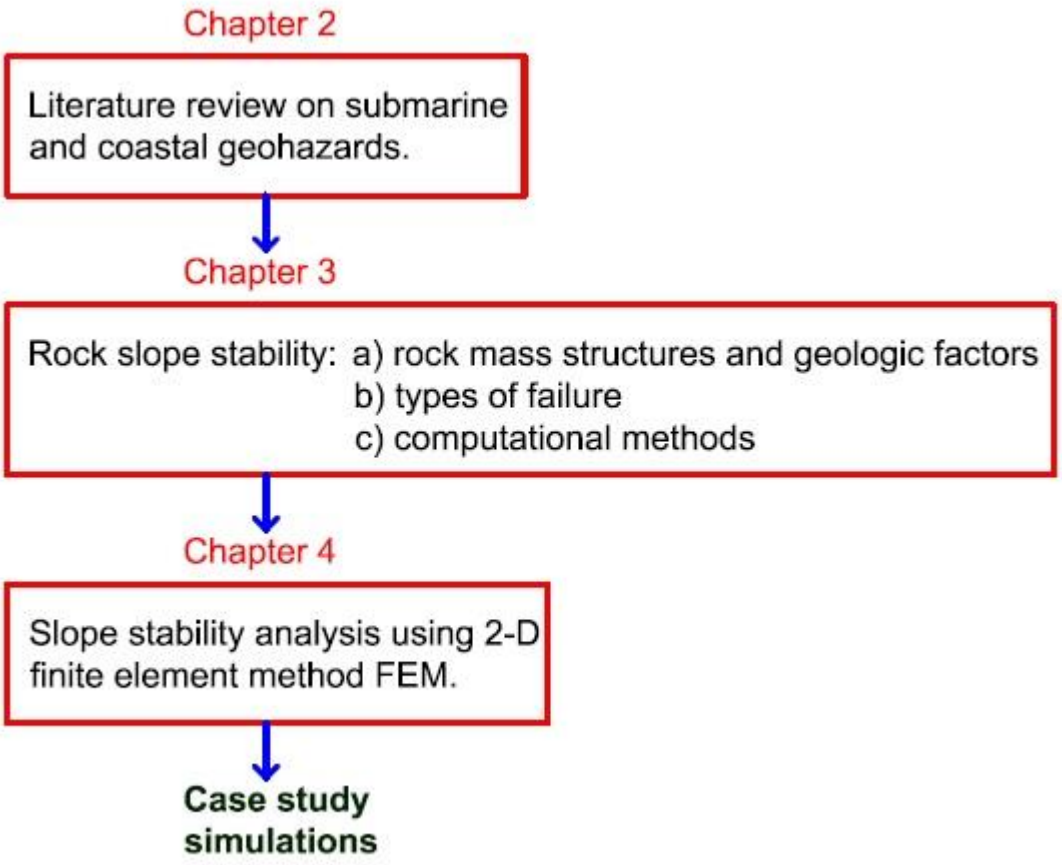

Figure 1.1: Structure of thesis

CHAPTER 2: LITERATURE REVIEW

2.1 INTRODUCTION

Because of the long, linear nature of pipeline corridors, they often cross areas that are highly susceptible to landslides. In addition to ground displacement, construction disturbance, ground settlement and movement due to freeze and thaw processes, pipelines are often threatened by earthquake shaking and by impact and displacement from landslides. Landslides that can affect pipeline corridors vary widely in type and in size. A landslide is a form of mass wasting that includes a wide range of ground movements, such as rockfalls, deep failure of slopes, and shallow debris flows. Landslide material ranging from bedrock with high intact compressive and shear strength to soil with low cohesion. Landslides can and have occurred underwater, called a submarine landslide, coastal and onshore environments in pipeline corridors throughout the world. Much of the hazard to pipelines from landslides derives from the long, linear nature of the corridors. With widths of up to one kilometer, pipeline corridors extend great distances through topography with wide varieties of susceptibility to landslides. Almost every pipeline that traverses areas in mountainous terrain has some vulnerability to landslide hazards.

The landslide susceptibility that can translate into high or insignificant hazard to the pipeline depends on various factors. Many pipelines are buried to depths of about one meter, so those landslides that penetrate to those depths, or induce damaging stresses at those depths will pose a real hazard to the pipe. Therefore, those failures that tend to be shallow and non-eroding to the surrounding terrain pose little hazard to pipelines. On the other hand, a large portion of commonly occurring landslides, such as falls and slides in soil and rock and debris flows, that tend to be triggered in great numbers in seismic or extreme precipitation events are significant threats for the pipeline integrity. When a slope failure happens, rock falls and slide in soil flows can transmit damaging stresses to surface and buried pipelines.

2.2 SUBMARINE GEOHAZARDS

In the last decades, environmental considerations in coastal and offshore zones have shown a remarkable increase. In this sense, the integrity of coastal facilities, offshore oil & gas installations and facilities, and various pipeline networks both offshore and onshore play an important role due to their significant economic feasibility and environmental sustainability.

Pipelines are static features within a dynamic environment with rivers, floodplains and coastal zones representing some of the most active areas within a landscape. These areas could also characterized by seismicity, and the integrity of any facility on these, is related to the earthquake-related geohazards. In addition to ground motion, the potential earthquake-related geohazards that may threaten the integrity of pipeline corridors include mainly active faults, coastal or submarine landslides and soil liquefaction phenomena. As shown in Figure 2.1 The offshore geohazards occur in all oceanic environments, but they concentrate on continental margins and comprise a number of geological phenomena, such as submarine slides, shallow gas and dissociation of gas hydrates, shallow water flow, volcanic island eruptions with flank collapse, and seismicity. Figure 2.2 shows a sketch summarizing the seafloor features linked to potential geohazards. This figure depicts an idealized continental margin with both natural geohazard-bearing features and main anthropogenic structures lying on the seafloor (e.g pipelines).

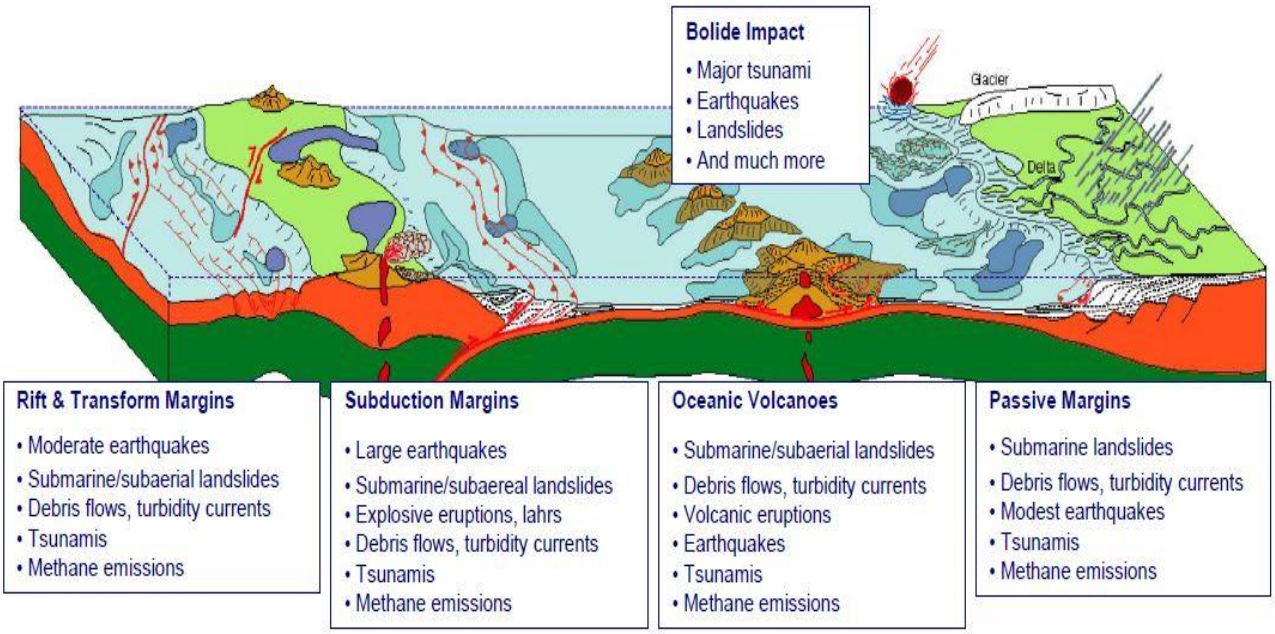

Figure 2.1: Offshore and coastal geohazards (Morgan et al. 2009)

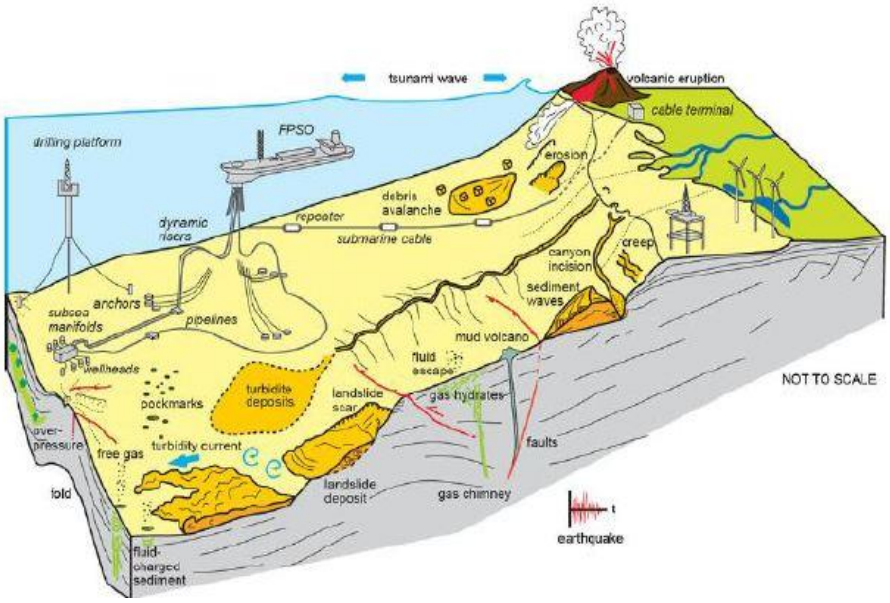

Figure 2.2: Sketch summarizing the seafloor features linked to potential geohazards (after Chiocci et al. 2011)

As mentioned above, the economic feasibility and environmental sustainability of the coastal and offshore or onshore facilities has a paramount of importance. The risk factor in these activities is very high. Structural risk is defined as the probability that a specific hazard will cause harm to a structure or infrastructure. According to Lacasse & Nadim (2007), risk is defined as the measure of the probability and severity of an adverse effect to life, health, environment and property. As shown in following expression, the estimation of structural risk requires:

a) the assessment of hazard (i.e. when, where, how frequently, magnitude)

b) the assessment of the structural vulnerability to this specific hazard (i.e. evaluation of the impact of the hazard on the examined structure or infrastructure).

$$\text{Risk} = \text{Hazard} \times \text{Vulnerability}$$

Obviously, if the hazard is an offshore or onshore geohazard, then the structural risk is a function of the geohazard under consideration. The triggering mechanisms of offshore and coastal geohazards could be natural, such as earthquake, tectonic faulting, temperature increase caused by climate change, excess pore pressure due to rapid sedimentation and gas hydrate melting due to climate change with increased sea water temperature after glacial periods; or man-made, such as anchor forces from ships or floating platforms, rock filling for pipeline supports, temperature change around oil and gas wells in the offshore field development area, underground blow-out, and reservoir depletion and subsidence (including induced seismicity). Figures 2.3 & 2.4 show a conceptual model of gas hydrates

and submarine landslides due to global warming and common modes of submarine landslide formation respectively.

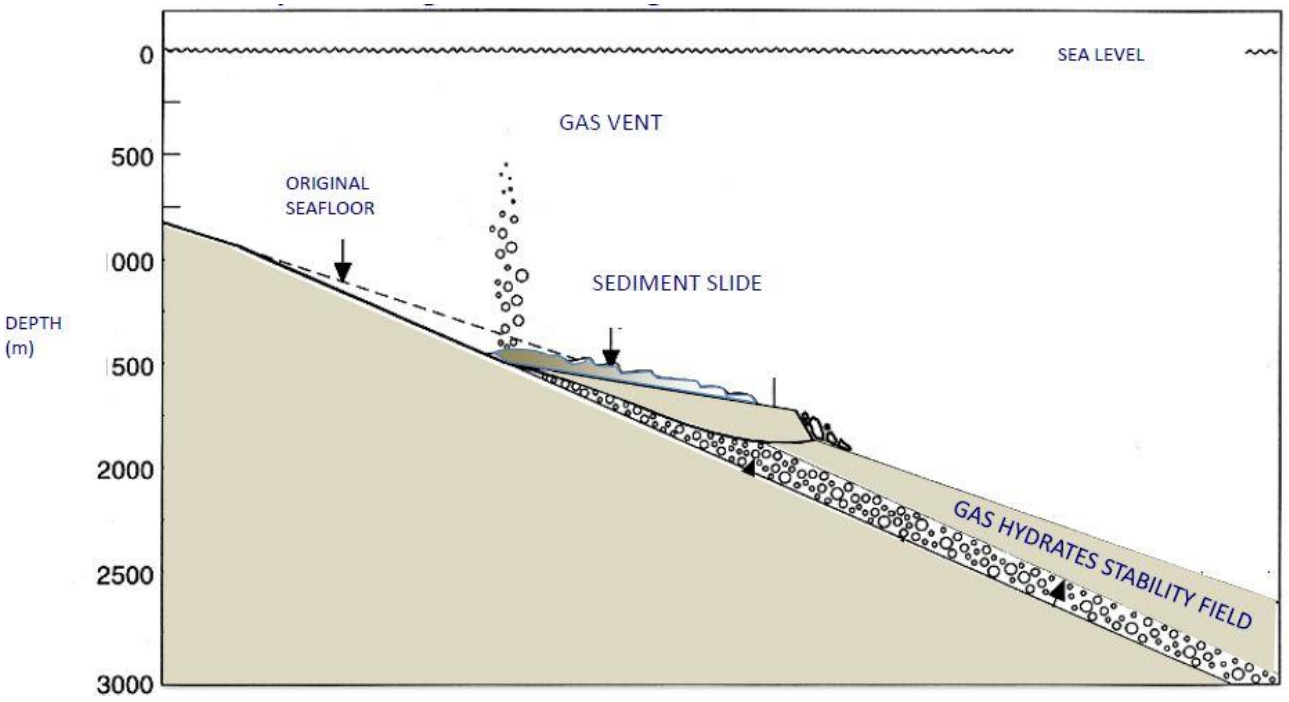

Figure 2.3: Gas hydrates and submarine landslides in response to climate change (Camerlenghi, EGU General Assembly, Vienna, 2013)

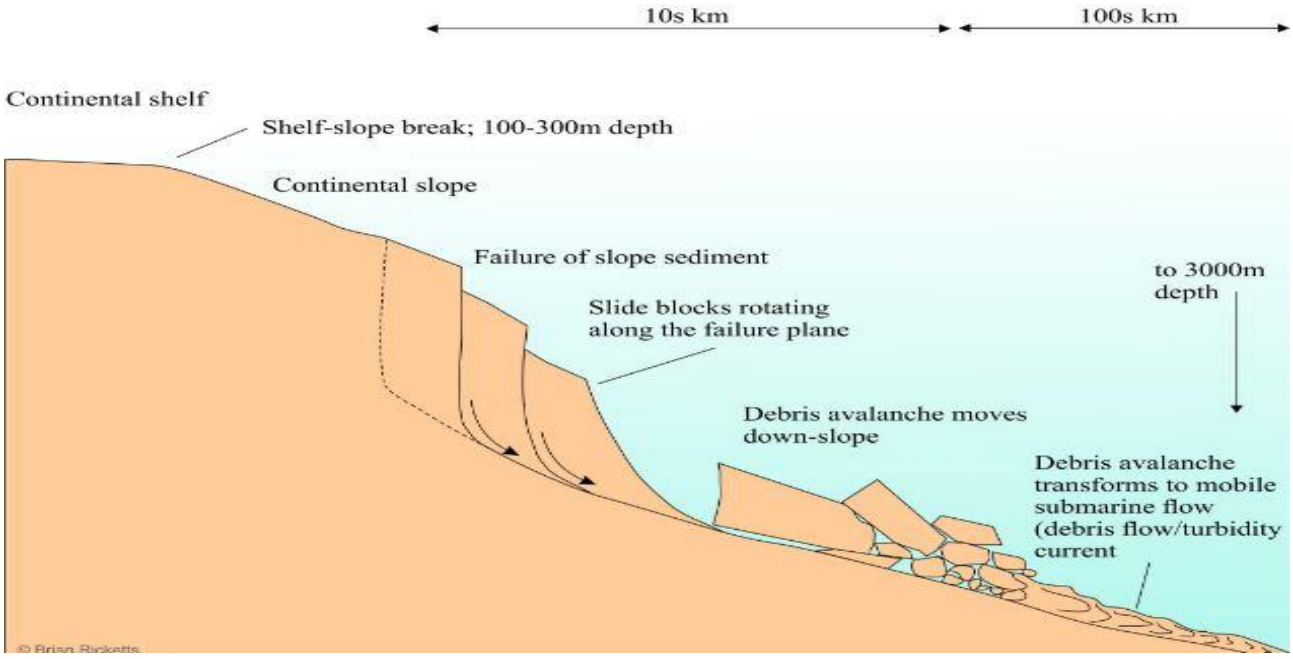

Figure 2.4: Common modes of submarine landslide formation

Source: http://www.geological-digressions.com

According to the above, some of the main earthquake-related geohazards that can damage offshore and coastal structures such as pipelines are, soil liquefaction submarine landslides, seismic waves ruptures seabed shaking and tsunamis.

Most of the major tsunamis are triggered by earthquakes, and the resulting waves are crossing regional basins before to hit the opposite coasts tens of minutes later. More local tsunamis may be generated as consequence of submarine sedimentary or volcanic failures; such events may quickly impact the neighboring coastlines where they may also induce important damages. The first three can cause permanent seafloor deformations which may be considered as quasi - static loading to a pipeline, while seabed shaking is a dynamic loading to any structure with various acceleration levels.

Seismic waves

Earthquake faults are the boundaries between the individual plates. Earthquake result from the relative movement of one plate with respect to its neighbor. Movement at the plate boundaries is sporadic, typically with at least decades between significant movements. Forces build over time, eventually fracturing the brittle Lithospheric rock. The sudden fracture and relative movement across the fault rupture surface releases built-up energy and generates seismic waves which propagate away from the fault rupture zone. The passage of these seismic waves causes the ground to shake back and forth. However, the ground shaking is transient: the shaking starts when seismic waves arrive at the site and ends when the waves have passed. The ground shaking may trigger landslides of marginally stable slopes, liquefaction and lateral spreading of saturated sandy soil, and settlements of the ground surface. Nevertheless, unlike the ground motion that triggers these ground movements, these deformations are permanent.

In terms of their effects on buried or surface pipelines the two general classes of seismic hazards are the wave propagation hazard and the permanent ground deformation (PGD) hazard. The wave propagation hazard is transient and corresponds to ground shaking. It results in transient strains in pipelines, strains that disappear when the shaking has stopped. The wave propagation hazards occur in every event and generally leads to low to moderate damage rates for pipelines. Contrariwise, the PGD hazard corresponds to permanent offset at a fault, permanent amounts of landslide movement and the like. It results in permanent strains in pipelines, strains that remain after the shaking has stopped. The PGD hazard does not necessarily occur in every event, but when it does it generally results in moderate to high damage rates for pipelines in the limited areas where it occurs.

Soil liquefaction

Soil liquefaction and related ground failures are commonly associated with large earthquakes. In common usage, liquefaction refers to the loss of strength in saturated, cohesionless soils due to the build-up of pore water pressures during dynamic loading. Sladen et al. (1985) define that liquefaction is a phenomenon wherein a mass of soil loses a large percentage of its shear resistance, when subjected to monotonic, cyclic, or shock loading, and flows in a manner resembling a liquid until the shear stresses acting on the mass are as low as the reduced shear resistance.

Liquefaction results from the tendency of soils to decrease in volume when subjected to shearing stresses. When loose, saturated soils are sheared the soil grains tend to rearrange into a more dense packing, with less space in the voids, as water in the pore spaces is forced out. If drainage of pore water is impeded, pore water pressures increase progressively with the shear load. This leads to the transfer of stress from soil skeleton to the pore water precipitating a decrease in effective stress and shear resistance of the soil. If the shear resistance of the soil becomes less than the static, driving shear strength, the soil can undergo large deformations and is said to liquefy (Martin et al. 1975; Seed and Idriss 1982). Liquefaction of loose, cohesionless soils can be observed under monotonic and cyclic shear loads.

A great number coastal zones are characterized by loose and cohesionless soils as mentioned above. Thus, it is obvious how disastrous can be a soil liquefaction in surface or buried pipelines at those areas. For example as the Figure 2.5 depict the support of a pipeline, it can registered that a soil liquefaction can cause the loss of pipeline support.

Figure 2.5: Pipeline support exposed to a soil liquefaction (Barry, Plains Mid American, 2014)

Submarine landslides

Landslides occur under water as well as on land; in fact, they are surprisingly abundant on the seafloor. Most reported submarine landslides occur in unlithified sediment, but some notable ones displace volume of rock. Other related phenomena are flow processes such as creep *(Silva and Booth, 1984*), debris flows (*Hampton, 1972*) and turbidity currents (*Kuenen and Migliorini, 1950*). Submarine slope failures can also occur on slopes as 1^0 and at depths ranging from a few 10s of meters to 1000s of meters and can evolve in several different ways. The two common types are large slides where relatively coherent blocks move down slope, and debris avalanches. Submarine landslides are characterized by lateral extent and can run out for 10s, even 100s of kilometers.

To evaluate the failure of submarine slope, a clear understanding is needed of underlying physical processes associated to both predisposition and triggering factors. Examples of the latter are: slope gradients, high sedimentation rates, fluid seepages, lithological discontinuities, loose sand and liquefaction, leaching and high sensitivity clay, hydrates occurrence, free gas generation and earthquake shaking, etc. Three main types of triggering mechanism can act in time and space to produce failure of submarine slopes: a) tectonic factors; b) eustatic changes in sea level and changes due to glacial-interglacial periods where sea level drops were in the orders of hundred meters; (c) high storm waves inducing overloading on shallow underconsolidated sediments. Such events can severally damage various offshore structures such as submarine cables, pipelines, e.t.c.

2.2.1 Landfall areas and Coastal edges

As the main objectives of offshore and coastal industries are to protect their investment, they have to choose areas of optimal conditions to locate their structure. For example, certain topographical features, such as sandy sea bottoms as opposed to rocky substrate may permit greater flexibility in the siting and construction of pipelines. In addition, other features in the coastal zone, like historical shipwrecks, serve to constrain pipeline placement. Because of the associated high risks to pipeline safety, industry would attempt to avoid laying a pipeline in areas classified as “restricted” by the military for weapons testing or practice purposes or where the sea bottom displays an exceptionally dynamic history. By locating pipelines in optimal positions and avoiding areas such as those described above, industry can be reasonably assured that risks to their investment will be minimized.

As defined earlier, siting considerations are those factors which influence the siting or location of pipelines. Both industrial and coastal resource considerations are described in terms of their geographic location. The aforementioned geohazards are present at coastal edges and landfall areas.

Coastal Edges

Coastal edges are those portions of land that are an integral part of the land-water interface, those areas where the land, tidal wetlands and tidal waters meet. They include such features as barrier islands, nearshore shallows, beaches, wetlands and bluffs. The land-water interface is a particularly dynamic and unpredictable area, reflecting the effects of both land and water physical processes. Land runoff, shoreline erosion rates, tidal and current patterns and frequency and intensity of storm surges act together to influence the composition and pipeline siting implications of various edge features.

The composition and texture of landfall soils in which surface or buried pipelines are a consideration in relation to the feature stability, and thus safety, of the pipeline. Soil conditions at the landfall site may be such that the shoreline dynamics and sediment supply characteristics are conducive to accelerated erosion. Traversing barrier spits could lead to a breach in the natural stability of the shoreline, with future inlet formation possibly resulting.

Figure 2.6: Erosion of rock; piles of boulders have gathered at the base of the cliff

Source: http://www.dailymail.co.uk/news/article-2274536/Walkers-warned-steer-clear-Beachy- Heads-cliff-sub-zero-temperatures-accelerated-pace-erosion-leaving-extremely-unstable.html

Landfall areas

Once the decision is made to construct a pipeline, consideration must be given to a site at which the pipeline can be brought ashore. Usually, a 50 to 100 foot right-of-way is the minimum requirement for a pipeline landfall. However, a pipeline shore terminal and a pumping facility may be required to increase pipeline pressure if the product is to be piped inland for processing.

The marine terminals and surge storage facilities are situated in landfall areas. Landfall areas can be defined as the land which is between the seaward limit and landward limit, and combine offshore and onshore facilities. If the terrain of the landfall area is mild with low inclination, it is usually consists of soft cohesive materials and saturated loose sandy materials. The latter have the potential of soil liquefaction phenomena under strong seismic waves which may impose a substantial distortion to the pipeline as shown in Figure 2.7. On the other hand, if the pipeline follows a steep terrain at the landfall, then the pipeline has to endure both the amplified ground motion due to the topography effects and the imposed permanent ground deformations due to the potential earthquake-triggered landslide. The geomorphology of steep slopes at the landfall areas change in time due to sea erosion, and thus, increase the risk of landsliding especially under seismic conditions (Fig. 2.8).

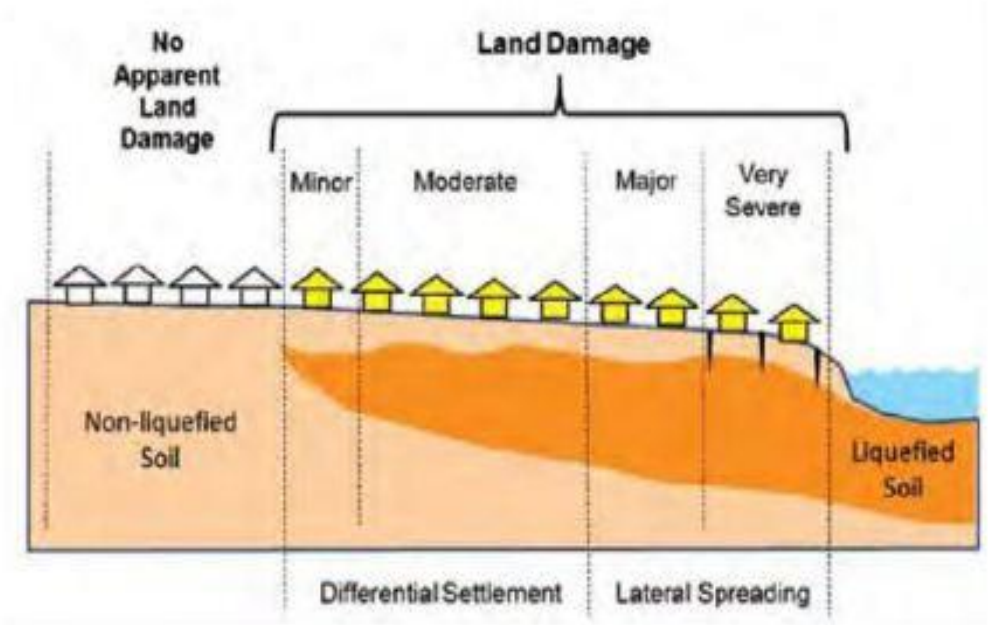

Figure 2.7: Sketch showing some of the geohazards at landfall areas (Psarropoulos & Antoniou, 2016)

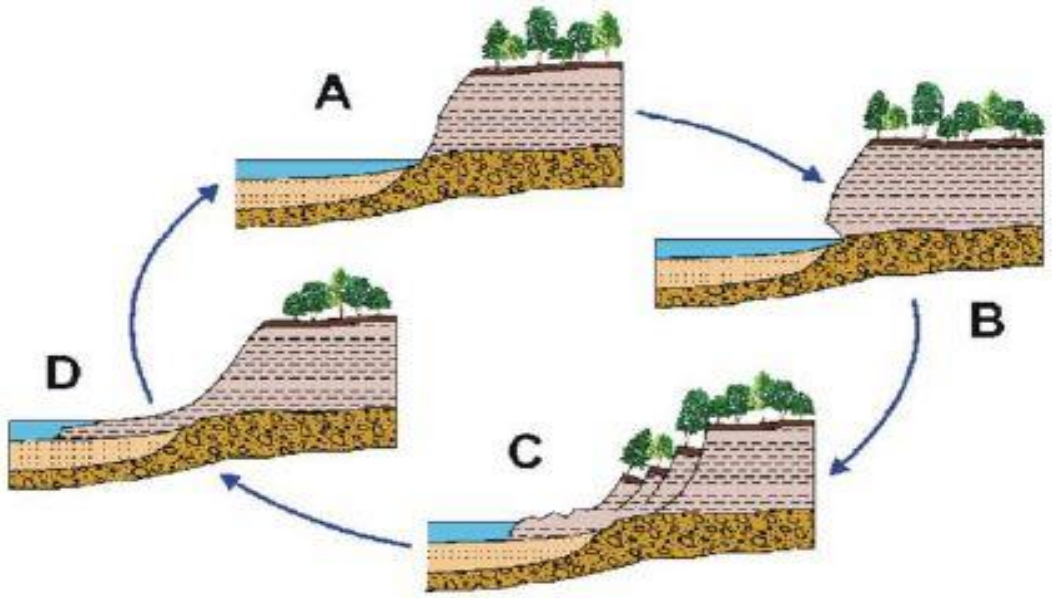

Figure 2.8: Sketch showing the phenomenon of sea erosion in a steep slope at landfall area (Psarropoulos & Antoniou, 2016)

2.3 GEOHAZARD IN ROCKY COASTAL AREAS

2.3.1 Introduction

Natural hazard on the coast is largely affected by processes of rapid sediment transfers produced by meteorological, oceanographic and geological forces. Coastal failure, mass wasting and floods are some of the processes that operate naturally in this environment and significantly influence the human use of coastal resources. The most of the part of coastal zones is consisted of rocky shores which include beaches that they are backed by bedrock cliffs or rocky uplands. The geological processes that regulate sediment transfer in these environments also cause major physical changes both onshore and at sea. According to the coastal zone concept, the term "rocky coast" is used to denote a spatial zone between the landward limit of marine influence and seaward limit of terrestrial influence (Carter 1988) composed of a rocky substrate retaining at the coastline the form of a cliff with different profiles.

Rocky coasts occur in a variety of geological settings with a wide range of morphologies depending on rock type, tectonics and climate. Rocky coastal areas can be associated with mountainous regions with active or recent tectonics or volcanic activity, or develop as low-relief cliffs along non-active margins, which limit seaward flattened areas. Steep coasts commonly occur also in glacial

environments such as fjords or lakes. In all these settings, slope instability represents the most effective hazardous process, which can erode and transfer large volumes of material directly, or via coastal streams, into the sea, lake or fjord (Fig. 2.9). Landslide activity has a significant impact on coastal facilities. Material eroded from rocky coasts is mostly delivered in the form of cliff debris, landslide accumulations, coarse-grained deltas and ultimately as fluvial turbidity flows. As a result of high-gradient sea-floor topography and often a narrow or non-existent shelf along rocky coasts, the eroded deposits often go straight to the open sea. Coastal evolution mainly depends on the balance between sediment availability and wave reworking processes. For rocky coasts, delivery of sediment is typically intermittent, and persistence of the displaced material in the littoral environment as natural armour for wave action is consequently low. This exposes rocky coasts to an irreversible loss of land human-scale periods.

Figure 2.9: Picture of an alluvial fan transfer and deposit

Source: https://devynba.weebly.com/water-erosion.html

2.3.2 Sediment transfer at rocky coast

Rocky are potentially subject to mass-wasting events over a range of magnitude and period of recurrence, which are able to transfer large amounts of material into coastal and open seas. Topographic gradients arise from volcanic and tectonic processes of deformation and uplift, which also have a primary effect on the denudation rate and coastline features. Besides coastal slope tectonic

activity shapes the seafloor morphology of marine areas, which is characterized by high gradients, narrow and abrupt continental margins, and submarine canyons close to the shoreline.

Sediment transfer at rocky coasts is typically intermittent, involving massive transport of rock, regolith sedimentary cover and soil which can damage buried or surface pipelines. The resulting deposits have a coarse-grained texture with relatively small quantities of fine sand and mud, and are transient through the shore zone and mostly redeposited at great depth. The combination of steep continental shelves, which are unable to dissipate wave energy and episodic coastal supply prevents the beach profile being maintained over a long period, although coastline progradation may occur as ephemeral alluvial deltas at stream mouths. Lack of extensive coastal plains on rocky coasts is further due to the capture of sand at the head of submarine canyons, with the result that sand is carried to the deep sea out of the coastal system.

Mass movement is a fundamental component of landscape evolution on rocky coasts that accounts for active cliff recession (Fig. 2.8), lateral collapse of coastal volcanic structures and rocky slopes, and sudden increases in sediment load in short coastal rivers. The catastrophic delivery of material exposes coastal zones to both mass wasting and tsunami hazards, the latter being produced by displaced waves as rock avalanches enter a lake or the sea. The understanding of all these hazardous processes is essential for the construction's sustainability because of the induced construction risk.

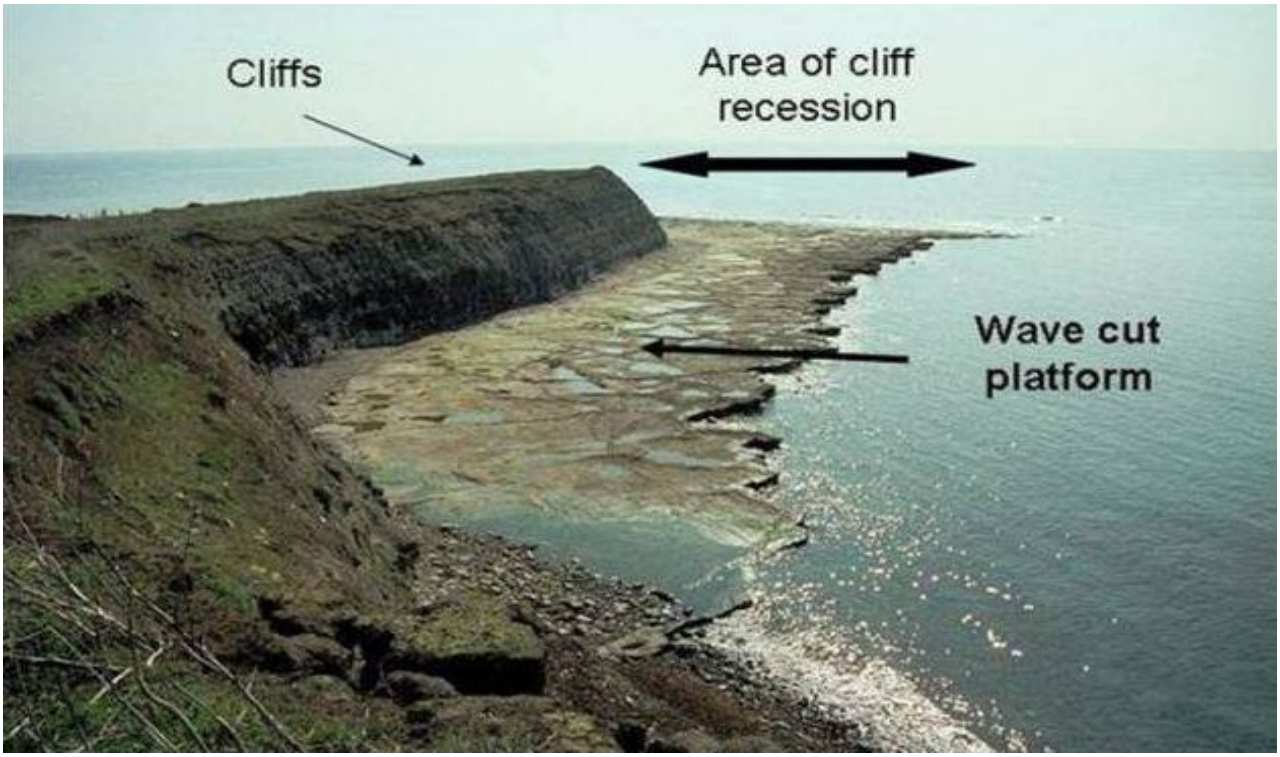

Figure 2.10: Cliffs and wave cut platforms

Source: http://thebritishgeographer.weebly.com/coasts-of-erosion-and-coasts-of-deposition.html

2.3.3 Sea-cliffs

An important source of sediments at rocky coasts is represented by colluvial deposits resulting from cliff recession (Fig. 2.11). Cliff erosion is produced by both wave and weathering action, which operate with varying intensity depending on local meteorological and oceanographic features, and rock resistance and results in an irreversible loss of land. Although basal erosion is a critical factor for cliff instability (Richards & Lorriman 1987, McGreal 1979), precipitation and infiltration of water resulting from rainfall events and groundwater may act as driving or forcing agents in the upper part of the cliff slope, significantly contributing to coastal changes (Lawrence 1994). Again, a major role is played by landslide activity of various magnitude, which can involve the rock substrate and loose superficial terrain transporting significant amount of materials to the cliff toe. The form and stability of rocky coasts is further related to factors inherited from past environmental conditions, characterized by different sea level and climate, which interact with contemporary erosive agents so that the sea may rework steep slopes initially formed by non-marine processes (Fig. 2.12; Sunamura 1992; Bray & Hook 1997; Trenhaile 2002).

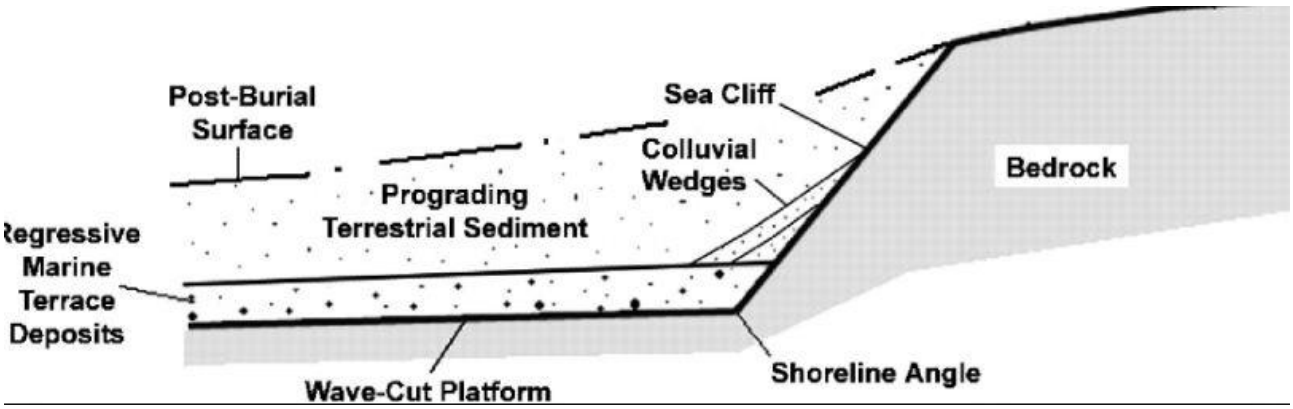

Figure 2.11: Colluvial deposits due to cliff recession (Shaller & Heron 2004)

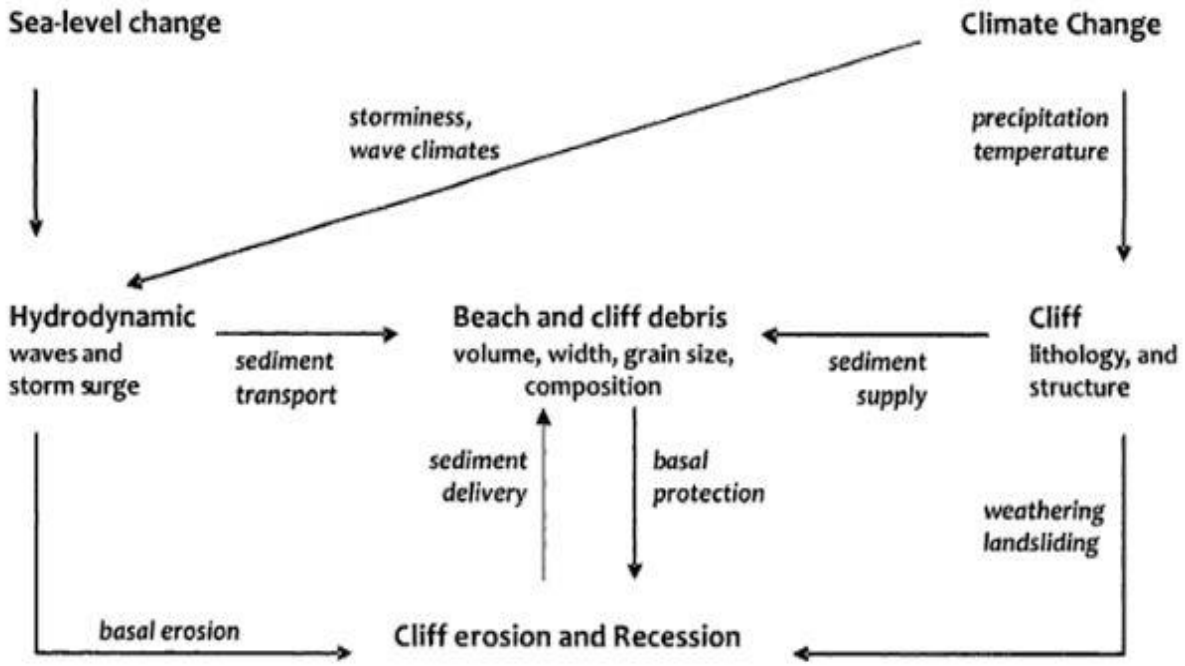

Figure 2.12: Factors influencing cliff erosion and recession (Violante 2009)

Mechanical strength and wave energy are the main elements affecting the recession of cliffed coasts (Sunamura 1992). The wave factor is greatly influenced by occurrence of loose sediments in coastal waters, which increase mechanical abrasion and wave impact. However, as the solid load increases to high values, wave energy is dissipated in moving and reworking sediments the coast is consequently protected. Therefore, fallen and/or fluvial-derived debris that accumulate in the form of a beach or as a landslide deposits at the cliff toe significantly reduces cliff instability. The persistence of such basal protective sediments depends upon the balance between hydrodynamic forcing (waves, tides, cross- and long-shore currents), and the type and amount of materials supplied. A general model for the evolution of a rocky coast, first proposed by Sunamura (1983), involves a cyclic process with phases of cliff retreat followed by failures and mass movements and longshore transport of the accumulated material, such that the cliff is exposed again to the wave action.

Another consequence of cliff retreat is the creation of shore platforms, which is mainly related to quarrying and abrasion activities with significant aid from bio-erosion and weathering. These structures are seldom horizontal, and often have a gentle seaward slope of up to 3%, possibly possibly covered by a small amount of sediment (Trenhaile 2004). Although associated with the rate of cliff retread, the occurrence of a shore platform in front of a cliff increasingly acts to dissipate wave energy as it develops landward, up to a critical platform width, beyond which waves are unable to erode or remove debris protecting the cliff face. Nevertheless, the dissipative effect may decrease as a result of platform downwearing, which reduces the platform height relative to sea level, thus maintaining

cliff retreat. Again, this process has a finite limit, as shear stress between the platform and the waves decreases with water depth.

The retreat of cliffed shore is the cumulative result of numerous variables acting on each other. Interaction between processes and products may result in self-regulation from negative feedback associated cliff debris that supports, protects or load the toe. In these cases the recession can stop and the cliff may be degraded by subaerial processes, or evolve through a cyclic process involving debris removal redistribution by hydrodynamics forces.

2.3.4 Cliff recession

The stability of a rocky coastal slope is greatly influenced by intrinsic geological features that determine material strength and rock mechanics. Lithology, patterns of fractures and faults. and strata attitude can vary significantly also at a local scale, affecting cliff response to wave energy (Allison 1989; Sunamura 1992; Bray & Hook 1997) and the types of mass movement. Mudflows and rotational slumps regularly develop in soft and weak lithologies, whereas on firm and rocky cliffs rockfalls and topples are predominant (Fig. 2.13 & Fig 2.14. More resistant lithologies are often characterized by the development of stress-release jointing resulting from decrease in the confining pressure as cliff retreat proceeds. Such tension cracks can cause a high degree of freedom for block movements, often resulting in toppling failures.

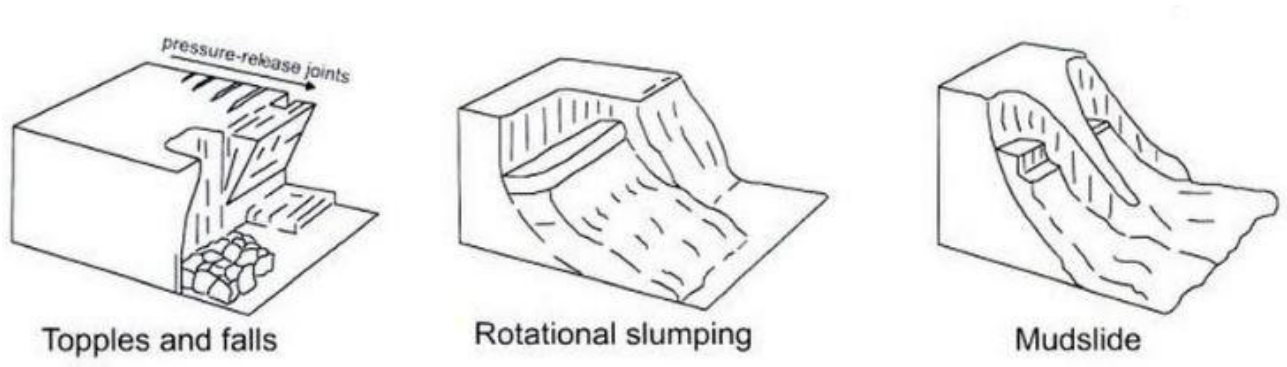

Figure 2.13: Types of mass movement affecting a sea-cliff (Violante 2009)

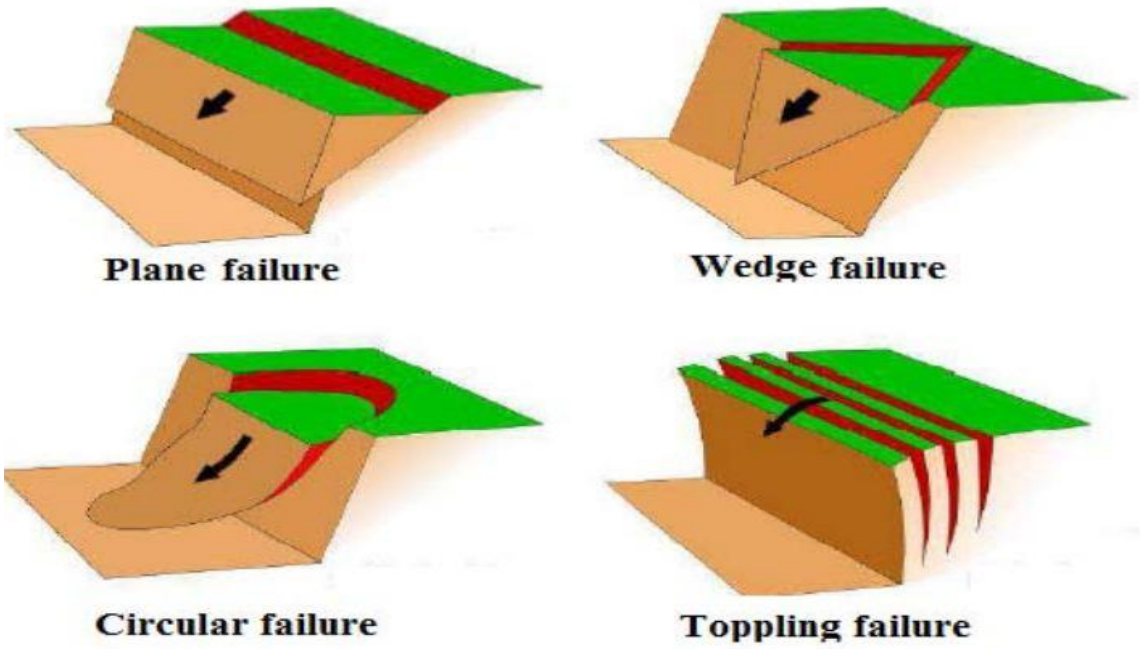

Figure 2.14: Types of slope failure

The types of mass movement are especially important because the affect the nature, size and amount of sediment released by cliff erosion. These characteristics influence the proportion of cliff input retained in the littoral area, which inhibits wave impact, thus reducing further recession. Coarse and block-size durable materials are more likely be retained on the upper shoreface and act as natural armour whereas sands are more susceptible to cross-shore transport induced by seasonal storms. However, local bathymetry and oceanographic factors can aloe the presence of wide sandy beaches that actively protect cliffs from marine erosion. Fine deposits of silt and clay do not contribute significantly to active shore profiles, as they are regularly removed from the littoral environment as suspended material and redeposited further offshore.

Coastal landslides are common where rocks incline or dip seawards, with the resultant cliff angle being largely determined by the dip angle. If strata dip landward or have a horizontal attitude, slope instability is significantly reduced and near-vertical cliffs faces may develop. In many Mediterranean coastal environments where the rock masses are carbonate nature, chemical weathering may exert an important effect through the activity of karst processes. For these coasts basal erosion often produces deep notches, formed by a combination of biological and physical activities, which effectively undermine the cliff and lead to slope failure. Seepage erosion also may facilitate major mass movements at coasts characterized by groundwater circulation with permeable strata that overlie or are interbedded with impermeable units. This is the case for the coastal bluffs of New England, where

ground waters remove material and reduce sediment strength, greatly enhancing slope instability (Kelley 2004).

The study of factors and eroding actions controlling the evolutionary dynamics of sea cliffs (Trehaile 1987; Sunamura 1992, 1997; Griggs 1994) suggest that retreat of coastal slopes largely depends on mechanical wave action. Besides mechanical rock strength, assessment of cliff recession has to take into account all the variables that influence the persistence of cliff-derived deposits or river-borne sediments in the littoral environment in the form of beaches and/or landslide deposits. These parameters commonly vary at local scale, and sectors with different erosional processes and types of landslide often characterize the evolution of a given rocky coastal area.

2.3.5 Large coastal slope failures

Coastal regions of high relief, such as tectonically active mountain chains or volcanic edifices, are prone to catastrophic slope failure that can mobilize large volumes of shattered rocks from $10^6 – 10^7$ m^3 to 10 – 100 km^3 (Moore & Moore 1984; Siebert 1984; Melosh 1987). Landslides resulting from massive rock and volcano slope failure (rock or debris avalanches) are important sources of geological hazard that can damage coastal facilities. The most widely quoted examples occurring in historical times include the volcanic sector collapses of the northern flank of St. Helens on 18 May 1980 (Voight *et al*. Glicken 1998). These rapid giant rock landslides fjords can cause tsunamis as they enter a lake or the sea.

Tsunamis are most frequently generated by large submarine earthquakes, and less frequently by volcanic activity and by landslides. They generally consist of a series of waves with periods ranging from minutes to hours, arriving in a so-called “internal wave train” and their destructive power can be enormous and they can affect not only coastal areas but entire ocean basins. They are generated when the sea level is displaced within a very short time over a large region by a disturbance involving sea bottom or the sea surface (Fig. 2.15). In addition, mass movements and volcanic slope collapses can cause tsunamis with catastrophic consequences. Mass movements (e.g coastal and submarine landslides) generate tsunami waves when they involve a large volume of material over an extensive area. Furthermore, volcanic slope collapses can be assimilated to mass movements (submarine or coastal), while the collapse of a volcanic caldera can be schematically seen as a sudden downward displacement of a sector of land that goes underwater: the rabid extension of the sea domain causes the seawater to flow and fill the caldera, and starts the tsunami.

Rock avalanches, whether volcanic or non-volcanic in origin, possess high mobility in terrestrial (Hsu 1975; Ui *et al*. 1986) as well as marine environments (e.g Moore *et al*. 1989; Watts & Masson 2001). The travel distance of displaced materials is of the order of some tens of kilometers and seems

to be greater for subaqueous than for subaerial events (Hampton *et al*. 1996). The mobility of large mass movements has been attributed to the collisions between grains (Hsu 1975), to layers of compressed air trapped beneath the sliding mass (Shreve 1968) or to mechanical and acoustic fluidization (Melosh 1979). For subaqueous landslides the hydroplaning effect (Mohrig *et al*. 1998) resulting from the presence of a basal layer of water offers a plausible and widely accepted explanation for the long travel distances and high velocities of many submarine flows even on very gentle slopes. Evaluation of the runout of slope failures is particularly important for subaerial rock avalanches, as it allows the potential distribution of hazard density from the source area to be determined (Crosta *et al*. 2006).

Tectonic deformation and uplift play crucial role in the development of threshold conditions for rock slope instability by increasing hillslope inclination or height. Also, tectonic stress along with lithology and weathering intensity exert a major control on geometric and strength characteristics of discontinuities and intact rock, with profound influence on the stability of rock slopes. As emphasized by numerical simulations (Bhasin & Kaynia 2004), decrease in the residual friction angle along rock discontinuities under active environmental and earthquake conditions is an important factor for sliding and rotation of blocks that may evolve into catastrophic rock avalanches.

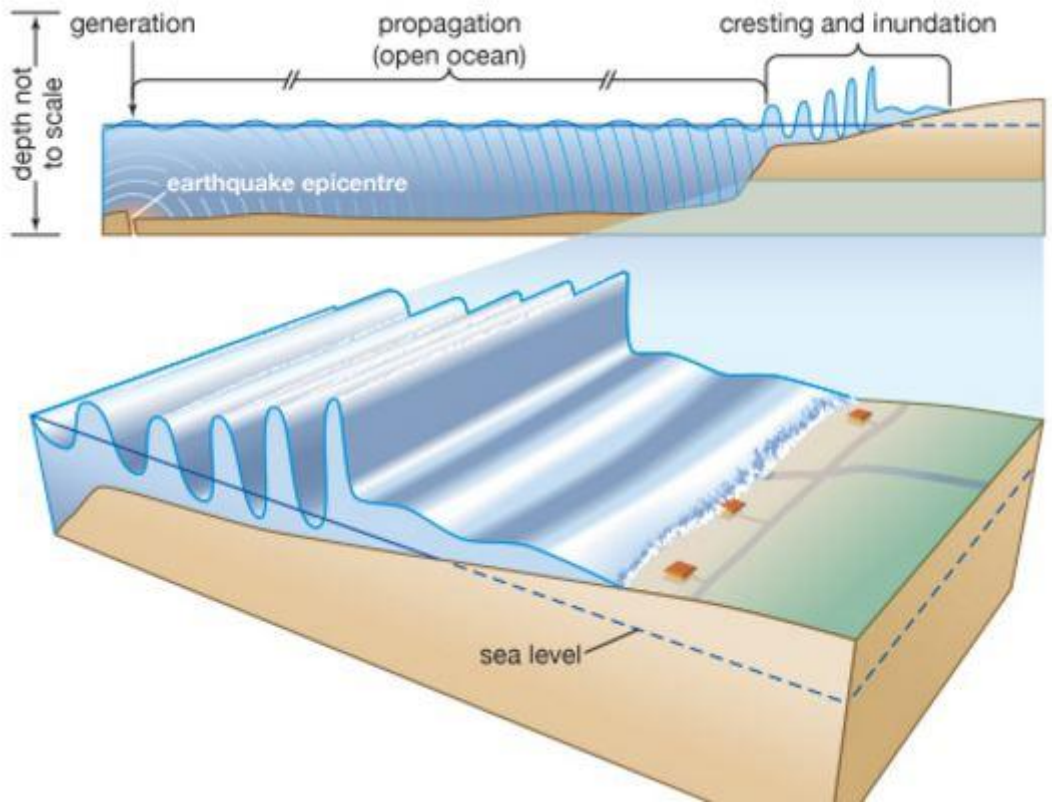

Figure 2.15: Sketch illustrating the origin of tsunami generated by faulting

Source: https://www.britannica.com/science/tsunami

CHAPTER 3: ROCK SLOPE STABILITY

3.1 INTRODUCTION

In recent years, the operation of infrastructures in mountainous terrain such as pipeline corridors often require stable slopes and control of rock falls. This applies to both excavated and natural slopes. The understanding of rock slope failure mechanisms has increased considerably during last decades in response to coastal and onshore facilities.

Structural features, such as folds, faults, and discontinuities, control rock mass (i.e., intact rock dissected by discontinuities) behavior and contribute to either the stabilization or destabilization of rock slopes, depending on their orientations and the intensity of associated tectonic damage. Glastonbury and Fell (2000) demonstrate how the geometry and composition of a rock slope and its structures determine the potential mechanism of a landslide, ranging from translational to complex multi-mechanism failure (Fig. 3.1).

a)  (b) 

c)  d) 

Figure 3.1: Key rock failure modes considered in slope stability analysis: a) planar/translational sliding, b) toppling, and c) wedge sliding, d) multi-translational failure (Palliser rockslide), demonstrating the complexity slope engineers may encounter

This chapter deals with rock stability, a subject that has shown remarkable development in the last twenty years relative to methods for estimating shear strength for discontinuities and methods of analysis.

3.2 BASIC ROCK MASS STRUCTURE

3.2.1 Introduction

This chapter consider various geologic factors and other significant features that may intervene in slope stability and which, sometimes, are responsible for the failure or the potential instability of a slope. The role of geology on slope problems and assessment is variable, according to the subsoil constituents and structure.

In slopes of limited extension entirely made of soil, the problem may be purely geotechnical. However, in larger areas, the variation in geology may lead to the formation of different types of soils with varying geotechnical properties. A geologic study can identify the different zones and physical factors, as well as their influence on the respective geotechnical properties.

In cases of slopes involving rocks, or mixtures of soils and rock, the geology plays a very important role. The methods of reconnaissance, subsoil investigation and identification of the geologic features that will describe the slope stability are different from traditional soils engineering, requiring specific methods.

Soil masses are often considered as a continuous and homogeneous constituents, but residual soils may inherit anisotropy and discontinuities such as planes of weakness (Fig. 3.2). Rock masses are generally divided by joints and discontinuities, which can constitute planes of weakness. Therefore, rock masses are considered a discontinuous media requiring specific methods of analysis.

Figure 3.2: Residual soil derived from gneiss, exhibiting different zones inherited from the parent rock, representing heterogeneity, anisotropy and planes of weakness along the structure (Ortigao & Sayao 2004)

3.2.2 Basic rock mass structure inherited from its genesis

Intrusive Igneous Rock

Igneous rock are crystalline solids which cool from magma: the liquid phase of rock. Magmas occur at depth in the crust where it cools and solidifies, forming crystalline rocks such as granite, gabbro, basalt, etc. When the cooling is quick the crystals are microscopic and when slow, medium large crystals are formed. During cooling, joints may be formed, and the forces of the intrusion may cause shearing failure planes (faults) within the intruded mass or in the neighbouring rock, dividing the rock mass into blocks of intact rock, as shown in Figure 3.3 & 3.4. Vertical dykes (vertical walls) or horizontal layers of diabase, a dark rock, or pegmatite, a white rock rich in quartz, may occur. These dense and hard bodies of rock may be present at surface due to diverse geologic processes (surface erosion, faulting, etc.).

As a result, intrusive rocks are generally homogeneous rocks, although discontinuous. Their strength is very high and their permeability is low (except when they are highly jointed or faulted) while seepage occurs along open joints. Their weathering (alteration from rock to soil) is gradual, being more intense at or near the surface. Near the top of the rock, in a transition zone between rock and soil, boulders can be present within the soil mass, representing individual blocks which are not entirely altered. These types of masses has their weight increased by the denser boulders, but their strength is controlled by the weaker soil.

Figure 3.3: A picture of an igneous rock mass mountain

Source: https://espanafascinante.com/parque-natural-de-espana/parques-naturales-en-castilla-la-mancha/piton-volcanico-de-cancarix-y-saladar-de-agramon-que-ver-que-hacer-comer-dormir-visitar/

Figure 3.4: Picture of an igneous rock mass mountain

Source: https://www.tenontours.com/history-and-formation-of-the-giants-causeway/

Sedimentary Rocks

In the most places on the surface, the igneous rocks which make up the majority of the crust are covered by a thin veneer of a loose sediment, and the rock which is made as layers of this debris get compacted and cemented together. Sedimentary rocks are called secondary, because they are often the result of the accumulation of small pieces broken off of pre-existing rocks. The original loose sediments can become consolidated by the weight of overburden, chemical precipitations, heat, pressure, etc. Depending on the degree of these diverse conditions, the sedimentary rocks may be harder or softer. This is why they are usually highly variable in nature and properties. Loose quartz sand particles can become a sandstone. Sandstone can be very weak and crumbling rock or a very hard and resistant rock, depending on the degree of cementation of chemical substances between grains. A sedimentary rock composed mostly of silt particles (siltstone) or clay (claystone, argillite, mudstone) may be very weak or of a medium strength depending on the degree of their consolidation (Fig 3.5 (a), (b)). When more compacted, the mudstone becomes a shale, presenting foliation planes or extremely jointed along the layers direction (bedding). Some clayey beds and most shales are expansive.

Most sedimentary rocks present a layered structure, with horizontal continuity but vertical heterogeneity (Fig. 3.6). They can also present a predominance of jointing coincident with bedding. The clayey rocks weather easily and produce clayey soils, some of which have poor geotechnical properties while the weathering of sandy rocks produce sandy soils, frictional but permeable.

In addition, sedimentary rocks may also originate from glacial activity. The most common glacial deposit is mixture of soil and rock fragments deposited together when the ice melts, called *moraine* or *till*. Consolidated it is called *tillite*. They consist of layers spread out horizontally, but with an irregular base (deposited over an older topographic surface), and quite heterogeneous. Since the matrix is earthy, it can accumulate water and weathers very easily.

Continuous accumulations of diverse chemical precipitates, resulting from water evaporation forms sedimentary rocks of chemical origin, for example limestone, gypsum. These rocks are soluble, The most common rock is limestone, composed of calcium carbonate (sometimes also with magnesium, which is called dolomite). Owing to its solubility, they may have solution cavities, channels, caves, large and deep sinkholes at the surface resulting from cavern collapse, offering excellent ways for waters to flow and escape.

a)  b) 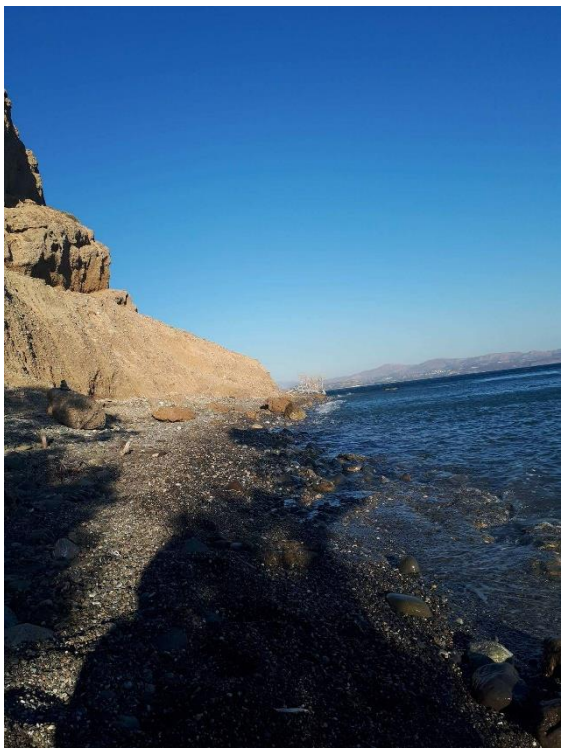

Figure 3.5: Natural coastal slope composed of mudstone. Upper part (a) corresponding to a medium strong rock. Lower part (a) corresponding to a weak and crumpling rock (Southern Crete, Heraklion, Greece)

Figure 3.6: Sedimentary rock horizontally jointed with horizontally continuity and vertical heterogeneity (Aegina, Greece)

Metamorphic Rocks

Metamorphic rocks (Fig. 3.7) are sedimentary or igneous rocks that have undergone high pressures and temperature, and were transformed into another rock, generally harder and more compact. The pressure may be confining pressure due to deep burial or due to tectonic forces. Rock structure may become deformed into folds formed by compressional stresses, as well as failure planes (faults and jointing), due to shearing stresses. The higher temperature, besides the pressure, may promote recrystallization, with the development of new minerals, changing the original mineral composition of the rock, as well as distortion of preserved minerals. The oriented pressure develops orientation of the structure and the development of schistosity (foliation) planes normally perpendicular to directed stress. Sandstones are transformed into quartzite, mudstones into shales and phyllites, and at higher degrees into schists or banded gneiss, limestones into marble, granite and similar rocks are transformed into gneiss.

Metamorphic rocks are usually deformed by folding and faulting, and can become very jointed, diminishing the size of the intact rock blocks. As a result, the structures of the rock masses are normally very complex, and geologic skill is required to understand them especially regarding the zones of different weathering, the location of weaker rocks, preferential percolation of ground water, and the identification of potential failure planes. The geological conditions are also complex.

One point to mention is that the intensely jointed rock mass, in large scale, may behave almost as a homogeneous media, due to higher degree of freedom of the individual blocks to move with respect to each other.

Figure 3.7: Picture of metamorphic rock

Source: http://www.rockclimbing.com/Articles/Geology_for_Climbers_Part_III_Metamorphic_Rocks_1595.html

3.2.3 Significant Geologic Features

There are some geologic features that have a paramount of importance as related to the geotechnical behavior of slopes.

Faults

The rupture of the rock mass by geologic (tectonic) action, followed by some displacement, causes the formation of a continuous plane of discontinuity, often accompanied by the fragmentation of the rock along this plane. This allows water percolation, and more weathering than in the adjoining rock mass. A fault plane can have a much lower friction coefficient with respect to the rest of the rock mass. An unfavorable orientation of this plane with respect to the cut is when it has a direction parallel or with low angles to the slope surface and dips towards the slope. If the plane is exposed in the excavation and if the friction angle of this plane is equal or smaller than the dip angle, it will cause the sliding of the rock mass above it.

Joints, Bedding planes, and Shear zones

These planes of discontinuity act in the same manner as faults, representing planes of weakness within the rock mass. When the joints are oriented in preferential spatial attitude and conform to jointing systems along which the mass is weaker with respect to shearing stresses, they become directions of weakness. These discontinuities can be critical when adversely oriented with respect to the slope. Figures 3.8, 3.9 present two examples of how jointed rock can affect slope stability. Figure 3.8 shows an example where jointing does not affect the slope stability and Figure 3.9 shows how jointing conditions affect the stability of the slope.

Stress relief joints

The slow natural removal of topsoil by erosion promotes the decrease in stresses acting on the rock due to the weight of the material. The rocks then tends to decompress, giving rise to tension in planes parallel to the topographic surface. As the rock has a low-tension strength, it fractures, forming a family of joints, which become more tightly spaced close to the rock surface. They are often weathered, as they constitute paths of entry for the waters infiltrating into the ground, besides the fact that after heavy rains they are saturated allowing the building up of high hydrostatic pressures.

Figure 3.8: Slope in rock mass crossed by vertical joint normal the slope face, which do not affect the slope stability (Kythera, Greece)

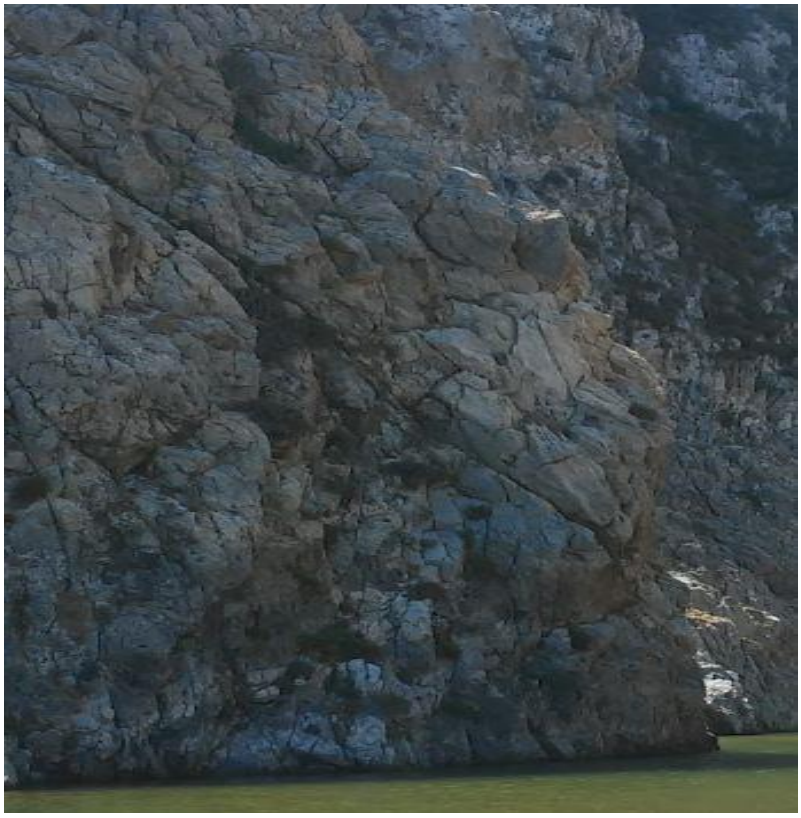

Figure 3.9: Slope in rock mass crossed by an oblique joint, which can affect the slope stability (Kythera, Greece)

Tension cracks

In clefts, where the slope is very steep, sometimes even vertical, and when the strength of the rock is low, vertical tension cracks may formed. In rainy periods the water infiltrates very easily within these fissures and, since their drainage is usually much slower than the infiltration rate, high hydrostatic pressures are built up, exerting hydrostatic lateral thrust on the thin vertical slice of rock, causing failures by toppling.

Sheared planes

In planes that underwent displacement in the geologic past, like bedding planes in folded strata and planar discontinuities, the friction angle decrease due to the destruction of the roughness during shear, and the friction coefficient also decreased, eventually attaining its residual strength.

Weak layers

The rock mass may contain layers of weaker material, which may represent potential zones of failure. This is commonly the case in stratified rock, examples being the presence of shales within harder rocks such as sandstone, limestone etc. Their adverse effect will also depend on the orientation of these layers with respect to the slope surface.

Permeable layers

The existence of more permeable layers covered by impermeable layers, such as the saprolite horizon covered by clayey soil, may help developing uplift pressures that decrease the strength of soils. Another undesirable condition may occur when, within the slope or at the foundation of high fills or dumps, there are permeable layers; in this situation, an artesian condition may occur if the piezometric level is high, decreasing the stability of slope.

Colluvium deposits

These deposits resultant from the accumulation of loose material transported by gravity or by erosion from the uppers parts of the hill. These deposits occur at the toe of the hill or at the hill slope in portions of lower inclination. Due to their mode of formation, they stayed practically at their natural angle of repose and also are quite irregular and under-consolidated. In tropical regions, where chemical weathering predominates, they have an earthy matrix and rounded rock fragments and boulders. They commonly show movements and instabilities in rainy seasons due to the rise of water level and decrease of its suction tension. In arid or semi-arid regions, under prevailing physical weathering, they may have a sandy matrix and angular rock fragments and are more commonly called talus. In any case, they are unstable deposits when subjected to cuts.

3.3 TYPES OF ROCK SLOPE FAILURE

3.3.1 Introduction

This chapter focuses on landslip types and presents their classification according to the kinematics, rate of movement and other features. Types of rock slope failure are major natural hazards that occur in many areas throughout the world. Slopes expose two or more free surfaces because of geometry. Plane, wedge, toppling, rockfall, and rotational (circular/non-circular) types of failure are common in slopes.

3.3.2 Plane Failure

A rock slope undergoes this mode of failure when combinations of discontinuities in the rock mass form blocks or wedges within the rock which are free to move. The pattern of the discontinuities may be comprised of a single discontinuity or a pair of discontinuities that intersect each other, or a combination of multiple discontinuities that are linked together to form a failure mode.

A planar failure of rock slope occurs when a mass of rock in a slope slides down along relatively planar failure surface. The failure surfaces are usually structural discontinuities such as bedding planes, faults, joints or the interface between bedrock and an overlying layer of weathered rock. Block sliding along a single plane (Fig. 3.10) represents the simplest sliding mechanism. In case of a plane failure, at least one joint set strike approximately parallel to the slope strike and dips toward the excavation slope and the joint angle is less the slope angle.

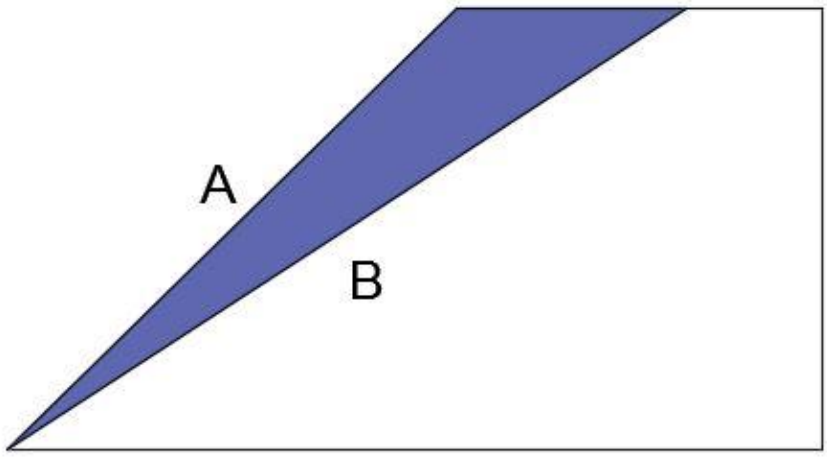

Figure 3.10: Typical view of plane failure (A = Sliding plane, B = Slope face)

3.3.3 Wedge Failure

Wedge failure of a rock slope results when rock mass slides along two intersecting discontinuities, both of which dip out of the cut slope at an oblique angle to the cut face, thus forming a wedge-shaped block (Fig. 3.11). Wedge failure can occur in rock mass with two or more sets of discontinuities whose lines of intersection are approximately perpendicular to the strike of the slope and dip towards the plane of the slope. This mode of failure requires that the dip angle of at least one intersect is greater than the friction angle of the joint surfaces and that the line of joint intersection intersects the plane of the slope.

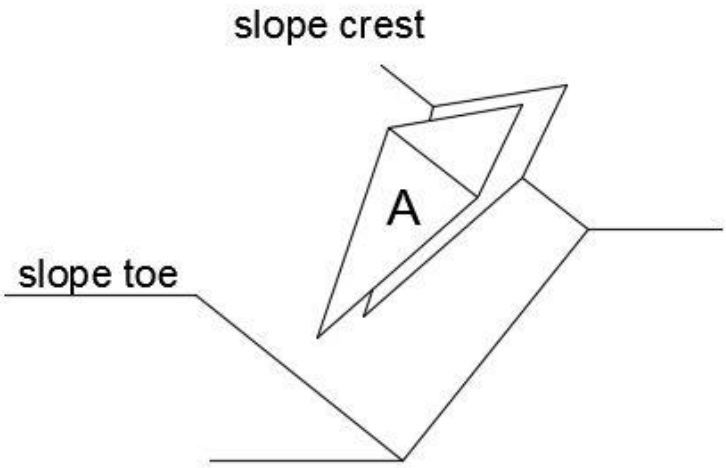

Figure 3.11: Typical view of wedge failure (A = Wedge block)

Depending upon the ratio between peak and residual shear strength, wedge failure can occur rapidly, within seconds or minutes, or over a much longer time frame in the order of several months. The size of a wedge failure can range from a few cubic meters to very large slides from which the potential for destruction can be enormous. The formation and occurrence of wedge failures are dependent primarily on lithology and structure of the rock mass (Piteau, 1972). Rock mass with well defined orthogonal joint sets or cleavages in addition to inclined bedding or foliation are generally favorable situations for wedge failure. Shale, thin-bedded siltstones, claystones, limestones and slaty lithologies tend to be more prone to wedge failure development than other rock types. However, lithology alone does not control development of wedge failures.

3.3.4 Toppling Failure

A topple, occurring is rock slopes, involves rock displacement from a slope. It occurs when columns of rock formed by steeply dipping discontinuities in the rock rotates about an essentially fixed point at or near the base of the slope followed by slippage between the layers (Fig. 3.12 (a), (b)). The center of gravity of the column or slab must fall outside the dimension of its base in toppling failure. Jointed rock mass closely spaced and steeply dipping discontinuity, sets that dip away from the slope surface, are necessary prerequisites for toppling failure. This type of slope failure may be further categorized depend on the mode such as flexural toppling and block toppling.

Flexural toppling

Flexural toppling is a mode of failure involving the bending of interacting rock columns formed by a single set of steeply dipping discontinuities, such as regular bedding planes, foliation, or joints as depicted schematically in Fig. 3.12a. Such a discontinuity system produces a rock mass composed of a stack of rock columns which can be visualized as an array of interactive cantilever beams fixed at a certain depth, and free to bend into the excavation. In such cases the rock columns bend forward under their own weight and transfer load to the underlying columns, thus giving rise to tensile and compressive bending stresses. Failure is initiated when the tensile (bending) stress in the toe column exceeds the tensile strength of the rock.

Block toppling

This type of failure is associated with sliding and toppling of rock columns (blocks, Fig. 3.12b) along a pre-existing basal failure plane formed by a discontinuity dipping into the excavation. It occurs when individual columns in a strong rock are formed by a set of discontinuities dipping steeply into the face. A second set of widely spaced orthogonal joints defines the column height. The short columns forming the toe of the slope are pushed forward by the loads from the longer overturning columns behind. This sliding of the toe allows further toppling to develop higher up the slope. The base of the failure generally consists of a stepped surface rising from one cross joint to the next. Typical geological conditions, in which block failure may occur, are bedded sandstone and columnar basalt in which orthogonal jointing is well developed.

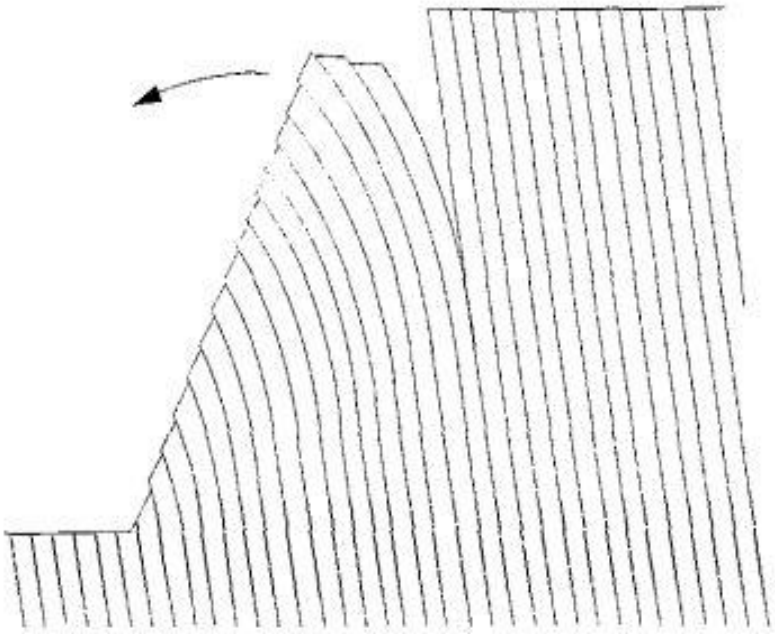

a) Flexural toppling failure

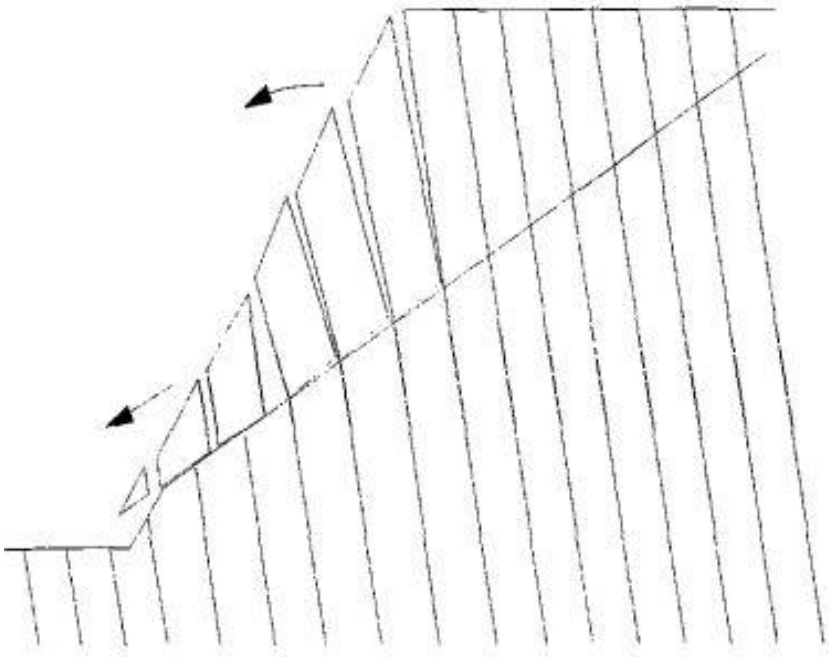

b) Block toppling failure

Fig. 3.12: Flexural and block toppling mechanisms (Adhikary, Dyskin, Jewell, and Stewart 1997)

3.3.5 Rockfalls

In rockfalls, a rock mass of any size is detached from a steep slope or a cliff along a surface on which little or no shear displacement takes place, and descends mostly through the air either by free fall, leaping, bouncing, or rolling (Fig. 3.13 & 3.14). It is generally initiated by some climatic or biological event that causes a change in the forces acting on the rock. These events may include pore pressure increase due to rainfall infiltration, erosion of surrounding material during heavy rain storms, freeze-thaw processes in cold climates, chemical degradation or weathering of the rock, root growth etc. In an active construction environment, the potential for mechanical initiation of a rock fall may probably be one or two orders of magnitude higher than the climatic or biological initiating events described above.

Movements are very rapid to extremely rapid. Rockfall may involve a single rock or a mass of rocks, and the falling rocks can dislodge other rocks as they collide with the cliff. Once movement of a rock perched on the top of a slope has been initiated, the most important factor controlling its fall trajectory is the geometry of the slope. In particular, dip slope face, such as those created by the sheet joints in granites are important, because they impart a horizontal component to the path taken by a rock after it bounces on the slope or rolls off the slope.

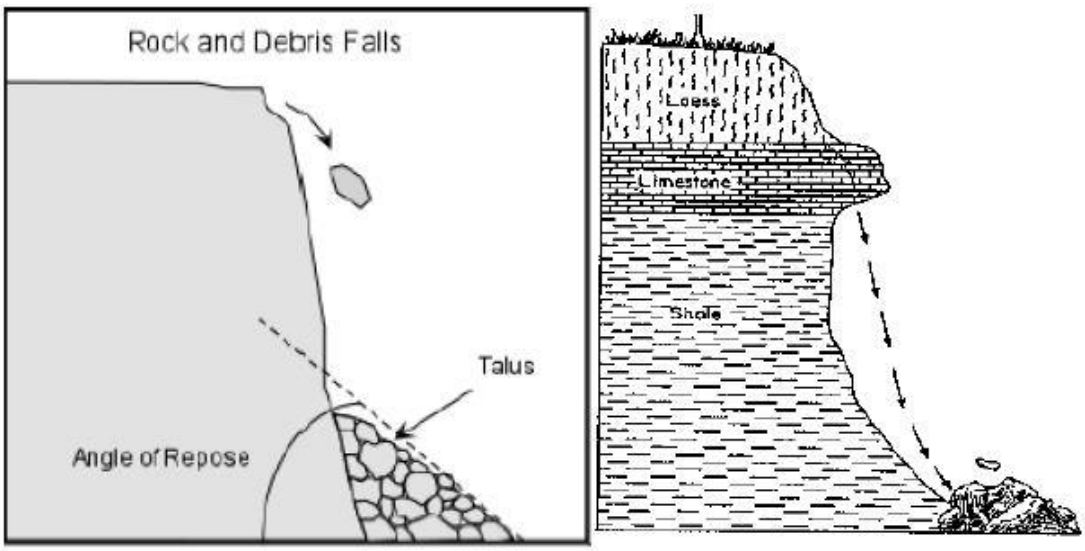

Figure 3.13: Typical view of a rockfall

Figure 3.14: Rockfall at Tempe in central Greece

Source: http://neoskosmos.com/news/en/rains-threaten-greek-highways

3.3.6 Rotational failure

In rotational slips the shape of the failure surface in section may be a circular arc or a non-circular curve. In general, circular slips are associated with homogeneous soil conditions and non-circular slips with non-homogeneous conditions. Translational and compound slips occur when the form of the failure surface is influenced by the presence of an adjacent stratum of significantly different strength. Translational slips tent to occur where the adjacent stratum is at a relatively shallow depth below the surface of the slope: the failure surface tent to be plane and approximately parallel to the slope. Compound slips usually occurs where the adjacent stratum is at greater depth, and the failure surface consisting of curved and plane sections.

The sliding of material along a curved surface called a rotational slide which commonly has two different shapes of failure surface as mentioned above: circular and non-circular. Whilst failures of this type do not necessarily occur along a purely circular arc, some form of curved failure surface is normally apparent. Circular shear failures are influenced by the size and the mechanical properties of the particles in the soil or the rock mass. Figure 3.15 shows a few typical modes of circular shear failure. This failure can occur in rock structures that exhibit no plane of weakness, and may not be associated with any underlying critical discontinuity.

A circular failure occurs when the individual particles in soil or rock mass are very small as compared to the size of the slope. The broken rock in a fill tends to behave as soil and fail in a circular mode, when the slope dimension is substantially greater than the dimension of the rock fragments. Highly weathered rocks, and rocks with closely spaced, randomly oriented by discontinuities also tend to fail in this manner. If soil conditions are not homogeneous or if geologic anomalies exist, slope failures may occur on non-circular shear surface (Fig. 3.16).

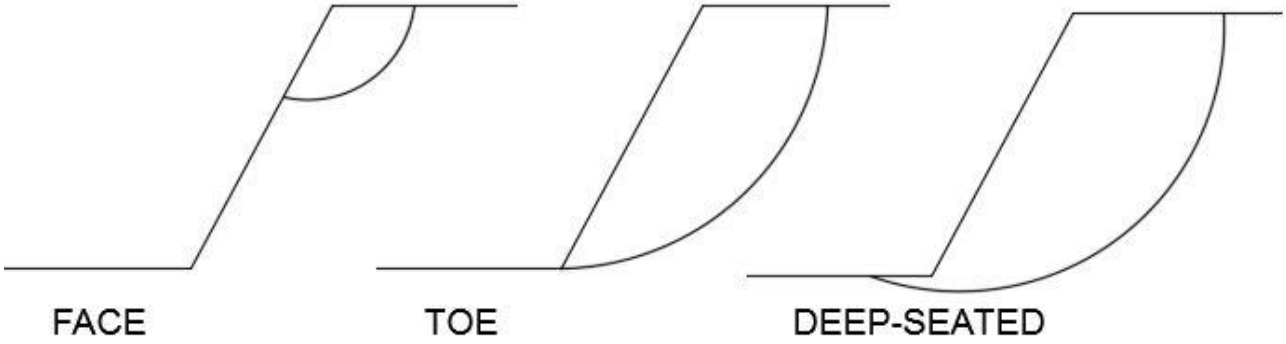

Figure 3.15: Typical view of Circular failure

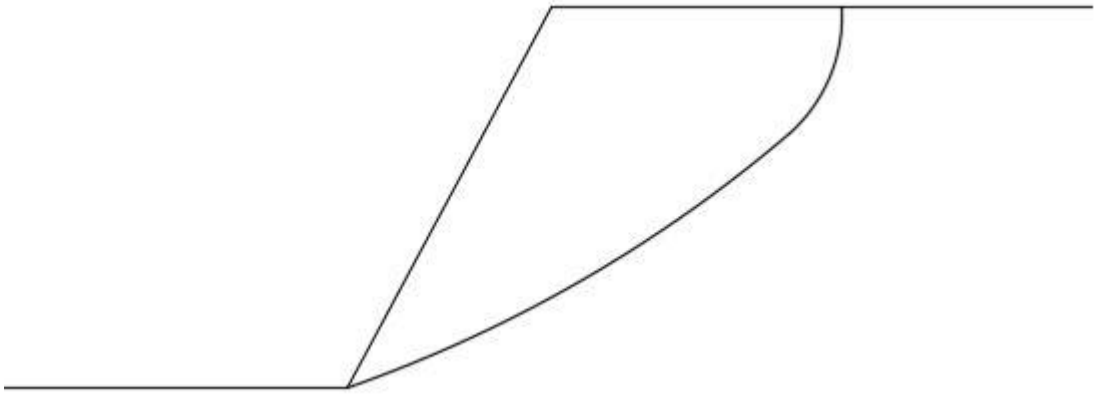

Figure 3.16: Typical view of Non-Circular failure

3.4 ROCK MASS STRENGTH PROPERTIES AND THEIR MEASUREMENT

3.4.1 Introduction

In analyzing the stability of a rock slope, the most important factor to be considered is the geometry of the rock mass behind the face. The relationship between the orientation of the discontinuities and of the excavated face will determinate whether parts of the rock mass are free to slide or topple. After geology, the next most important factor governing stability is the shear strength of the potential sliding surface, which is the subject of this chapter.

3.4.2 Scale effects and rock strength

The sliding surface in a slope may consist of a single plane continuous over the full area of the surface, or a complex surface made up both discontinuities and fractures through the intact rock. Determination of a reliable shear strength value is a critical part of a slope design, because small changes in shear strength can result in significant changes in the safe height or angle of a slope. The choice of appropriate shear strength values depends not only on the availability of test data, but also on a careful interpretation of these data in light of the behavior of the rock mass that makes up the full-scale slope. For example, it may be possible to use the results obtained from a shear test on a joint in designing a slope in which failure is likely to occur along a single joint similar to the one being tested. However, these shear test results could not be used directly in designing a slope in which a complex failure process involving several joints and some failure of intact rock is expected.

The selection of an appropriate shear strength of a slope depends to a great extent on the relative scale between the sliding surface and structural geology. More specifically, if the dimensions of an overall slope are much greater than the discontinuity length, any failure will pass through the joint rock mass, and the appropriate rock strength to use in design of the slope is that of the rock mass. Because of these scale effects the rock mass can categorized in three classes of rock:

i. *Discontinuitie*s: Single bedding planes, joints or faults. The properties of discontinuities that influence shear strength include the shape and the roughness of the surfaces, the rock on the surface which may be fresh or weathered, and infillings that may be low strength or cohesive.
ii. *Rock mass*: The factors that influence the shear strength of a jointed rock mass include the compressive strength and friction angle of the intact rock, and the spacing of the discontinuities and the conditions of their surfaces.
iii. *Intact rock*: A factor to consider in measuring the strength of the intact rock is that the strength could diminish over the design life of the slope due to weathering.

3.4.3 Classes of rock strength

Based on scale effects and geological conditions, it can be seen that sliding surfaces can form either along discontinuities surfaces, or through the rock mass as illustrated in Fig. 3.17. The importance of the classification shown in Fig. 3.17 is that in essentially all slope stability analysis it is necessary to use the shear strength properties of either the discontinuities, or of the rock mass.

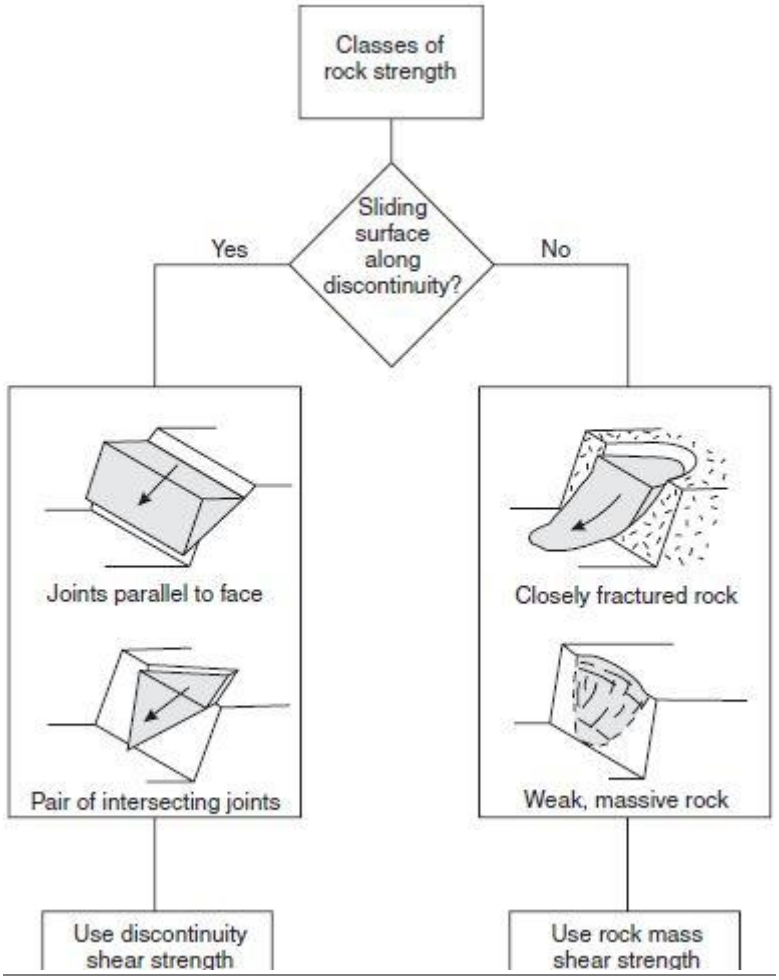

Figure 3.17: Relationship between geology and classes of rock strength (Wyllie & Mah, 4th edition 2005)

As a further illustration of the effects of geology on shear strength, relative strength parameters for three types of discontinuity and two types of rock mass are shown on the Mohr diagram in Fig 3.18. The slope of these lines represents the friction angle, and the intercept with the shear stress axis represents the cohesion.

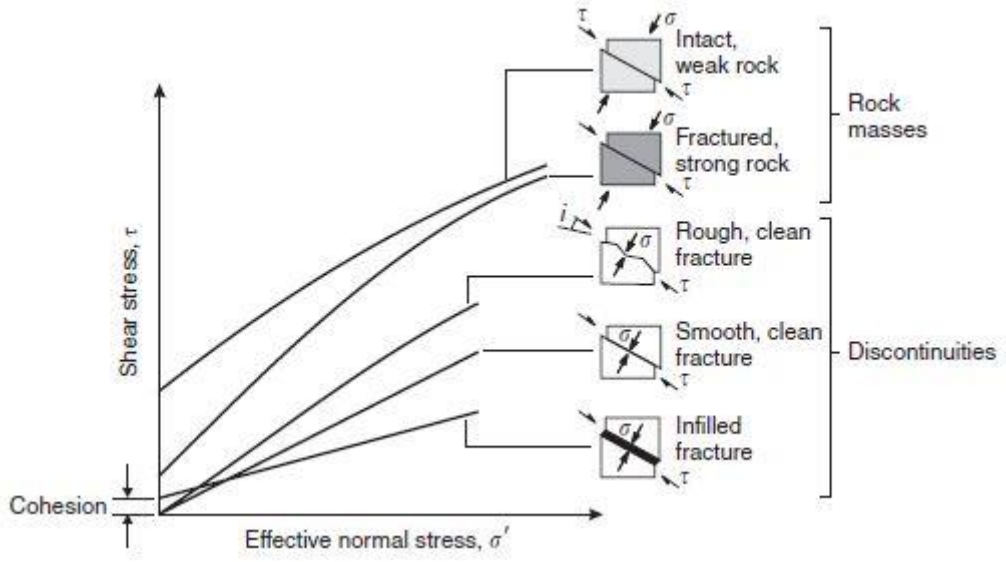

Figure 3.18: Relationships between shear and normal stresses on sliding surface for five different geological conditions (Transportation Research Board, 1996)

A description of these conditions on Fig. 3.18 is as follows:

Curve 1 Infilled discontinuity: If the infilling is a weak clay or fault gouge, the infilling friction angle (φ_{inf}) is likely to be low, but there may be some cohesion if the infilling is undisturbed. Alternatively, if the infilling is strong calcite for example, which produces a healed surface, then the cohesive strength may be significant.

Curve 2 Smooth discontinuity: A smooth, clean discontinuity will have zero cohesion, and the friction angle will be that of the rock surfaces (φ_r). The friction angle of the rock is related to the grain size, and is generally lower in fine-grained rocks than in coarse-grained rocks.

Curve 3 Rough discontinuity: Clean, rough discontinuity surfaces will have zero cohesion, and the friction angle will be made up of two components. First, the rock material friction angle (φ_r), and second, a component (i) related to the roughness (asperities) of the surface and the ratio between the rock strength and the normal stress. As the normal stress increases, the asperities are progressively sheared off and the total friction angle diminishes.

Curve 4 Fractured rock mass: The shear strength of fractured rock mass, in which the sliding surfaces lies partially on discontinuity surfaces and partially passes through intact rock, can be expressed as a curved envelope. At low normal stresses where there is little confinement of the fractured rock and the individual fragments may move and rotate, the cohesion is low but the friction angle is high. At higher normal stresses, crushing of the rock fragments begins to take place with the result that the

friction angle diminishes. The shape of the strength envelope is related to the degree of fracturing, and the strength of the intact rock.

Curve 5 Weak intact rock: A rock mass which is composed of fine-grained material that has a low friction angle and contains no discontinuities, has a higher cohesion in comparison to a strong intact rock that is closely fractured.

The range of shear strength conditions that may be encountered in rock slopes, clearly demonstrates the importance of examining both the characteristics of the discontinuities and the rock strength during the site investigation.

3.4.4 Shear strength of discontinuities

If geological mapping and/or diamond drilling identify discontinuities on which shear failure could take place, it will be necessary to determine the friction angle and cohesion of the sliding surface in order to carry out stability analyses. The investigation program should also obtain information on characteristics of the sliding surface that may modify the shear strength parameters. Important discontinuity characteristics include continuous length, surface roughness, and the thickness and characteristics of any infilling, as well as the effect of water on the properties of the infilling.

Shear strength of plane rock discontinuities

Suppose that a number of samples of a rock are obtained for shear testing. Each sample contains a through-going bedding plane that is cemented: in other words, a tensile force would have to be applied to the two halves of the specimen in order to separate them. The bedding plane is absolutely planar, having no surface irregularities or undulations. As illustrated in Fig. 3.19, in a shear test each specimen is subjected to a stress σ_n normal to the bedding plane and the shear stress τ, required to cause a displacement δ, is measured.

The shear strength will increase rapidly until the peak strength is reached. This corresponds to the sum of the strength of the cementing material bonding the two halves of the bedding plane together and the frictional resistance of the matching surfaces. As the displacement continues, the shear strength will fall to some residual value that will remain constant, even for large shear displacements.

Plotting the peak and residual shear strengths for different normal stresses results in the two lines illustrated in Fig. 3.19. For planar discontinuity surfaces the experimental points will generally fall along straight lines. The peak strength line has a slope of φ and an intercept of c on the shear strength axis. The residual strength line has a slope of φ_r.

The relationship between the peak shear strength τ_p and the normal stress σ_n can be represented by the Mohr-Coulomb equation:

$$\tau_p = c + \sigma_n tan\varphi \tag{3.1}$$

where, *c* is the cohesive strength of the cemented surface and

φ is the angle of friction.

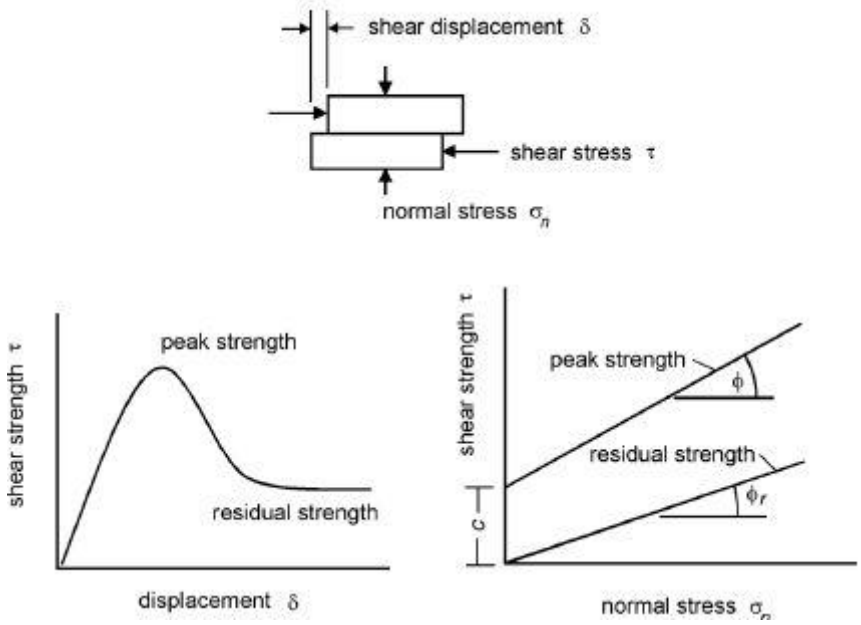

Figure 3.19: Shear testing of discontinuities

In the case of the residual strength, the cohesion *c* has dropped to zero and the relationship between φ_r and σ_n can be represented by:

$$\tau_p = \sigma_n tan\varphi_r \tag{3.2}$$

where, φ_r is the residual angle friction.

For the residual strength condition, the cohesion is lost once displacement has broken the cementing action; on the Mohr diagram this is represented by the strength line passing through the origin of the graph. Also, the residual friction angle is less than the peak friction angle because the shear displacement grinds the minor irregularities on the rock surface and produces a smoother, lower friction surface.

In addition, for a planar, clean (no infilling) discontinuity, the cohesion will be zero and the shear strength will be defined solely by the friction angle. The friction angle of the rock material is related to the size and shape of the grains exposed on the fracture surface. Thus, a fine-grained rock, and rock with a high mica content aligned parallel to the surface, such as a phyllite, will tend to have a low friction angle, while coarse-grained rock such as granite, will have a high friction angle. Table 3.1

shows typical ranges of friction angles for a variety of rock types (Barton, 1973; Jaegar and Cook, 1976). The friction angles listed in Table 3.1 should be used as a guideline only because actual values will vary widely with site conditions.

Table 3.1: Typical ranges of friction angles for variety of rock types

Rock class	Friction angle range	Typical rock types
Low friction	20-27°	Schists (high mica contect), shale, marl
Medium friction	27-34°	Sandstone, siltstone, chalk, gneiss, slate
High friction	34-40°	Basalt, granite, limestone, conglomerate

Shear strength of rough surfaces

All natural discontinuity surfaces exhibit some degree of roughness, varying from polished and slickensided sheared surfaces with very low roughness, to rough and irregular tension joints with considerable roughness. These surface irregularities are given the general term *asperities*, and because they can have a significant effect on the stability of slope, they should be accounted for appropriately in design. Patton (1966) found that asperities can be divided into two classes: first- and second-order asperities as shown in Fig. 3. 20. The first-order asperities are those that correspond to the major undulations on the bedding surfaces, while the second-order asperities are small bumps and ripples on the surface and have higher *i* values. In order to obtain reasonable agreement between field observations of the dip of the unstable bedding planes shown in Fig. 3.21 and the ($\varphi + i$) values, it was necessary to measure only the first-order asperities.

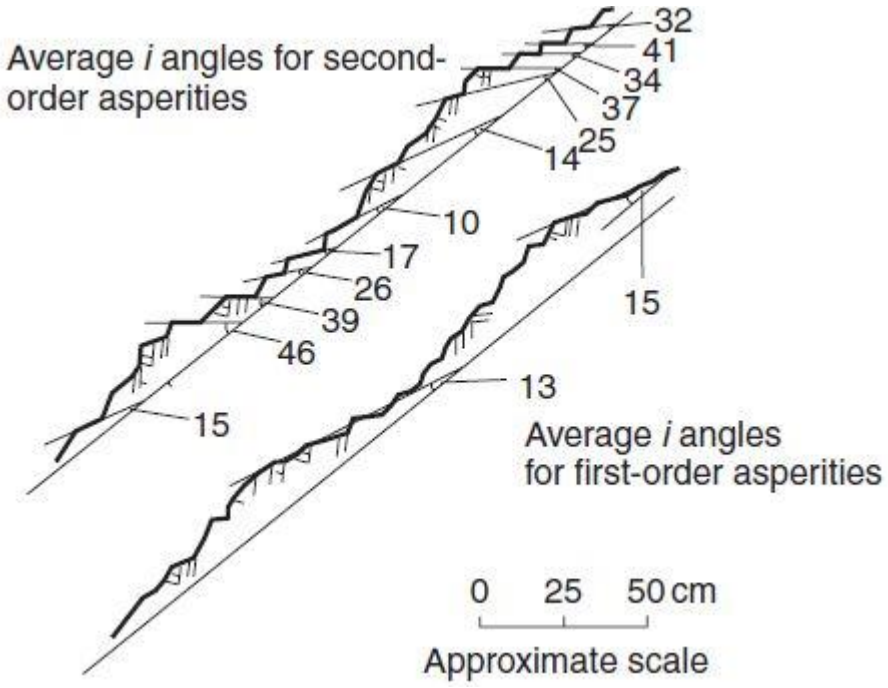

Figure 3.20: Measurement of roughness angles *i* for first- and second-order asperities on rough rock surfaces (Patton, 1966)

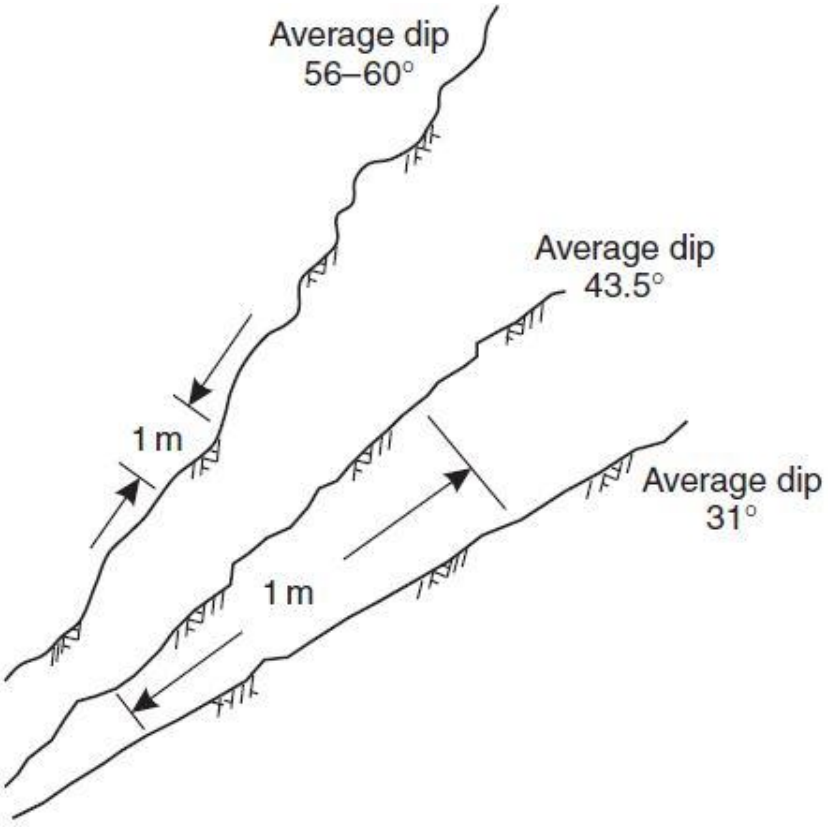

Figure 3.21: Patton's observations of bedding plane traces in unstable limestone slopes (Patton, 1966)

Later studies by Barton (1973) showed that Patton's results were related to the normal stress acting across the bedding planes in the slopes that he observed. At low normal stresses, the second-order projections come into play and Barton quotes ($\varphi + i$) values in the range of 69-80° for tests conducted at low normal stresses ranging from 20 to 670 kPa (Goodman, 1970; Paulding, 1970; Rengers, 1971). Assuming a friction angle for the rock of 30°, these results show that the effective roughness angle i varies between 40 and 50° for these low normal stress levels.

The actual shear performance of discontinuity surfaces in rock slopes depends on the combined effects of the surface roughness, the rock strength at the surface, the applied normal stress and the amount of shear displacement. This is illustrated in Fig. 3.22 where the asperities are sheared off, with a consequent reduction in the friction angle with increasing normal stress. That is, there is a

transition from dilation to shearing of the rock. The degree to which the asperities are sheared will depend on both the magnitude of the normal force in relation to the compressive strength of the rock on the fracture surface, and the displacement distance.

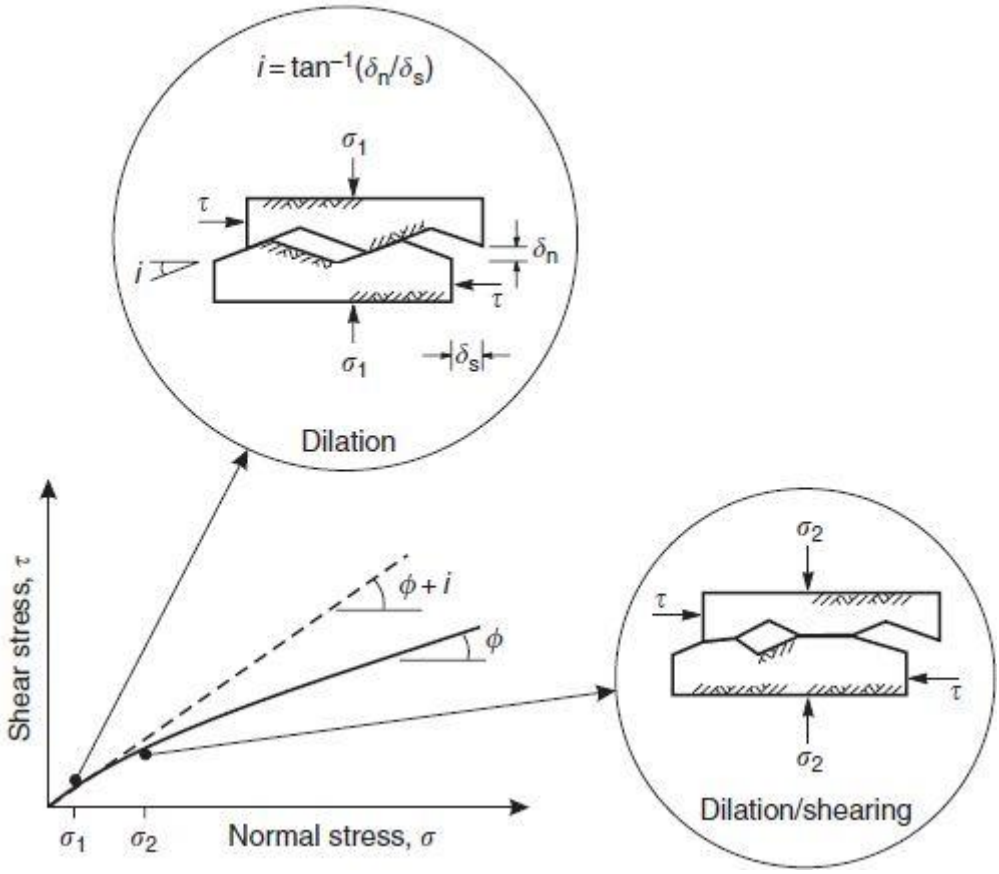

Figure 3.22: Effect of surface roughness and normal stress on friction angle of discontinuity surface (Transportation Research Board, 1996)

A rough surface that is initially undisturbed and interlocked will have a peak friction angle of $(\varphi + i)$. With increasing normal stress and displacement, the asperities will be sheared off, and the friction angle will progressively diminish to a minimum value of the basic, or residual, friction angle of the rock. This dilation-shearing condition is represented on the Mohr diagram as curved strength envelope with an initial slope equal to $(\varphi + i)$, reducing to φ_r at higher normal stresses.

The shear stress-normal stress relationship shown in Fig. 3.22 can be quantified using a technique develop by Barton (1973) based on the shear strength behavior of artificially produced rough, clean "joints". The study showed that the shear strength of a rough rock surface depends on the relationship

between the roughness, the rock strength and the normal stress, and can be defined by the following empirical equation:

$$\tau = \sigma' \tan(\varphi + JRC \log_{10}(\frac{JCS}{\sigma'})) \quad (3.3)$$

where, *JRC* is the joint roughness coefficient

JCS is the compressive strength of the rock at the fractured surface

σ' is the effective normal stress.

Barton developed his first non-linear strength criterion for rock joints (using the basic friction angle φ), and with Choubey in 1977 revised the above equation to:

$$\tau = \sigma' \tan(\varphi_r + JRC \log_{10}(\frac{JCS}{\sigma'})) \quad (3.4)$$

where φ_r is the residual friction angle.

Barton and Choubey suggests that φ_r can be estimated from:

$$\varphi_r = (\varphi_b - 20) + 20(r/R) \quad (3.5)$$

where *r* is the Schmidt rebound number on wet and weathered fracture surfaces and *R* is the Schmidt rebound number on dry unweathered sawn surfaces.

The joint roughness coefficient *JRC* is a number that can be estimated by comparing the appearance of a discontinuity surface with standard profiles published by Barton and others. One of the most useful of these profile sets was published by Barton and Choubey (1977) and is reproduced in Fig. 3.23.

The appearance of the discontinuity surface is compared visually with the profiles shown and the *JRC* value corresponding to the profile which most closely matches of the discontinuity surface is chosen. In the case of small scale laboratory specimens, the scale of the surface roughness will be approximately the same as that of the profiles illustrated. However, in the field the length of the surface of interest may be several meters or even tens of meters and the *JRC* value must be estimated for the full scale surface.

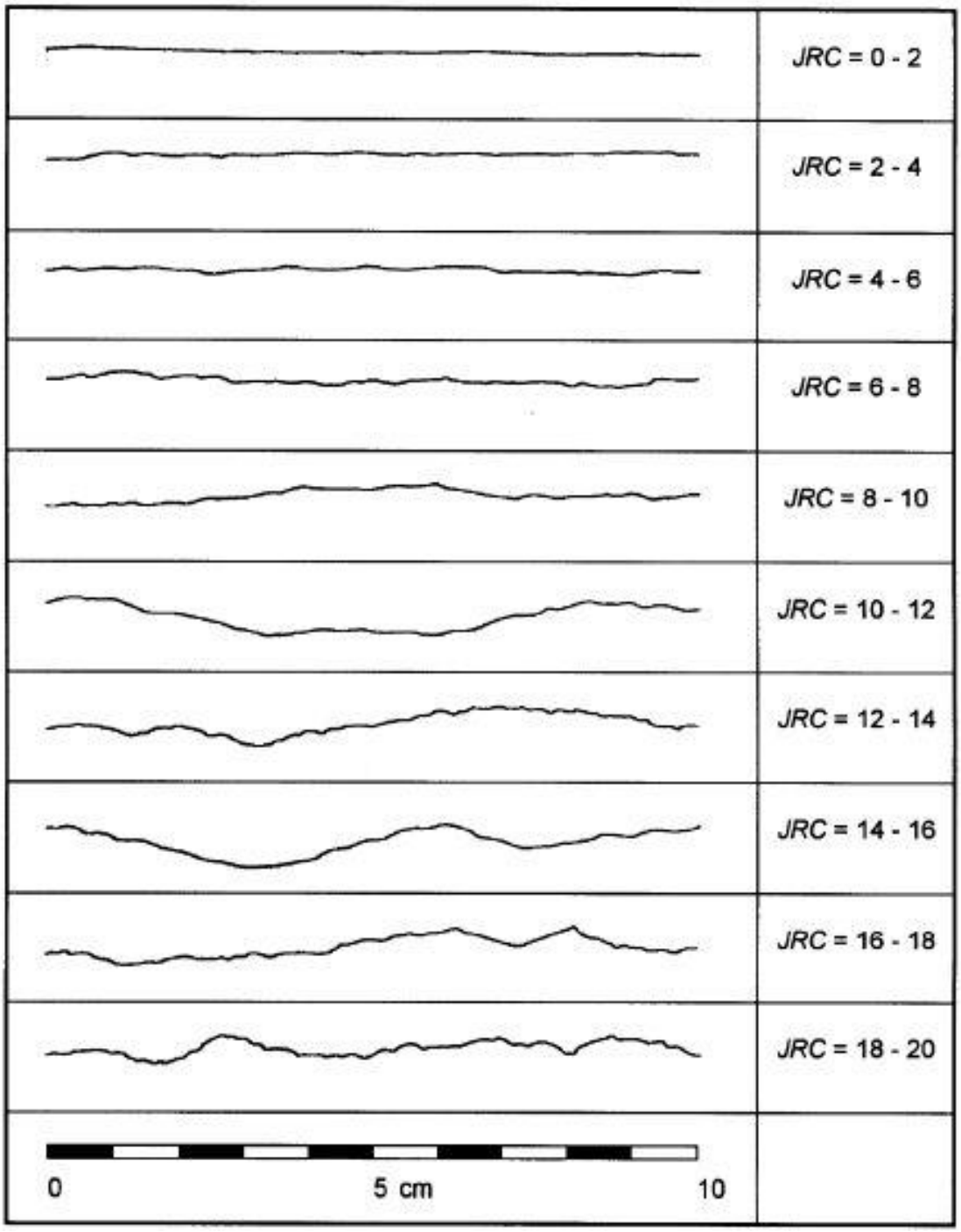

Figure 3.23: Roughness profiles and corresponding *JRC* values (After Barton and Choubey 1977)

Influence of water on shear strength of discontinuities

The most important influence of water in a discontinuity is the diminished shear strength resulting from the reduction of the effective normal shear stress acting on the surface. The effective normal stress is the difference between the weight of the overlying rock and the uplift pressure produced by water pressure. The effect of water pressure *u* on the shear strength can be incorporated into the shear strength equation as follows:

$$\tau = c + (\sigma - u)tan\varphi - peak\ strength \tag{3.6a}$$

or

$$\tau = c + (\sigma - u)tan\varphi_r - residual\ strength \tag{3.6b}$$

These equations assume that the cohesion and friction angle are not change by the presence of water on the surface. In most hard rock and gravels, the strength properties are not significantly altered by water. However, many clays, shales and mudstones, and similar materials will exhibit significant reduction in strength with changes in moisture content.

3.5 ROCK SLOPE STABILITY ANALYSIS

3.5.1 Introduction

Rock slope stability analyses are routinely performed and directed towards assessing the safe and functional design of excavated slopes and/or the equilibrium conditions of natural slopes. The analysis technique chosen depends on both site conditions and the potential mode failure, with careful consideration being given to the varying strengths, weaknesses and limitations inherent in each methodology.

In our days, a vast range of slope stability analysis tools exist for both rock and mixed rock-soil slopes; this range from simple infinite slope and planar failure limit equilibrium techniques to elasto-plastic analysis using the finite element codes. A difficulty with all the equilibrium methods is that they are based on the assumption that failing mass can be divided into slices. This is in turn necessitates further assumptions relating to side force directions between slices, with consequent implications for equilibrium. The assumption made about the side forces is one of the main characteristics that distinguishes one limit equilibrium method from another, and yet is itself an entirely artificial distinction. On the other hand, a finite element approach (FE) to slope stability analysis does not need assumptions about the shape or location of the failure surface. Failure occurs 'naturally' through the zones within the rock mass in which the rock shear strength is unable to sustain the applied shear stresses. Furthermore, while there is no concept of slices in the FE approach, there is no need for assumptions about slice surfaces. The FE method preserves global equilibrium until failure is reached.

3.5.2 Limit equilibrium methods

Planar analysis

The planar failure consists of a slip of a rock mass according to a plane failure surface. The analysis consists of a two-dimensional wedge failure, as shown in Fig. 3.24. The factor of safety is calculated considering equilibrium equations of vertical and horizontal forces. The factor of safety is given by the following equation:

$$FS = \frac{C'(H-Z)COS\psi_p + (Wcos\psi_p - U - Vsin\psi_p)tan\varphi'}{Vcos\psi_p + Wsin\psi_p} \quad (3.7)$$

where, *c'* is the effective cohesion

φ' is the effective friction angle

ψ_p is the dip of slide plane

W is the weight of block

U is the uplift force due to water pressure along slide plane

V is the force due to water pressure in tension crack

H is the slope height

z is the tension crack depth

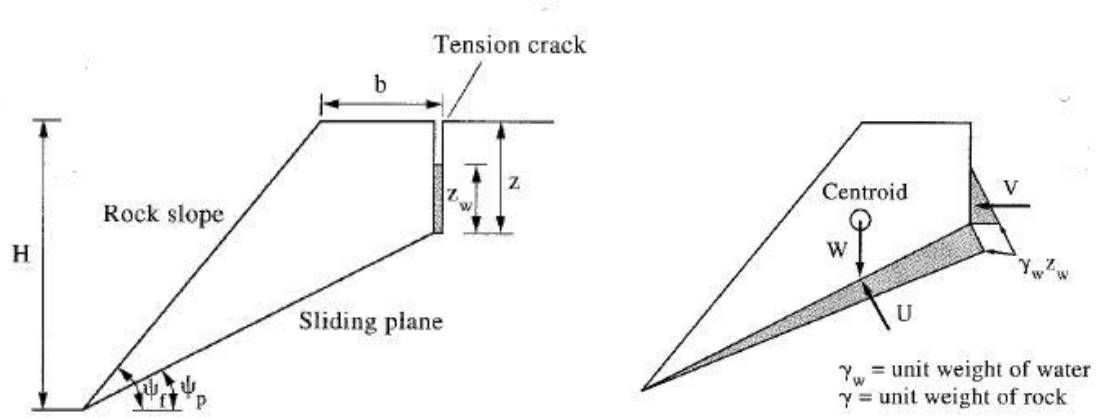

Figure 3.24: Limit equilibrium solution for planar failure (after Hudson & Harrison 1997)

Wedge analysis

Failure of a slope in the form of wedge can occur when the rock masses contain discontinuities striking obliquely to the slope face where, sliding of a wedge of rock take place along the line of intersection of two such planes (Fig. 3.25). The factor of safety is:

$$FS = \frac{(R_A + R_B)tan\varphi}{Wsin\psi_i} \tag{3.8}$$

and

$$R_A + R_B = \frac{Wcos\psi_i sin\beta}{\sin(0.5\delta)} \tag{3.9}$$

where, φ is the friction angle

ψ_i is the dip of the line of intersection

W is the weight of block

β,δ is the wedge geometry factors

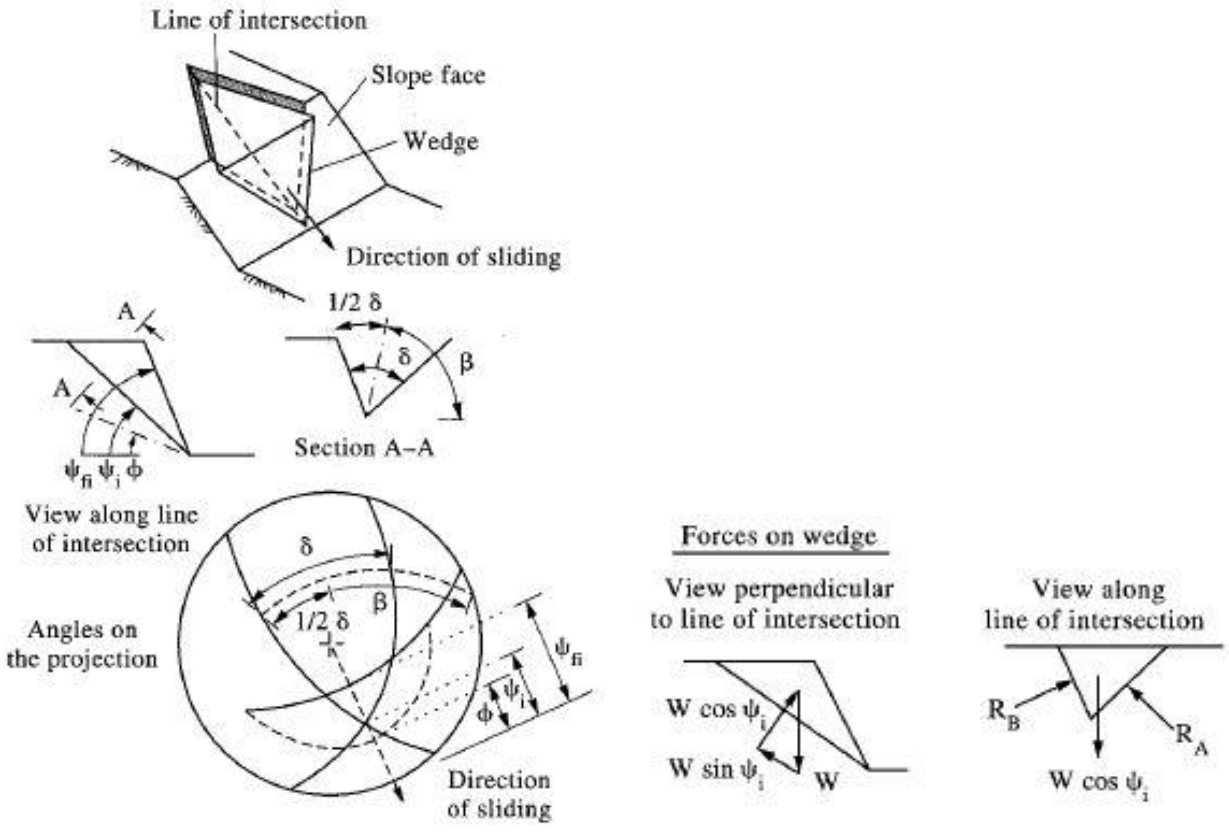

Figure 3.25: Limit equilibrium solution for wedge failure under dry conditions and with frictional strength only (after Hudson & Harrison 1997)

Toppling analysis

Direct toppling occurs when the center of gravity of a discrete block lies outside the outline of the base of the block, with the result that a critical overturning moment develops. Other considerations include the possibility that the block will slide, or that both sliding and toppling will occur simultaneously (Fig 3.26).

Limit equilibrium analysis of toppling failure must consider both the possibility of toppling and/or sliding. Fig. 3.27 shows the acting forces and limit equilibrium conditions for toppling and sliding of a single 2-D block on a stepped base.

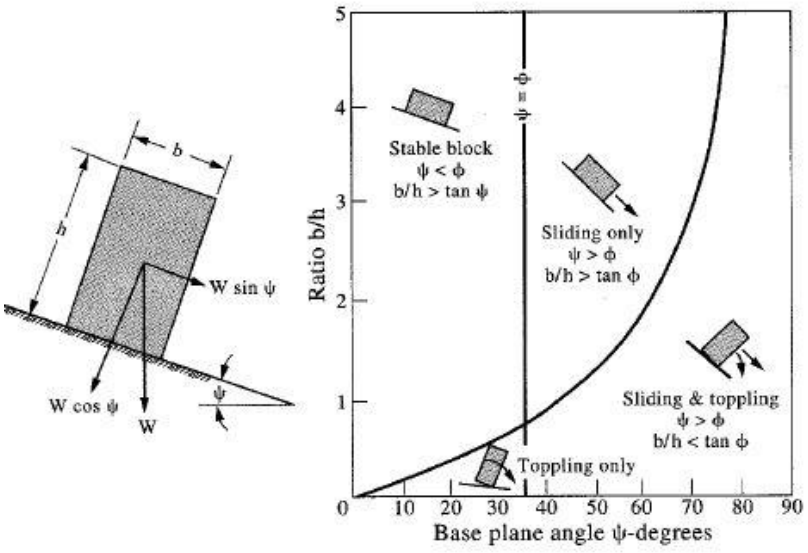

Figure 3.26: Sliding and toppling instability of a block on an inclined plane (after Hoek & Bray 1991)

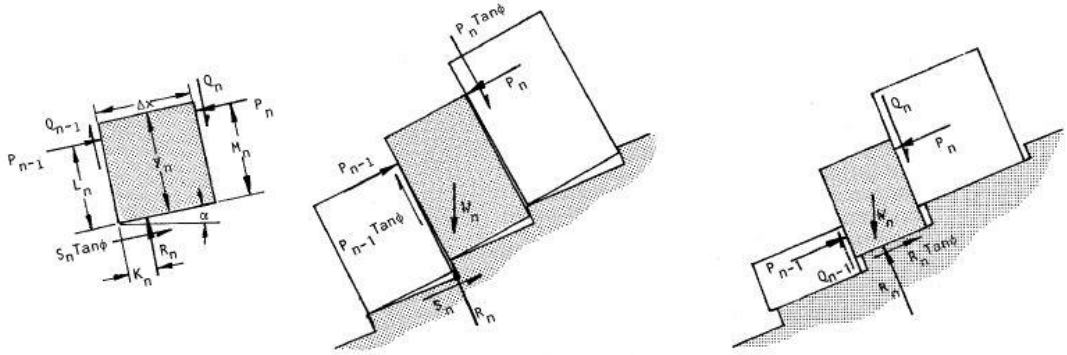

Figure 3.27: Limit equilibrium conditions for toppling and sliding, with input variables illustrated in the corresponding diagrams (after Hoek & Bray 1991)

$$P_{n-1} = \frac{P_n(M_n - \Delta x \tan\varphi) + (\frac{W_n}{2})(y_n \sin\alpha - \Delta x \cos a}{L_n} \quad (3.10)$$

$$P_{n-1} = P_n - \frac{W_n(\tan\varphi \cos a - \sin a)}{1 - \tan^2\varphi} \quad (3.11)$$

Rotational analysis

For very weak rock, where the intact material strength is of the same magnitude as the induced stresses, the structural geology may not control stability resulting in rotational failures. In analyzing the potential for failure, consideration must be given to the location of the critical slip surface and the determination of the factor of safety along it. Iterative procedures are used, each involving the selection of a potentially unstable slide mass, the subdivision of the mass into slices (i.e, *Method of Slices*), and considerations of those force and moment equilibrium acting on each slice (Fig. 3.28). For a circular failure the safety of factor is given by equation:

$$FS = \frac{\sum SF(Sseca)}{\sum(Wsina)+Hz/R} \tag{3.12}$$

where, S is the effective shear strength (i.e. $S/\Delta b = c' + \sigma_n tan\varphi'$)

α is the dip of base of slice

W is the weight of slice

H is the hydrostatic thrust from tension crack

z is the depth of tension crack (relative to 0)

R is the length of moment arm

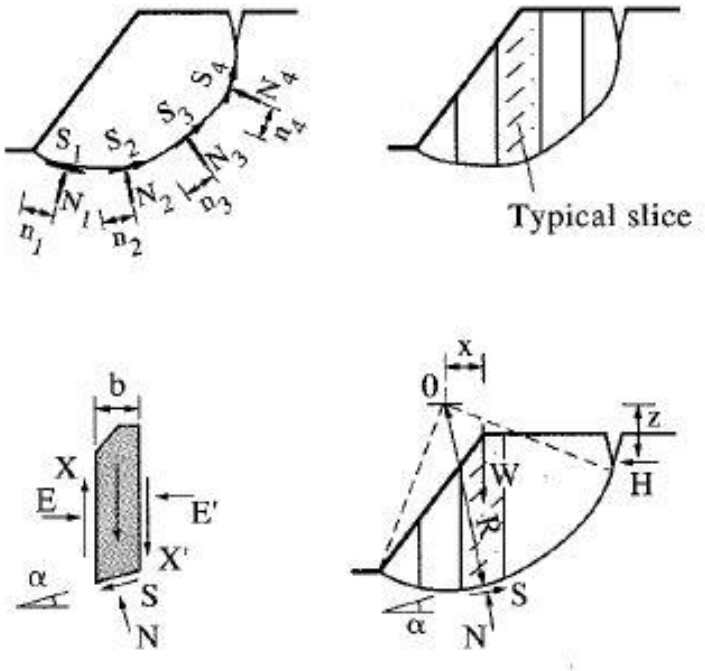

Figure 3.28: Limit equilibrium solution for circular failure (after Hudson & Harrison 1997)

3.5.3 Finite element method (FEM)

This section reviews the basics of the finite element method. The first step of any element simulation is to *discretize* the actual geometry of the structure using a collection of *finite elements*. Each finite element represents a discrete portion of the physical structure. The finite elements are joined by shared *nodes*. The collection of nodes and finite elements is called the *mesh*. The number of elements per unit of length, area, or in a mesh is referred to as the *mesh density*. In a stress analysis the displacements of the nodes are fundamental variables that Abaqus calculates. Once the nodal displacements are known, the stresses and strains in each finite element can be determined easily.

At this point to mention, that a displacement function is associated with each finite element. Every interconnected element is linked, directly or indirectly, to every other element through common interfaces, including nodes and/or boundary lines and/or surfaces. By using known stress/strain properties for the material making up the structure, one can be determinate the behavior of a given node in terms of the properties of every other element in the structure. The total set of equations describing the behavior of each node results in a series of algebraic equations best expressed in matrix notation.

For example, a three-dimensional body occupying a volume *V* and having a surface *S* is shown in Fig. 3.29. Points in the body are located by x, y, z coordinates. The boundary is constrained on some region, where displacement is specified.

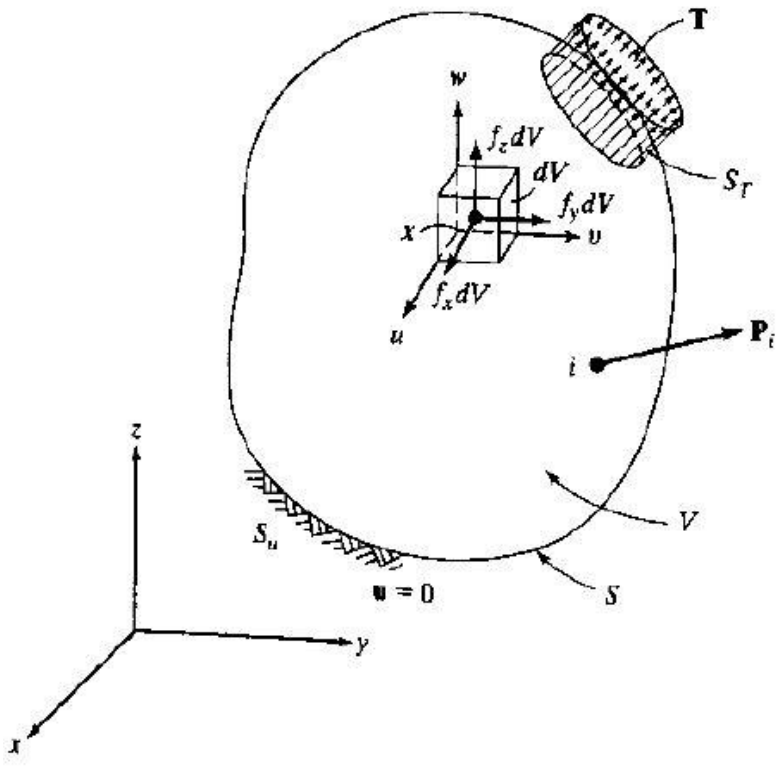

Figure 3.29: Three-dimensional body

One part of the boundary, distributed force per unit area T, also called traction, is applied. Under the force, the body deforms. The deformation of a point $x(=[x,y,z]^T)$ is given by the three components of its displacement:

$$u = [u,v,w]^T \tag{3.13}$$

The distributed force per unit volume, for example, the weight per unit volume is the vector f given by:

$$f = [f_x, f_y, f_z]^T \tag{3.14}$$

The body force acting on the elemental volume *dV* is shown in Fig. 3.25. The surface traction T may be given by its component values at points on the surface:

$$T = [T_x, T_y, T_z]^T \tag{3.15}$$

Examples of traction are distributed contact force and action of pressure. A load P acting at a point *i* is represented by its three components:

$$P_i = [P_x, P_y, P_z]i^T \tag{3.16}$$

The stresses acting on the elemental volume *dV* are shown in Fig. 3.30. When the volume *dV* shrinks to a point, the stress tensor is represented by placing its components in a (3 X 3) symmetric matrix. However, the stress is represented by the six independent components as in:

$$\sigma = [\sigma_x, \sigma_y, \sigma_z, \tau_{yz}, \tau_{xz}, \tau_{xy}]^T \tag{3.17}$$

where $\sigma_x, \sigma_y, \sigma_z$ are normal stresses and $\tau_{yz}, \tau_{xz}, \tau_{xy}$, are shear stresses.

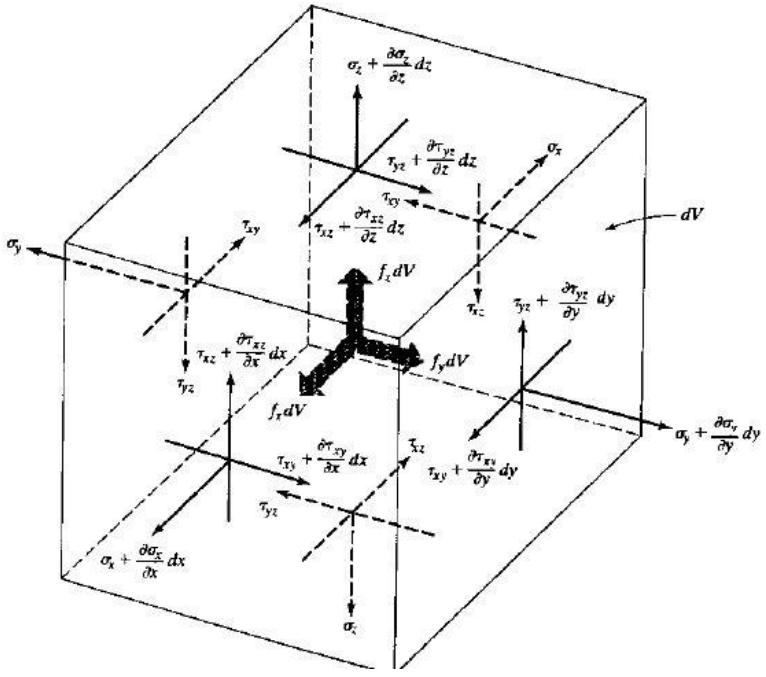

Figure 3.30: Equilibrium of elemental volume

Writing, $\sum F_x = 0, \sum F_y = 0$ and $\sum F_z = 0$ and recognizing $dV = dxdydz$ the equilibrium conditions of the elemental volume in Fig. 3.29 are defined by the following equations:

$$\frac{\partial \sigma_x}{\partial x} + \frac{\partial \tau_{xy}}{\partial y} + \frac{\partial \tau_{xz}}{\partial z} + f_x = 0$$

$$\frac{\partial \tau_{xy}}{\partial x} + \frac{\partial \sigma_y}{\partial y} + \frac{\partial \tau_{yz}}{\partial z} + f_y = 0 \tag{3.18}$$

$$\frac{\partial \tau_{xz}}{\partial x} + \frac{\partial \tau_{yz}}{\partial y} + \frac{\partial \sigma_z}{\partial z} + f_z = 0$$

Furthermore, referring to Fig. 3.29 resulting that there are displacement boundary conditions and surface-loading conditions. If *u* is specified on part of the boundary denoted by S_u then *u* is given by:

$$u = 0 \text{ on } S_u \tag{3.19}$$

Boundary conditions such as u=a where a is given displacement, can be considered. Fig. 3.31 shows an elemental tetrahedron *ABCD*, where *DA, DB* and *DC* are parallel to the x-, y-, and z-axes, respectively, and area *ABC*, denoted by dA, lies on the surface. If $n = [n_x, n_y, n_z]^T$ is the unit normal to dA, then area *BDC* = $n_x dA$, and *ADC* = $n_y dA$, and area *ADB* = $n_z dA$. Consideration of equilibrium along the three axes directions gives:

$$\sigma_x n_x + \tau_{xy} n_y + \tau_{xz} n_z = T_x$$

$$\tau_{xy} n_x + \sigma_y n_y + \tau_{yz} n_z = T_y \tag{3.20}$$

$$\tau_{xz} n_x + \tau_{yz} n_y + \sigma_z n_z = T_z$$

These conditions must be satisfied on the boundary, S_T, where the tractions are applied. In this description, the point loads must be treated as loads distributed over small, but finite areas.

Regarding the strain- displacement relations, strains are represented in a vector form that corresponds to the stresses in Eq. 3.17:

$$\varepsilon = [\varepsilon_x, \varepsilon_y, \varepsilon_z, \gamma_{yz}, \gamma_{xz}, \gamma_{xy}]^T \tag{3.21}$$

where $\varepsilon_x, \varepsilon_y, \varepsilon_z$ are normal strains and $\gamma_{yz}, \gamma_{xz}, \gamma_{xy}$ are the engineering shear strains. Fig. 3.32 gives the deformation of $dx - dy$ face for small deformations, which are considered here. Also considering other faces, it can be written:

$$\varepsilon = \left[\frac{\partial u}{\partial x}, \frac{\partial v}{\partial y}, \frac{\partial w}{\partial z}, \frac{\partial v}{\partial z} + \frac{\partial w}{\partial y}, \frac{\partial u}{\partial z} + \frac{\partial w}{\partial x}, \frac{\partial u}{\partial y} + \frac{\partial v}{\partial x}\right]^T \tag{3.22}$$

These strain relations hold for small deformations.

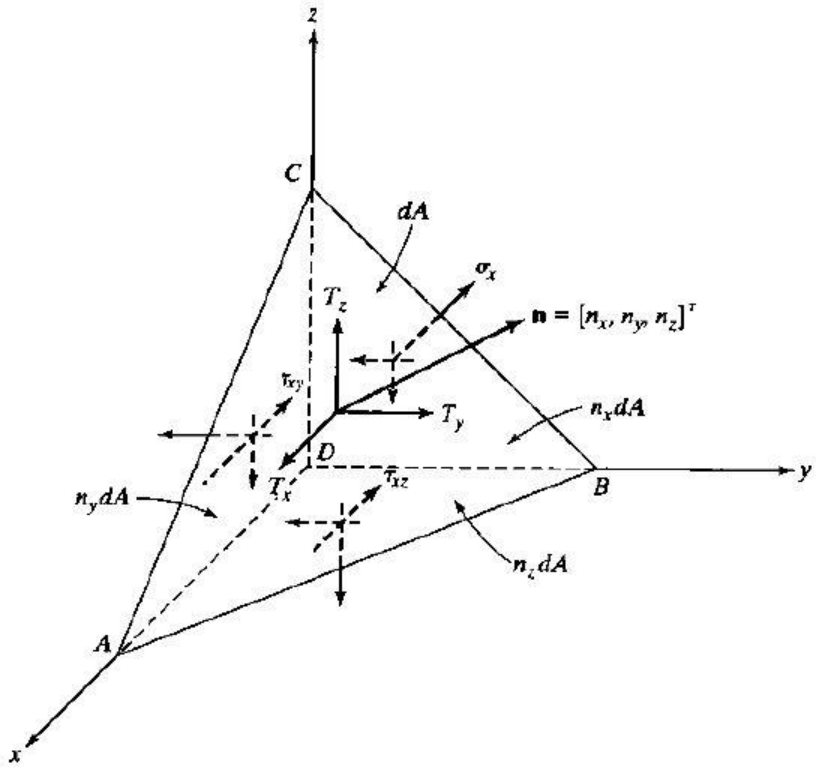

Figure 3.31: An elemental volume at surface

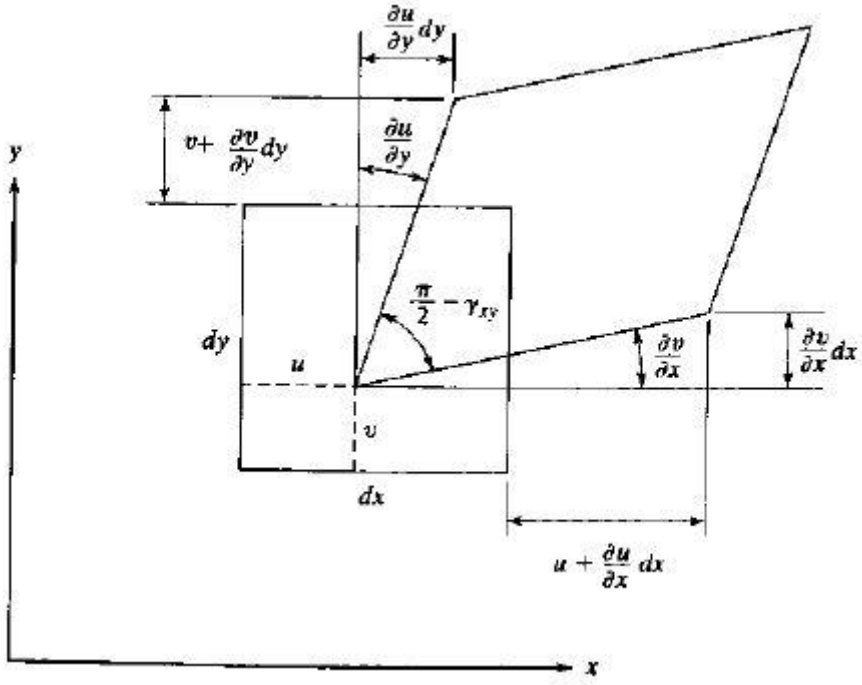

Figure 3.32: Deformed elemental surface

For linear elastic materials, the stress-strain relations come from the generalized Hooke's law. For isotropic materials, the two materials properties are Young's modulus (or modulus of elasticity) *E* and Poisson's ration *v*. Considering an elemental cube inside the body, Hooke's law gives:

$$\varepsilon_x = \frac{\sigma_x}{E} - \nu\frac{\sigma_y}{E} - \nu\frac{\sigma_z}{E}$$

$$\varepsilon_y = -\nu\frac{\sigma_x}{E} + \frac{\sigma_y}{E} - \nu\frac{\sigma_z}{E} \tag{3.23}$$

$$\varepsilon_z = -\nu\frac{\sigma_x}{E} - \nu\frac{\sigma_y}{E} + \frac{\sigma_z}{E}$$

$$\gamma_{yz} = \frac{\tau_{yz}}{G}$$

$$\gamma_{xz} = \frac{\tau_{xz}}{G}$$

$$\gamma_{xy} = \frac{\tau_{xy}}{G}$$

The shear modulus (or modulus of rigidity), *G*, is given by:

$$G = \frac{E}{2(1+\nu)} \tag{3.24}$$

From Hooke's relationships note that:

$$\varepsilon_x + \varepsilon_y + \varepsilon_z = \frac{(1-2\nu)}{E}(\sigma_x + \sigma_y + \sigma_z) \tag{3.25}$$

or

$$\sigma = D\varepsilon \tag{3.26}$$

where *D* is the symmetric (6 X 6) material matrix given by:

$$D = \frac{E}{(1+\nu)(1-2\nu)}\begin{bmatrix} 1-\nu & \nu & \nu & 0 & 0 & 0 \\ \nu & 1-\nu & \nu & 0 & 0 & 0 \\ \nu & \nu & 1-\nu & 0 & 0 & 0 \\ 0 & 0 & 0 & 0.5-\nu & 0 & 0 \\ 0 & 0 & 0 & 0 & 0.5-\nu & 0 \\ 0 & 0 & 0 & 0 & 0 & 0.5-\nu \end{bmatrix} \tag{3.27}$$

Plane stress

In two dimensions problem such as the rock mass slope examined in this study (see chapter 4), the above equations revised to:

$$\varepsilon_x = \frac{\sigma_x}{E} - \nu\frac{\sigma_y}{E}$$

$$\varepsilon_y = -\nu\frac{\sigma_x}{E} + \frac{\sigma_y}{E} \tag{3.28}$$

$$\gamma_{xy} = \frac{2(1+\nu)}{E}\tau_{xy}$$

$$\varepsilon_z = -\nu\frac{\sigma_x}{E} - \nu\frac{\sigma_y}{E}$$

$$\begin{Bmatrix}\sigma_x\\ \sigma_y\\ \tau_{xy}\end{Bmatrix} = \frac{E}{(1-\nu^2)}\begin{bmatrix}1 & \nu & 0\\ \nu & 1 & 0\\ 0 & 0 & \frac{1-\nu}{2}\end{bmatrix}\begin{Bmatrix}\varepsilon_x\\ \varepsilon_y\\ \gamma_{xy}\end{Bmatrix} \tag{3.29}$$

which is used as $\sigma = D\varepsilon$

In two dimensions, the problems are modeled as plane stress and plain strain.

Plane stress is denoted by the Eq. 3.28 & 3.29 where a thin planar body subjected to in-plane loading on its edge surface and is said to be in plane stress.

Plane strain

If a long body of uniform cross section is subjected to transverse loading along its length, a small thickness in the loaded area can be treated as subjected to plain strain. The stress-strain relations can be obtained directly from Eq. 3.26 & 3.27:

$$\begin{Bmatrix}\sigma_x\\ \sigma_y\\ \tau_{xy}\end{Bmatrix} = \frac{E}{(1+\nu)(1-\nu)}\begin{bmatrix}1-\nu & \nu & 0\\ \nu & 1-\nu & 0\\ 0 & 0 & \frac{1}{2}-\nu\end{bmatrix}\begin{Bmatrix}\varepsilon_x\\ \varepsilon_y\\ \gamma_{xy}\end{Bmatrix} \tag{3.30}$$

where *D* is a (3 X 3) matrix, which relates three stresses and three strains.

Anisotropic bodies, with uniform orientation, can be considered by using the appropriate D matrix for the material.

3.5.3.1 Jointed Material Model

Overview

As is discussed in Chapter 4, a jointed material model (Fig. 3.33) is used to simulate the jointed rock mass slope. The jointed material model is intended to provide a simple continuum model for a material containing a high density of parallel joint surfaces where each system of parallel joints is associated with particular orientation, such as a sedimentary rock. The spacing of the joints of a particular orientation is sufficiently close compare to characteristic dimensions in the domain of the model such that the joints can be smeared into a continuum of slip systems. It provides for opening or frictional sliding of the joints in each of these systems (a "system" in this context is a joint orientation in a particular direction at a material calculation point) and assumes that the elastic behavior of the material is isotropic and linear when all joints at a point are closed.

Joint opening/closing

The jointed material model is intended primarily for applications where the stresses are mainly compressive. The model provides a joint opening capability when the stress normal to the joint tries to become tensile. In this case the stiffness of the material normal to the joint plane becomes zero instantaneously. Abaqus/Standard uses a stress-based joint opening criterion, whereas joint closing is monitored based on strain. Joint system α opens when the estimated pressure stress across the joint (normal to the joint surface) is no longer positive:

$$p_a \leq 0 \tag{3.31}$$

In this case the material is assumed to have no elastic stiffness with respect to direct strain across the joint system. Open joints thus create anisotropic elastic response at a point. The joint system remains open as long as

$$\varepsilon_{\alpha n(ps)}^{el} \leq \varepsilon_{\alpha n}^{el} \tag{3.32}$$

Where $\varepsilon_{\alpha n}^{el}$ is the component of direct elastic strain across the joint and $\varepsilon_{\alpha n(ps)}^{el}$ is the component of direct elastic strain across the joint calculated in plane stress as

$$\varepsilon_{\alpha n(ps)}^{el} = -\frac{v}{E}(\sigma_{a1} + \sigma_{a2}) \tag{3.33}$$

Where E is the Young's modulus of the material, v is the Poisson's ratio, and σ_{a1}, σ_{a2} are the direct stresses in the plane of the joint.

The shear response of open joints is governed by the shear retention parameter, f_{sr}, which represents the fraction of the elastic shear modulus retained when the joints are open (f_{sr} = 0 means no shear

stiffness associated with open joints, while f_{sr} = 1 corresponds to elastic shear stiffness in open joints; any value between these two extremes can be used). When a joint opens, the shear behavior may be brittle, depending on the shear retention factor used for open joints. In addition, the stiffness of the material normal to the joint plane suddenly goes to zero. For these reasons, in situations where the confining stresses are low or significant regions experience tensile behavior, the joint system may experience a sequence of alternate opening and closing states from iteration to iteration. Typically, such behavior manifests itself as oscillating global residual forces. The convergence rate associated with such discontinuous behavior may be very slow and, thus, prohibit obtaining a solution. This type of failure is more probable in cases where more than one joint system is modeled.

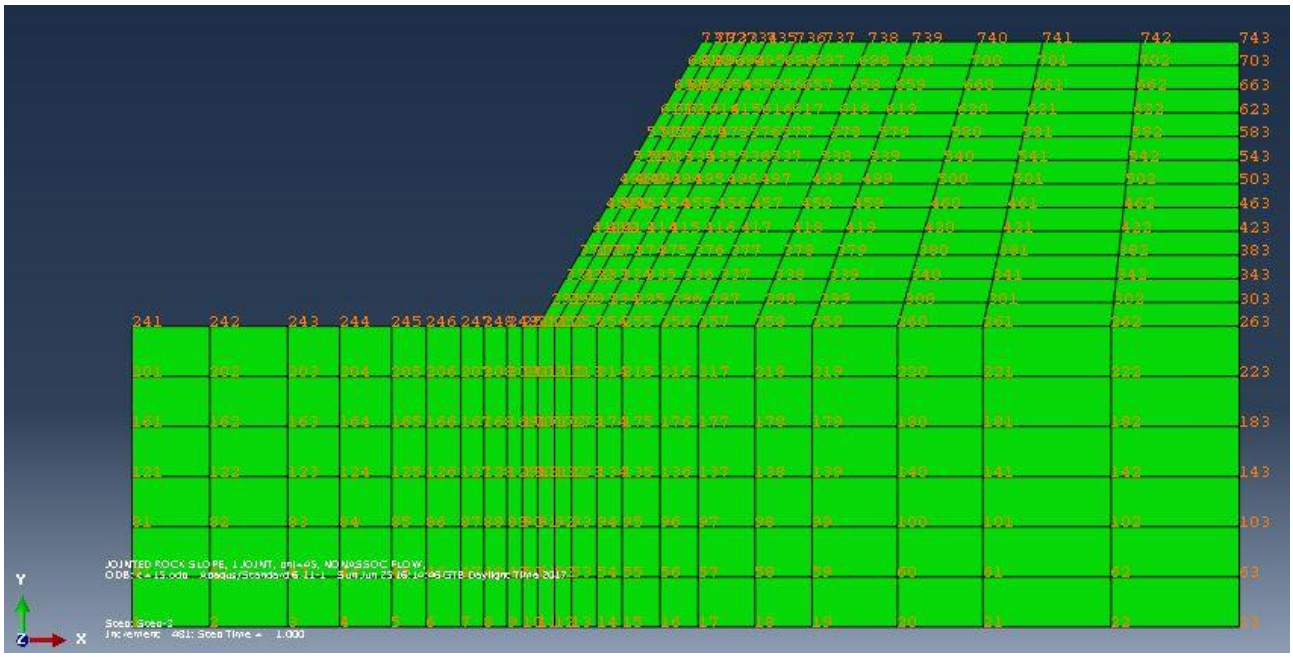

Figure 3.33: Illustration of jointed model with two joint systems

3.5.4 Seismic analysis of rock slopes

In seismically active areas of the world, the design of rock slopes should take into account the effects on stability of earthquake-induced ground motions. Studies of the number and distribution of landslides and rock falls near earthquakes has shown that concentrations of landslides can be as high as 50 events per square kilometer. These data have been used to assess the geological and topographical conditions for which the landslide and rock fall hazard is high (Keefer, 1992). It has also been found that the following five slope parameters have the greatest influence stability during earthquakes:

i. *Slope angle:* Rock falls and slides rarely occur on slopes with angles less than about 25°.
ii. *Weathering:* Highly, weathered rock comprising core stones in a fine soil matrix, and residual soil are more likely to fail than the fresh rock.
iii. *Induration:* Poorly indurated rock in which the particles are weakly bonded is more likely to fail than stronger, well-indurated rock.
iv. *Discontinuity characteristics:* Rock containing closely spaced, open discontinuities are more susceptible to failure than massive rock in which the discontinuities are closed and healed.
v. *Water:* Slopes in which the water table is high, or where there has been recent rainfall, are susceptible to failure.

The relationship between these five conditions and the slope failure hazard is illustrated in the decision tree in Fig. 3.34.

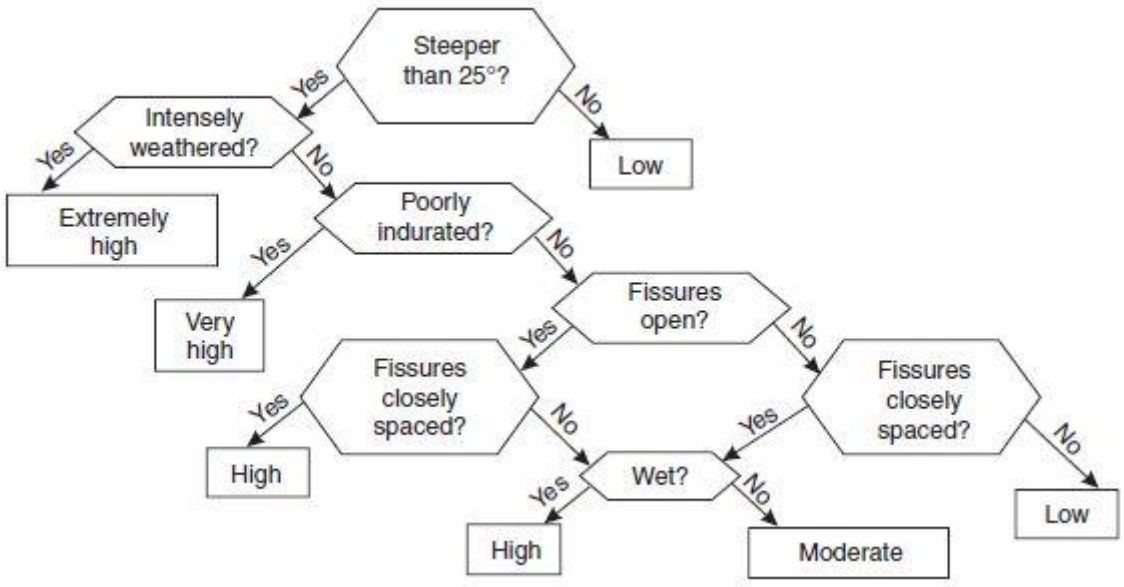

Figure 3.34: Decision tree for susceptibility of rock slopes to earthquake-induced failure (Keefer, 1992)

Furthermore, there is a hazard for slopes with local relief greater than about 2000 m, probably because seismic shaking is amplified by the topography (Harp and Jibson, 2002) and possible freeze-thaw action at high altitude that loosens the surficial rock. The decision tree shown in Fig. 3.34 can be used, for example, as a screening tool in assessing rock fall and slide hazards along transportation and pipeline corridors.

The design of slopes that may be subjected to seismic ground motion requires quantitative information on the magnitude of the motion (Abrahamson, 2000). This information may be either the peak ground acceleration (PGA) or the acceleration-time history of the motions, depending on the method of stability analysis that is to be used. The process by which the design motion parameters are established is term "seismic hazard" analysis which involves the following three steps (NHI, 1998; Class, 2000):

i. Identification of seismic sources capable of producing strong ground motions at the site.
ii. Evaluation of seismic potential for each capable source.
iii. Evaluation of the intensity of design ground motions at the site

Implementation of these three steps involves the following activities.

Seismic sources

Earthquakes are the result of fault movement, so identification of seismic sources incudes establishing the types of faults and their geographic location, depth, size and orientation. This information is usually available from publications such as geological maps and reports prepared by government geological survey groups and universities, and any previous projects that have been undertaken in this area. Also, the identification of faults can be made from the study of aerial photographs, geological mapping, geophysical surveys and trenching. On aerial photographs, such features as fault scarplets, rifts, fault slide ridges, shutter ridges and fault saddles, and off-sets in such features as fence lines and road curbs (Cluff *et al*., 1972) may identify active faults. In addition, records of seismic monitoring stations provide information on the location and magnitude of recent earthquakes that can be correlated to fault activity.

Seismic potential

Movements of faults within the Holocene Epoch (approximately the last 11,000 years) is generally regarded as the criterion for establishing that the fault is active (USEPA, 1993). Although, the occurrence interval of some earthquakes may be greater than 11,000 years, and not all faults rupture to the surface, lack of evidence that movement has occurred in Holocene is generally sufficient evidence to dismiss the potential for ground surface rupture. In regions where there is no surface

expression of fault rupture, seismic source characterization depends primarily on micro-seismic studies and the historical record of felt earthquakes.

Ground motion intensity

Once the seismic sources capable of generating strong ground motions at the site have been identified and characterized, the intensity of the ground motions can be evaluated either from public codes and standards, or from seismic hazard analysis as discussed above. The building codes of countries with seismic areas publish maps in which the country is divided into zones showing, for example, the effective peak accelerations levels (as a fraction of gravity acceleration) with 10% probability of being exceeded in a 50-year period (Frankel *et al*., 1996). These published accelerations can be used in geotechnical design and have the value of promoting standard designs within each zone.

3.5.5 Pseudo-static stability analysis

Pseudo-static method, involves simulating the ground motions as a static horizontal force acting in a direction out of the face. The magnitude of this force is the product of a seismic coefficient k_H (dimensionless) and the weight of the sliding block *W*. The value of may be taken as equal to the design PGA, which is expressed as a fraction of the gravity acceleration (i.e. k_H = 0.1 if the PGA is 10% of gravity). However, this is a conservative assumption since the actual transient ground motion with a duration of a few seconds is being replaced by a constant force acting over the entire design life of the slope.

In the design of soil slopes and earth dams, it is common that k_H is fraction of the PGA, provided that there is no loss of shear strength during cyclic loading (Seed, 1979; Pyke, 1999). Study of slopes using Newmark analysis (not mentioned) with a yield acceleration k_y equal to 50% of the PGA (i.e. $k_y = 0.5\ a_{max}/g$) showed that permanent seismic displacement would be less than 1 m (Hynes and Franklin, 1984). Additionally, for rock slopes there are two conditions for which it may be advisable to use k_H values somewhat greater than 0.5 times PGA. First, where the slope contains a distinct sliding surface for which there is likely to be a significant decrease in shear strength with limited displacements; sliding planes on which the strength would be sensitive to movement include smooth, planar joints or bedding planes with no infilling. Second, where the slope is a topographic high point and some amplification of the ground motions may be expected.

Under circumstances where it is considered that the vertical component of the ground motion will be in phase with, and have the same frequency, as the horizontal component, it may be appropriate to use both horizontal and vertical seismic coefficients in stability analysis. If the vertical coefficient is

k_V and the ratio of the vertical to the horizontal components is r_k (i.e. $r_k = \frac{k_V}{k_H}$), then the resultant seismic coefficient k_T is:

$$k_T = k_H(1 + r^2{}_k)^{1/2} \tag{3.31}$$

Fig. 3.35 & 3.36 shows forces acting on active wedge according to the above.

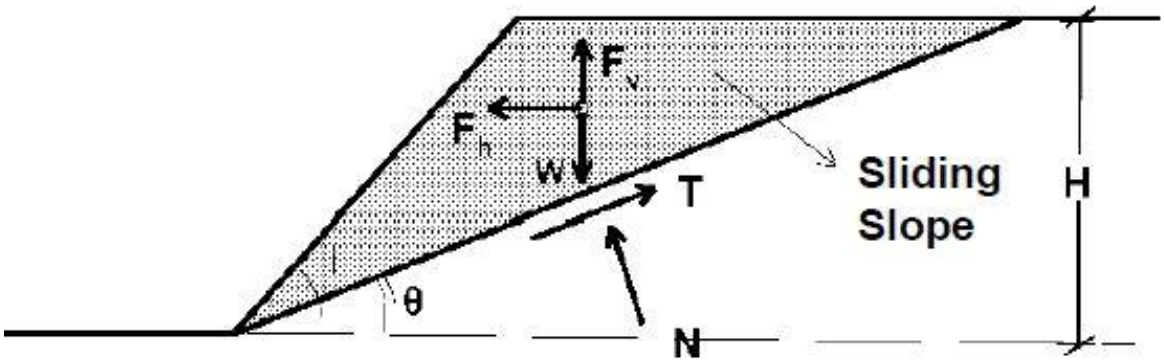

Figure 3.35: Forces acting on active wedge

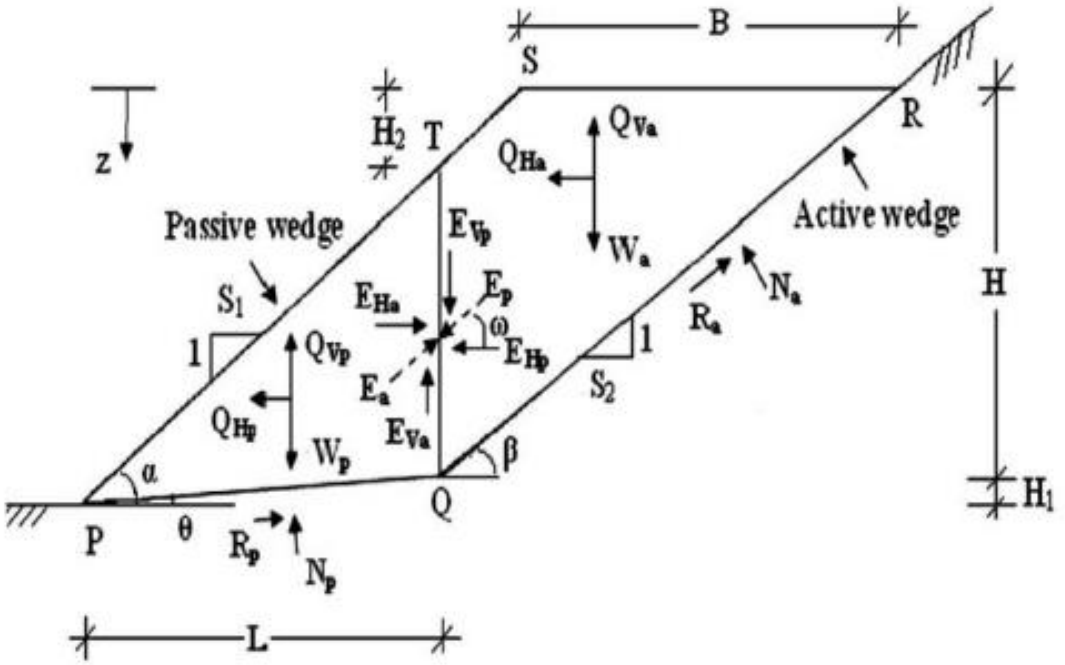

Figure 3.36: Forces acting on the active and passive wedges of the landfill (Santhosh, Babu, Chaithra &Ering, 2013)

CHAPTER 4: SLOPE STABILITY ANALYSIS USING 2-D FINITE ELEMENT METHOD

4.1 INTRODUCTION

Slope stability has been an important issue in geotechnical problems. Conducting stability analyses of rock slopes plays a vital role in many engineering projects such as an excavation and onshore pipeline construction. The most rock slopes that we meet in the practical engineering contain weak structural surfaces such as joints, faults and cracks. It makes big difference in physical and mechanical properties in all directions, and makes obvious distinctions in discontinuity, heterogeneous, anisotropic and inelastic.

Various methods have been proposed for determining rock slope stability. Numerous sophisticated slope stability software packages such as SLOPE/W, FLAC and ABAQUS, have made graphical methods and charts obsolete. ABAQUS software uses the finite element (FE) method which first introduced into geotechnical engineering by Clough and Woodward (1967). The FE is a great tool to solve geotechnical problems due its ability to model nonlinear stress-strain behavior of materials.

4.2 THE JOINTED ROCK MASS

The presence of joints in rock has been accounted for non-linear analysis by either considering isolated discrete joints, or distribution of planes of weakness throughout elements of finite size. This later proposal made by Zienkiewicz *et al.* did indeed include the possibility of multiple planes of weakness. However, with standard analysis procedures it was found difficult to implement such behavior.

The behavior of joints in general is non-linear and Figure 4.1 shows typical stress-strain curves when subjected to monotonic loads either in the direction normal or tangential to the joint. Such curves by themselves are of little value in describing the behavior which we shall characterize by:

i. purely elastic within the yield envelope;
ii. incapable of withstanding any tensile stress in the direction normal to the joint;
iii. shear strength on the joint is dependent on a certain value of cohesion and frictional resistance dependent on the normal stress;
iv. The joints have full memory of their excursions in the tensile zone and are subsequently able to transmit compressive stresses in the normal direction only when total normal strain $(\varepsilon_q) < 0$.

In general both cohesion as well as the frictional coefficients may be strain dependent thus allowing for strain hardening/softening.

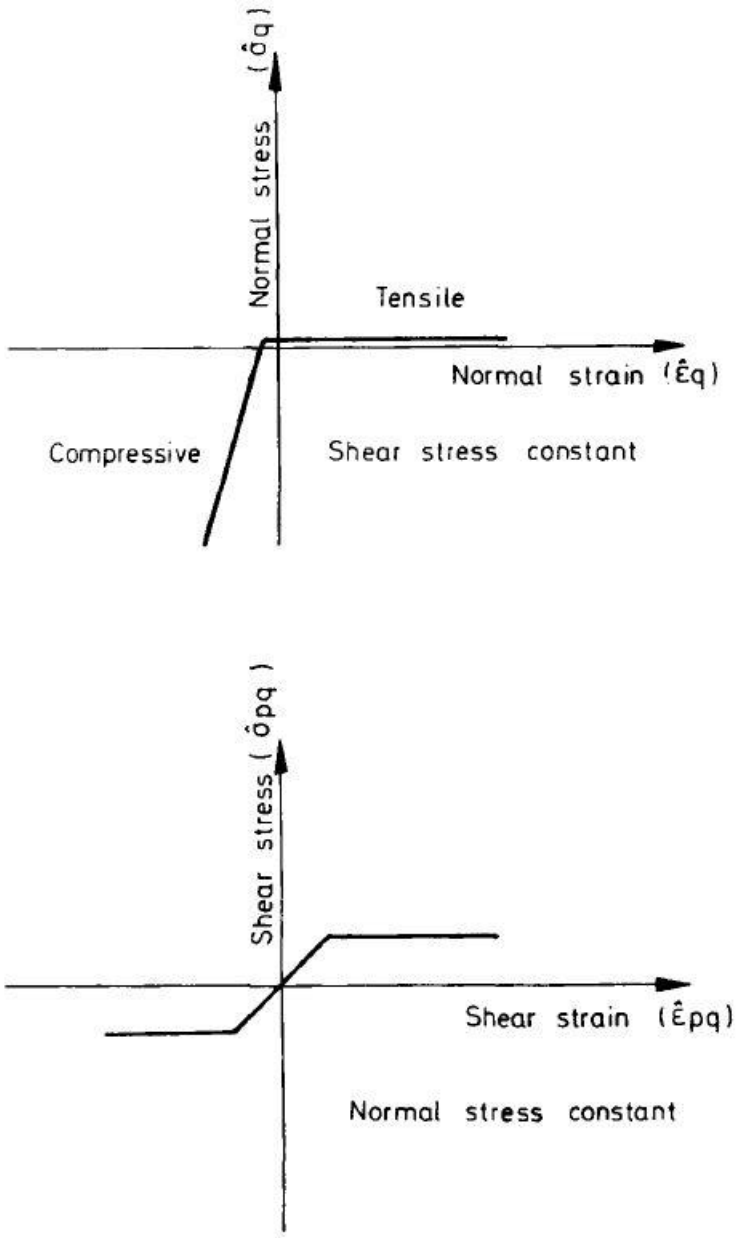

Figure 4.1: Typical idealized normal stress-normal strain and shear stress-shear strain relationships of joints (Zienkiewicz & Pande, 1977)

4.2.1 Complex failure surfaces

Experimental evidence has shown that shear strength envelopes of rock joints may be non-linear. A typical shear stress-shear displacement and shear stress-normal stress relationship is shown in Figure

4.2. It is generally accepted that after small shear displacement, cohesion intercept and coefficient of friction drop to their residual values.

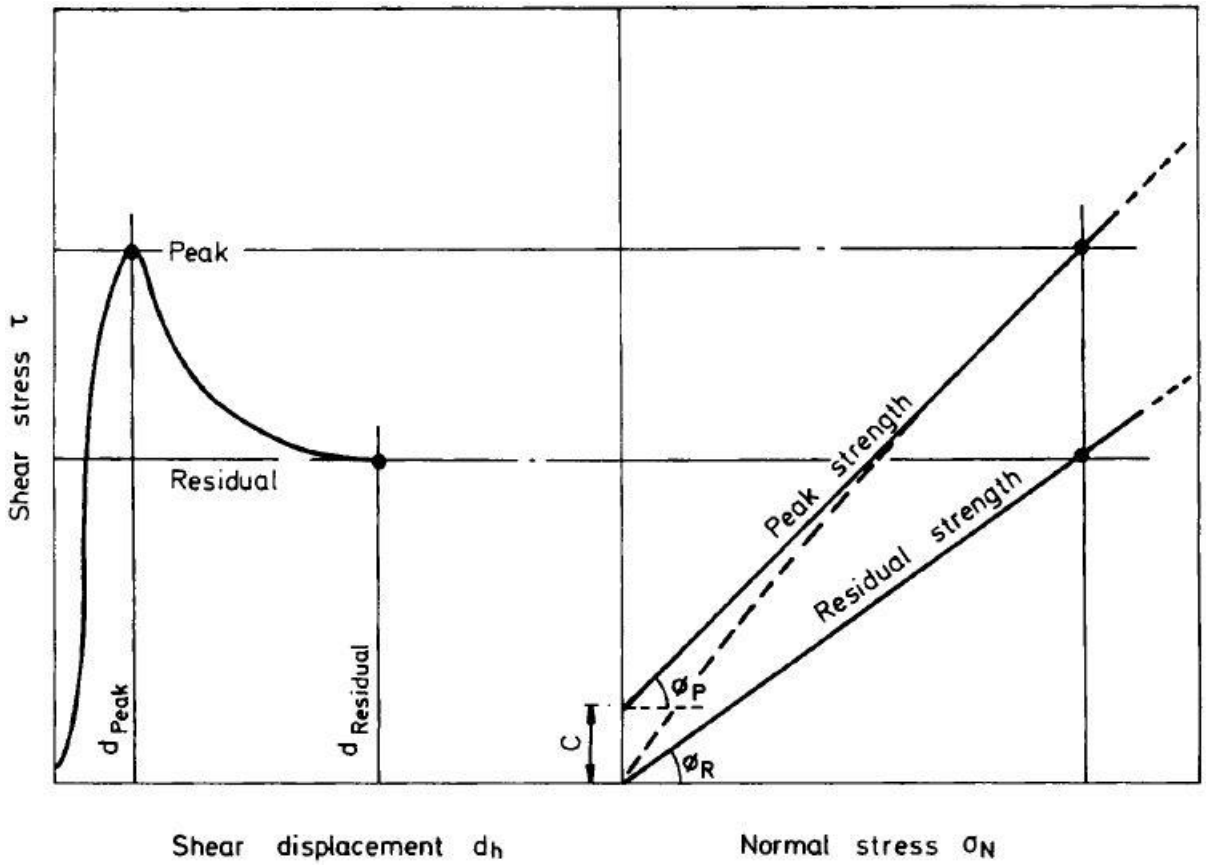

Figure 4.2: The simplified direct shear characteristics of an interlocking joint surface (Zienkiewicz & Pande, 1977)

Barton has done an extensive review of reported shear strength investigations combined with observations of the behavior of rough model tension joints and presented analytical expressions for shear strength of rock joints. Lundborg has suggested an analytical expression for dependence of coefficients of friction on normal stress. Any such relationships can be readily incorporated in the computer code.

4.3 MODELING THE JOINTED ROCK SLOPE

In this chapter a joint material model is presented, which is created to simulate the jointed rock mass and how the parameters of rock slopes influence their stability, by finite element analysis software ABAQUS. This model 70 m in height dipping 60^0 regards the rock slope mass as a material full of joints. The basic model used in this study consists of six parameters, as shown in Table 4.1. It also assumes two sets of jointed planes: one vertical set of joints and one set of inclined joints with inclination angle 52.5^0. The element used in the 2-D finite element model in this dissertation including

the 4-node fully integrated elements that subjected to bending. The boundary condition on the bottom and on the edges is hinged ($u_x = u_y = 0$), which is restricted on vertical and horizontal displacements. The plane strain model analyzed is shown in Figure 4.3.

Table 4.1: Six-parameter rock mass model

φ	Friction angle
c	Cohesion
ψ	Dilation angle
E	Young's modulus
ν	Poisson's ratio
γ	Unit wait

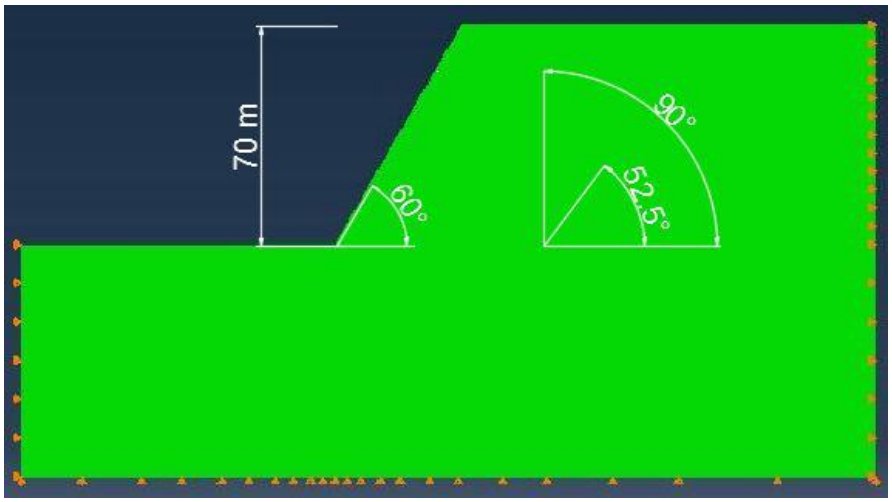

Figure 4.3: Assumed geometry for 2-D FEM modelling of rock slope mass

4.4 DEFINING THE ANALYSIS

As mentioned before, this study aims to research how the geometric and main parameters of the rock slopes with joint planes covered by: Shear retention, unit weight, friction angle, cohesion and angles between the joint planes impact on the stability of rock slopes. The methods are to imitate the jointed rock slopes by the large-scale finite element simulation software ABAQUS, analyze and study the distribution or size of the equivalent plastic strain zones and displacements with control variable method.

4.4.1 Static analysis with gravity loading

In this problem a nonzero state of stress was assumed before an excavation took place: This consists of a vertical stress that increases linearly with depth to equilibrate the weight of the rock and horizontal stresses caused by tectonic effects. The initial state of stress is capturing from the following equations:

$$\sigma_y = \rho g h \tag{4.1}$$

$$\sigma_x = \sigma_z = K_0 \sigma_y \tag{4.2}$$

where, ρ is the mass density of rock

g is the acceleration due to gravity

h is the depth of the point under consideration below the virgin rock level (assumed horizontal)

K_0 is the coefficient of initial stress

The effect of excavation was obtained by applying equivalent nodal forces on the excavated boundary. If the initial stress state is different, the response of the system will be different. Thus, the response of the system to external loading depends on the state of the system when that loading sequence begins and the need of nonlinear analysis is inevitability.

4.4.2 Pseudo-static analysis for seismic action

After the excavation and static analysis with body weight loads, was made an effort to compose on the rock slope seismic forces. For the purpose of the pseudo-static analysis, the seismic action represented by a set of horizontal static forces equal to the product of the gravity forces. In other words, an equivalent static force is assumed for seismic acceleration in unstable region.

National territories subdivided by the National Authorities into seismic zones, depending on the local hazard. By definition, the hazard within each zone is assumed to be constant and is described in terms of a single parameter, i.e., the value of the reference ground acceleration on type A ground, a_g.

In this research, the seismic zones were selected by the new map of seismic zones in Greece as are shown below (Fig. 4.4).

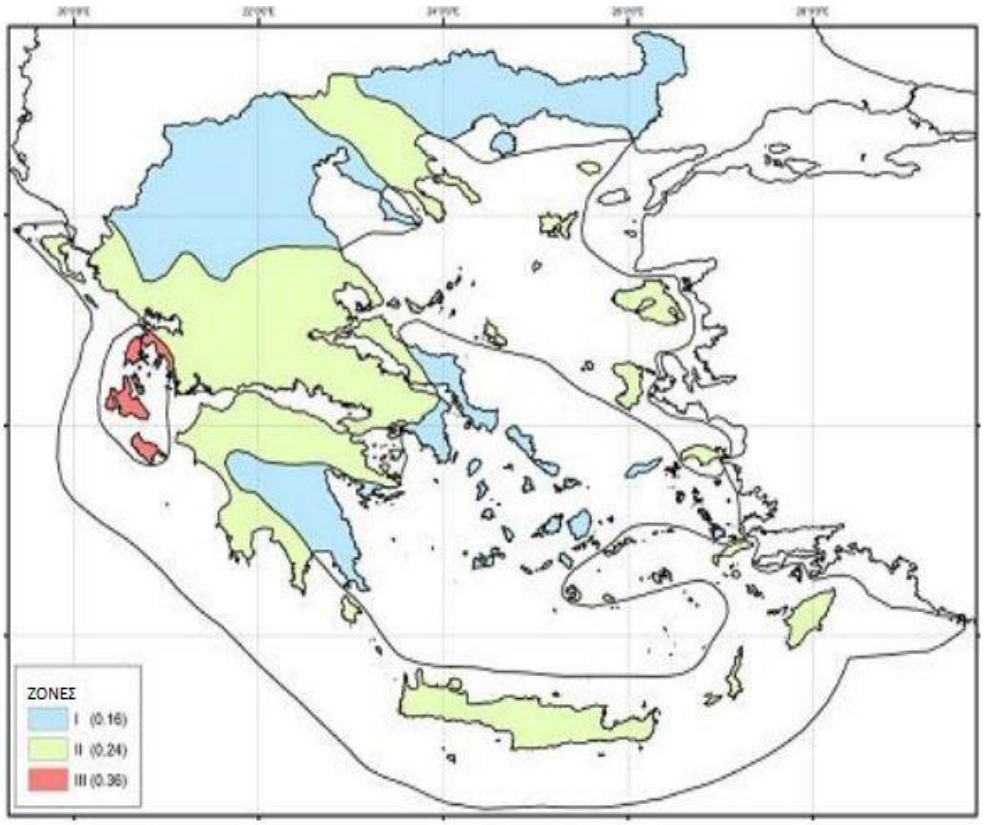

Figure 4.4: Map of seismic risk zones in Greece

Source: The Greek seismic hazard map "EC-8"

Seismic zonation has been based on the reference peak ground acceleration with 10% probability of exceedance in 50 years, i.e., 475years mean return period. Three seismic zones (I, II, III) have been introduced, and five soil types are defined (Table 4.2). The PGA values assigned to each zone refer to soil type A, (stiff soil, rock). With respect to seismic risk, soil are divided into five classes A, B, Γ, Δ, X

Table 4.2: Peak Ground Acceleration for soil type A

Seismic zone	a_g
I	0.16g
II	0.24g
III	0.36g

Source: Greek seismic building code "EAK-2000"

Table 4.3: Soil Classes

Class	Description
A	Rock or other rock-like geological formation, including at most 5 m weaker material surface.
B	Deposits of very dense sand, gravel, of very stiff clay, at least several tens of meters in thickness, characterized by a gradual increase of mechanical properties with depth.

Class	Description
C	Deep deposits of dense or medium-dense sand, gravel or stiff clay with thickness from several tens to many hundreds meters.
D	Deposits of loose-to-medium cohesionless soil (with or without some soft cohesive layers), or of predominantly soft-to-firm cohesive soil.
E	A soil profile consisting of a surface alluvium layer with v_s values of type C or D and thickness varying between about 5 m and 20 m, underlain by stiffer material with $v_s > 800$ m/s.
S_1	Deposits consisting, or containing a layer at least 10 m thick, of soft clay/silts with high plasticity index (PI > 40) and high water content.
S_2	Deposits of liquefiable soils, of sensitive clays, or any other soil profile not included in types A-E or S_1

Source: European standard "EC-8"

4.5 PARAMETRIC STUDY

The stability of rock slopes with joint planes analyzed using finite element software ABAQUS. A jointed rock mass slope may collapse due to displacements becoming very large, thus distorting the individual elements badly and prohibiting further time stepping.

Several study cases were conducted to analyze the stability of the rock slopes with control variable method. Results from the analysis are presented in Appendix A and shows the distribution of the equivalent plastic strain zones. Six study cases carried out with static analysis for very good quality rock mass to observe how the geometry and main parameters of rock slopes affect their stability. Additionally, seismic forces imposed on the rock slope as it is described above, to note the influence of seismic loads on jointed rock slopes.

The first six study cases follow the static analysis with gravity loading. The geometry of the rock mass slope is shown in Figure 4.3. It is assumed a very good quality jointed rock mass slope and the initial adopted parameters are summarized in Table 4.4. In the 2-D FE analysis two steps are created. The first step refers to state of initial stress and the second step simulates an excavation. After the analysis in geostatic conditions, an excavation is modeled in a static analysis by interrupting boundaries on the upper surface of the slope.

STATIC ANALYSIS

4.5.1 Case study 1: The influence of slope angle β to the stability of the rock slope

Table 4.4: Main parameters of the rock slope

c (kPa)	φ (^{0})	γ (kN/m^3)	H (m)	E (GPa)	ν
30	45	25	70	28	0.3

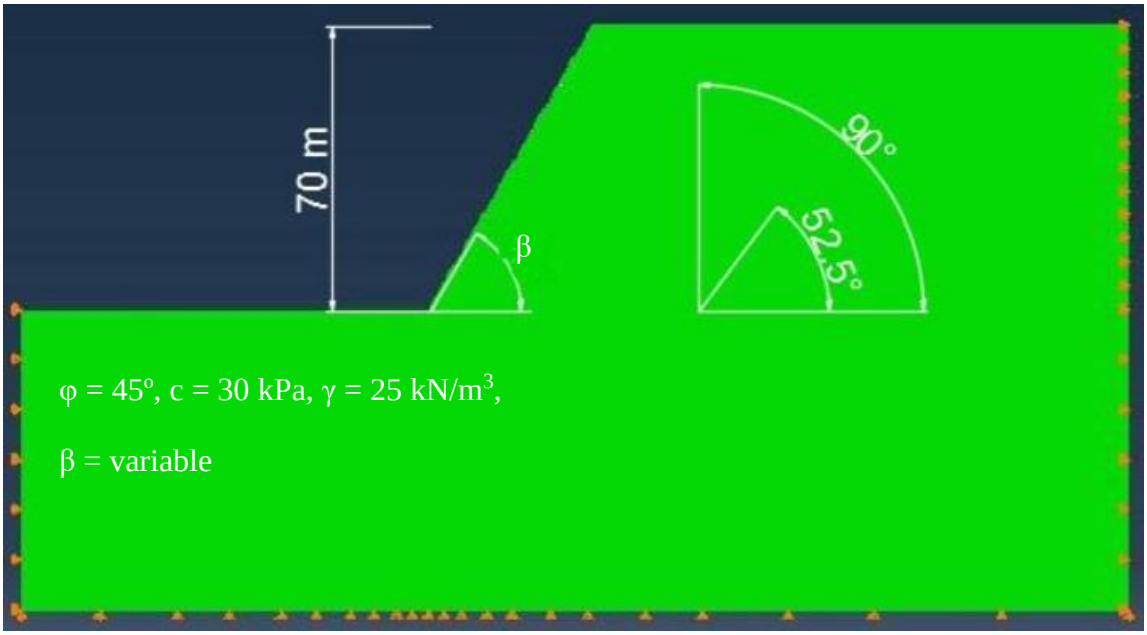

Figure 4.5: Parameters for case study 1

Results and conclusions

The overall results are presented in Appendix A. The contours indicate the location of potential slip surface formed in the failing slope. The different contours can indicate the location where the progressive failure will begin. From the deformed meshes and the PEMAG contours is obvious, that when the slope angle increases gradually from 45^0 to 65^0 to the horizontal, equivalent plastic strain amplitude also increases. That means, the steeper a slope is, the more unstable is. When the slope angle is small the plastic zone is flat to slope surface and slope toe. As the slope is being steeper, plastic zones develop from the toe to the slope inner a circular slip surface.

4.5.2 Case study 2: Unit weight γ influence to the stability of the rock slope

Table 4.5: Constant parameters of the rock slope in case study 2

c (kPa)	φ (^{0})	β (^{0})	H (m)	E (GPa)	ν
30	45	60	70	28	0.3

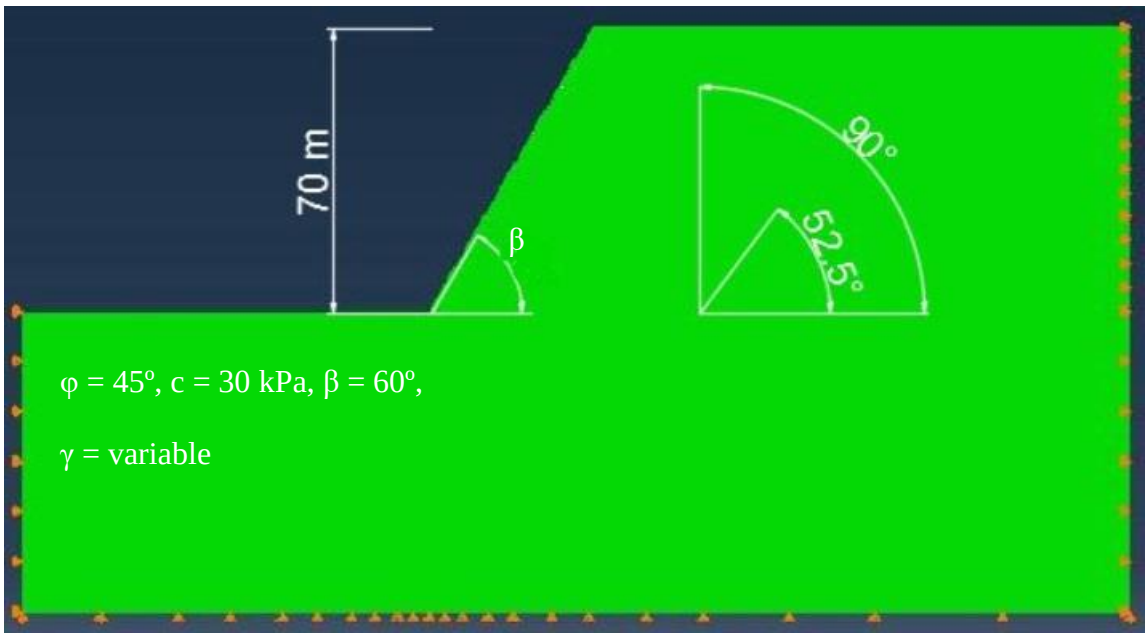

Figure 4.6: Parameters for case study 2

Results and conclusions

Density is also an important factor in slope stability. As it is presented in Appendix A, a relatively increase in unit weight of rock mass increases the vertical stress due to gravity loading, as it is captured in the equation 4.1. In this way the deformation of the rock slope is even bigger. As well as, in the case of different values of the slope angle, it is observed that plastic zones are developed between the middle and toe of the slope. The constant parameters of the slope are shown in Table 4.5.

4.5.3 Case studies 3, 4: The impact of the friction angle φ and cohesion c to the stability of the rock slope

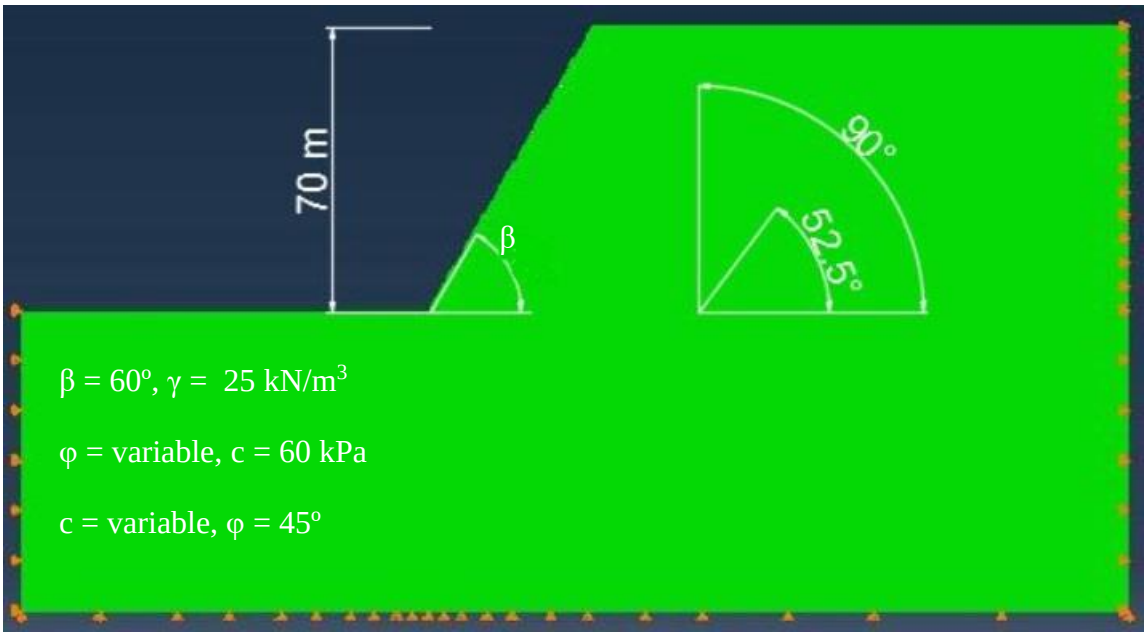

Figure 4.7: Parameters for case study 3 & 4

Results and conclusions

In case studies 3 and 4, it is examined the influence of joint plane's friction angle and cohesion on the rock mass slope stability respectively. The friction angle φ ranging from 35^0 to 50^0 and cohesion from 30 kPa to 120 kPa. In both cases small values of the above strength parameters, make the rock slope more unstable. Maximum values of equivalent plastic strain (PEMAG) are rounded up near the toe of the inclined surface. As the values increase, the slope becomes more stable. As a result, the plastic strain contours comes with the deformed meshes as shown in Appendix A, indicate a potential slip surface in wider area.

4.5.4 Case studies 5, 6: The impact of the joint plane angle to the stability of the rock slope

Table 4.6: Constant parameters of the rock slope in case studies 5 & 6

c (kPa)	γ (kN/m^3)	φ (^{0})	β (^{0})	H (m)	E (GPa)	ν
100	25	45	60	70	28	0.3

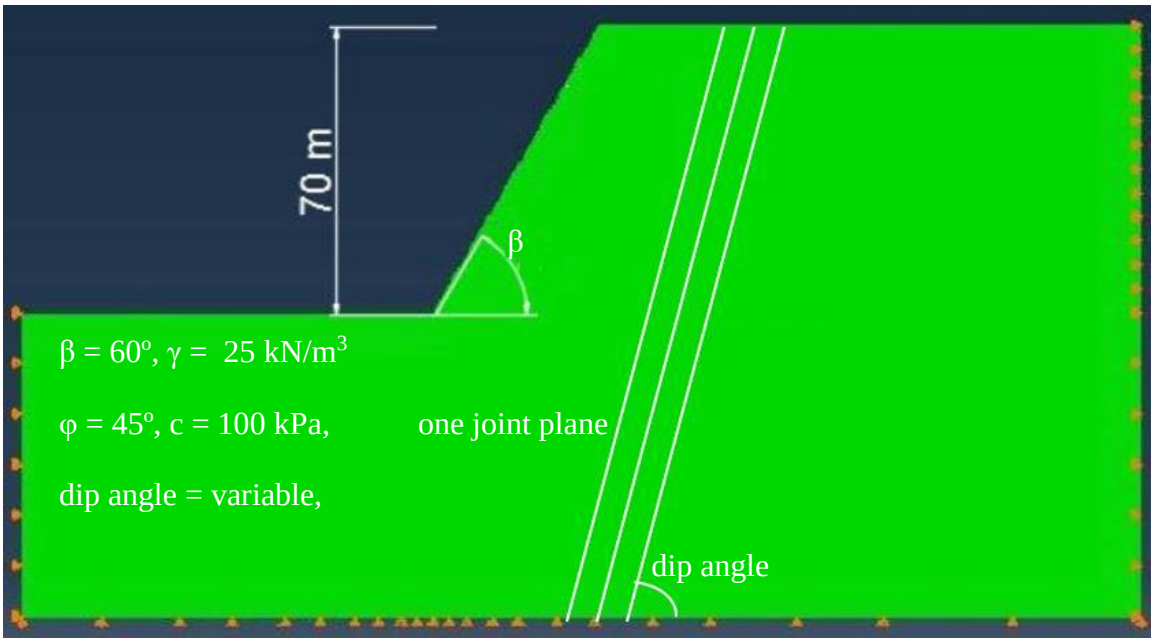

Figure 4.8: Parameters for case study 5

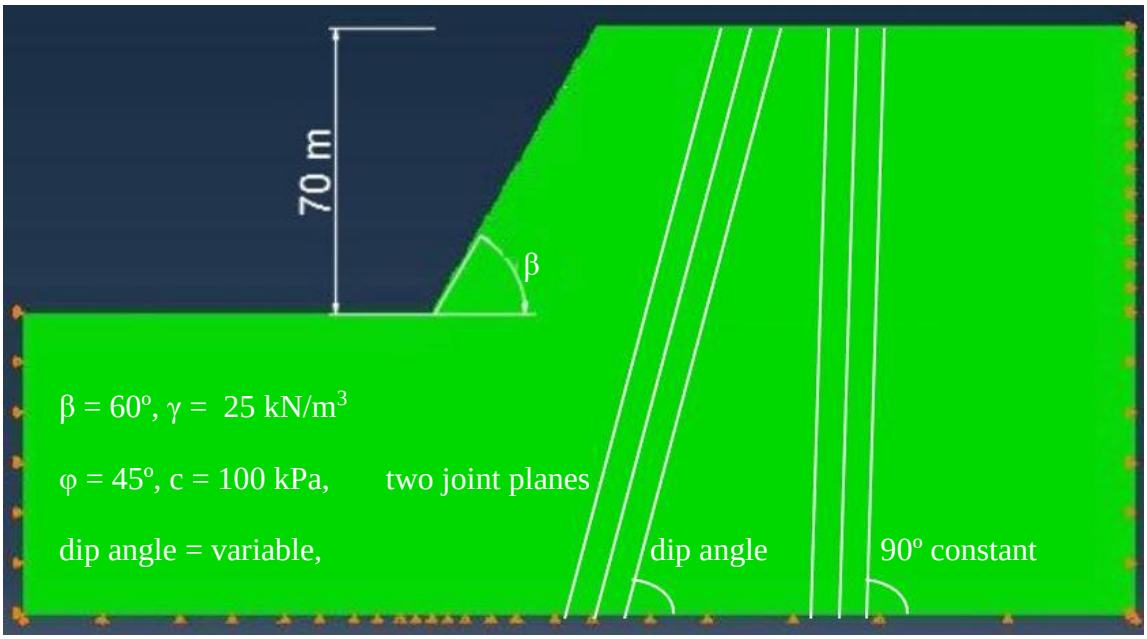

Figure 4.9: Parameters for case study 6

Results and conclusions

There are usually one or over one set joint planes in a rock slope. In this dissertation the model has two joint planes. For this analysis one joint plane kept perpendicular to the cross section and the dip angle of the other joint set ranges from 20^0 to 70^0. The basic parameters of the rock slope are showed in Table 4.6.

When the dip angle ranges from 20^0 to 40^0 the equivalent plastic strain amplitude increases from 3.729×10^{-5} to 5.891×10^{-5}. Plastic strain zone is concentrated downward inside of the slope and with the increase of joint angle *a* is noticed a smaller slip surface area. Moreover, when the dip angle ranges from 50^0 to 70^0, values of equivalent plastic strain amplitude increase slowly and from 3.025×10^{-5} to 3.168×10^{-5}. That means when the dip angle of discontinuity increase and become sub parallel to the slope angle the slope become relatively stable. However further increase in dip angle in discontinuity make is liable to undergo toppling failure.

In the case of one joint plane the behavior of the slope is similar. Generally, it can be observed from the contours in Appendix A that the magnitude of equivalent plastic strain is less than the case of two joint planes. Additional, when the dip angle is the very same with the slope angle, videlicet 60^0, plastic strain zones are negligible. Particularly, plastic zones are developed inside the slope and as the dip angle ranges from 20^0 to 40^0 the equivalent plastic strain amplitude getting larger. After that, as the dip angle increases till 70^0 the equivalent plastic strain amplitude decreases and plastic zones are developed in the toe of the slope. When the dip angle increases to 80^0 PEMAG also increases and then reduces again, as it is shown in the contour of 90^0.

PSEUDO-STATIC ANALYSIS

Seismic waves passing through rock adds stress which causes fracturing in the rock mass. In the follow cases. In the follow case studies the seismic waves are simulated with a third step in the analysis which applies an additional horizontal gravity load to the rock mass slope.

4.5.5 Case studies 7, 8, 9: Impact of the seismic loads on the rock mass slope stability of the rock slope

Results and conclusions

In these case studies it is examined a poor quality rock mass to notice a bigger range of plastic zones. The analysis has been conducted for three main magnitudes of seismic load and for variable values of cohesion c. The main parameters where used in this analysis are shown in the Table 4.7.

Table 4.7: Main parameters of the rock slope for pseudo-static analysis

a_g	γ (kN/m^3)	φ (^{0})	β (^{0})	H (m)	E (GPa)	ν
0.16g	25	45	60	70	5	0.3
0.24g						
0.36g						

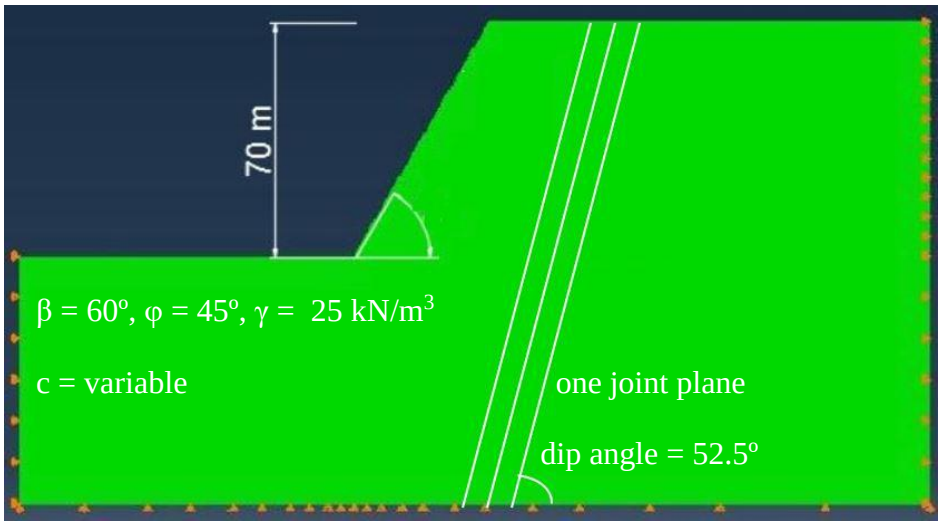

Figure 4.10: Parameters for case studies 7, 8 & 9

Firstly, it is obvious that in all case studies when the initial value of cohesion is 15 kPa plastic zones are developed from the toe to the crest of the slope. The deformed area of the slope is large and from the contours with scale factor = 6e+03 it can been seen the strong effect of seismic loads in slope stability.

Maximum values of equivalent plastic strain are measured on the crest. For a seismic load with magnitude 0.16g and 0.36g the equivalent plastic strain amplitude is 2.971×10^{-3} and 9.558×10^{-3} respectively. In other words with the seismic load increased from 0.16g to 0.36g the plastic zones extend in larger area and PEMAG also increases.

Furthermore, it can be remarked that in all cases, when cohesion increases from 15 kPa to 25 kPa the reduction velocity of plastic zone area is big. With 10 kPa gain increase of cohesion, maximum equivalent plastic strain amplitude is decreased by 78%, 55%, 40%, corresponding to 0.16, 0.24g, 0.36g seismic force amplitude. In the first seismic zone which refers to 0.16g seismic load amplitude, with the increase of cohesion plastic zones are concentrating lower to the surface of the slope in less steps compared with the two others seismic zones.

4.6 CONCLUSION

The angle of slope, unit weight, friction angle, cohesion and dip angle of joint planes have a paramount of importance to the slope stability and failure surfaces. Through the analysis of above case studies it is observed that:

- When the angle and unit weight of slope increase, the slope is getting more unstable. Plastic zones are concentrated near to the toe of slope and develop internal.
- Friction angle and cohesion of joint planes have an importance influence to the slope stability. The bigger they are, the less unstable is the slope. With the increase of their values the equivalent plastic strain amplitude decreases and the plastic zone area reduces.
- Concerning the dip angle of joint planes it is observed that when it is smaller than the slope angle, with its increase the equivalent plastic strain amplitude also increases and the slope become unstable. When it is sub parallel with slope angle plastic zones are reduced and the slope become more stable.
- As it is expected, an additional load in the appropriate direction will contribute to the collapse of the slope. As are imposed on seismic forces to the slope plastic zones are expanding to the crest of the slope. The bigger is the magnitude of the force, the bigger is the equivalent plastic strain amplitude.

  Consequently, the slope is easier to collapse under seismic forces. Plastic zones areas are extensive with increased equivalent plastic strain and therefore displacements in these areas will have considerable values.

In the following charts, are presented displacements with variable cohesion, in horizontal U1 and vertical U2 direction on the crest of slope as shown in Figures 4.11, 4.12, 4.13, 4.14, 4.15 for the three seismic zones as are described in 4.3.2 section. The main parameters which are corresponding with the following charts are summarized in Table 4.7.

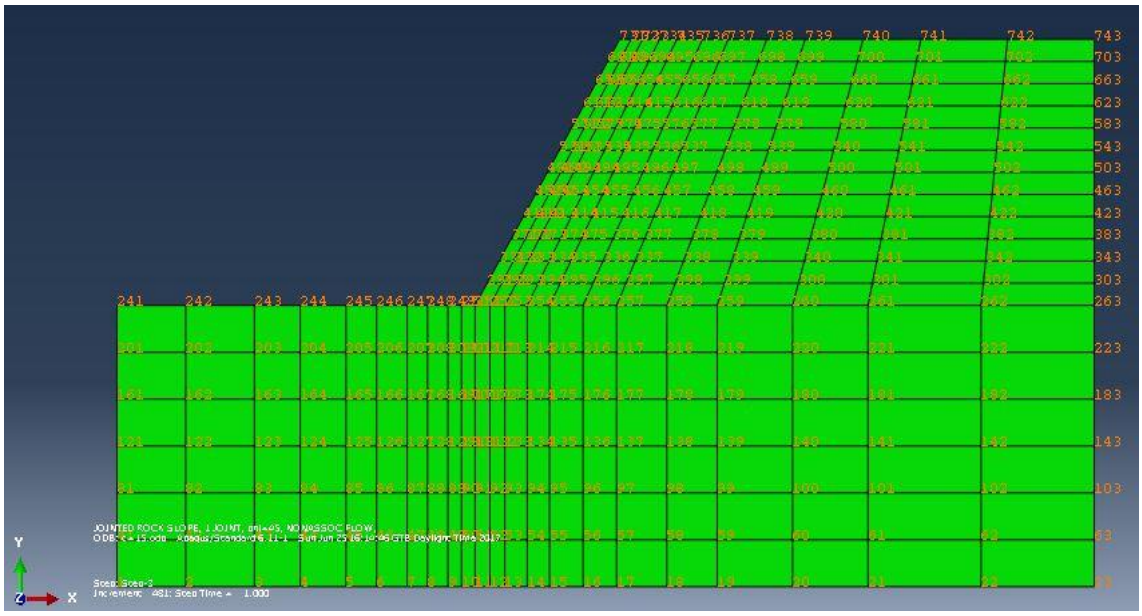

Figure 4.11: Depiction of nodes in the jointed slope model

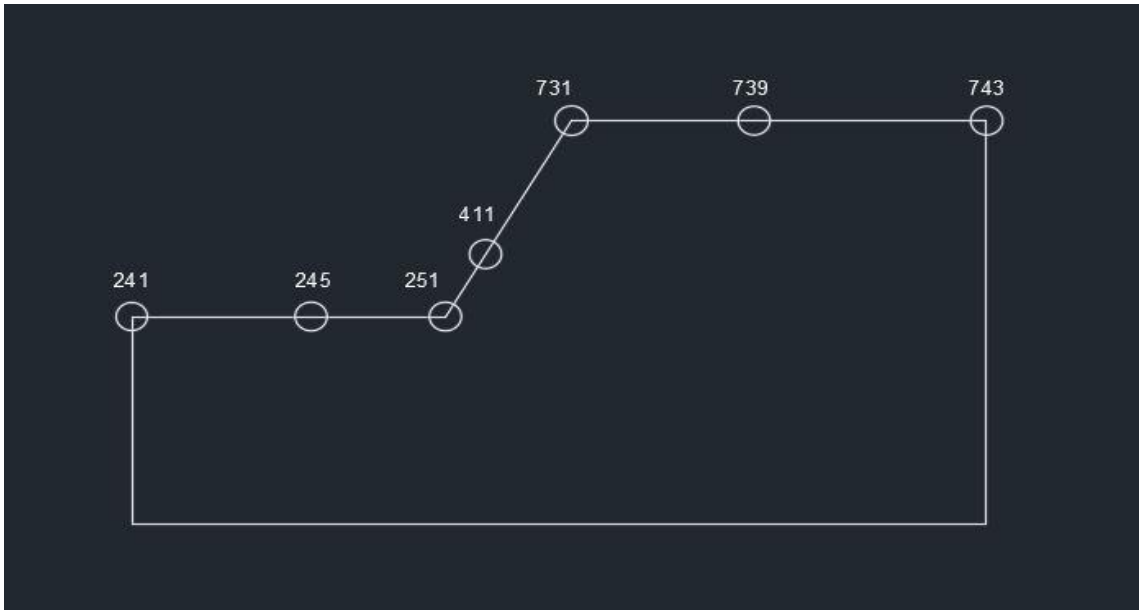

Figure 4.12: Critical point at node 731

0,16g

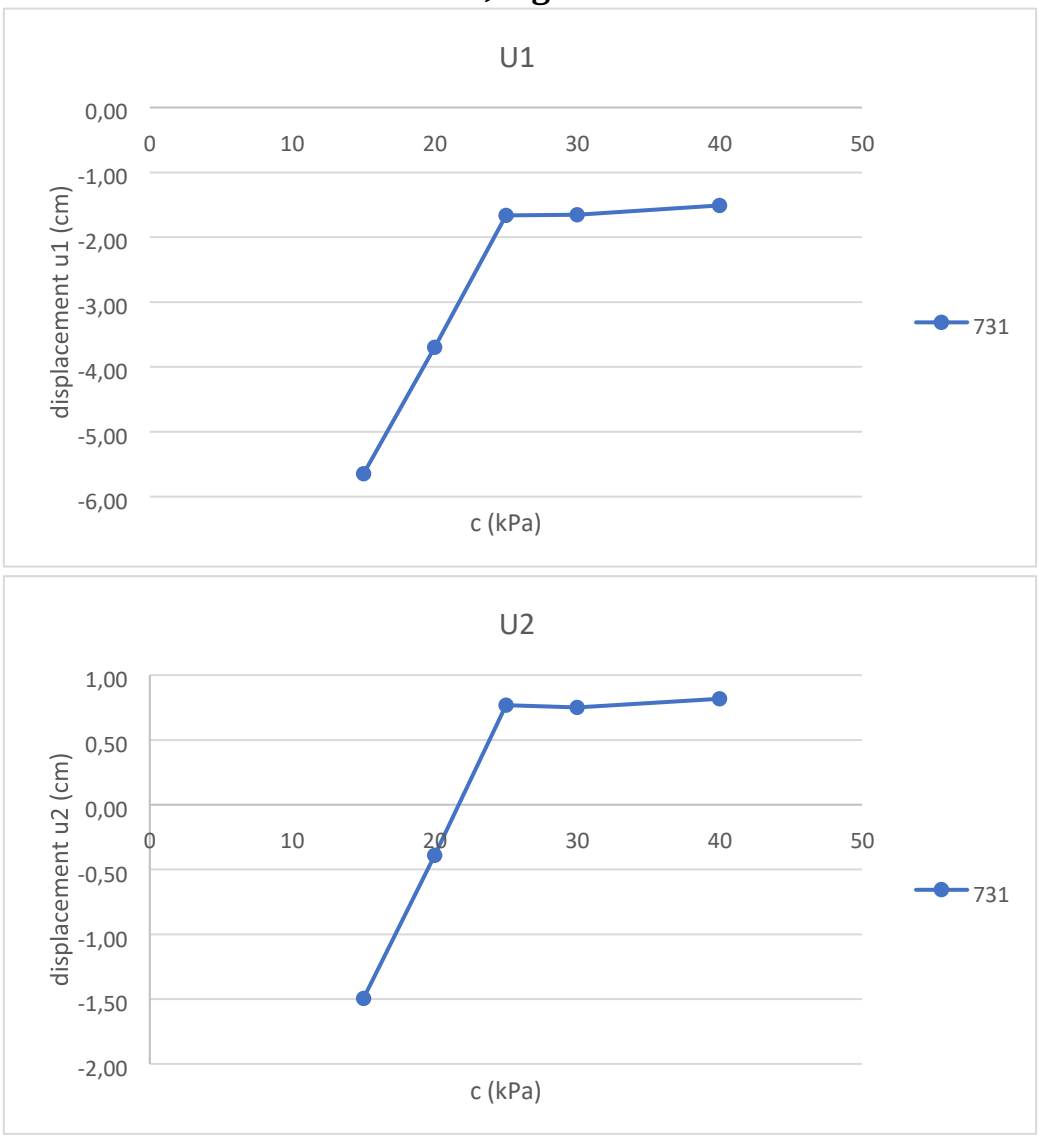

Figure 4.13: Variation of displacement u1 & u2 for different values of cohesion. Seismic zone I

0,24g

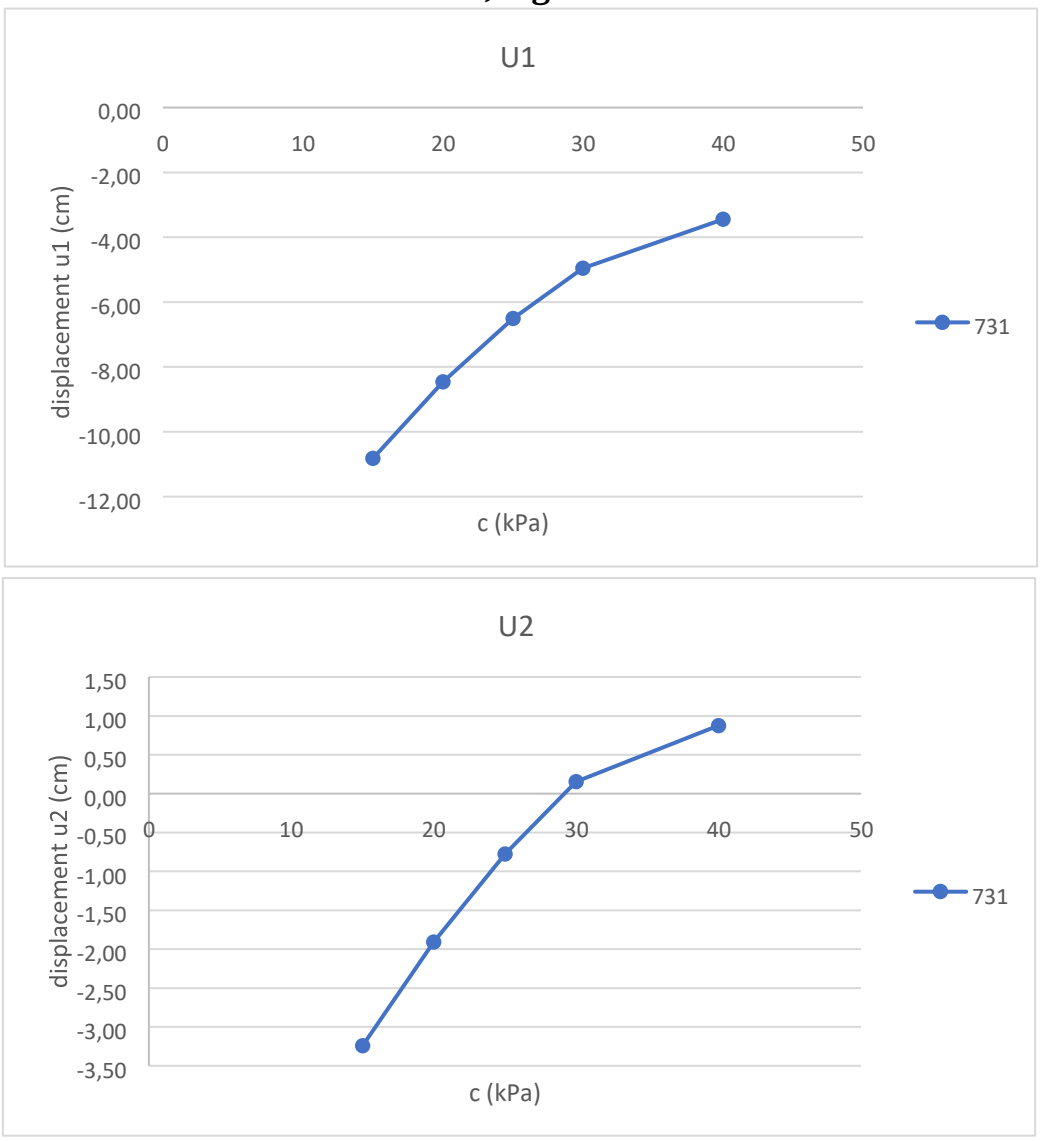

Figure 4.14: Variation of displacement u1 & u2 for different values of cohesion. Seismic zone II

0,36g

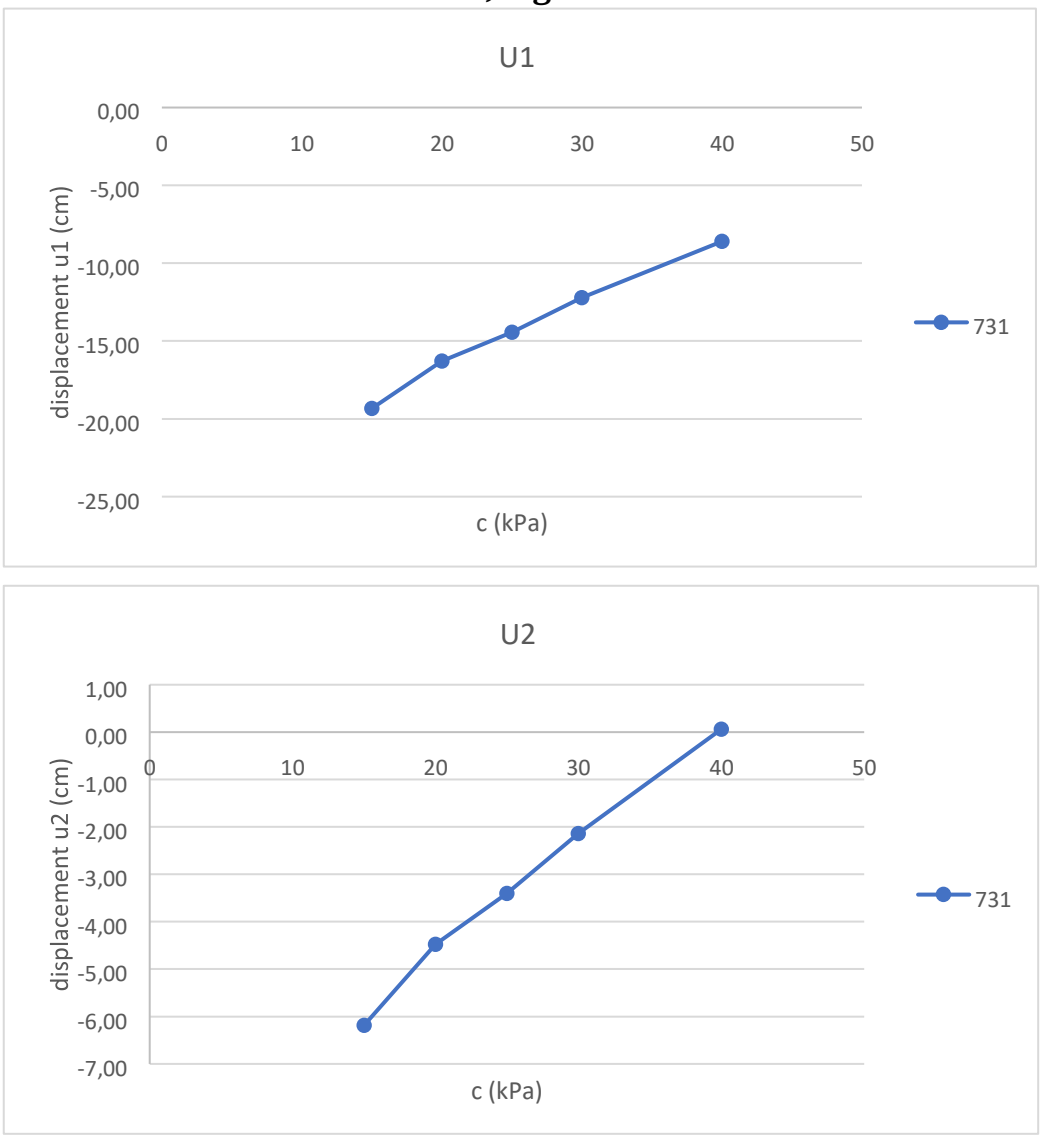

Figure 4.15: Variation of displacement u1 & u2 for different values of cohesion. Seismic zone III

The above charts validate that larger seismic forces create bigger displacements. When the seismic force increase from 0.16g to 0.36g the maximum displacement U1 at node 731 is 0.056m and 0.19m in absolute values, respectively. In vertical direction maximum displacement U2 in absolute values, is 0.015m and 0.06m corresponding to 0.16g and 0.36g seismic force.

REFERENCES

1. J. A. R. Ortigao & Alberto S. F. J. Sayao, 2004. Handbook of Slope Stabilization. New York: Springer-Verlag Berlin Heidelberg.

2. Duncan C. Wyllie & Christopher W. Mah, 2005. Rock Slope Engineering, Civil and Mining. 4th ed. Taylor & Francis e-Library.

3. Jamie Woodward, 2009. The Physical Geography of the Mediterranean. New York: Oxford University Press Inc.

4. G. P. Giani, 1992. Rock Slope Stability Analysis. Netherlands: A. A. Balkema Publishers.

5. R. Debin, D. Zheng, Y. Xiaotong, L. Shipeng, 2016. Stability Analysis on Factors of Jointed Rock Slopes. Atlantis Press, 19 - 23.

6. I-Hsuan Ho, 2014. Parametric studies of slope stability analyses using three-dimensional finite element technique: Geometric effect. Journal of GeoEngineering, Vol. 9, No. 1, pp. 33 - 43.

7. D. V. Griffiths, P. A. Lane, 1999. Slope Stability Analysis by Finite Elements. Geotechnique **49**, No. 3, 387 - 403.

8. Doug Stead, Andrea Wolter, 2015. A critical review of rock slope failure mechanisms: The importance of structural geology. Journal of structural geology 74, 1 - 23.

9. O. C. Zienkiewicz & G. N. Pande, 1977. Time-Dependent Multilaminate model of Rocks-A Numerical Study of Deformation and Failure of Rock Masses. International Journal for Numerical and Analytical Methods in Geomechanics, Vol. 1, 219-247.

10. Barton N., 1971. Progressive Failure of Excavated Rocks Slopes. Proceedings of the 13th Symposium on Rock Mechanics, Illinois, pp. 139 - 170.

11. Hoek E., 1970. Estimating the Stability of Excavated Slopes in Open Cast Mines. Trans. Inst. Min. and Metal., Vol. 79, pp. 109 - 132.

12. M. Amini, M. Gholamzadeh, M. H. Khosravi, 2015. Physical and Theoretical modeling of rock slopes against block-flexure toppling failure. International Journal of Min. & Geo-Engineering, Vol. 49, No. 2, pp. 155-171.

13. R. C. Viesca, J., R., Rice, 2008. Friction and basic Slope Stability, Landslide Phenomena. Based on notes for Mon. 5 Nov. 2007 lecture, Harvard University.

14. Aydan O., Shimizu Y., Ichikawa Y., 1989. The effective failure modes and stability of slopes rock mass with two discontinuity sets. Rock Mechanics and Rock Engineering, 22, 163 - 188.

15. Eberhardt E., Stead D., Coggan JS., 2004. Numerical Analysis of Initiation and progressive failure in natural slopes-the 1991 Randa rockslides, Rock Mechanics and Mining Sciences, 41, 69-87.

16. Hoek E., Carranza-Torres C., Corkum B., 2002. Hoek-Brown Failure Criterion- Edition, Rocscience.

17. ABAQUS, 2011, ABAQUS Documentation, Version 6.11,: ABAQUS/ Keywords Edition/ Analysis User's Manual, Vol I, II, III, IV, V. Dassault Systemes Simulia Corp., Providence, RI, USA.

18. CIESM, 2011. Marine geo-hazards in the Mediterranean. NO, 42 in CIESM Workshop Monographs [F. Briand Ed.], 192 pages, Monaco

19. A. Antoniou, P. Psarropoulos. 2016. The geohazards of the Mediterranean Sea that potentially threaten the offshore oil & gas facilities. Offshore Pipeline Technology Conference, Amsterdam, Netherlands.

20. Rex L. Baum, Devin L., Galloway, Edwin L. Harp, 2008. Landslide and Land Subsidence Hazards to Pipelines. Cooperation with the U.S Department of Transportation, Pipeline Research Council International, and DGH Consulting Inc.

21. Michael J., O' Rourke, (Jack) X. Liu, 2012. Seismic Design of Buried and Offshore Pipelines. Monograph MCEER, University at Buffalo, State University of New Work.

22. G., Biscontin., J. M. Pestana, F. Nadim, 2003. Seismic Triggering of Submarine slides in soft cohesive soil deposits. Internation Journal of Marine Geology, Geochemistry, Geophysics 203, pp. 341-354.

Appendix A

Results from ABAQUS analysis are presented in Appendix A for very good and poor quality rock mass slope with Young's modulus $E = 28\ GPa$ and $E = 5\ GPa$ respectively.

Very good quality rock mass slope, E = 28000 MPa, static analysis

<u>Case study 1: Variable parameter is slope angle β</u>

- $\beta = 45^0$

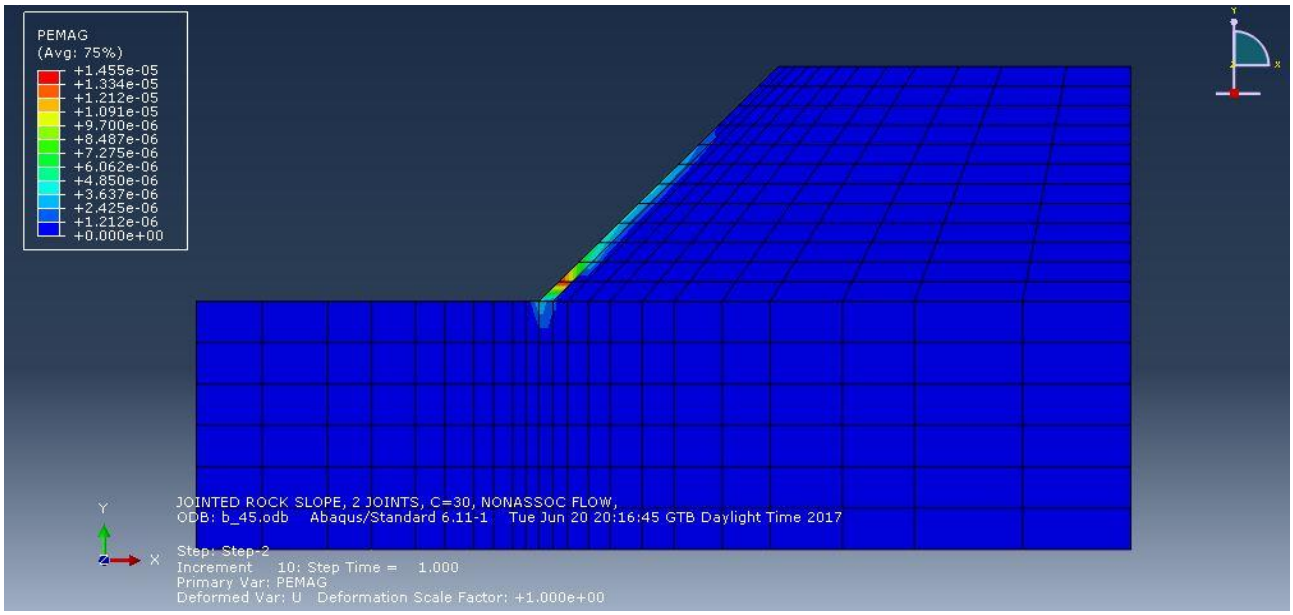

scale factor = 1e+00

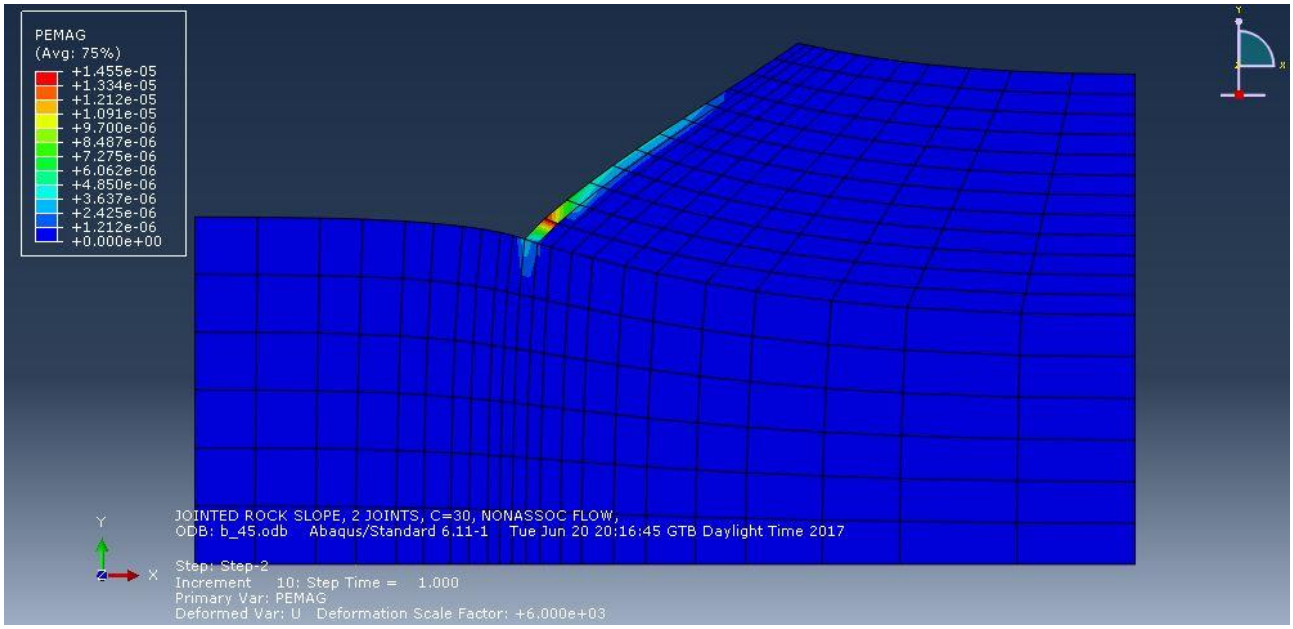

scale factor = 6e+03

- $\beta = 50^0$

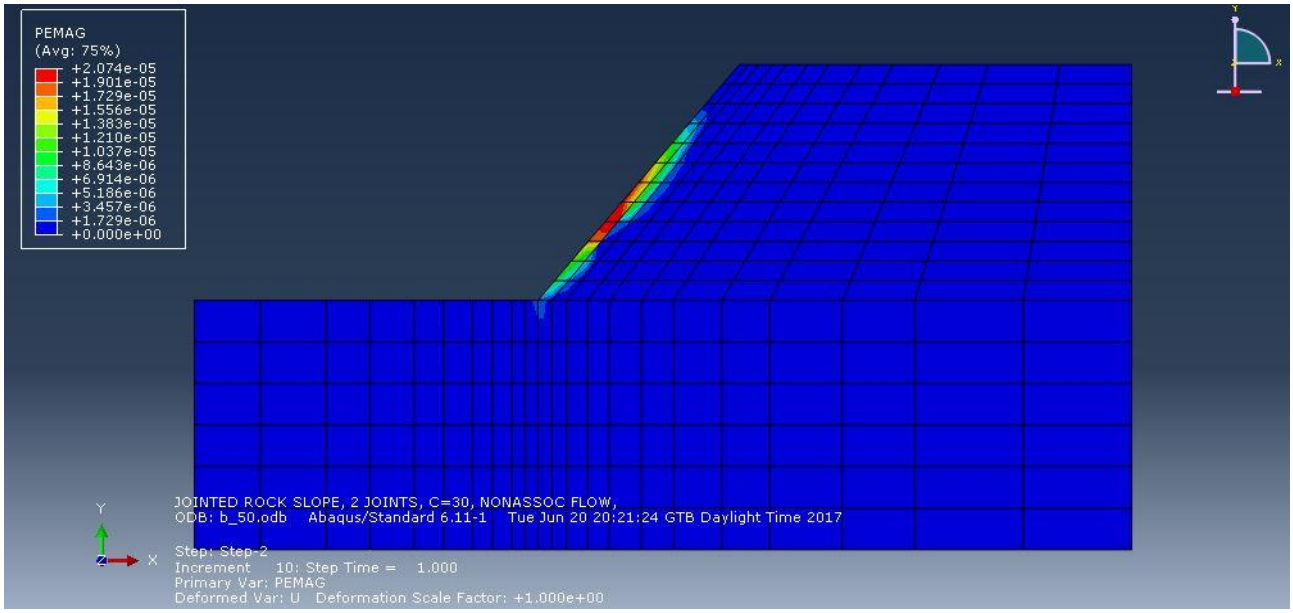

scale factor = 1e+00

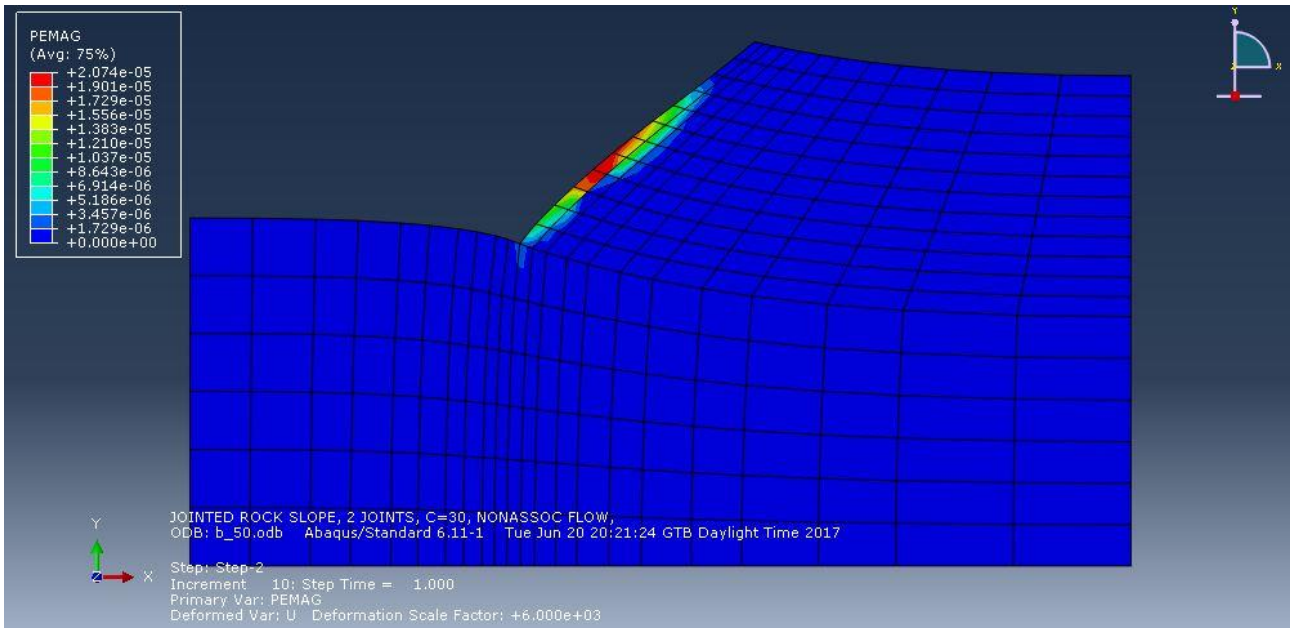

scale factor = 6e+03

- $\beta = 55^0$

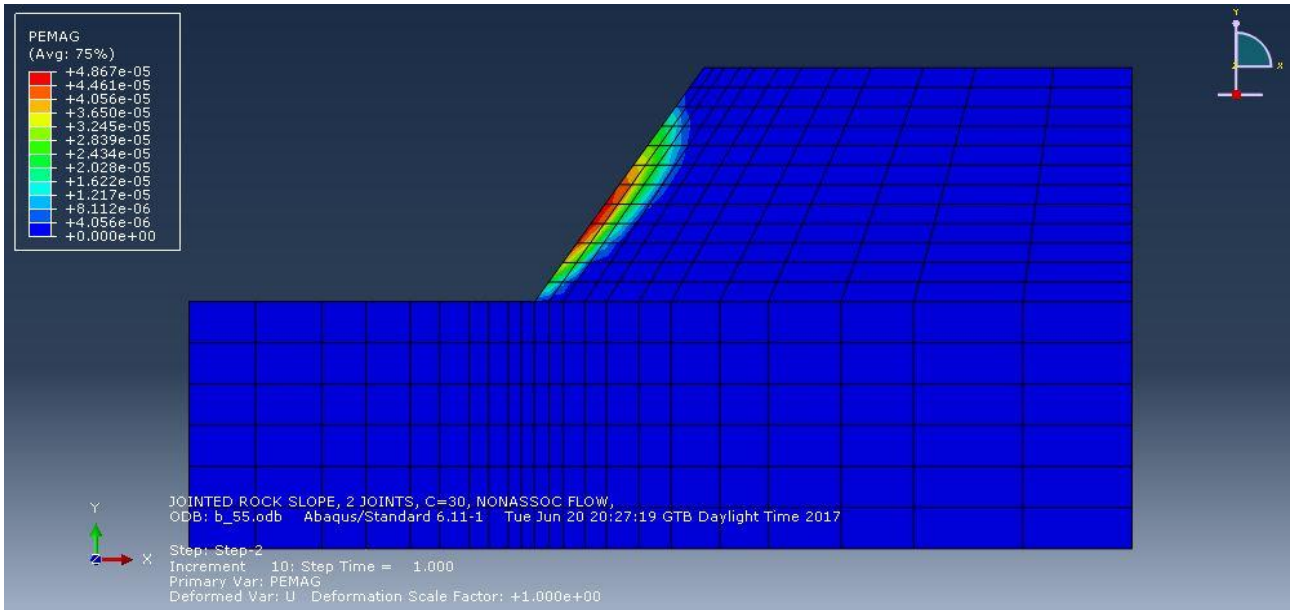

scale factor = 1e+00

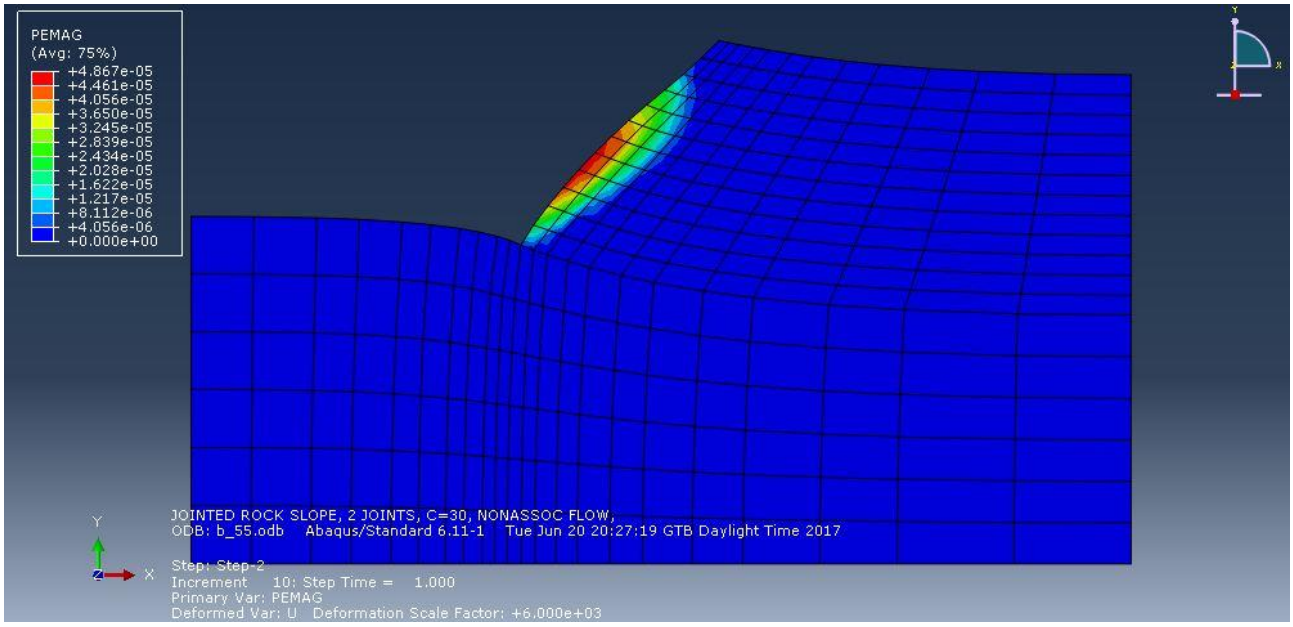

scale factor = 6e+03

- $\beta = 60^0$

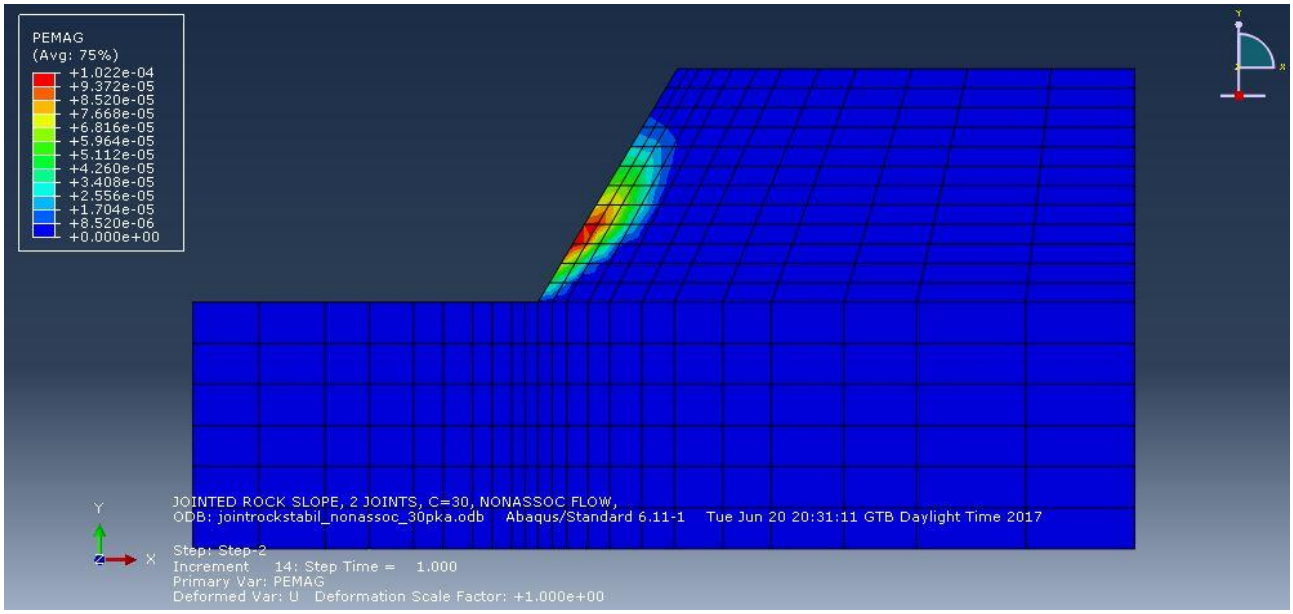

scale factor = 1e+00

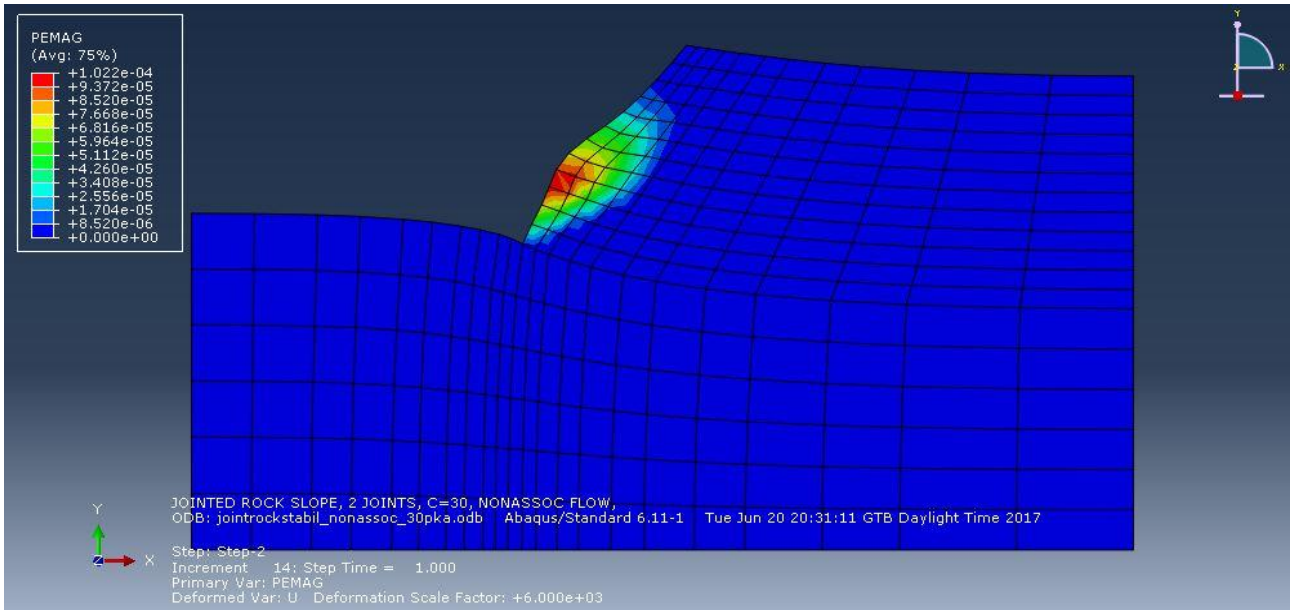

scale factor = 6e+03

- $\beta = 65^0$

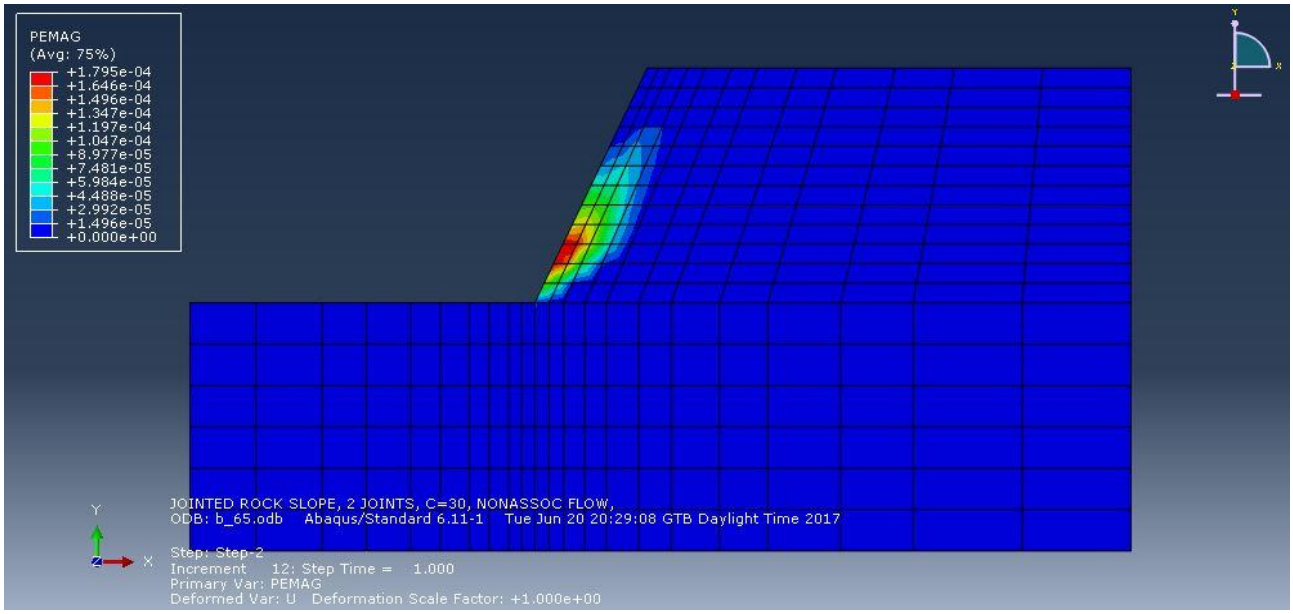

scale factor = 1e+00

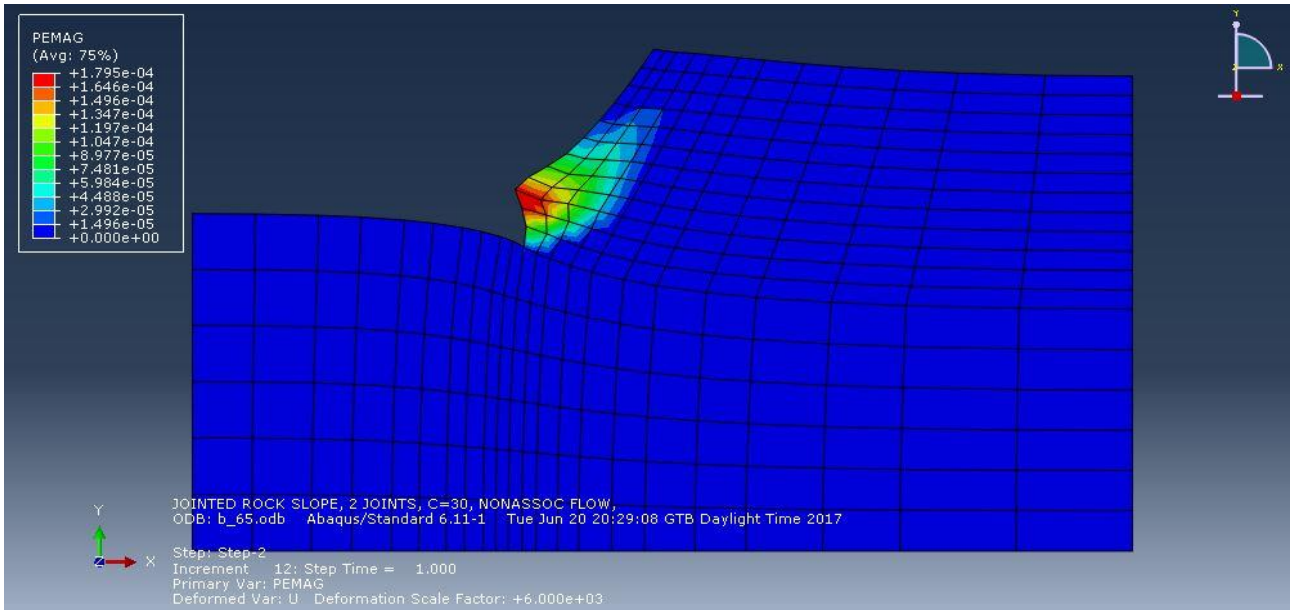

scale factor = 6e+03

Case study 2: variable parameter is unit weight γ

- γ =20 kN/m^3

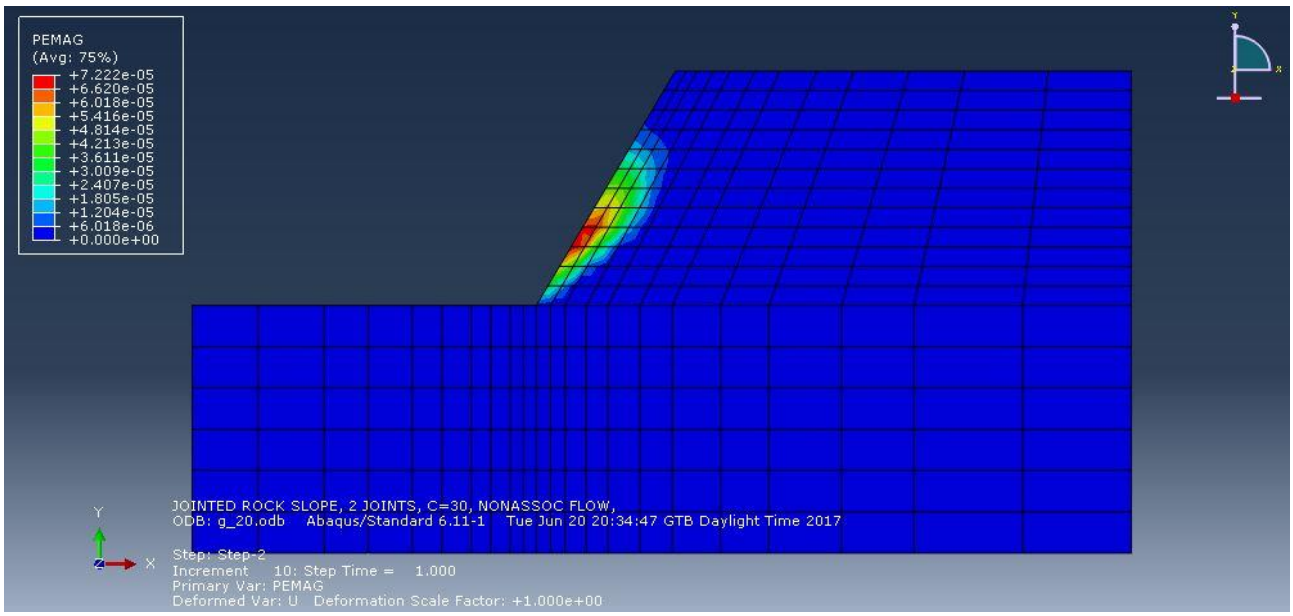

scale factor = 1e+00

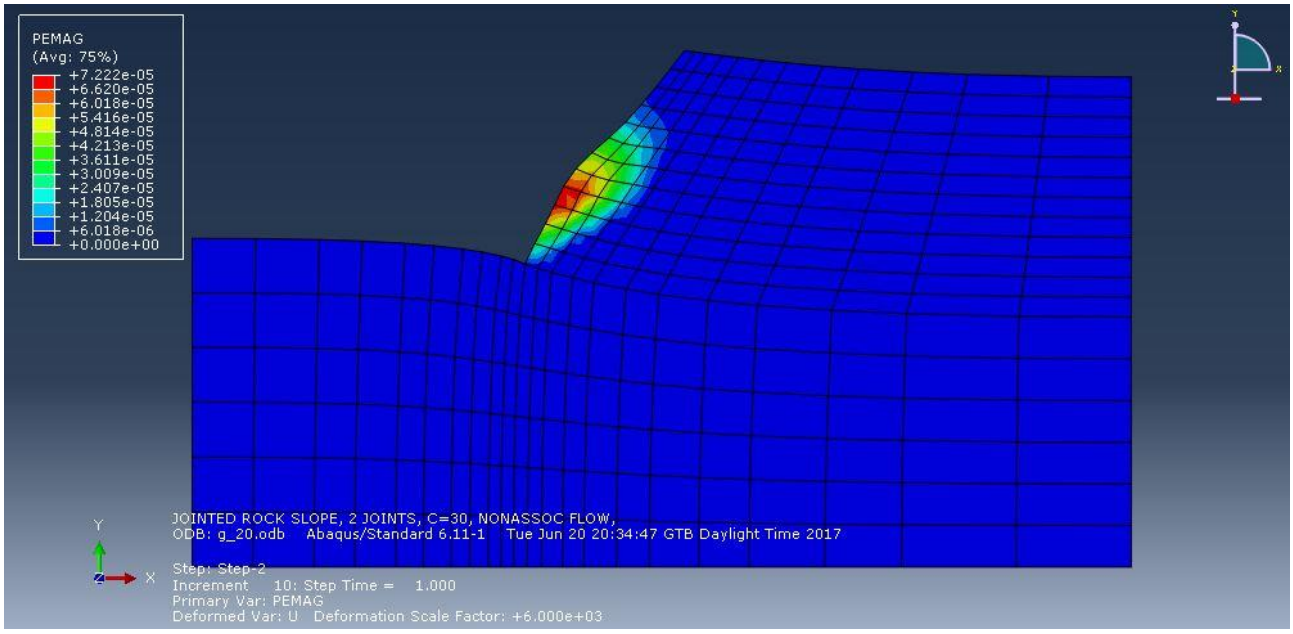

scale factor = 6e+03

- $\gamma = 21\ kN/m^3$

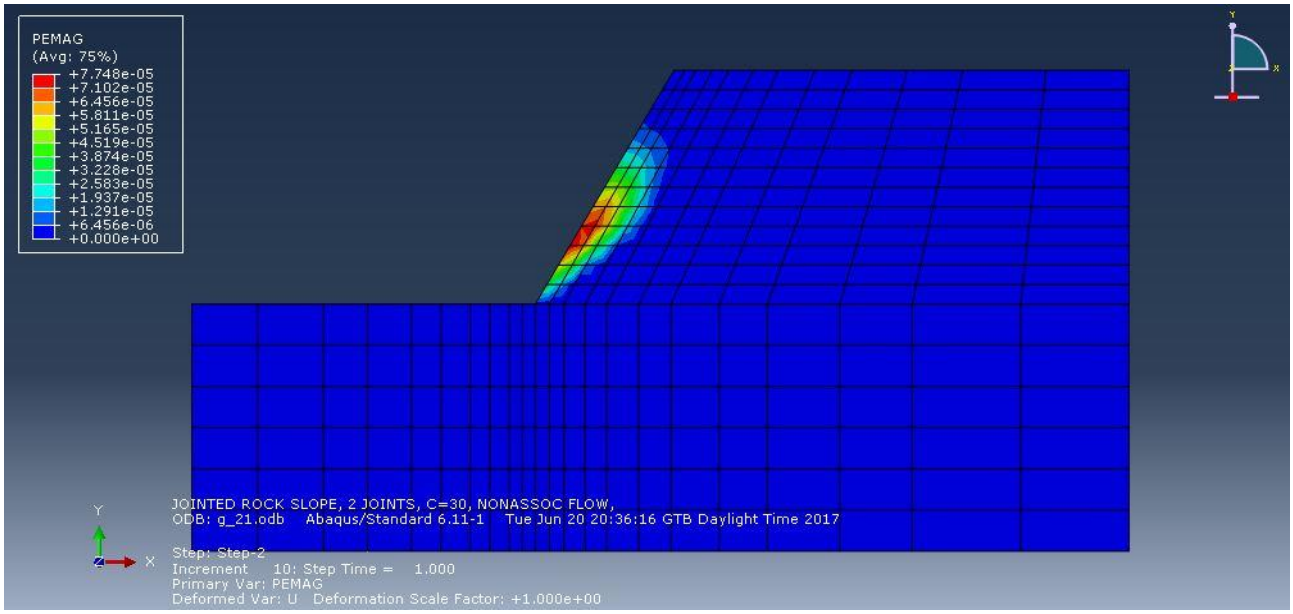

scale factor = 1e+00

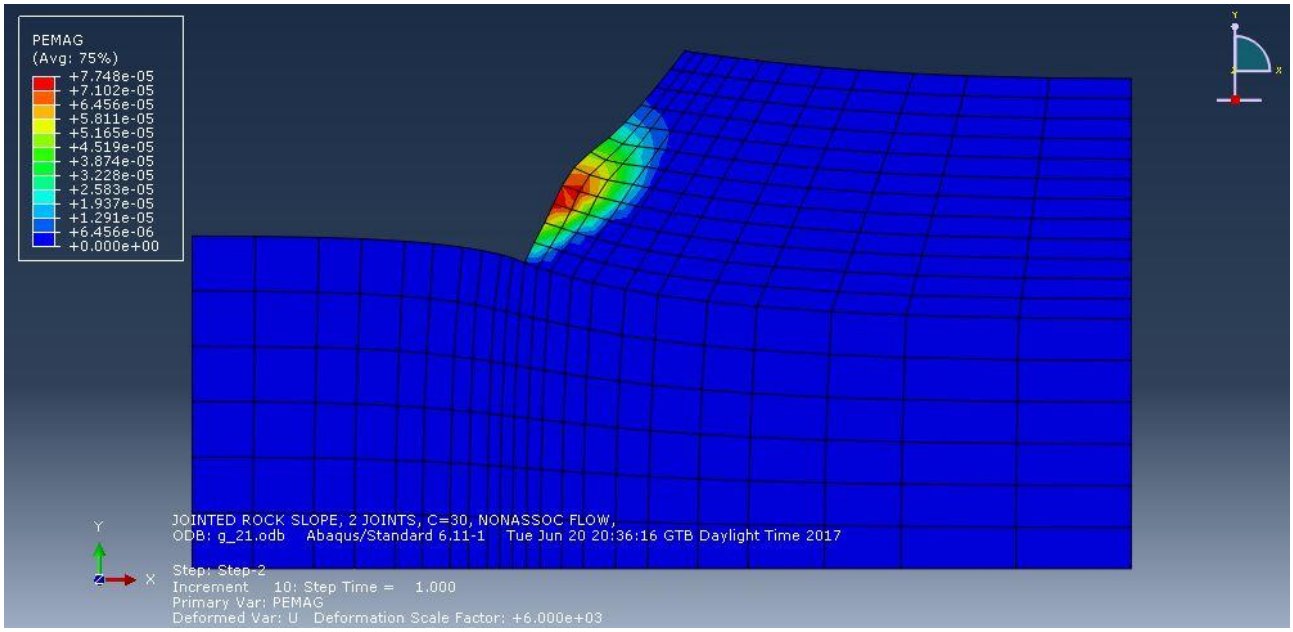

scale factor = 6e+03

- $\gamma = 22\ kN/m^3$

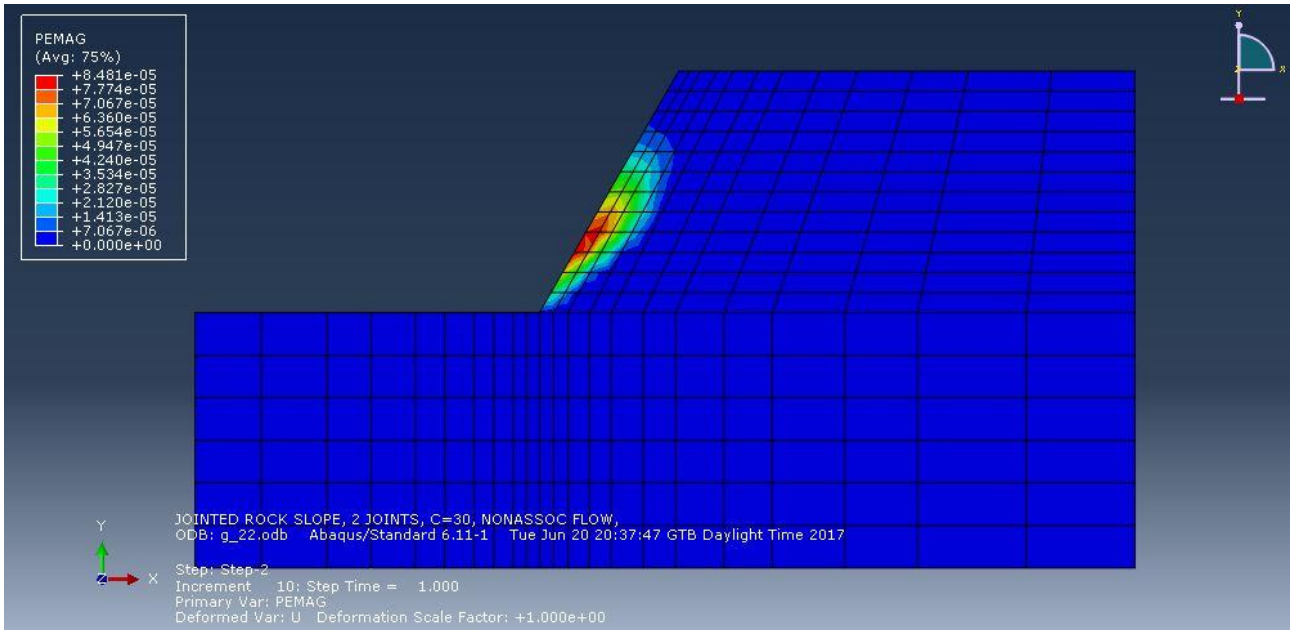

scale factor = 1e+00

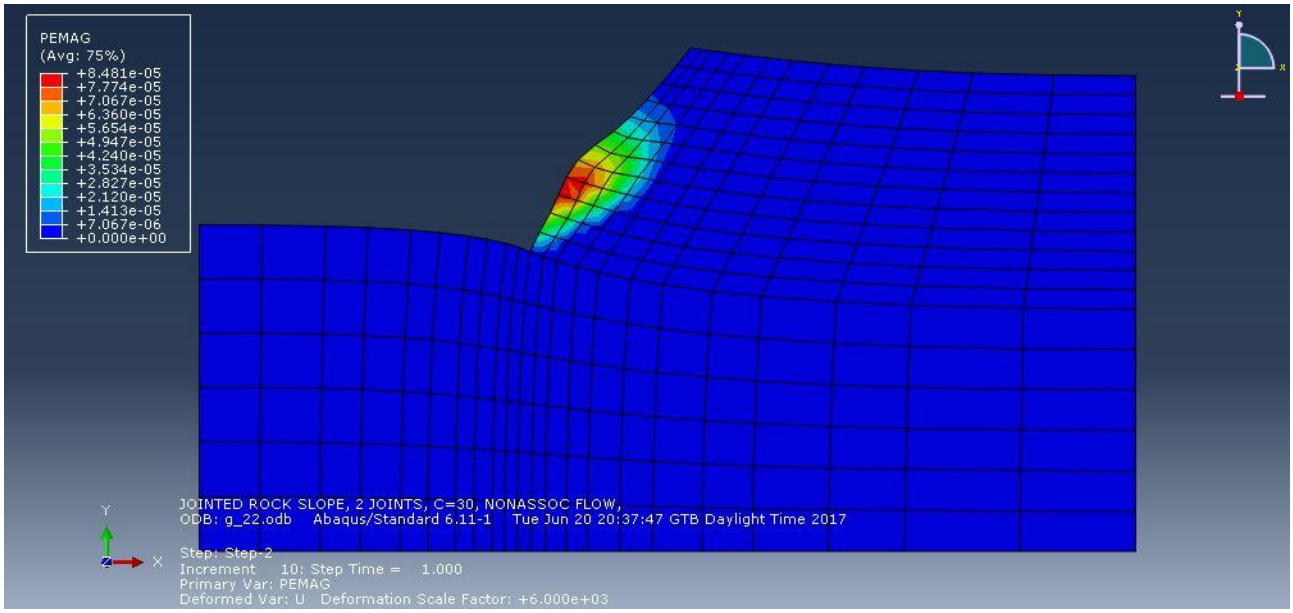

scale factor = 6e+03

- $\gamma = 23\ kN/m^3$

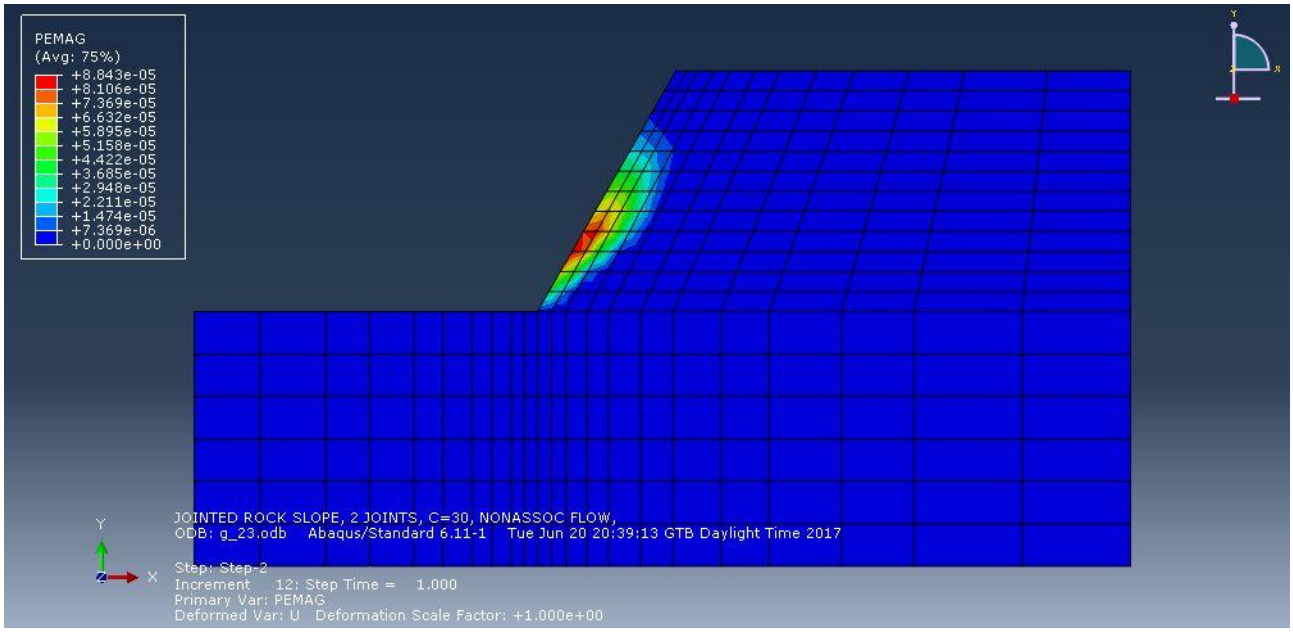

scale factor = 1e+00

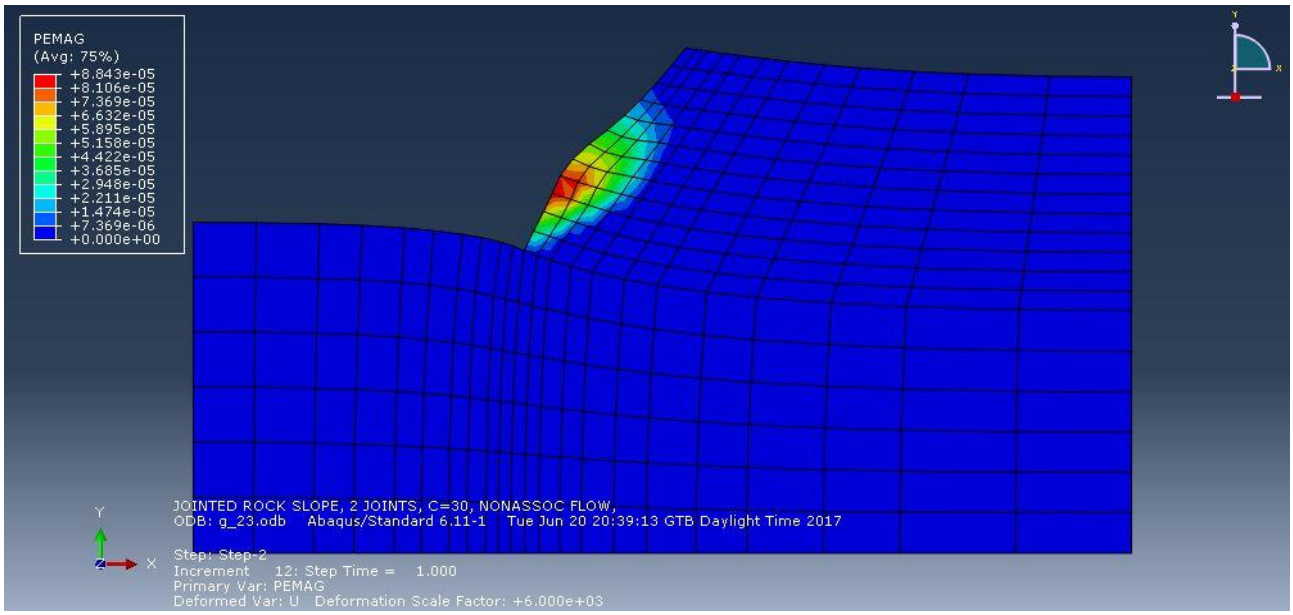

scale factor = 6e+03

- $\gamma = 24\ kN/m^3$

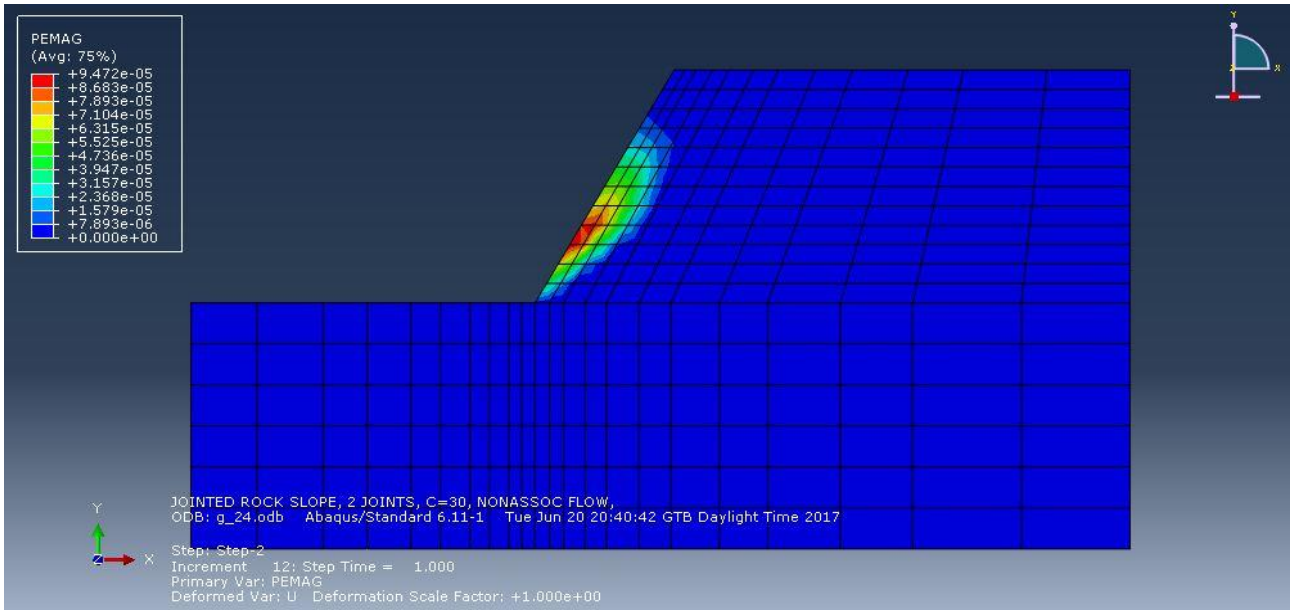

scale factor = 1e+00

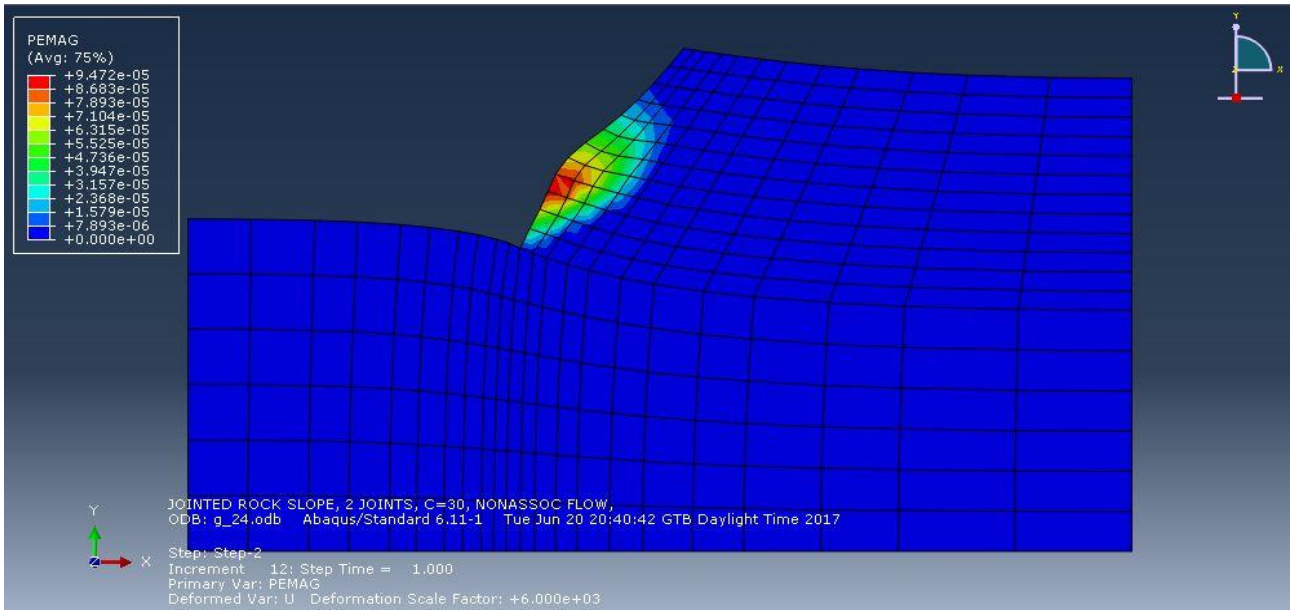

scale factor = 6e+03

- $\gamma = 25\ kN/m^3$

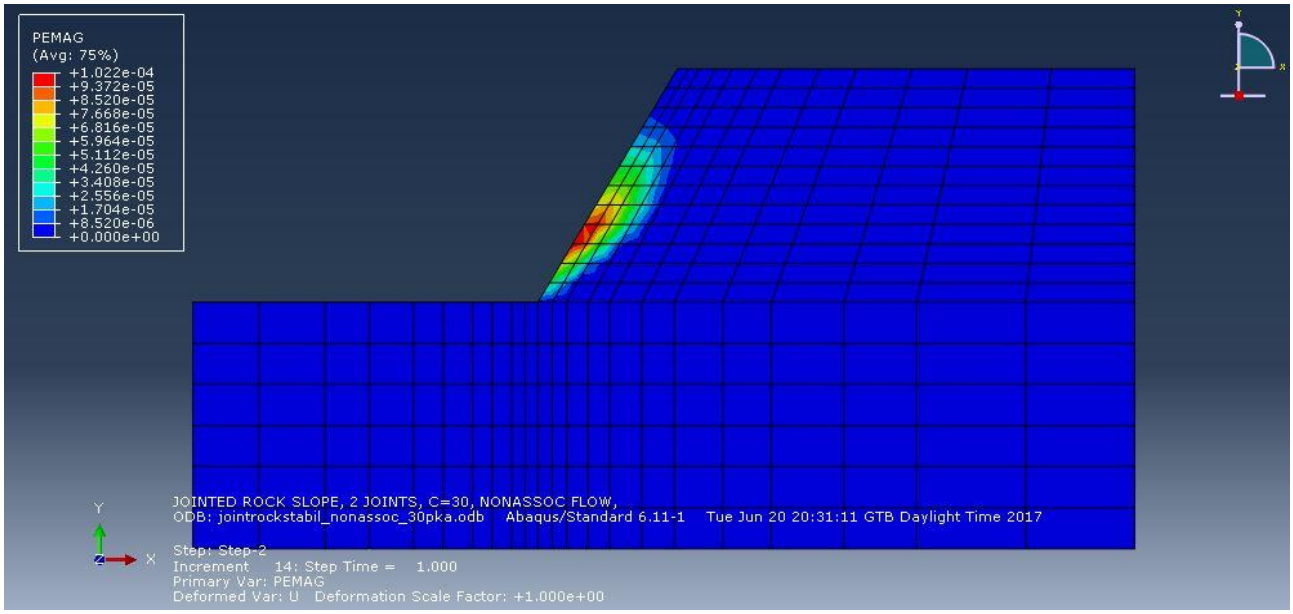

scale factor = 1e+00

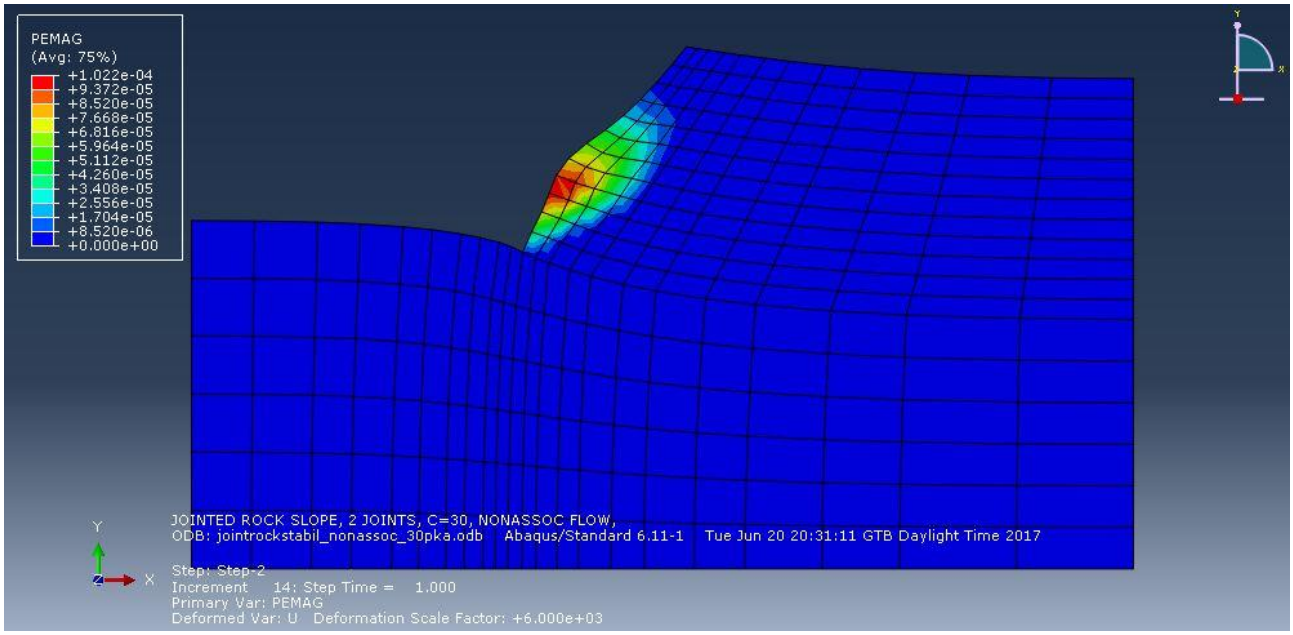

scale factor = 6e+03

- $\gamma = 26\ kN/m^3$

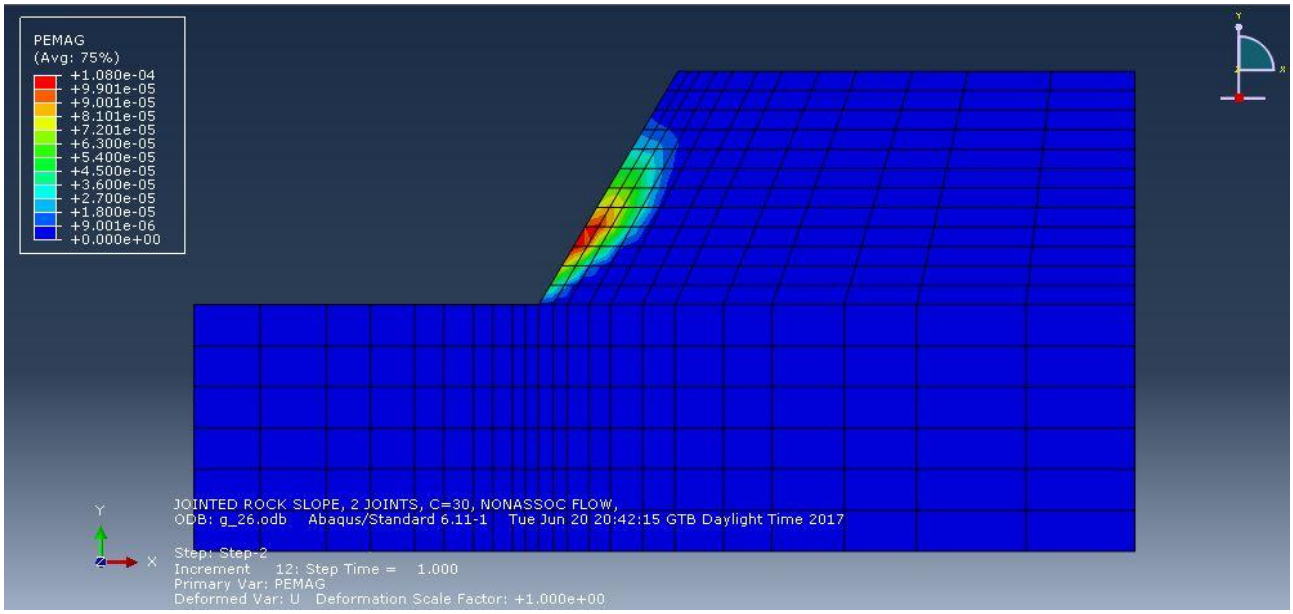

scale factor = 1e+00

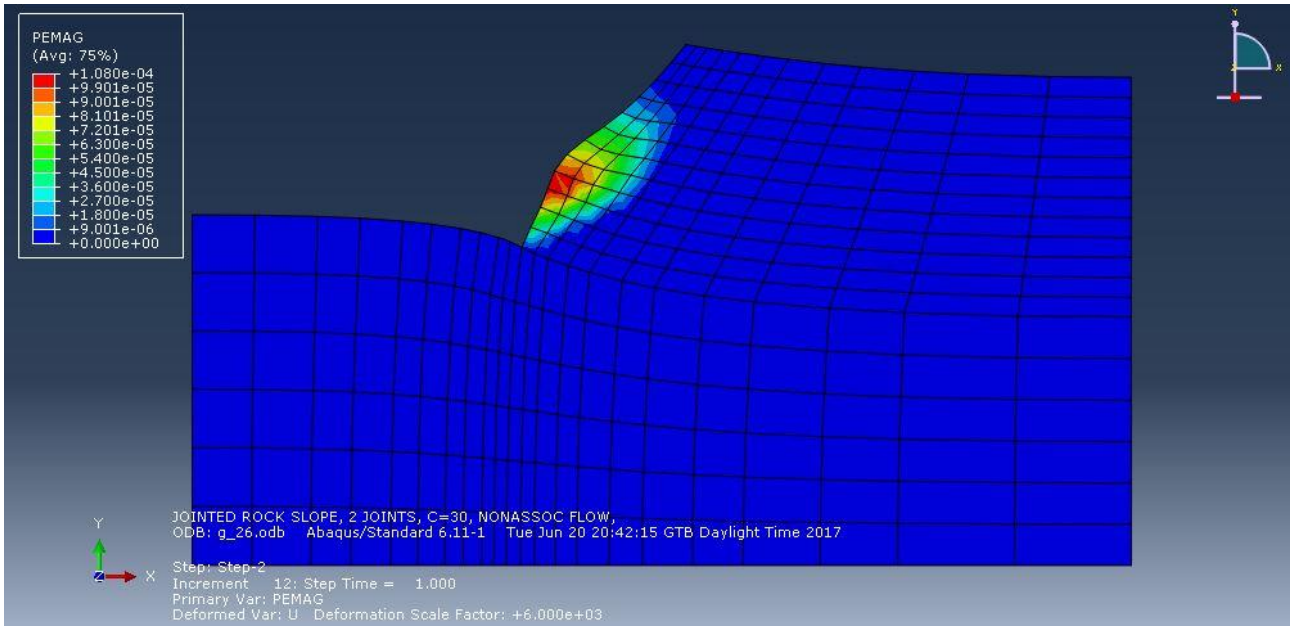

scale factor = 6e+03

Case study 3: variable parameter is friction angle φ

- $\varphi = 35^0$

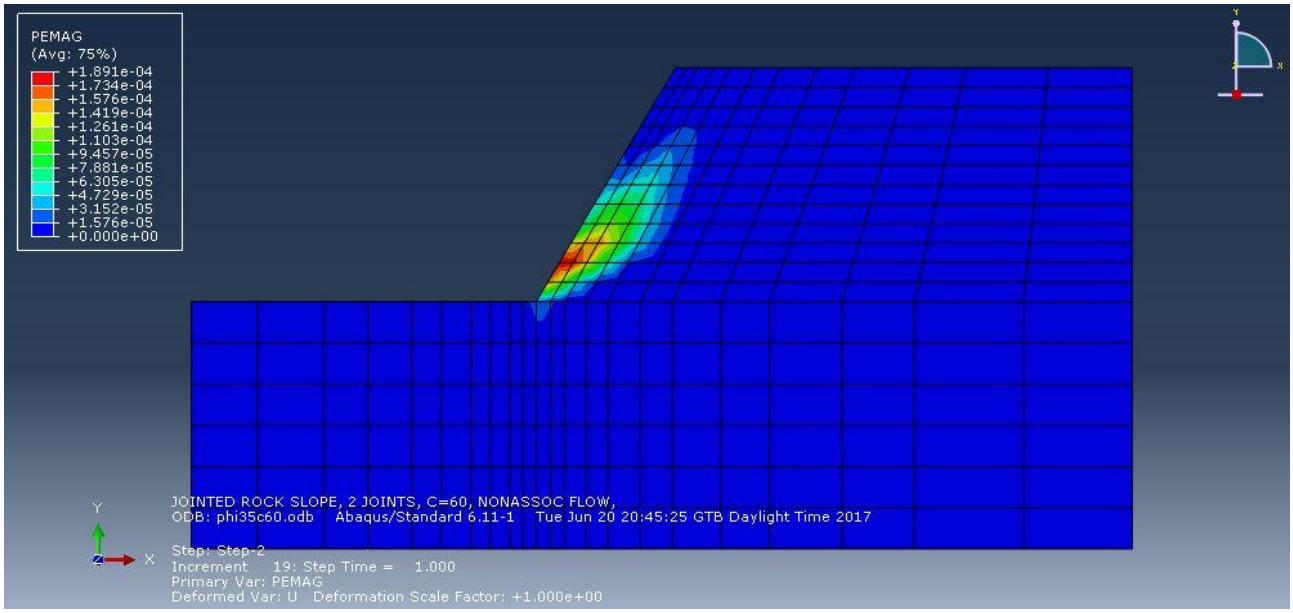

scale factor = 1e+00

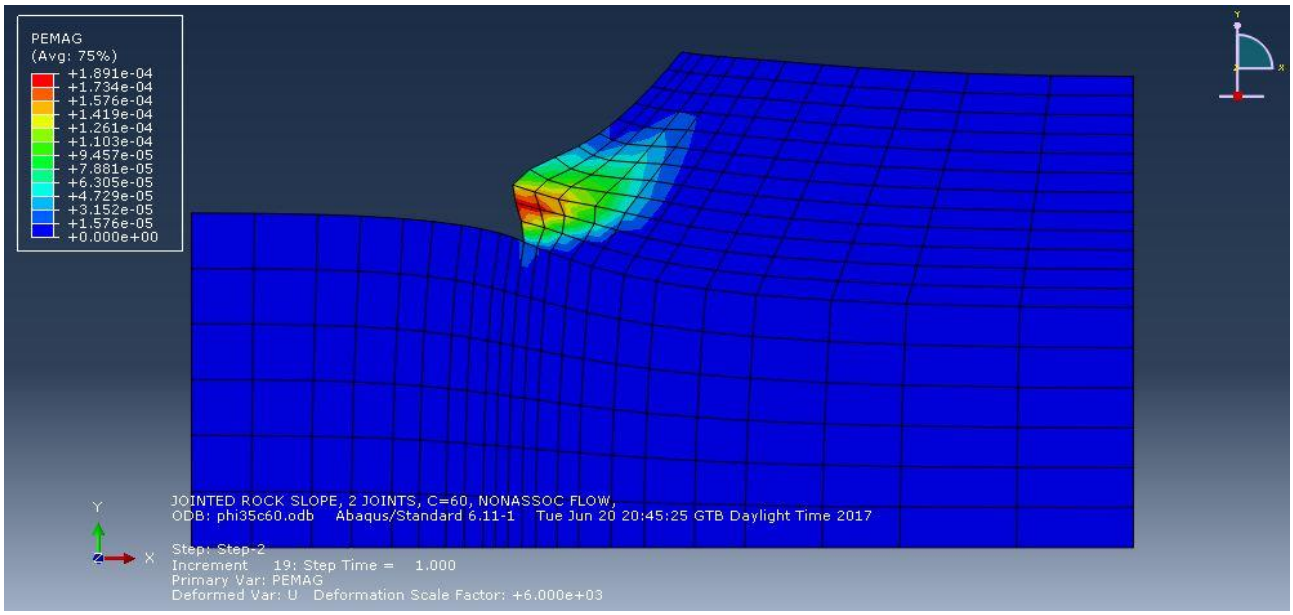

scale factor = 6e+03

- $\varphi = 40^0$

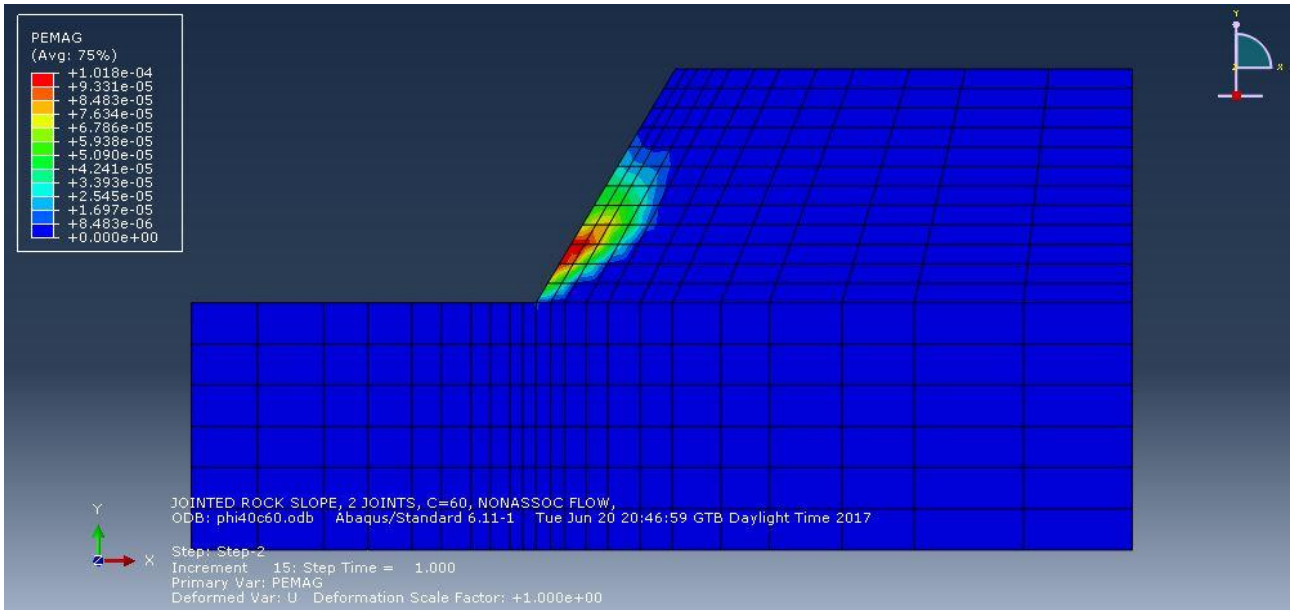

scale factor = 1e+00

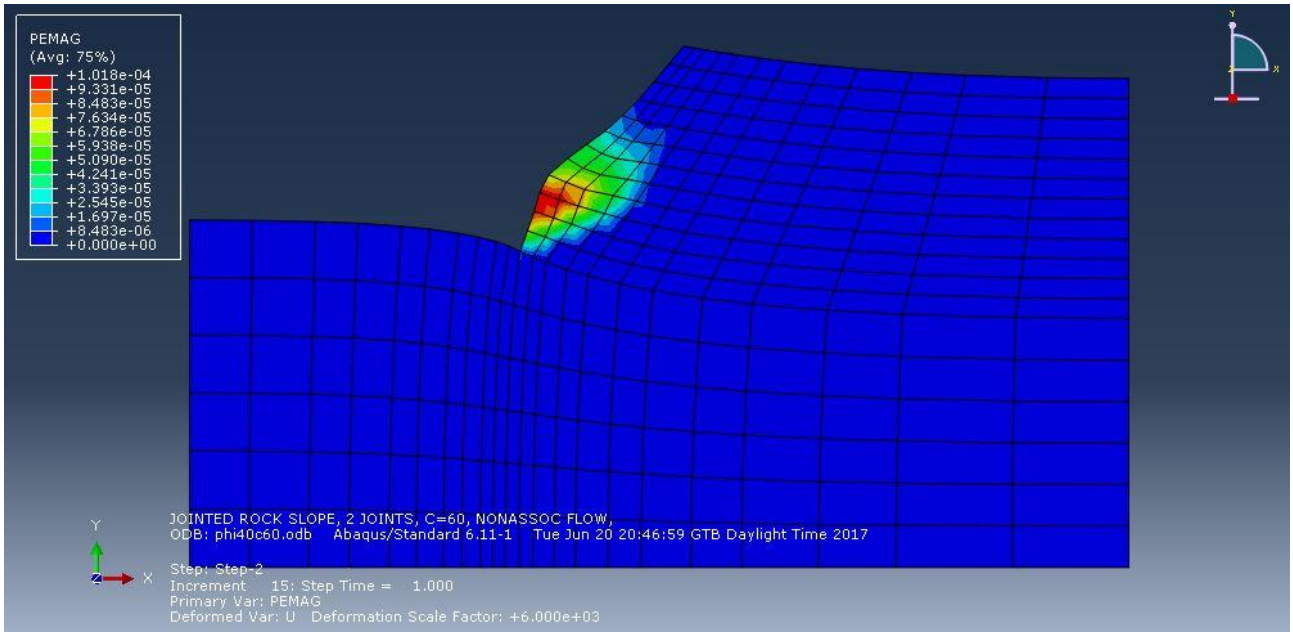

scale factor = 6e+03

- $\varphi = 45^0$

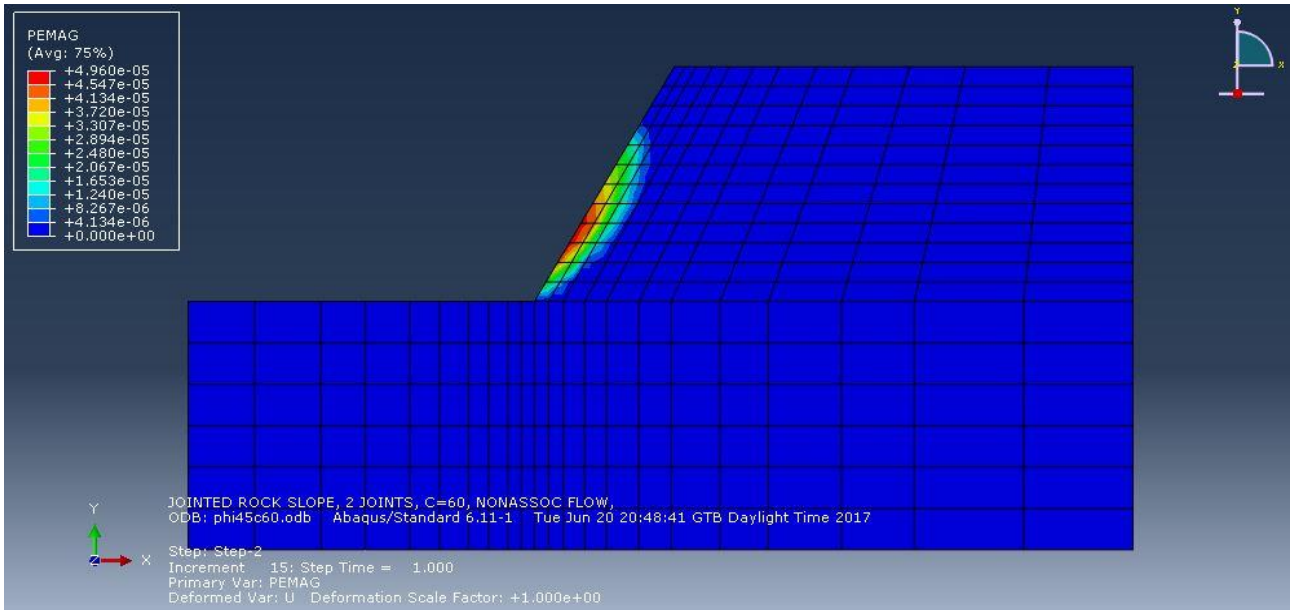

scale factor = 1e+00

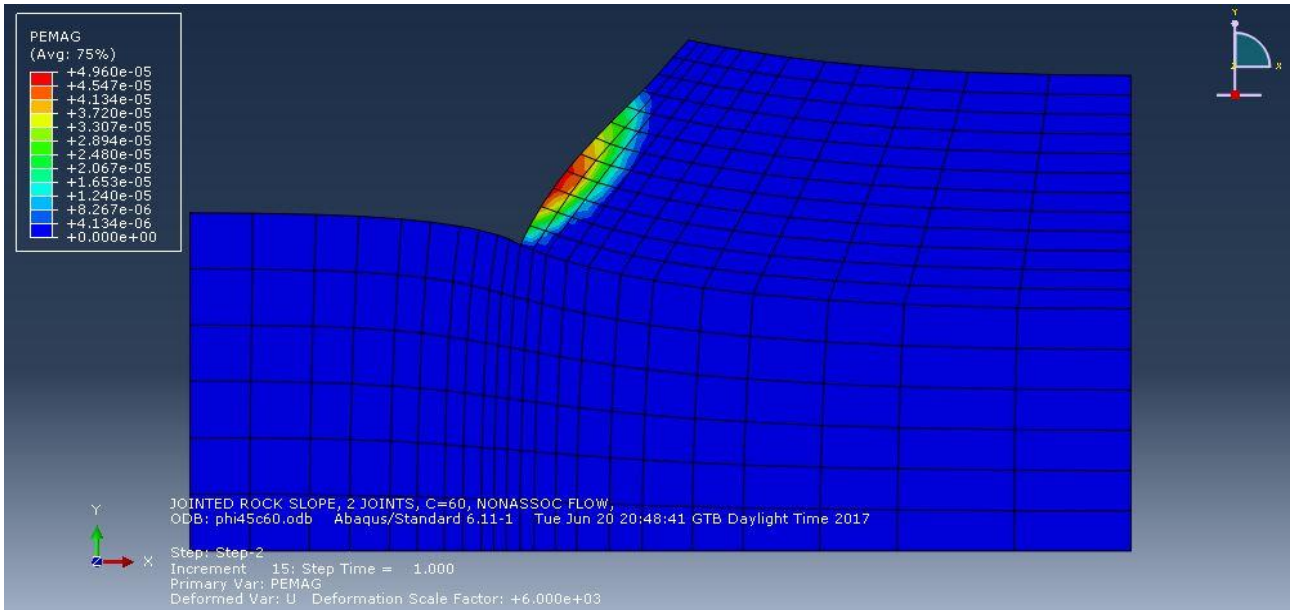

scale factor = 6e+03

- $\varphi = 50^0$

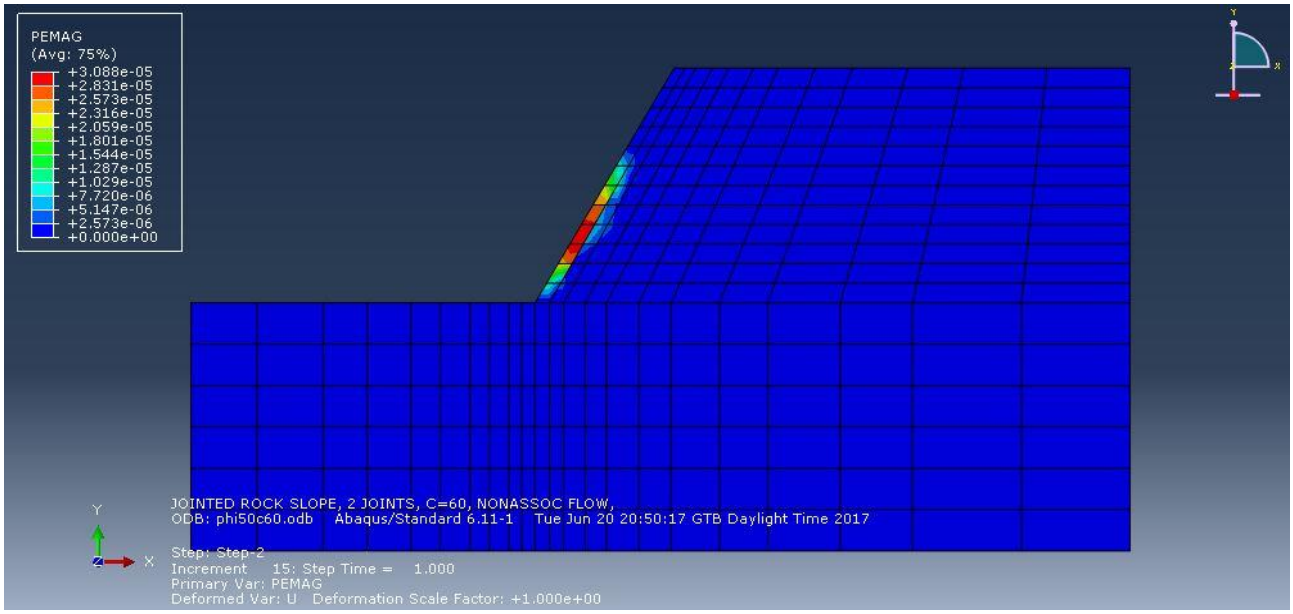

scale factor = 1e+00

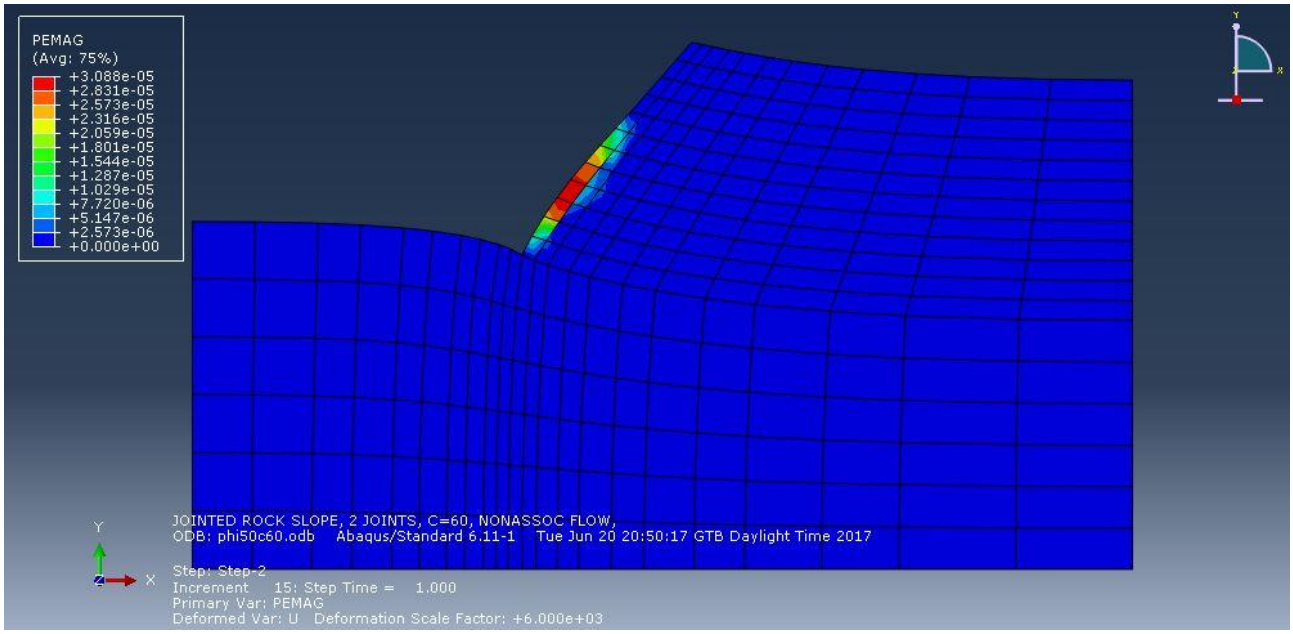

scale factor = 6e+03

Case study 4: variable parameter is cohesion c

- c = 30 kPa

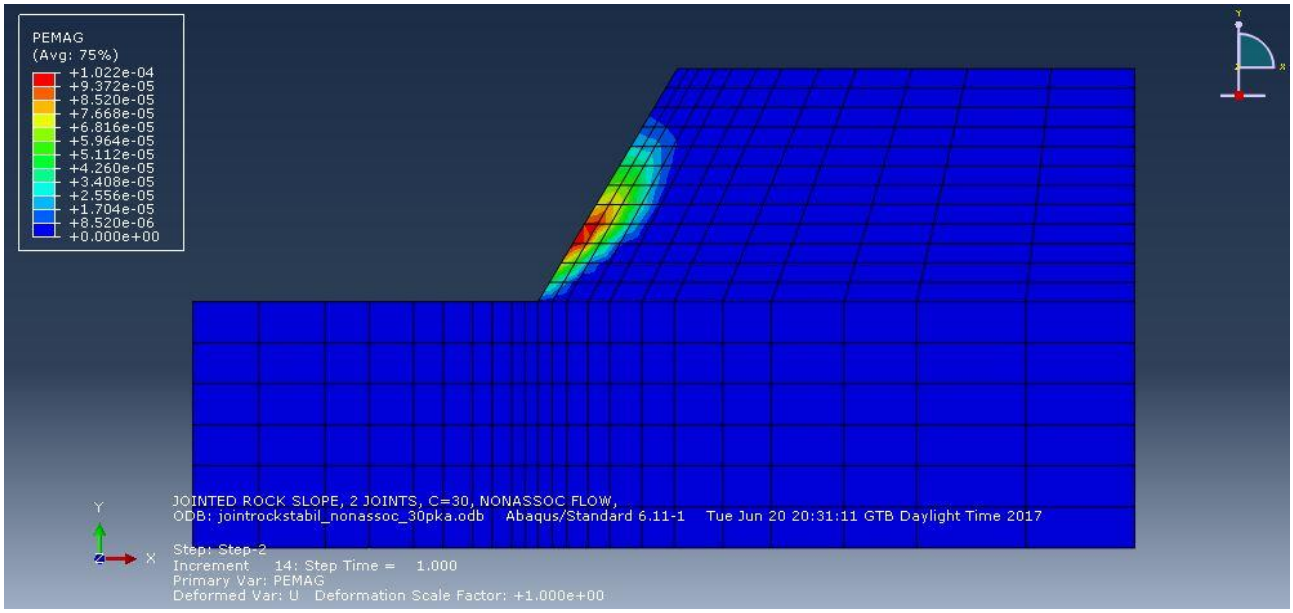

scale factor = 1e+00

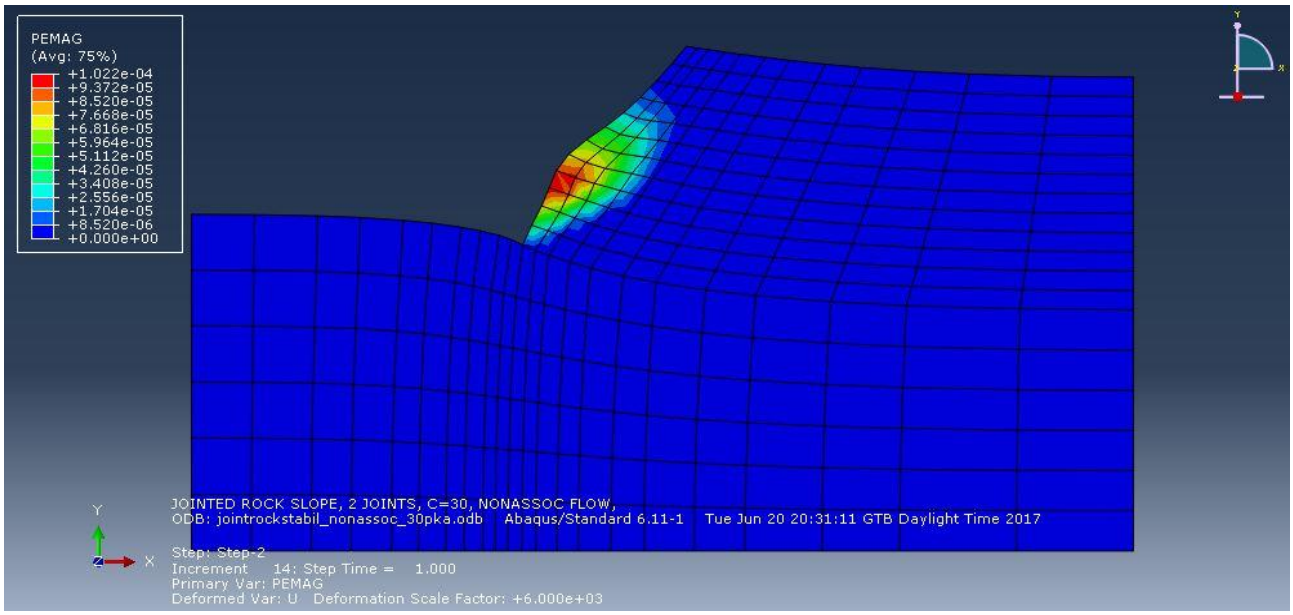

scale factor = 6e+03

- c = 50 kPa

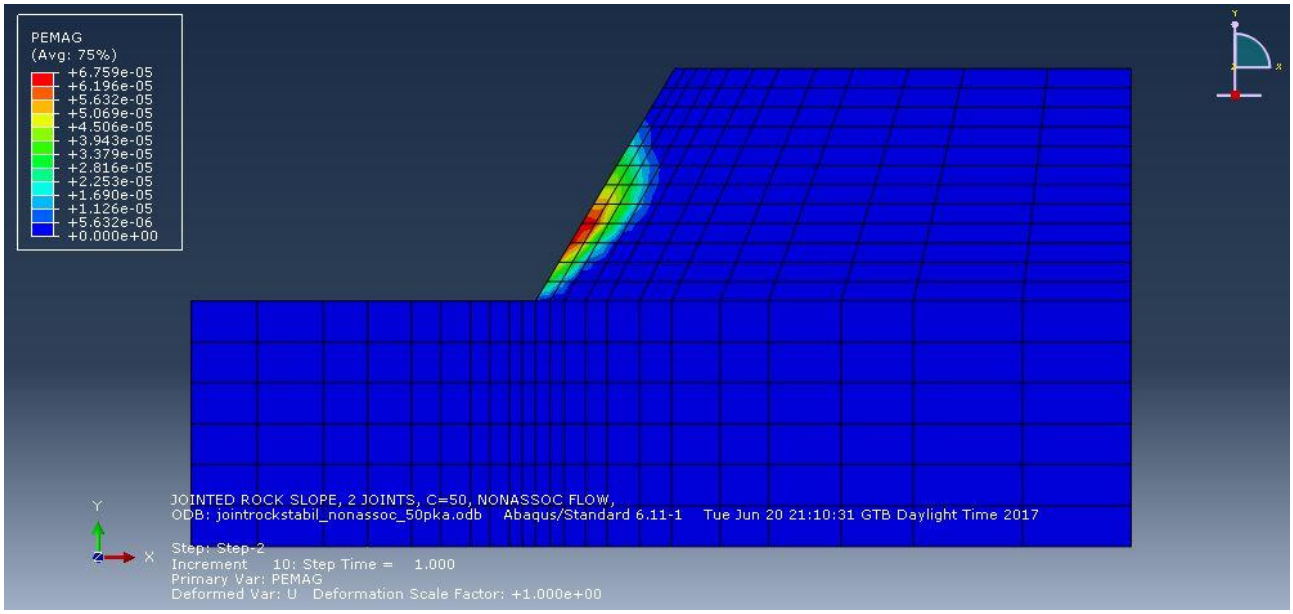

scale factor = 1e+00

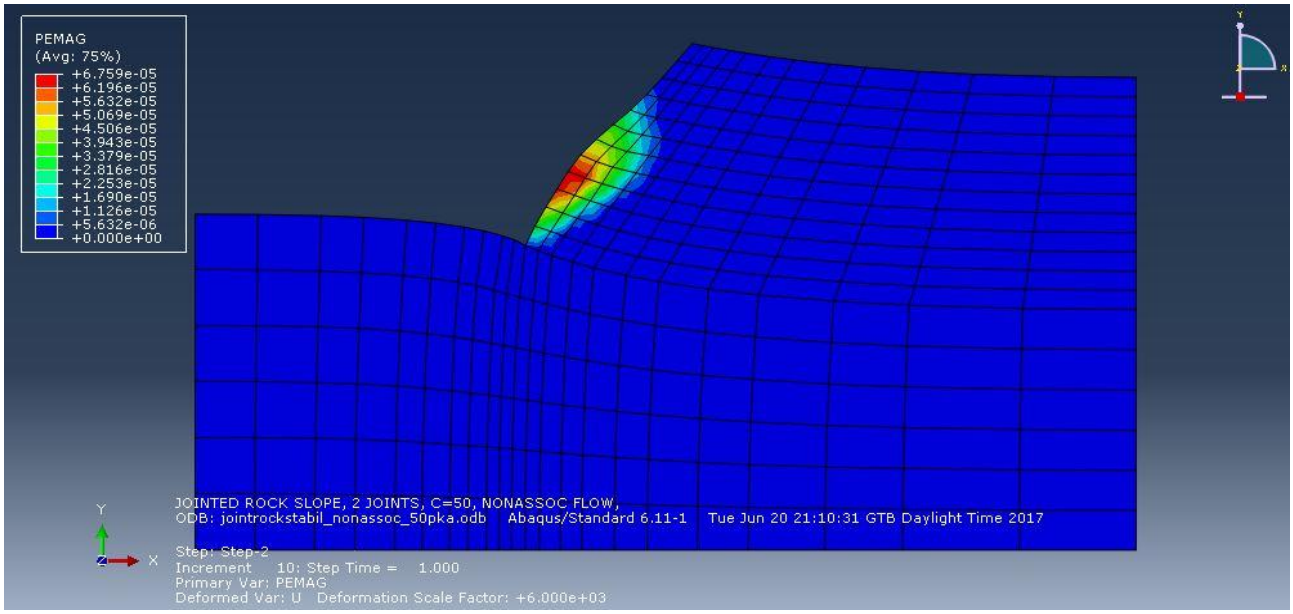

scale factor = 6e+03

- c = 80 kPa

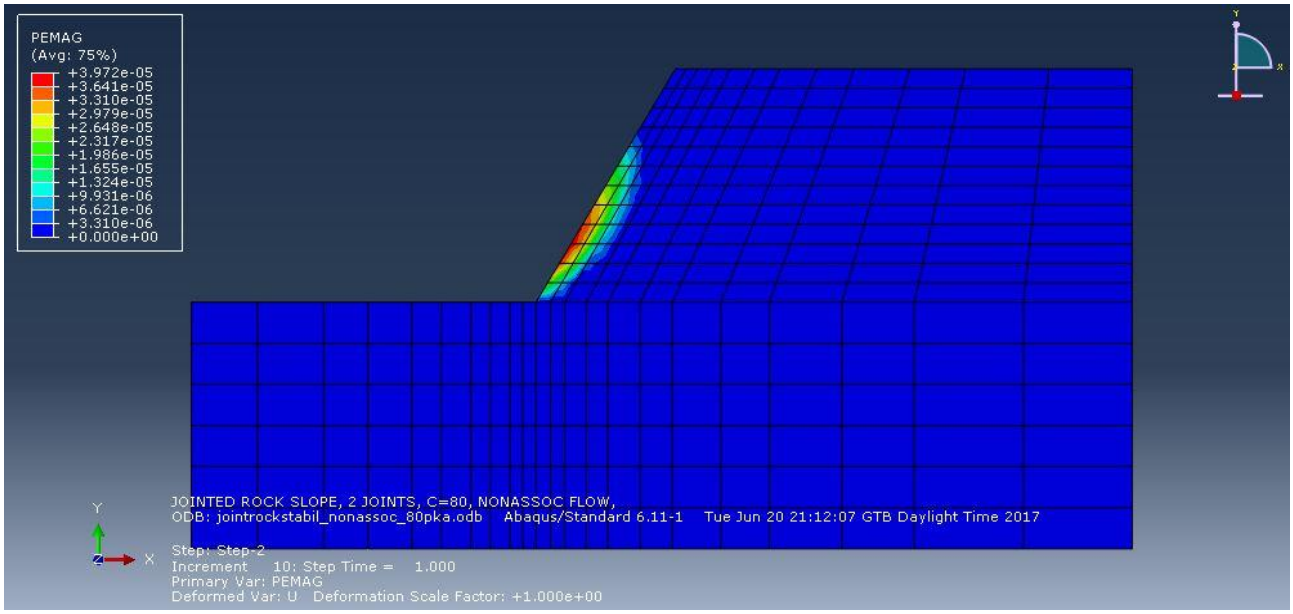

scale factor = 1e+00

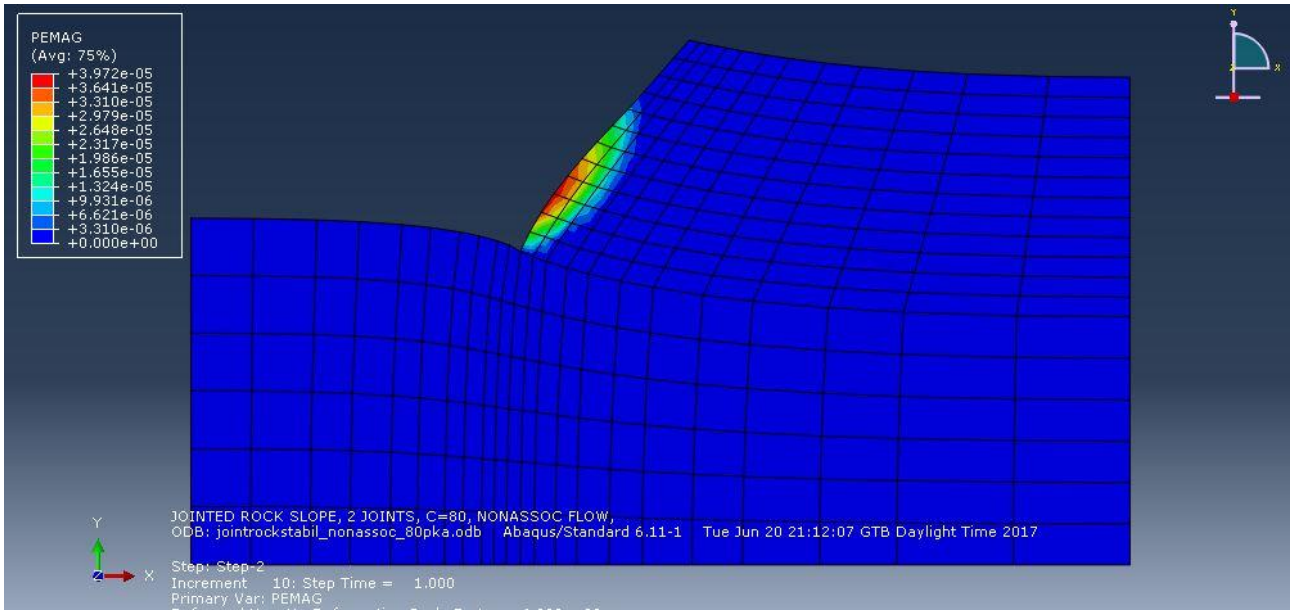

scale factor = 6e+03

- c = 100 kPa

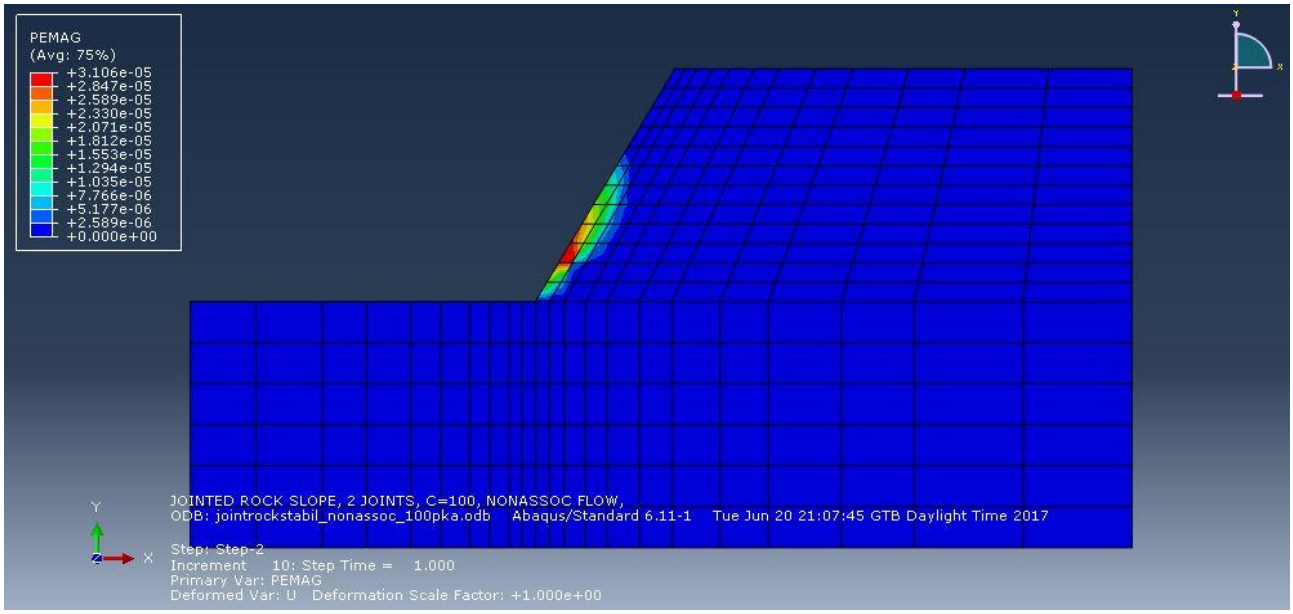

scale factor = 1e+00

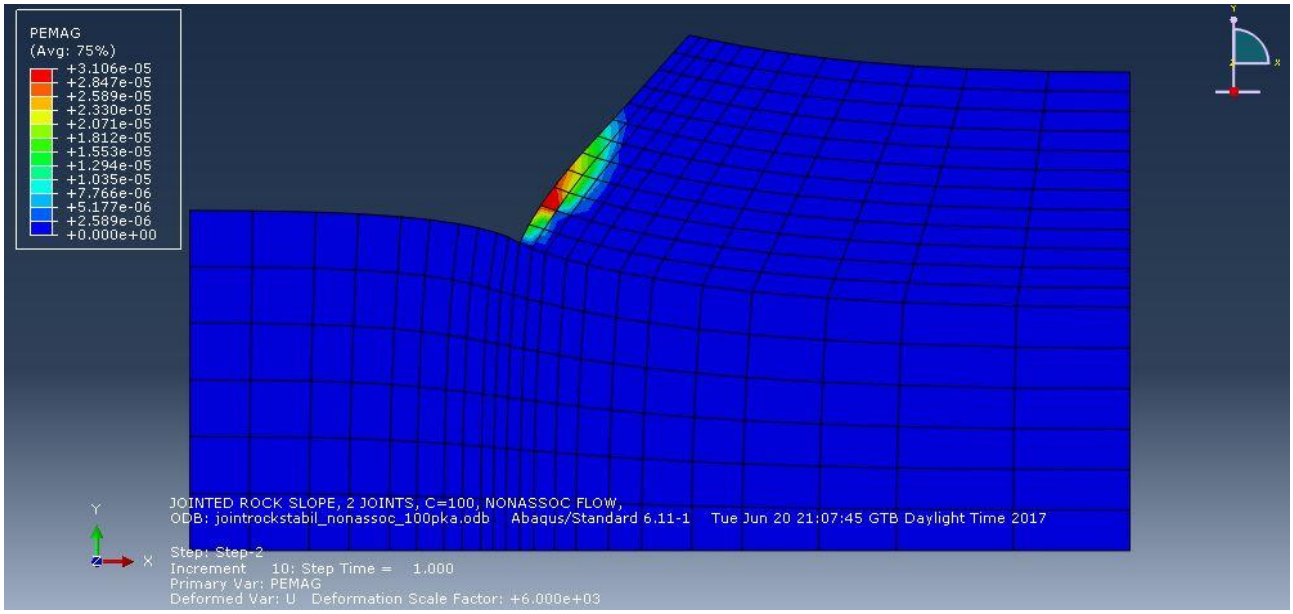

scale factor = 6e+03

- c = 120 kPa

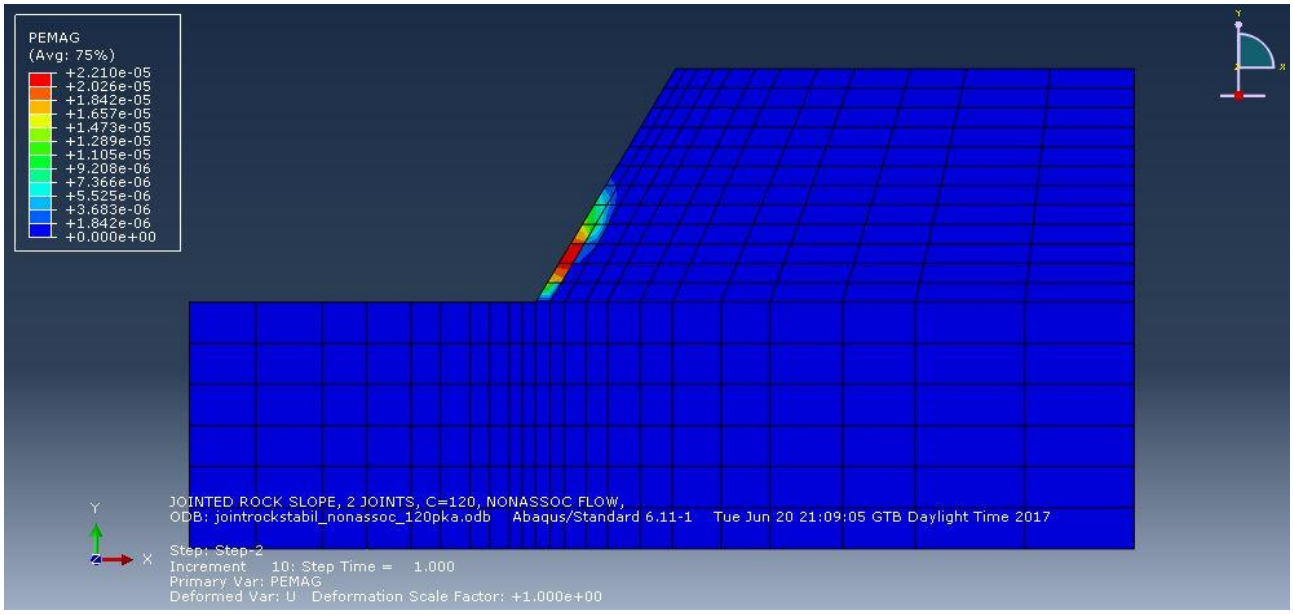

scale factor = 1e+00

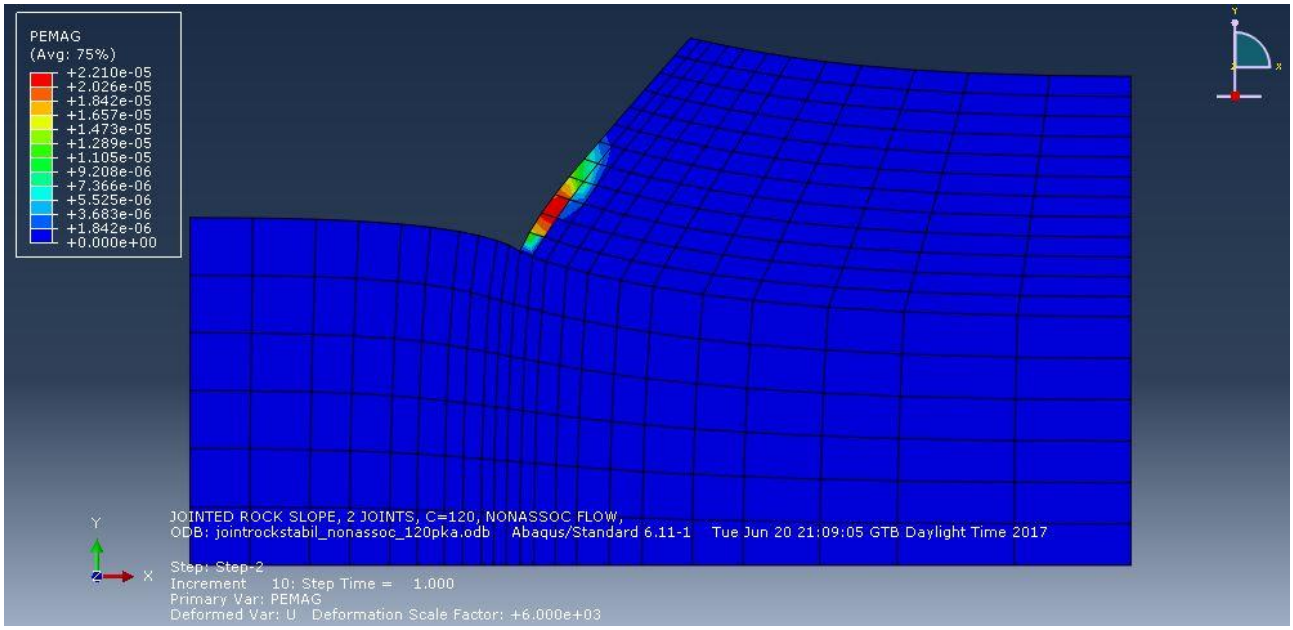

Case study 5: variable parameter is joint angle one of the joint sets (constant joint angle = 90^0)

- joint angle = 20^0

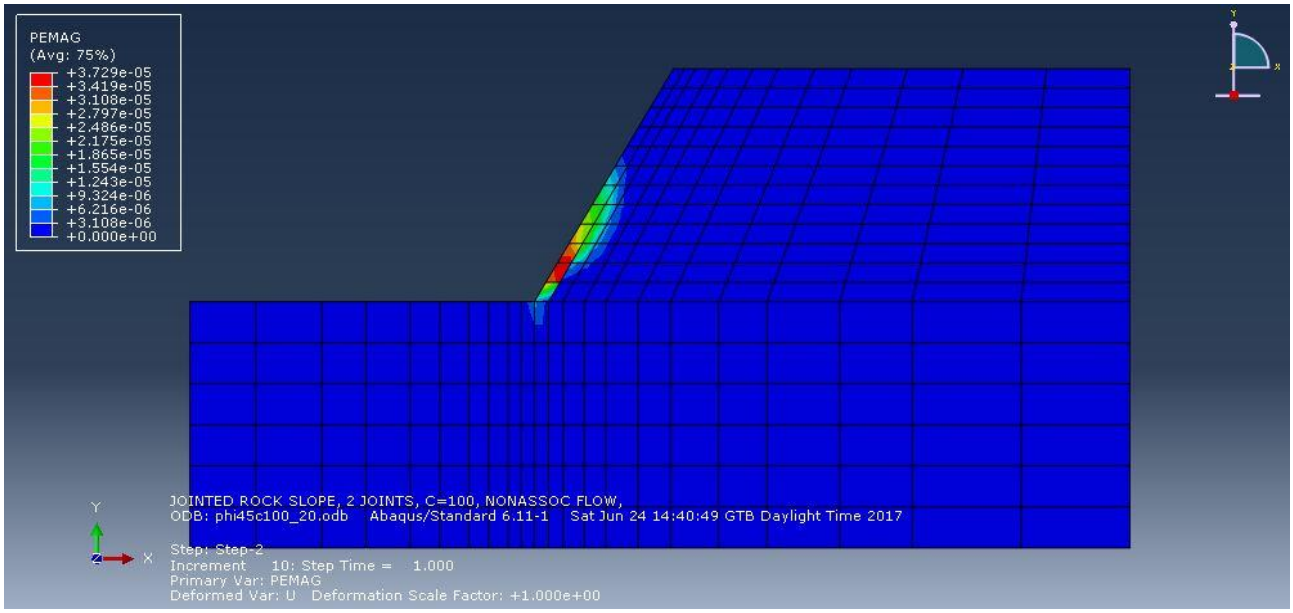

scale factor = 1e+00

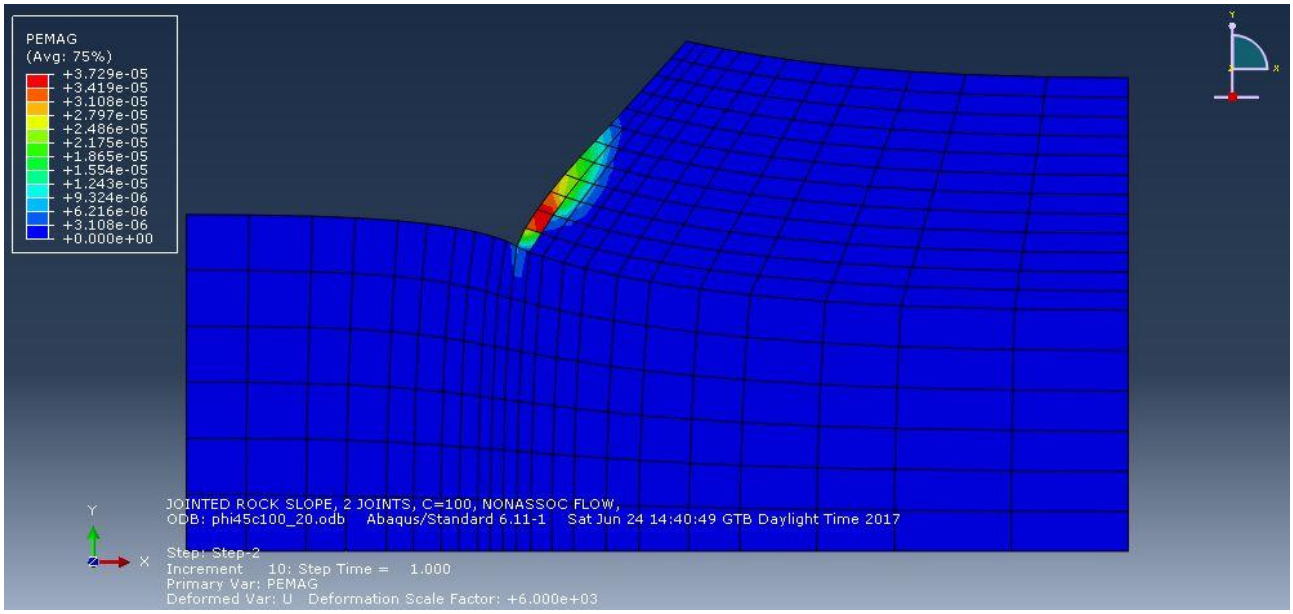

scale factor = 6e+03

- joint angle = 30^0

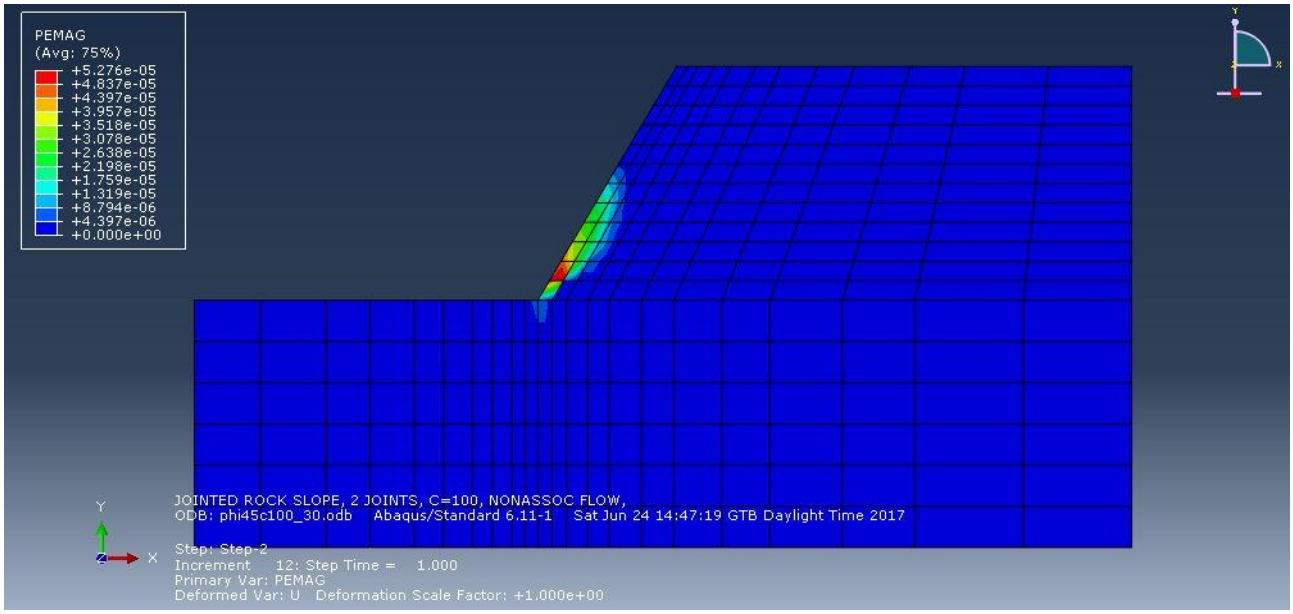

scale factor = 1e+00

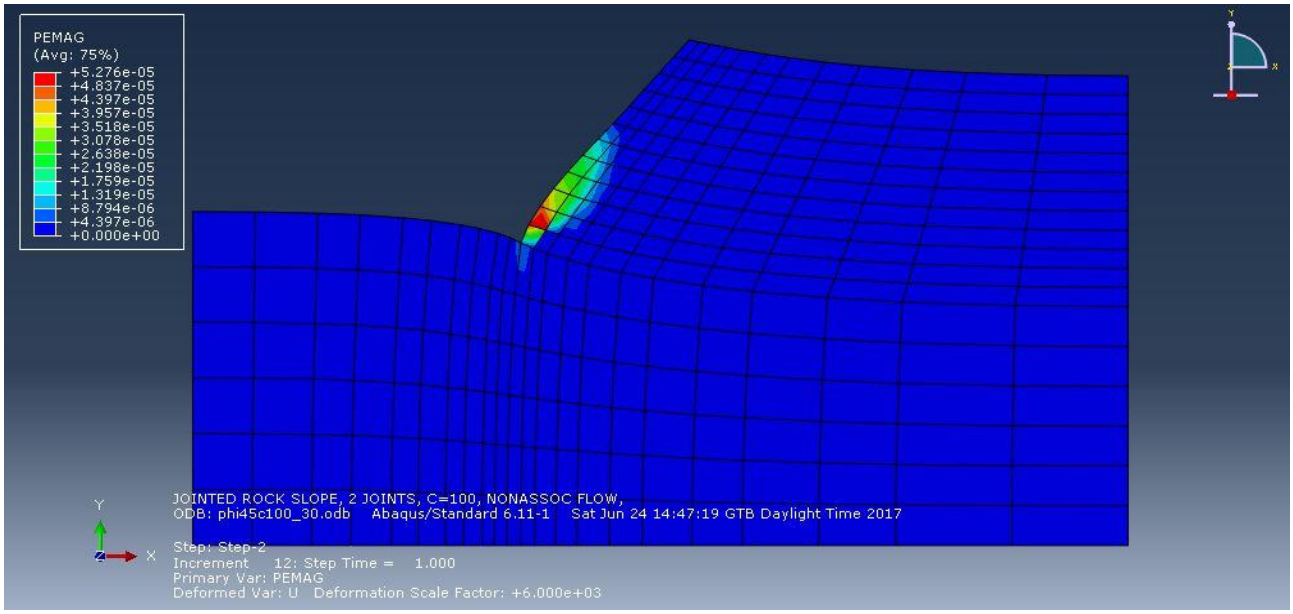

scale factor = 6e+03

- joint angle = 40^0

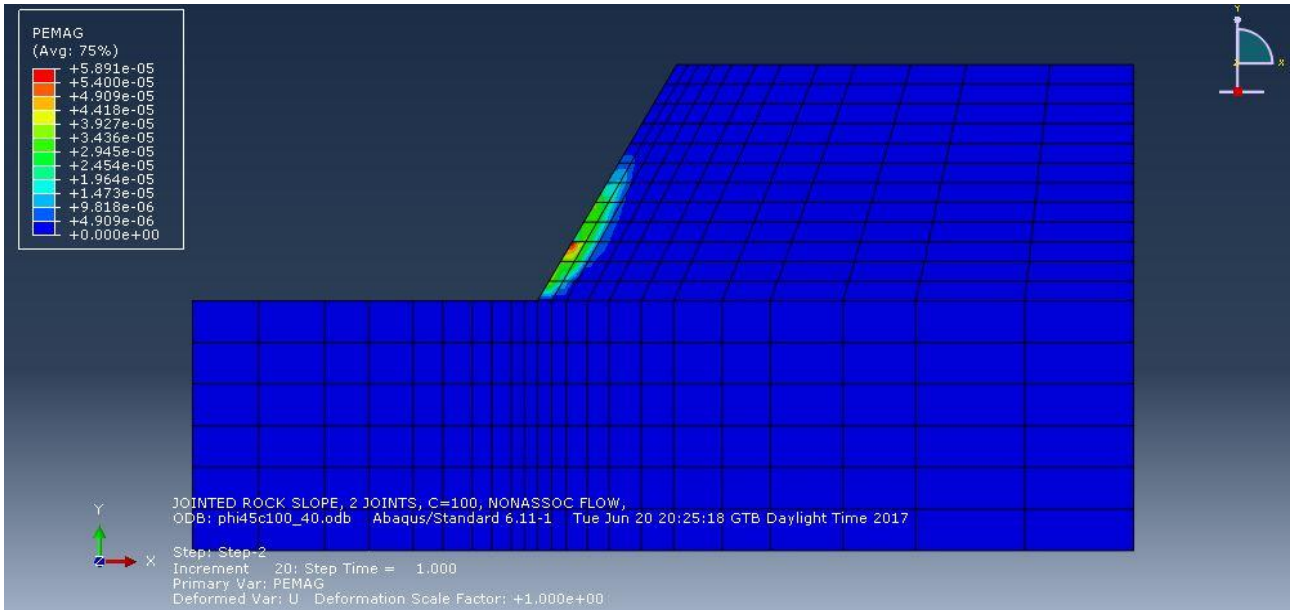

scale factor = 1e+00

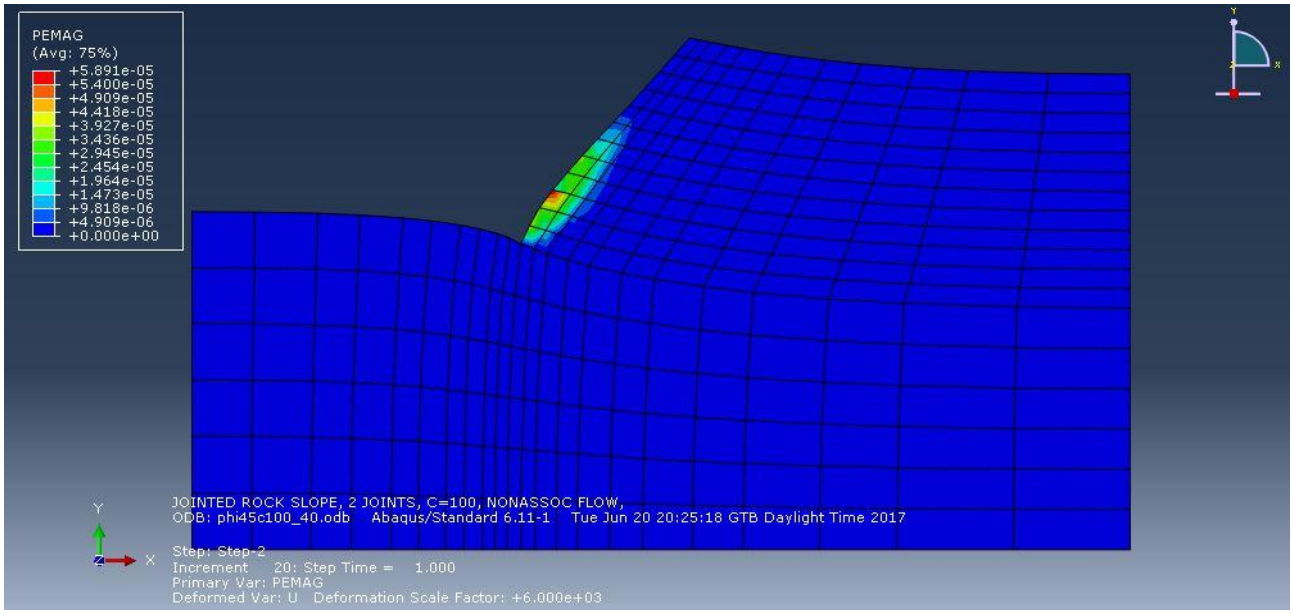

scale factor = 6e+03

- joint angle = 50^0

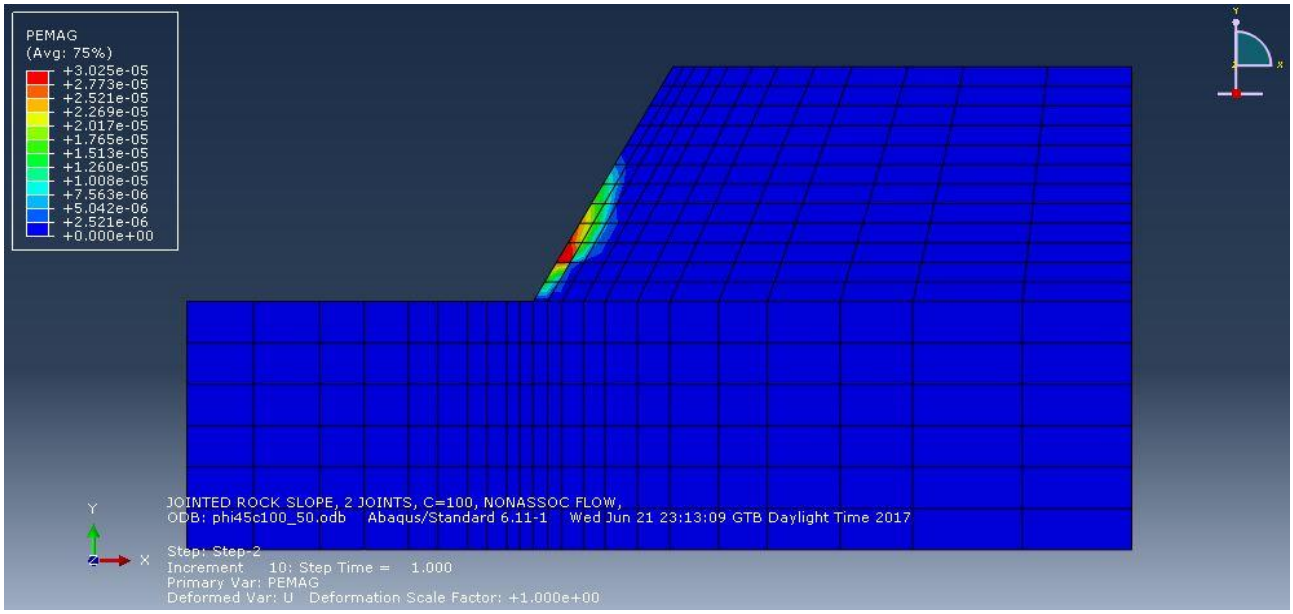

scale factor = 1e+00

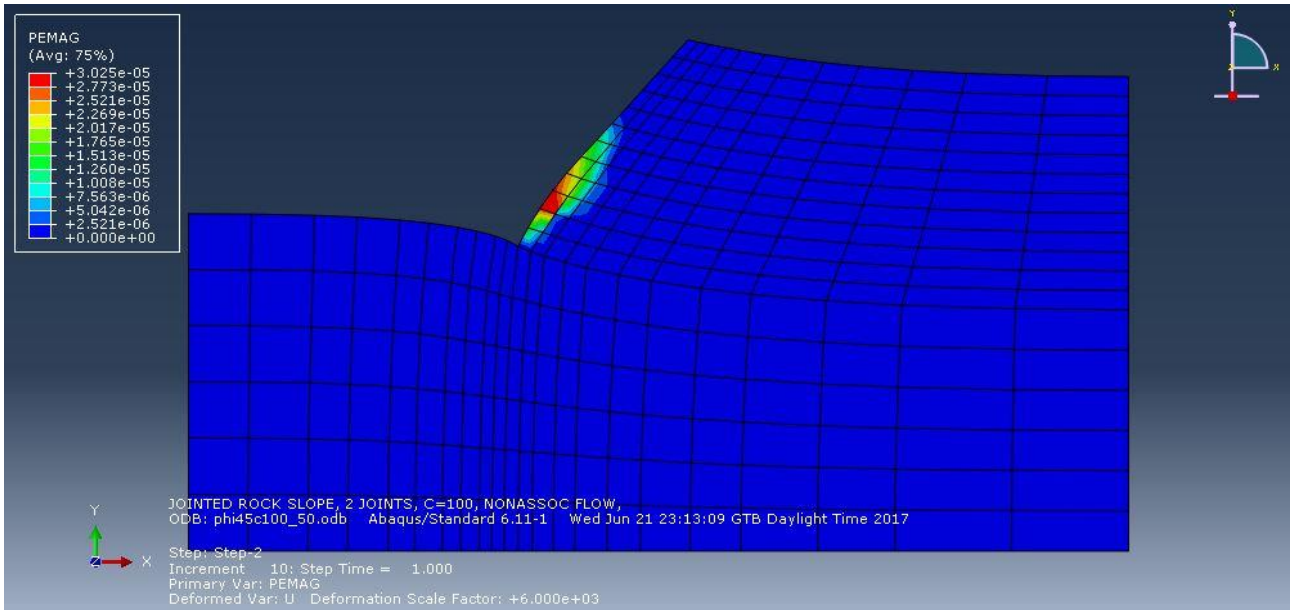

scale factor = 6e+03

- joint angle = 60^0

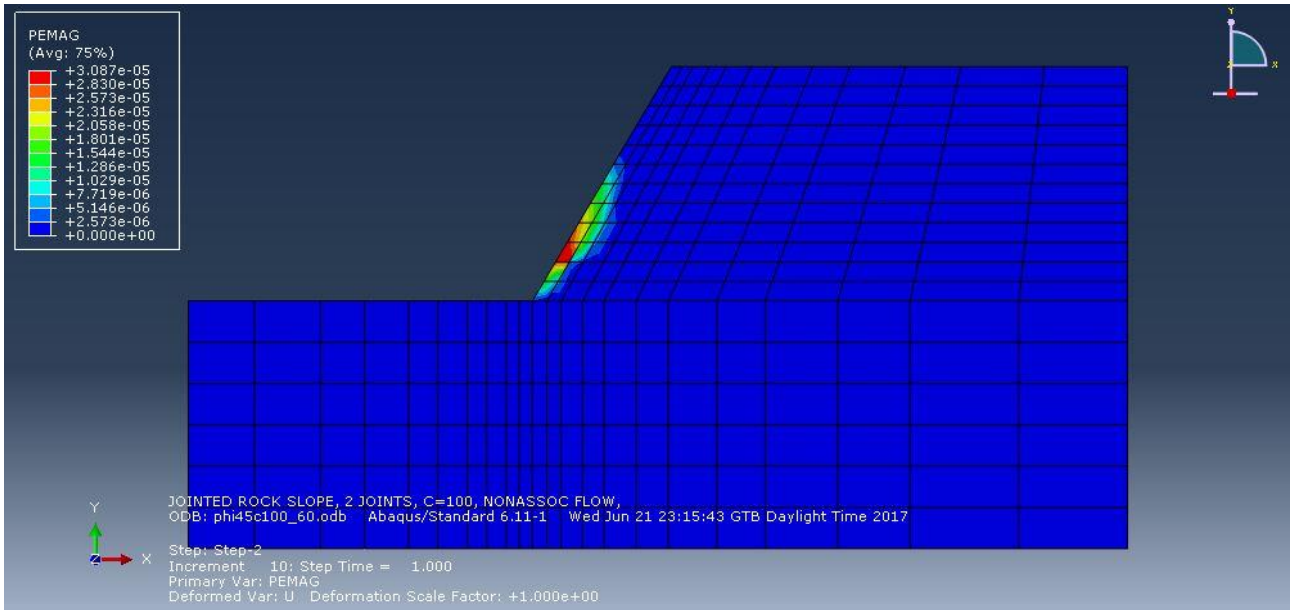

scale factor = 1e+00

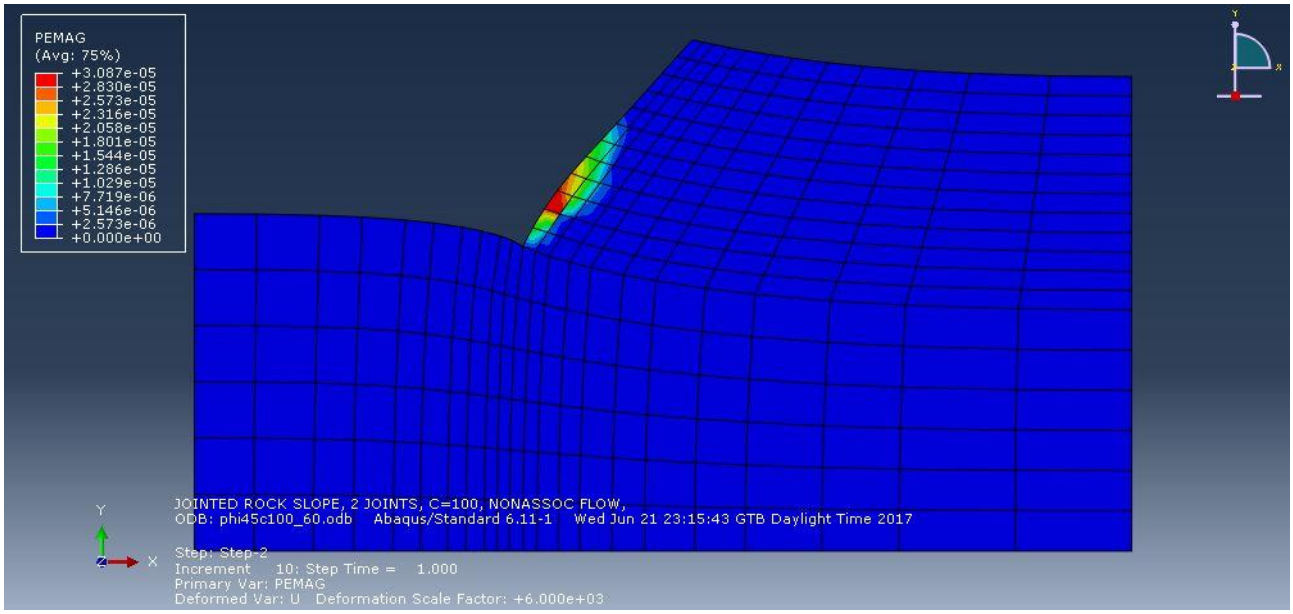

scale factor = 6e+03

- joint angle = 70^0

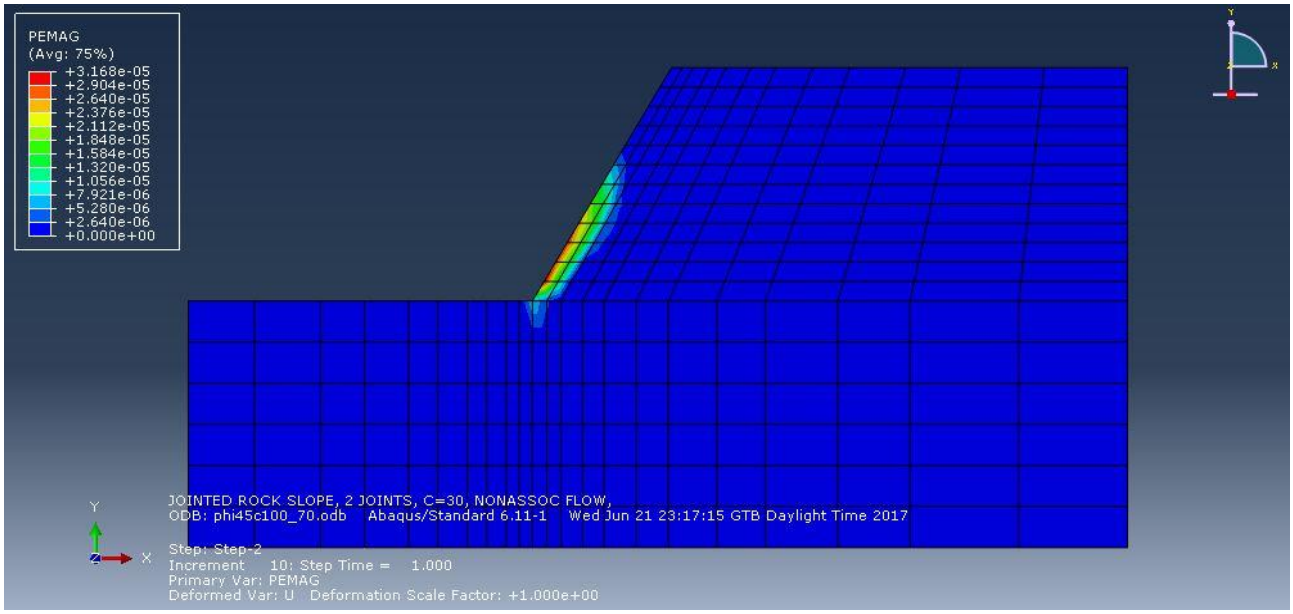

scale factor = 1e+00

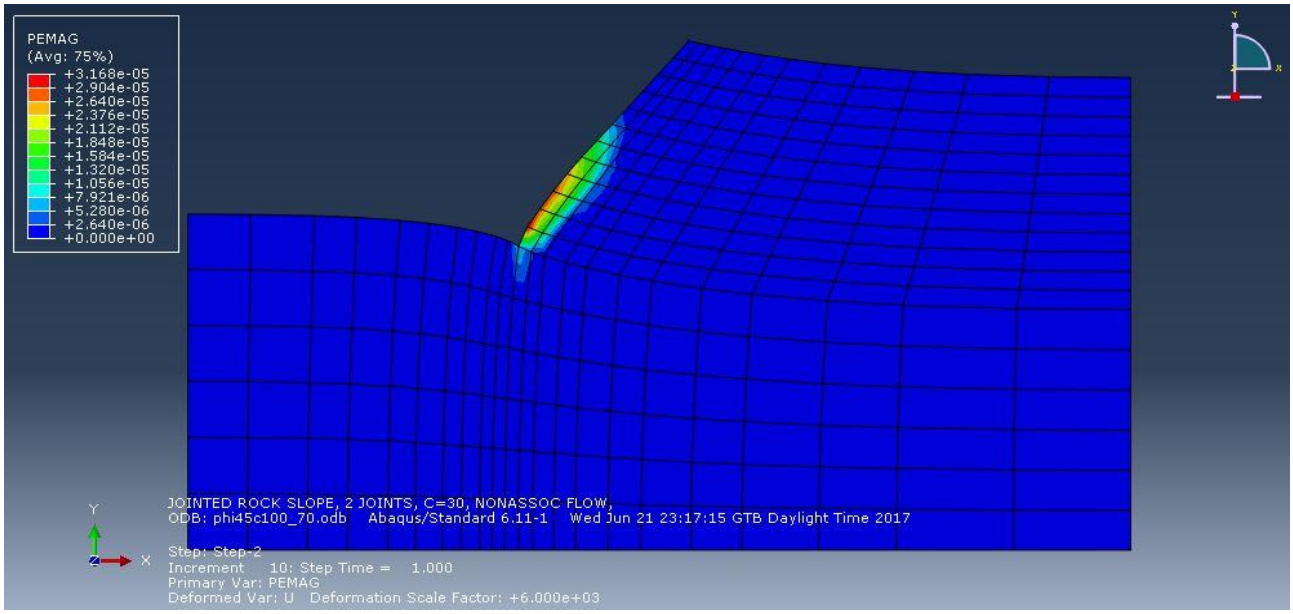

scale factor = 6e+03

Case study 6: rock slope with one joint set, variable parameter is joint angle

- joint angle = 20^0

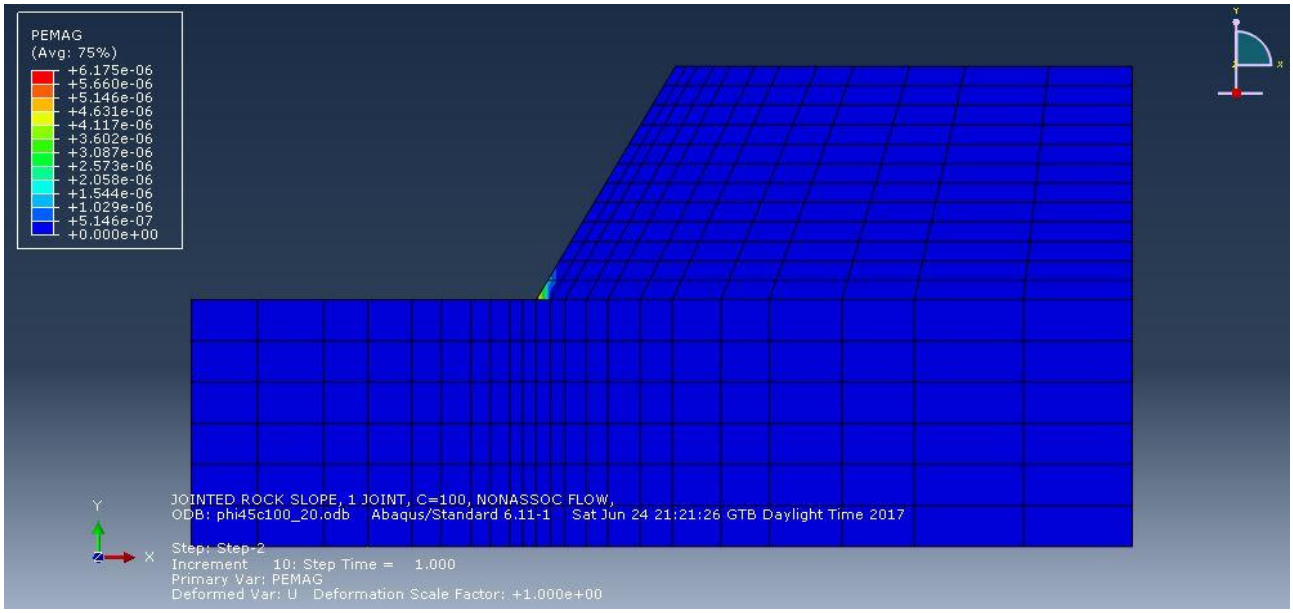

scale factor = 1e+00

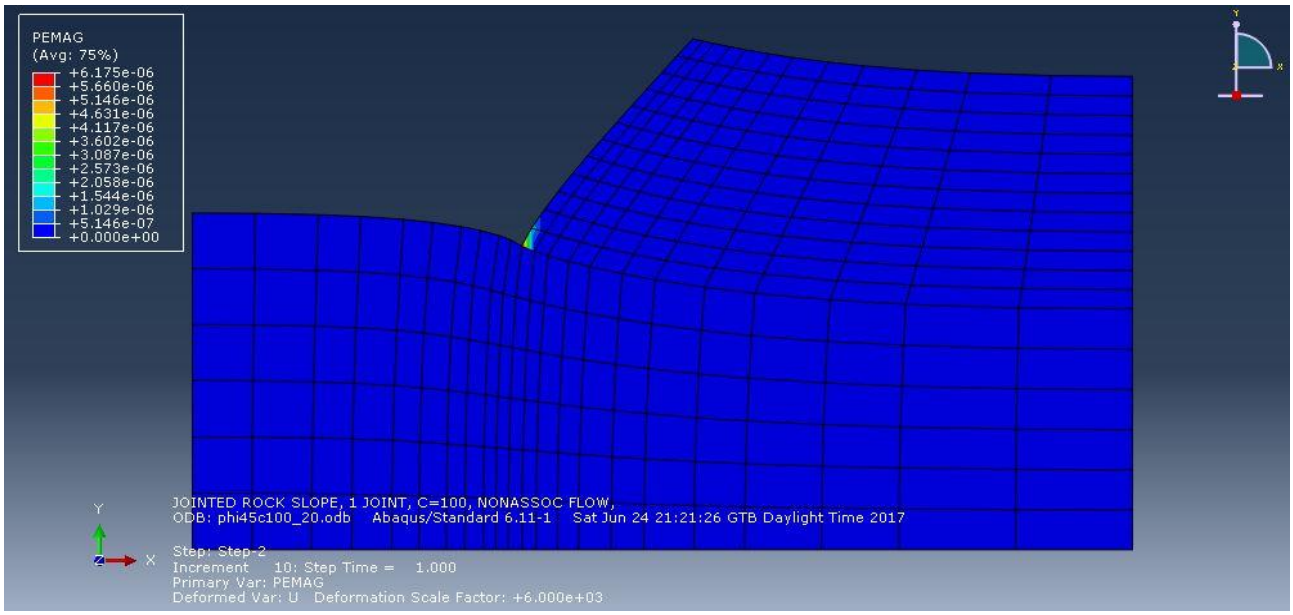

scale factor = 6e+03

- joint angle = 30^0

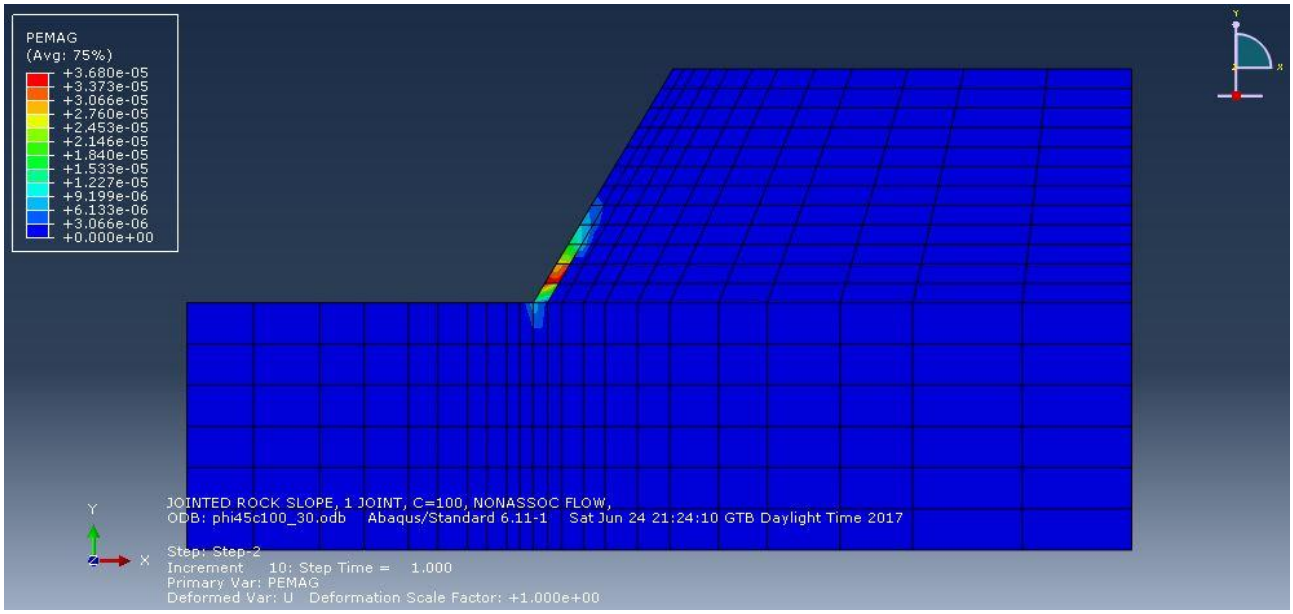

scale factor = 1e+00

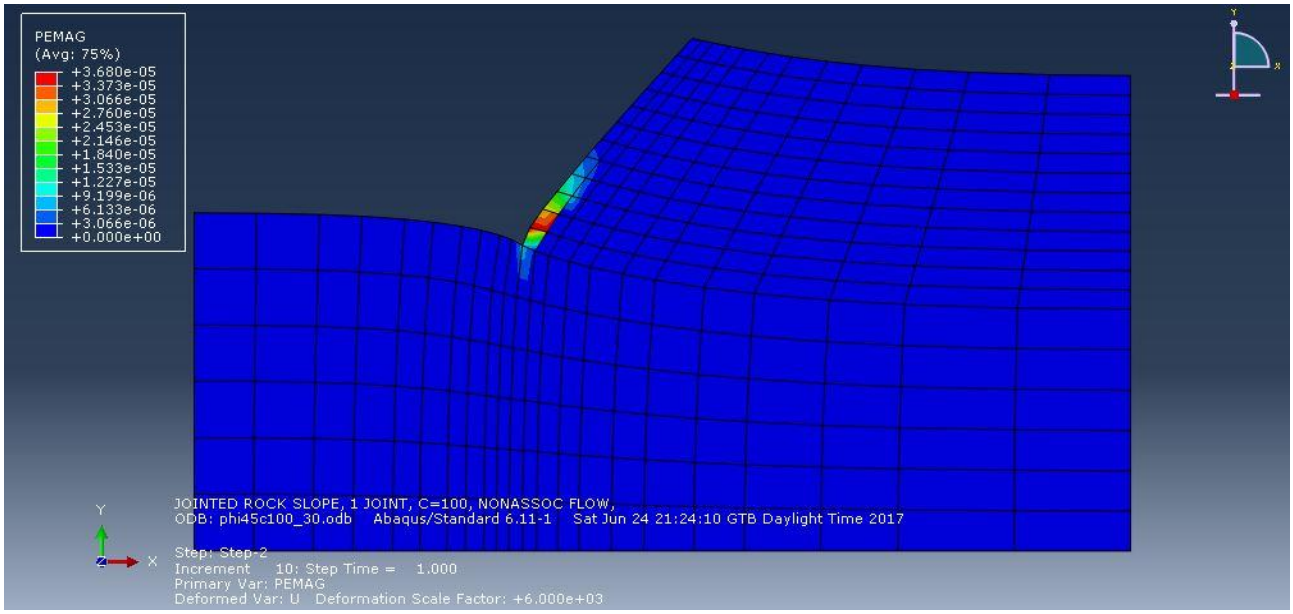

scale factor = 6e+03

- joint angle = 40^0

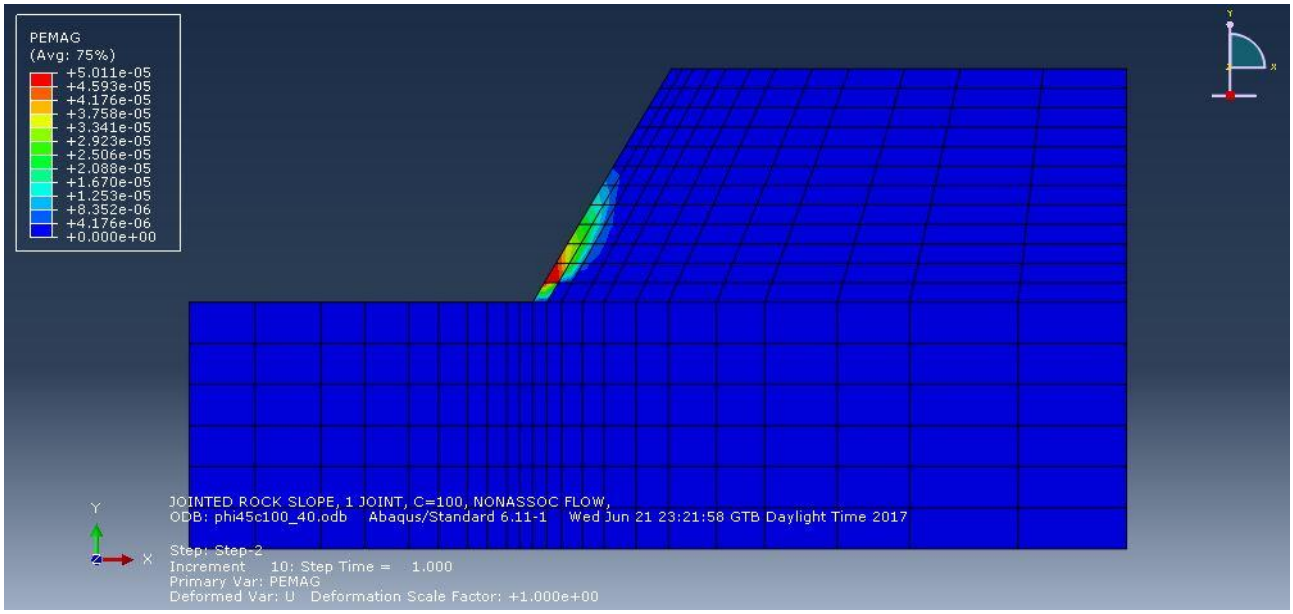

scale factor = 1e+00

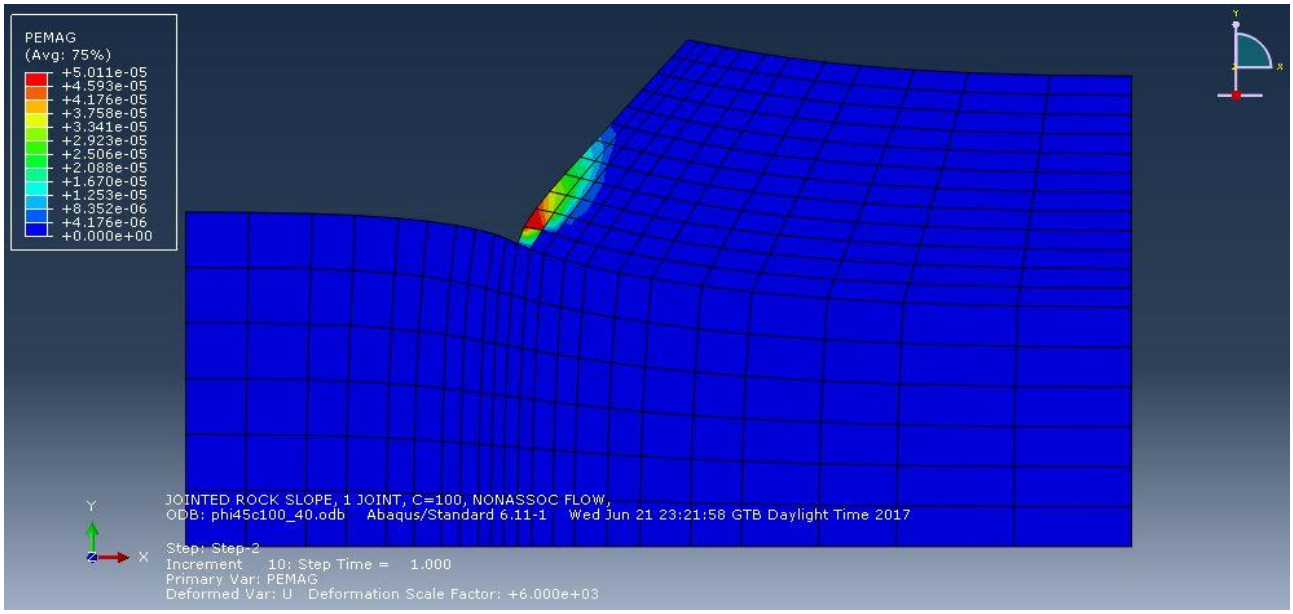

scale factor = 6e+03

- joint angle = 50^0

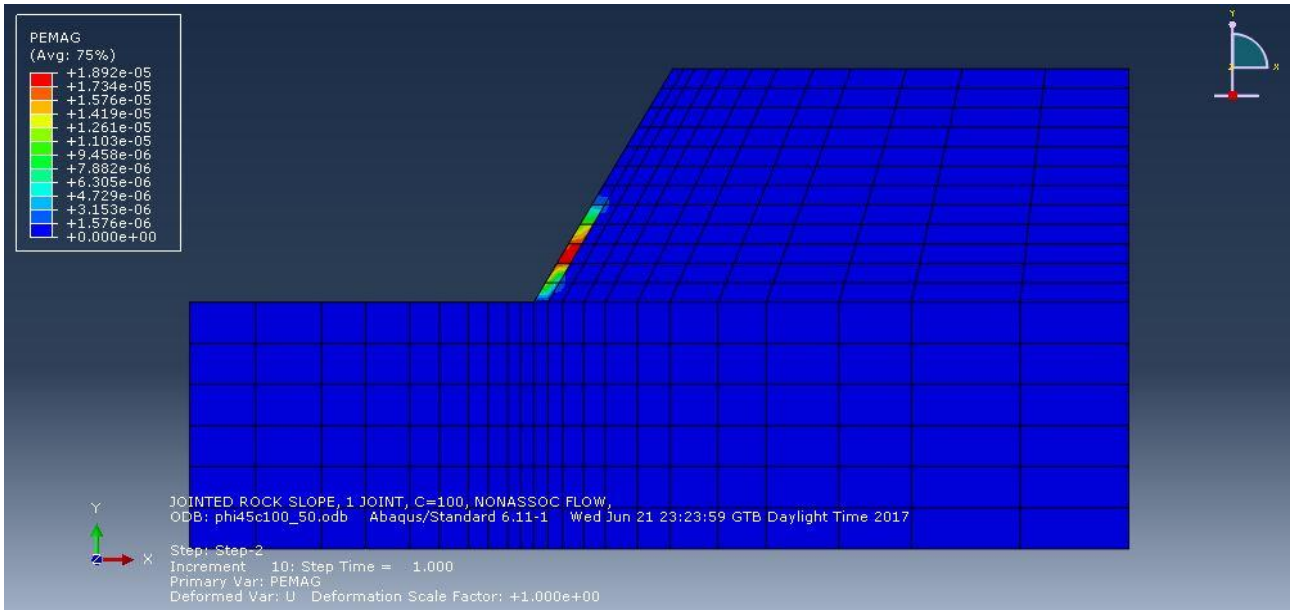

scale factor = 1e+00

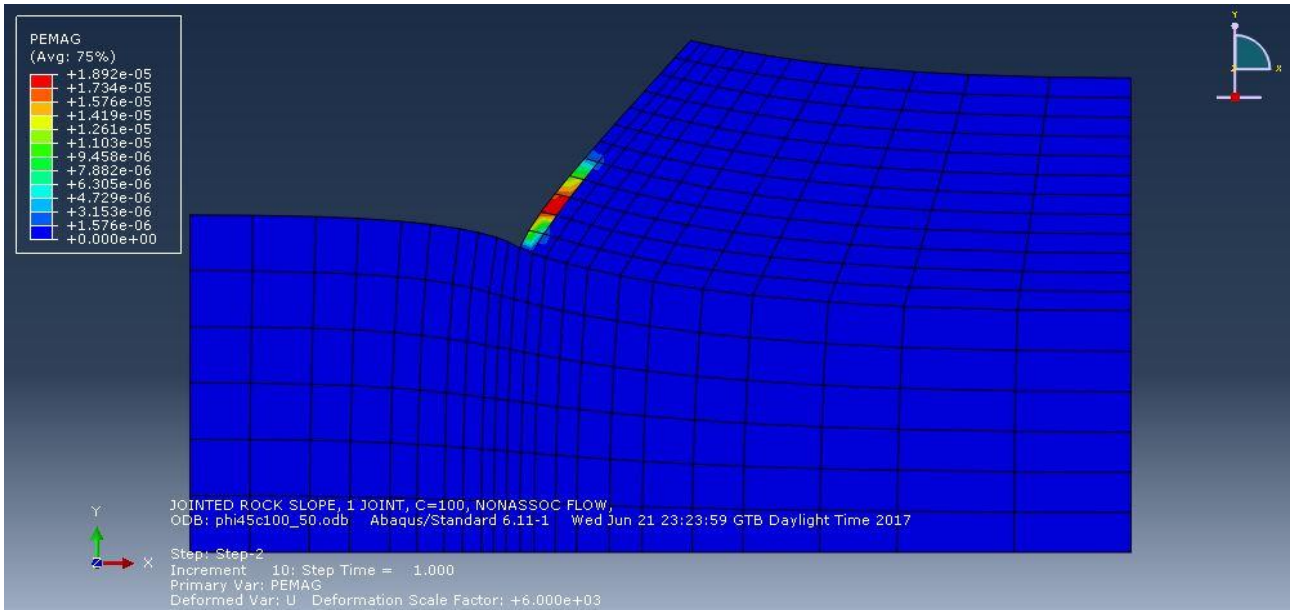

scale factor = 6e+03

- joint angle = 60^0

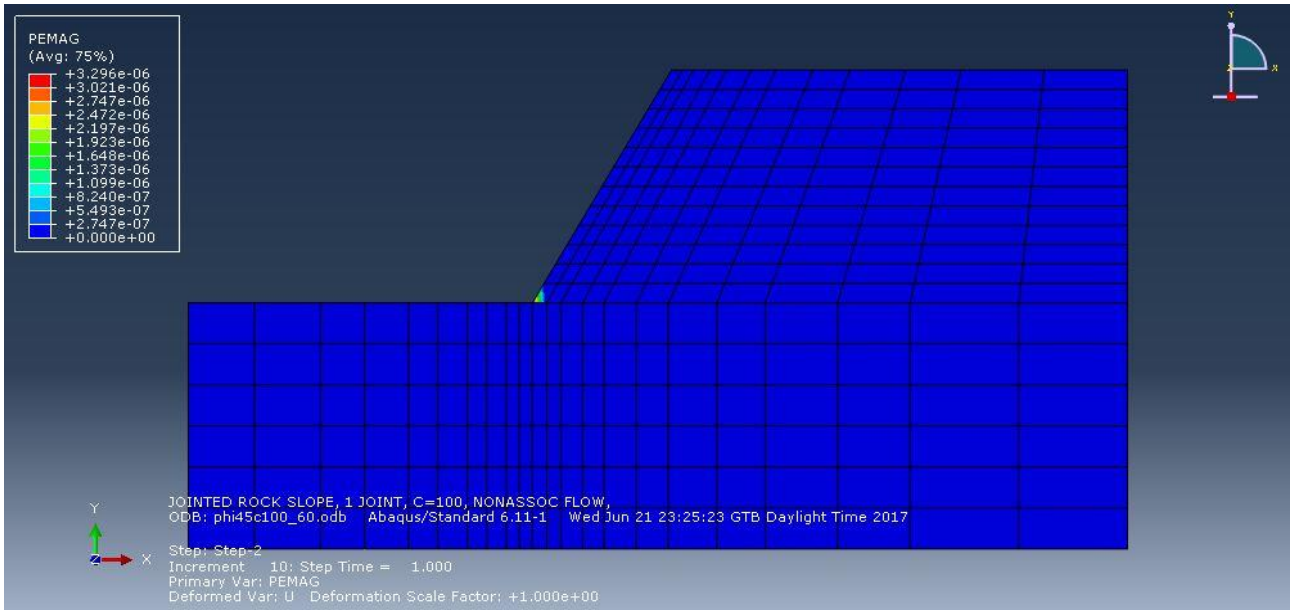

scale factor = 1e+00

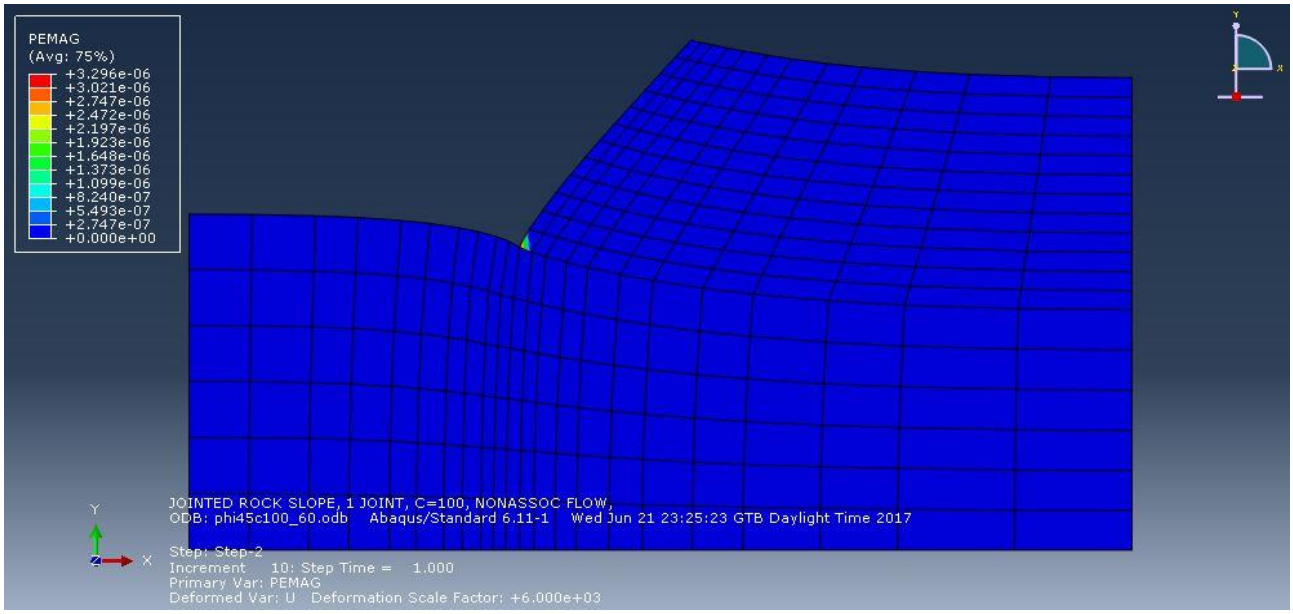

scale factor = 6e+03

- joint angle = 70^0

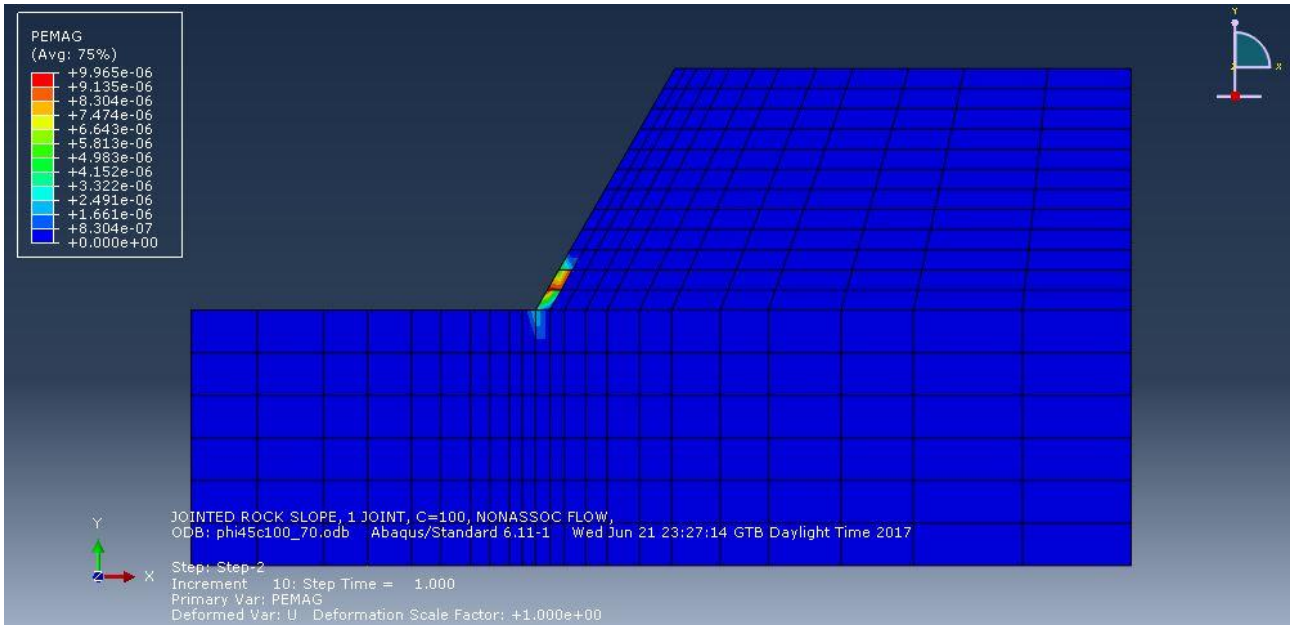

scale factor = 1e+00

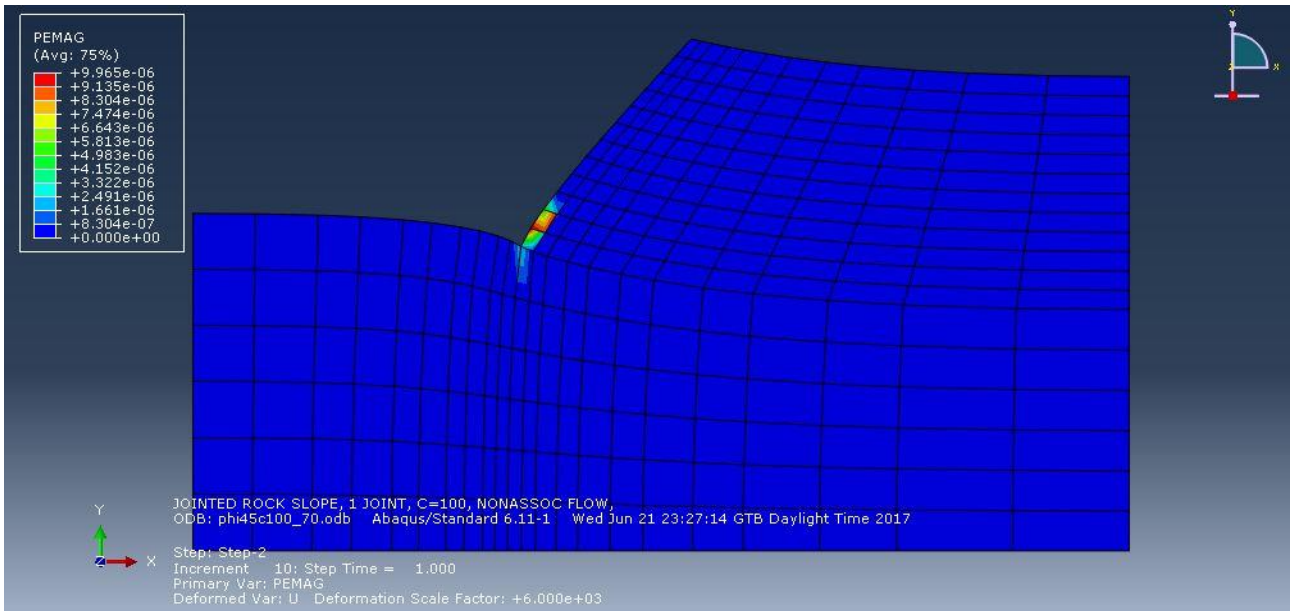

scale factor = 6e+03

- joint angle = 80^0

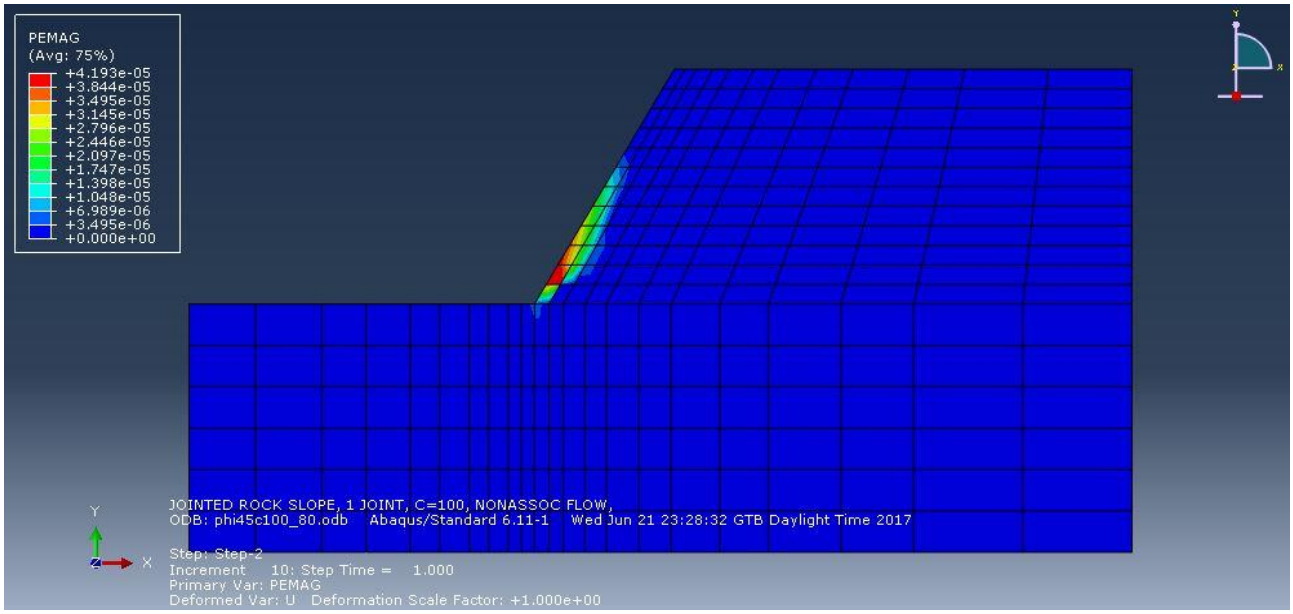

scale factor = 1e+00

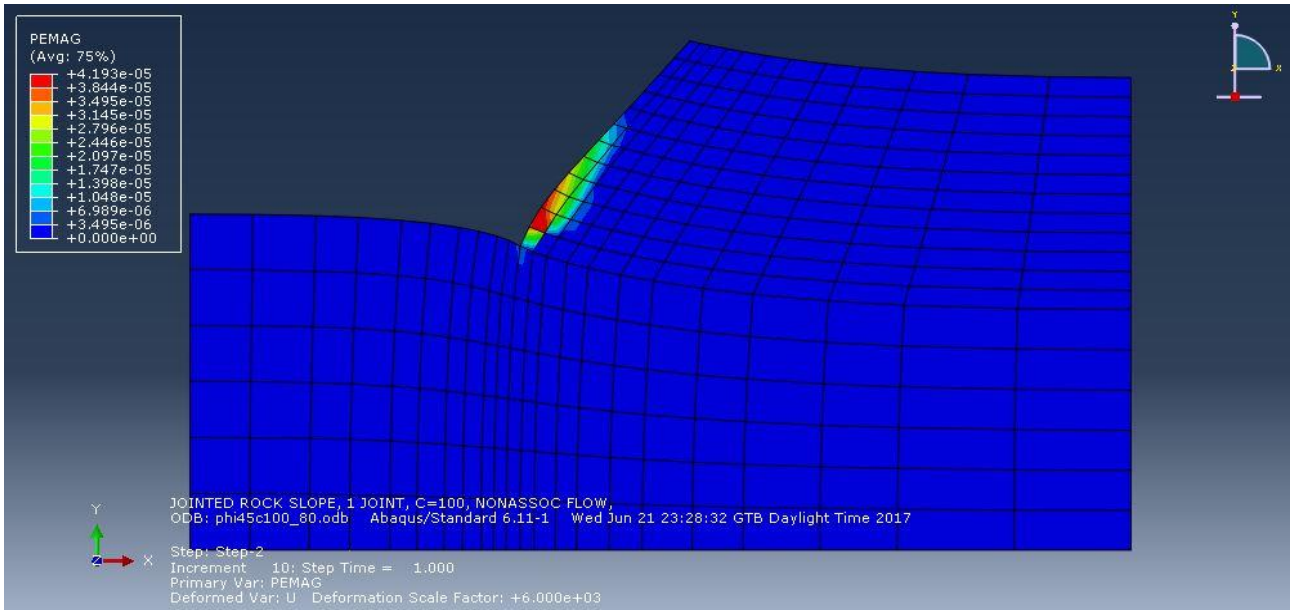

scale factor = 6e+03

- joint angle = 90^0

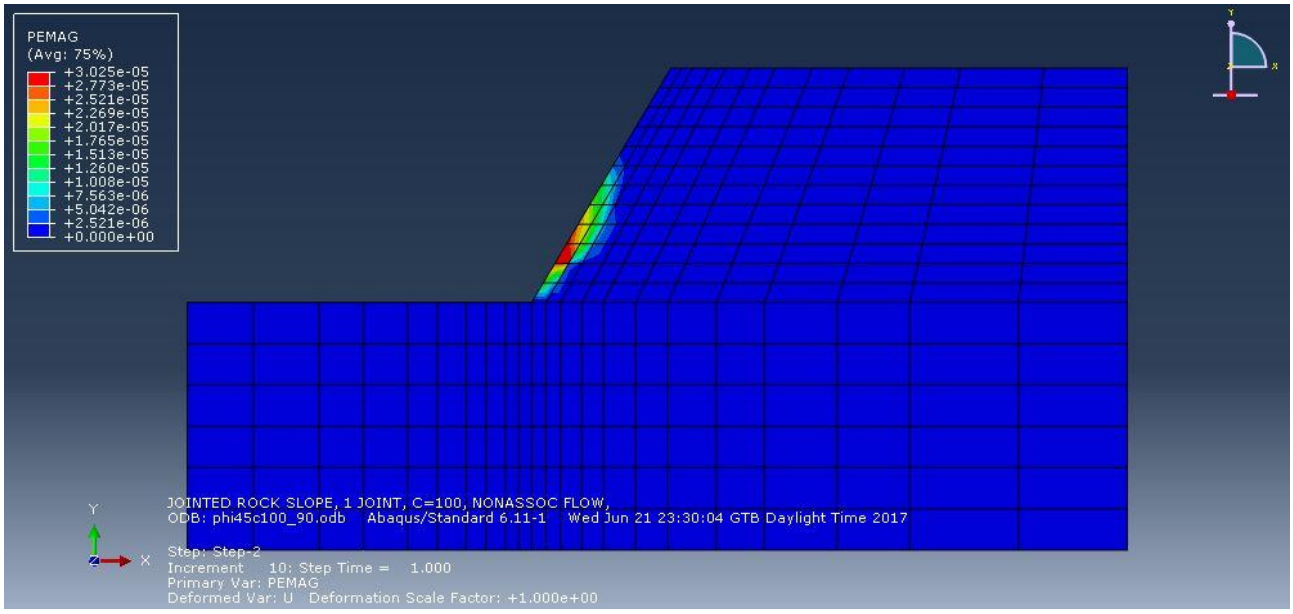

scale factor = 1e+00

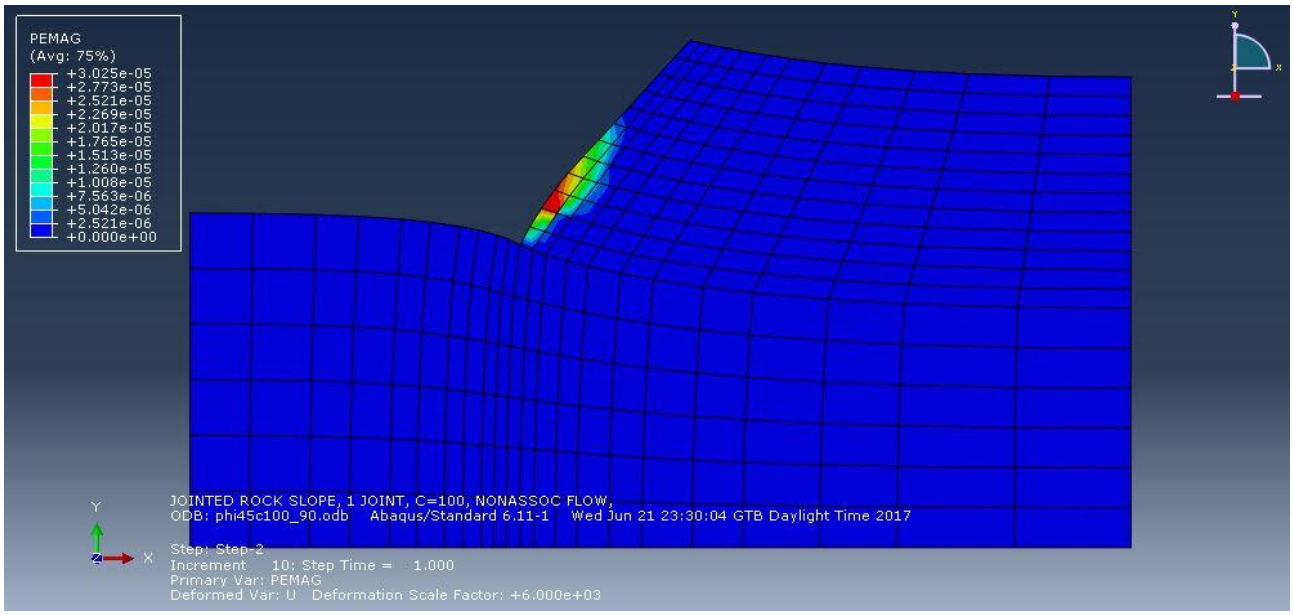

scale factor = 6e+03

Poor quality rock mass slope, E = 5000 MPa, pseudo-static analysis

Case study 7: a_g = 0.16g, variable parameter is cohesion c

- c = 15 kPa

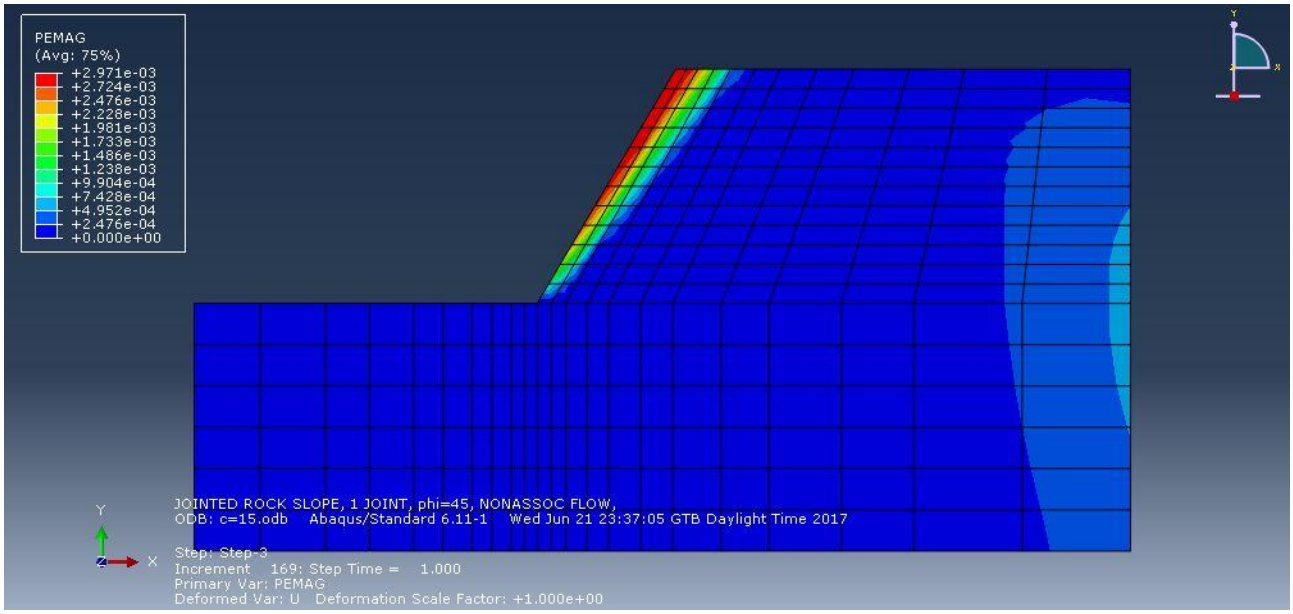

scale factor = 1e+00

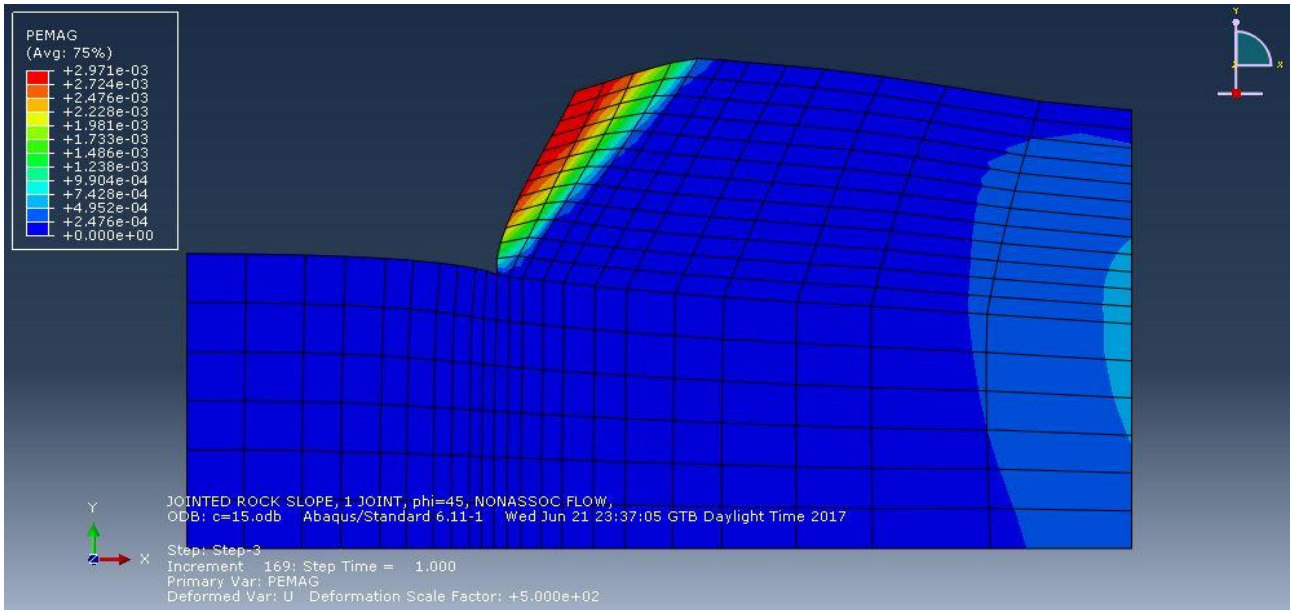

scale factor = 5e+02

- c = 25 kPa

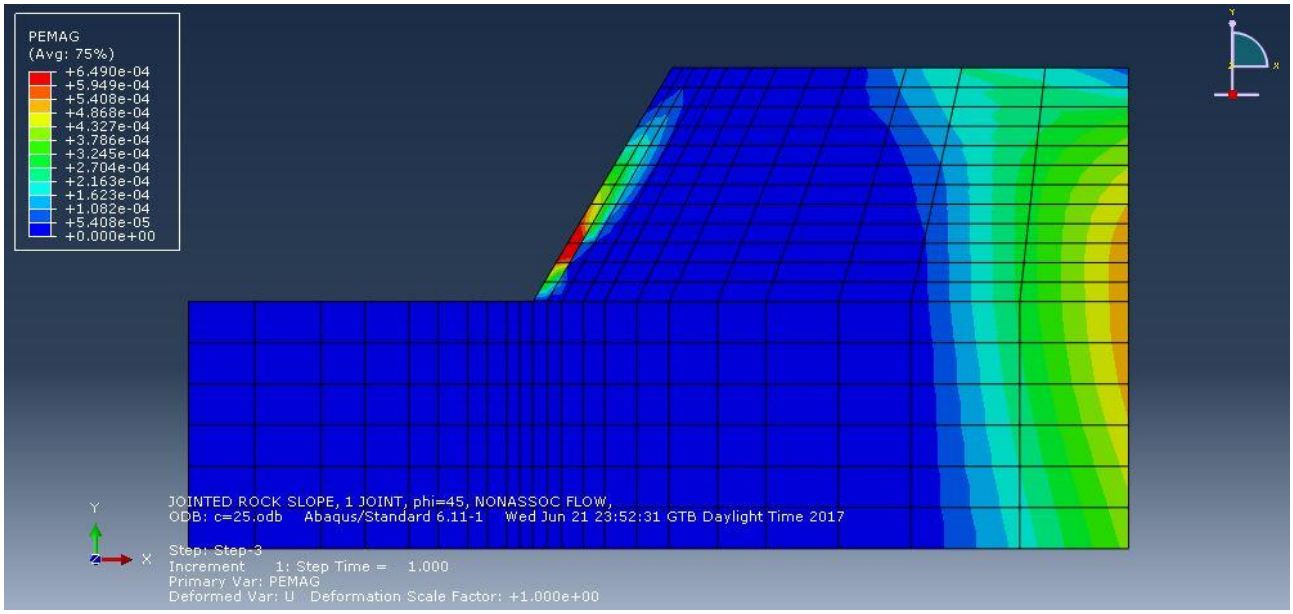

scale factor = 1e+00

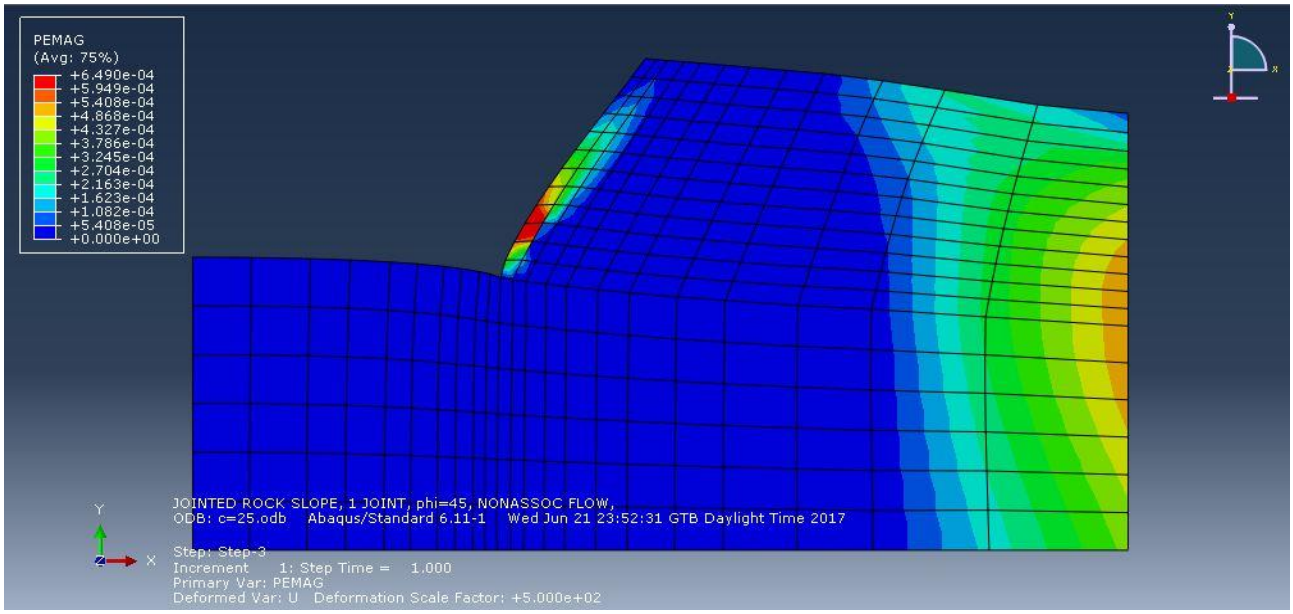

scale factor = 5e+02

- c = 40 kPa

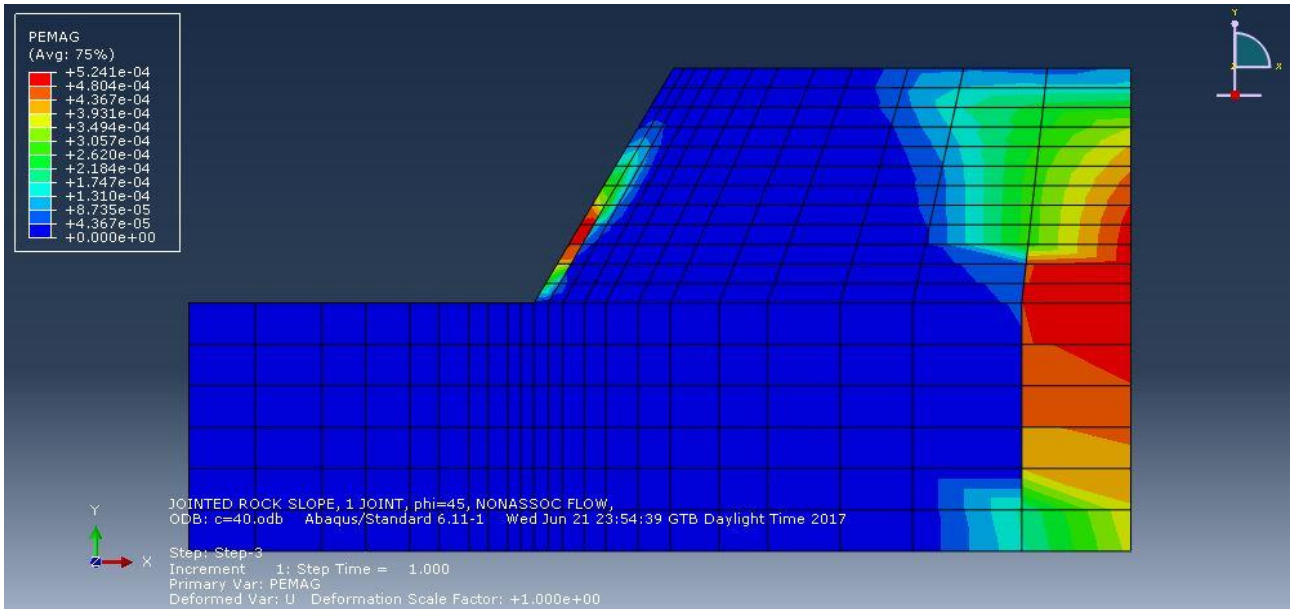

scale factor = 1e+00

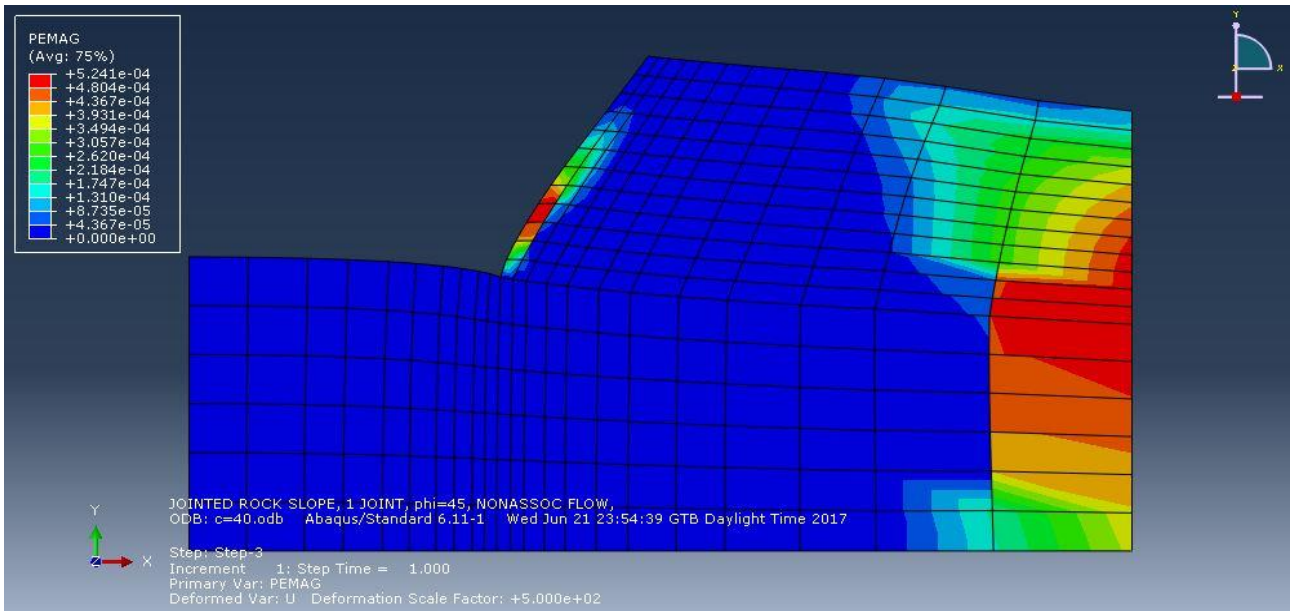

scale factor = 5e+02

Case study 8: a_g = 0.24g, variable parameter is cohesion c

- c = 15 kPa

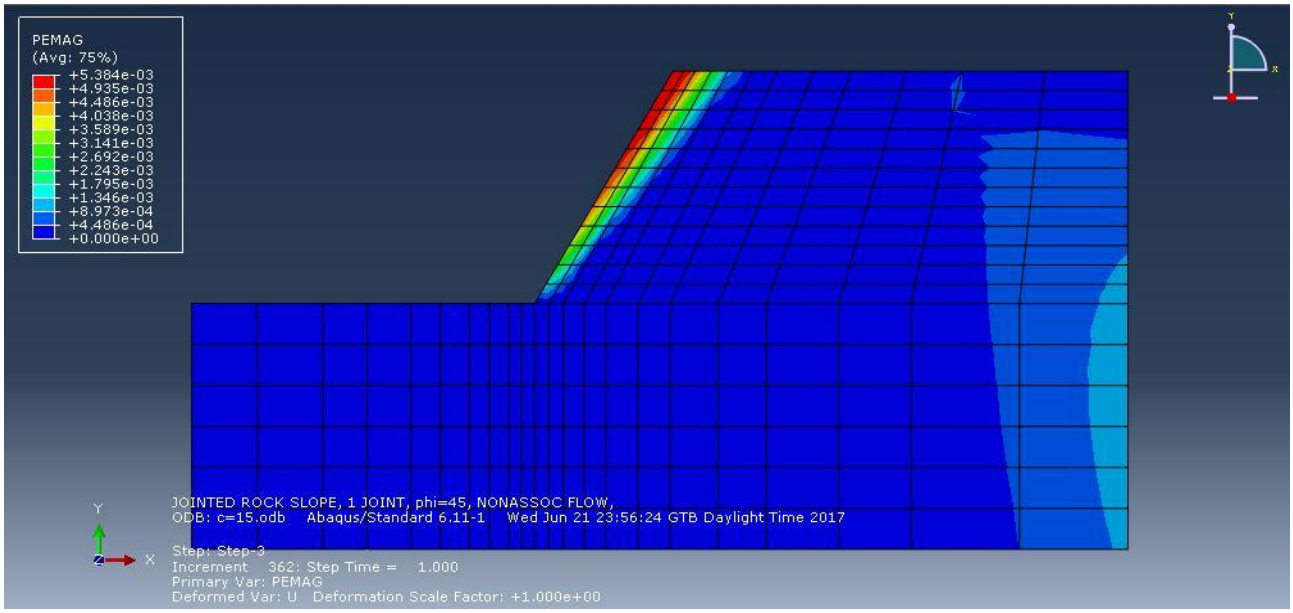

scale factor = 1e+00

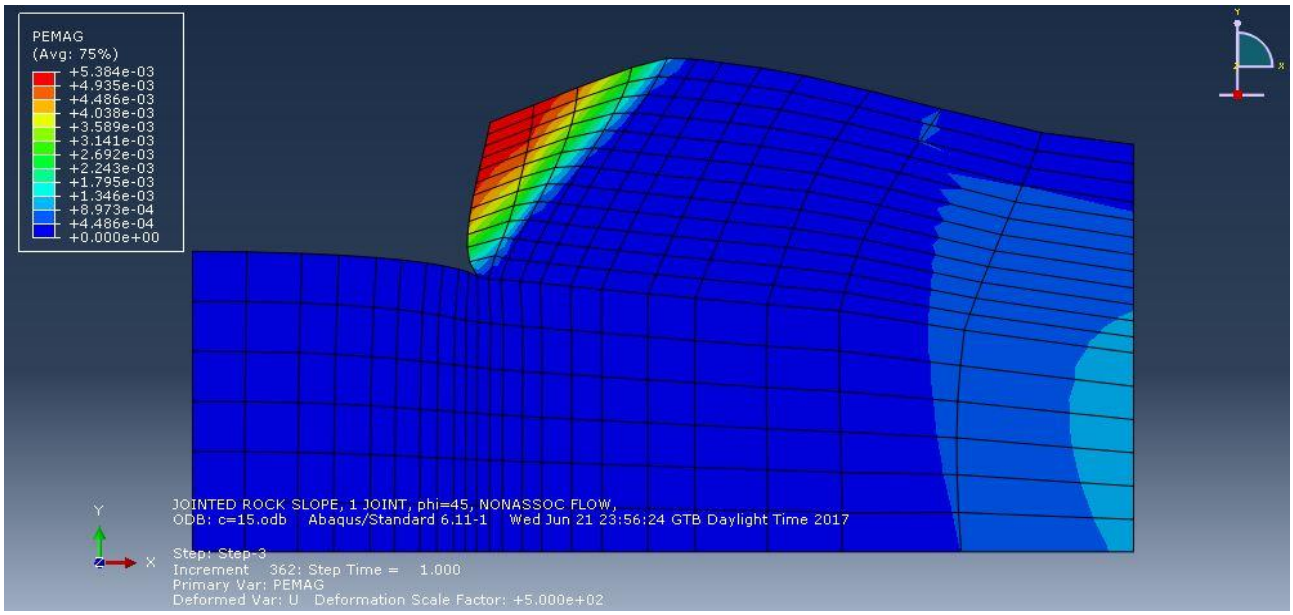

scale factor = 5e+02

- c = 25 kPa

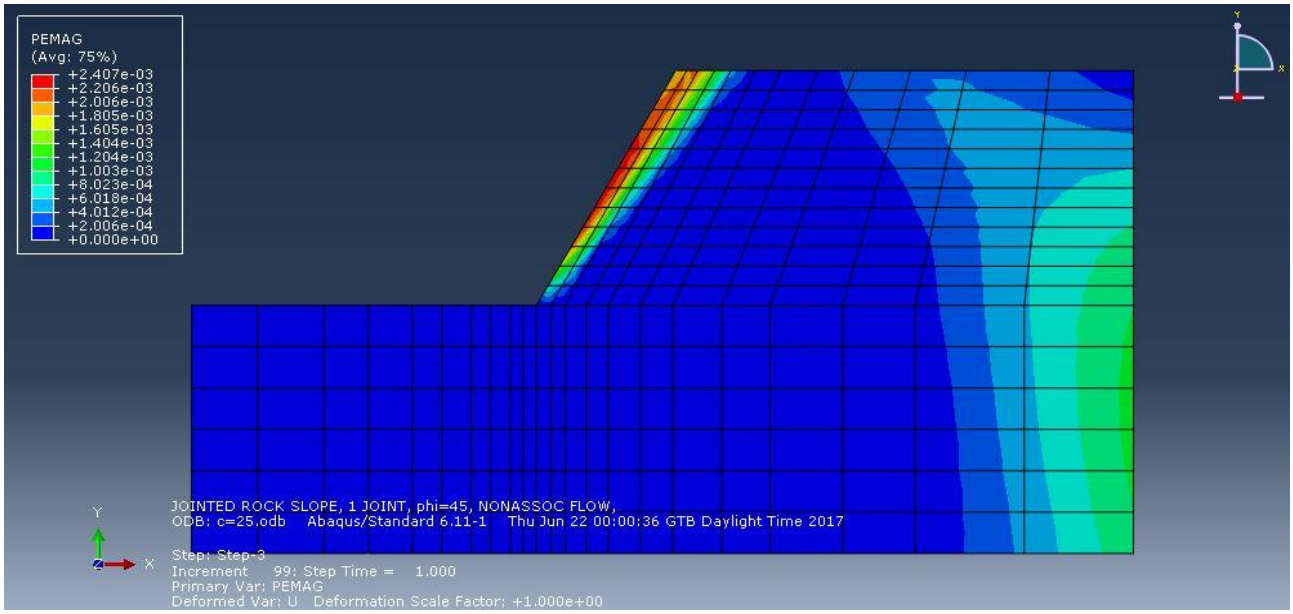

scale factor = 1e+00

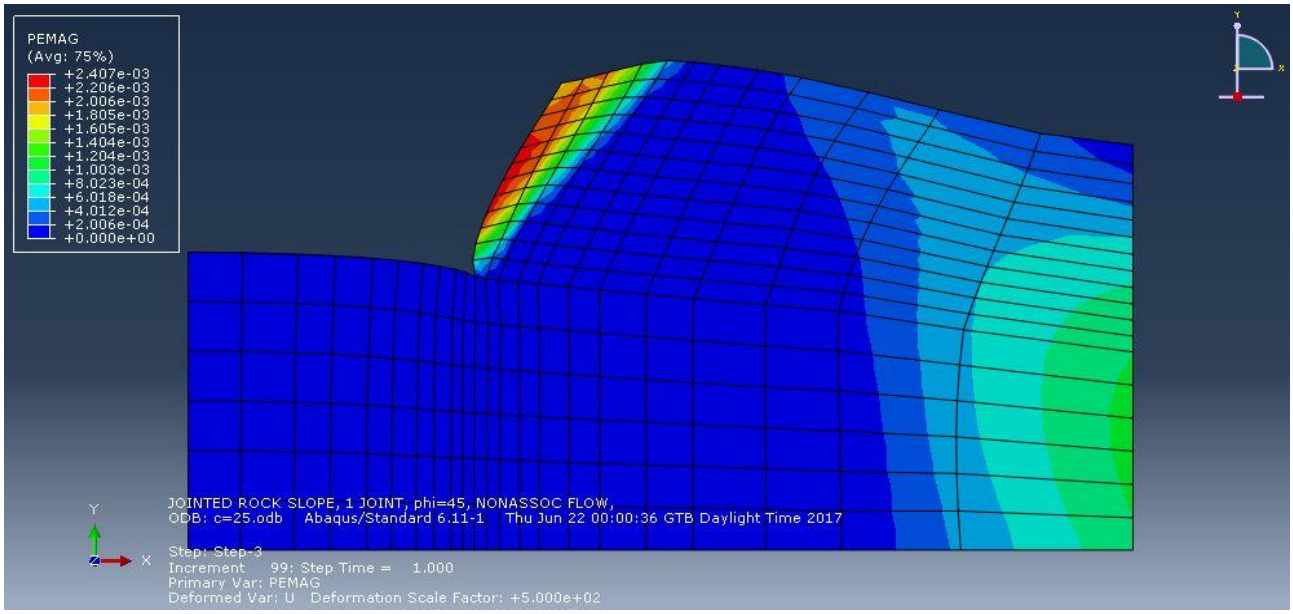

scale factor = 5e+02

- c = 40 kPa

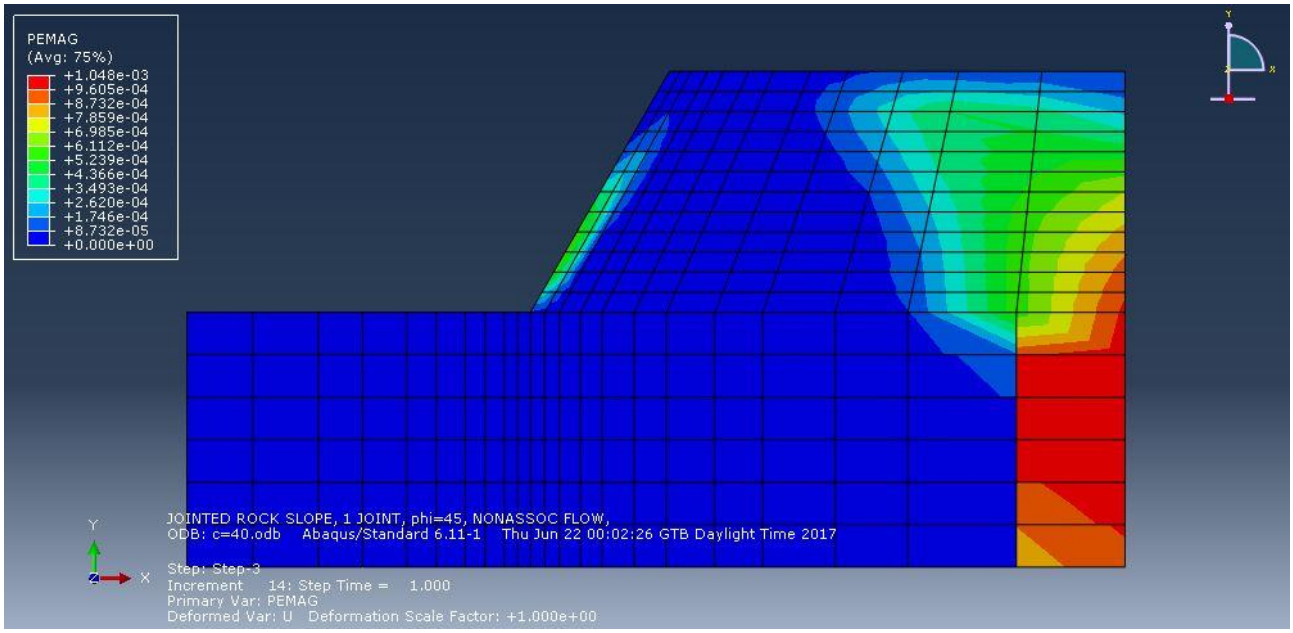

scale factor = 1e+00

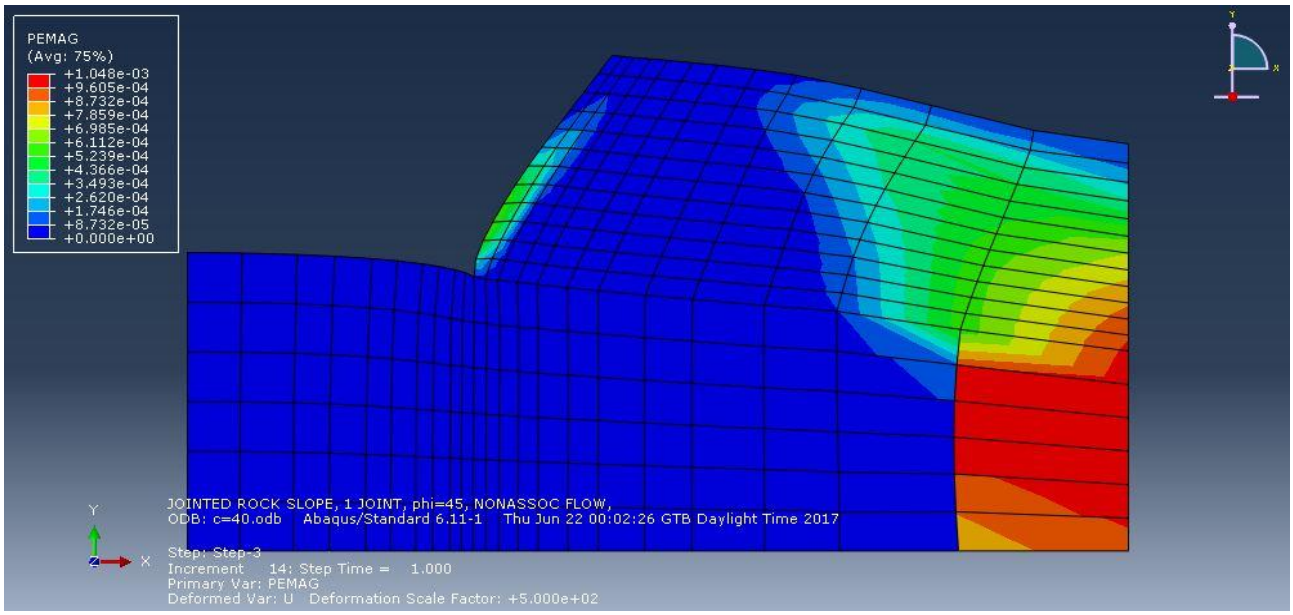

scale factor = 5e+02

Case study 9: a_g = 0.36g, variable parameter is cohesion c

- c = 15 kPa

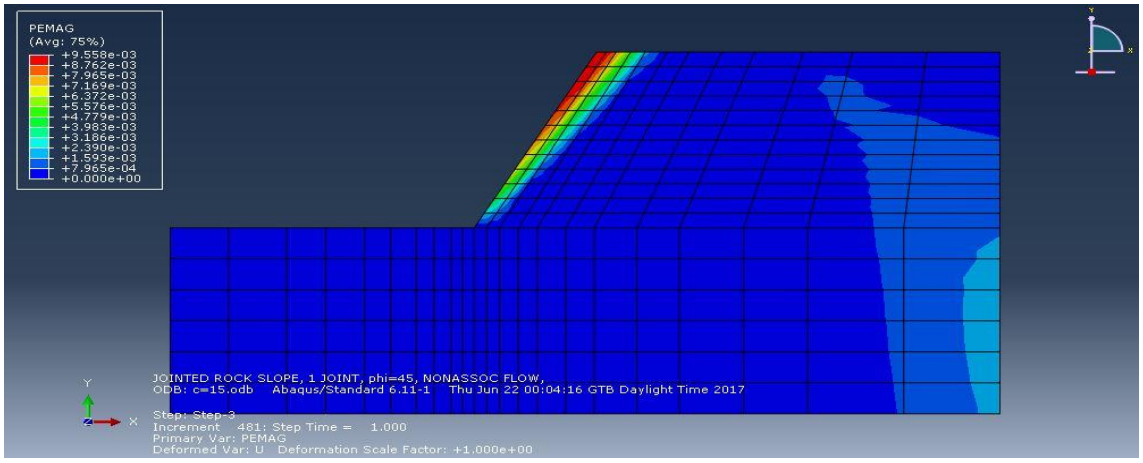

scale factor = 1e+00

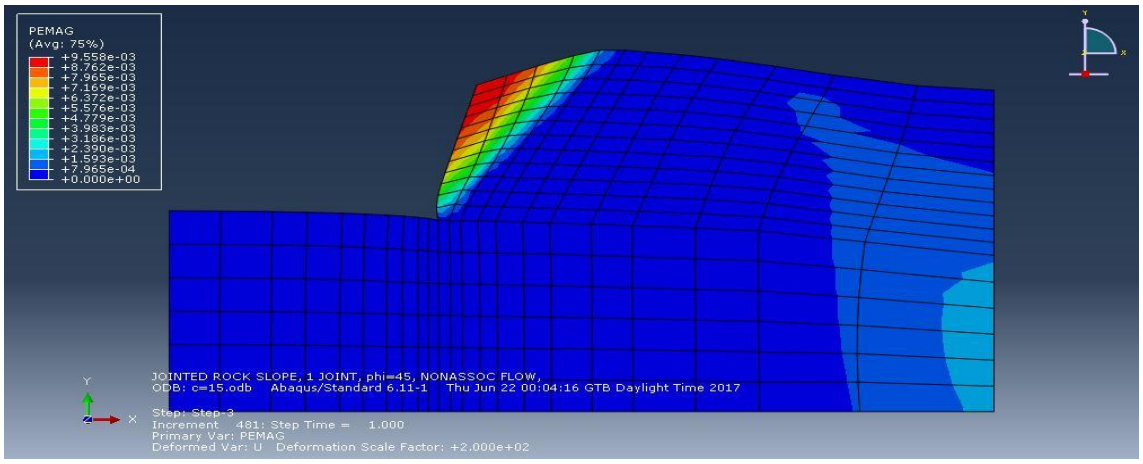

scale factor = 2e+02

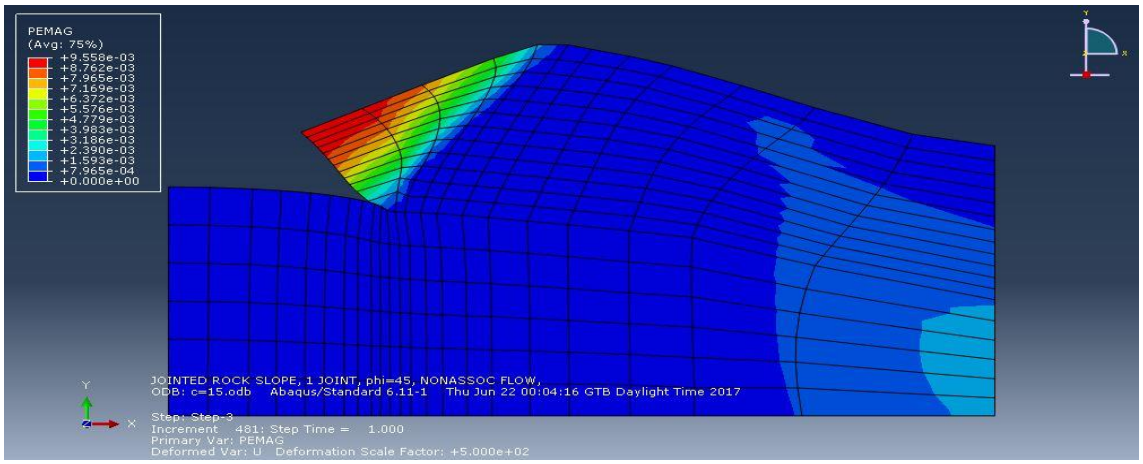

scale factor = 5e+02

- c = 25 kPa

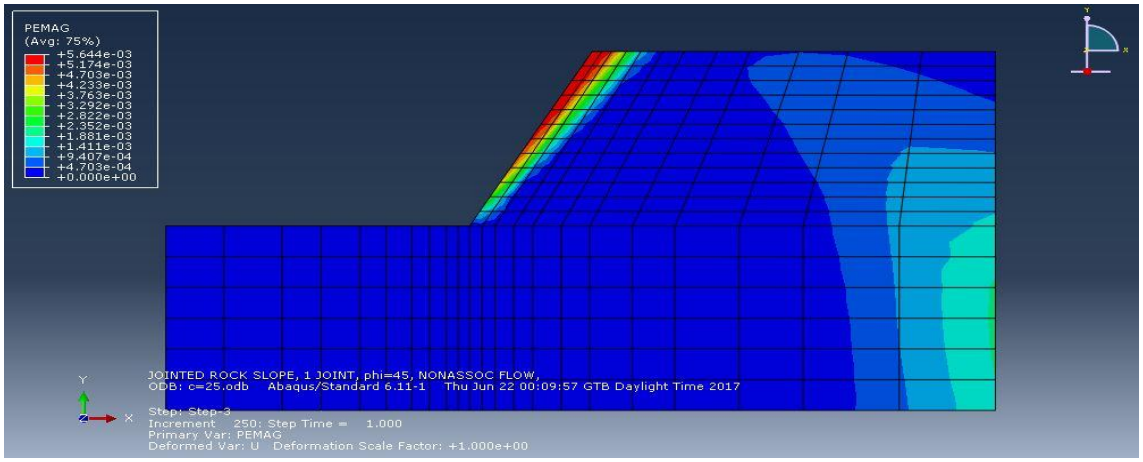

scale factor = 1e+00

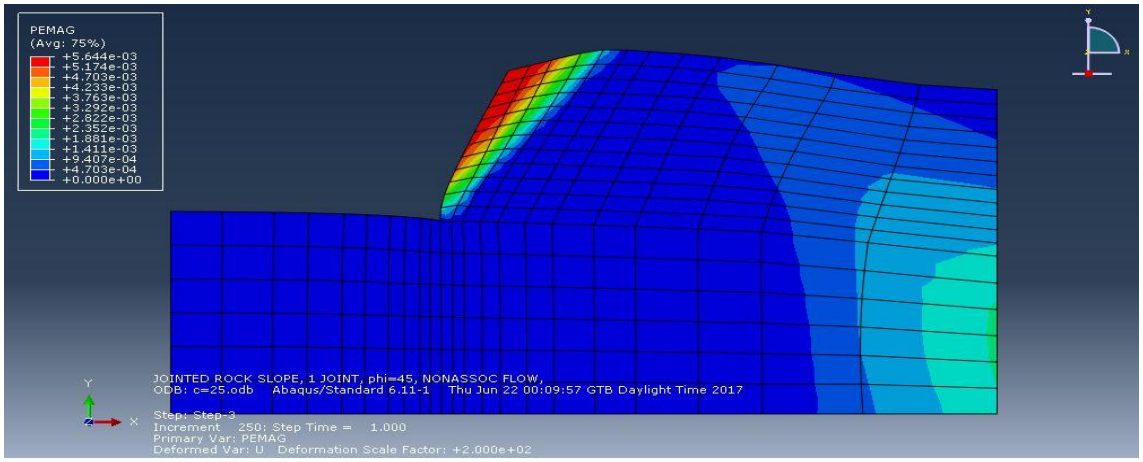

scale factor = 2e+02

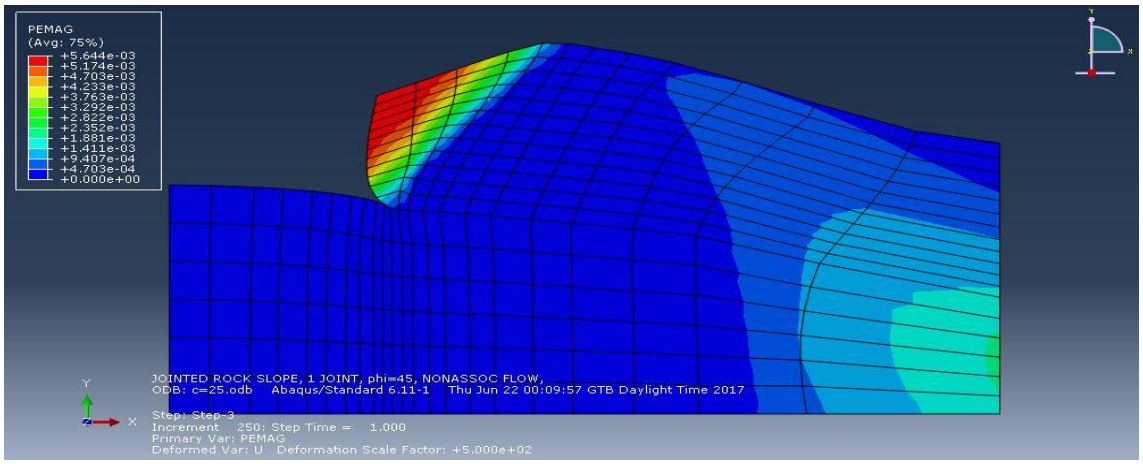

scale factor = 5e+02

- c = 40 kPa

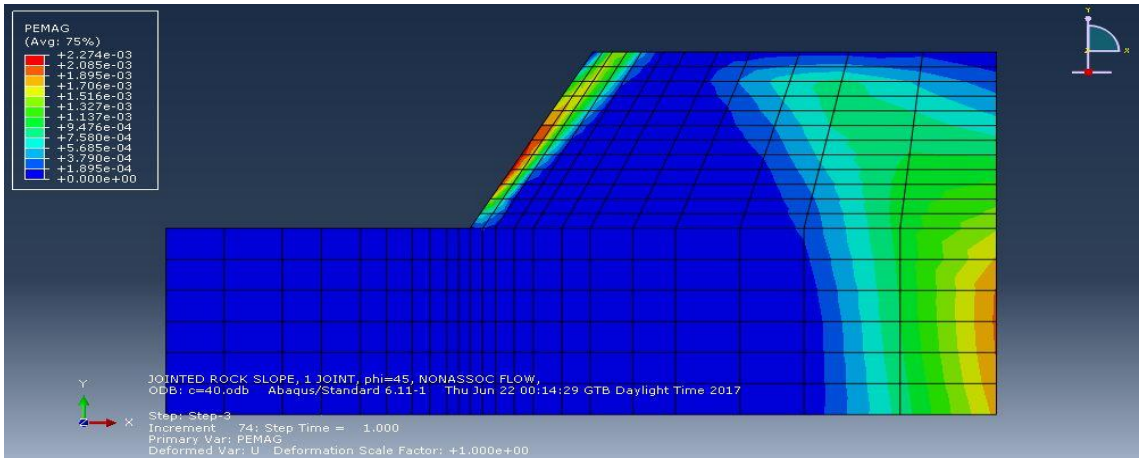

scale factor = 1e+00

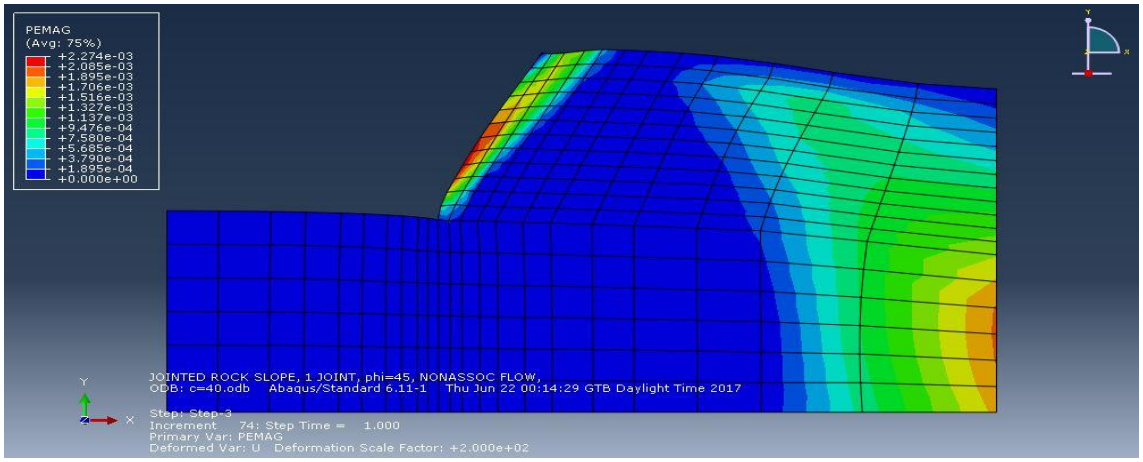

scale factor = 2e+02

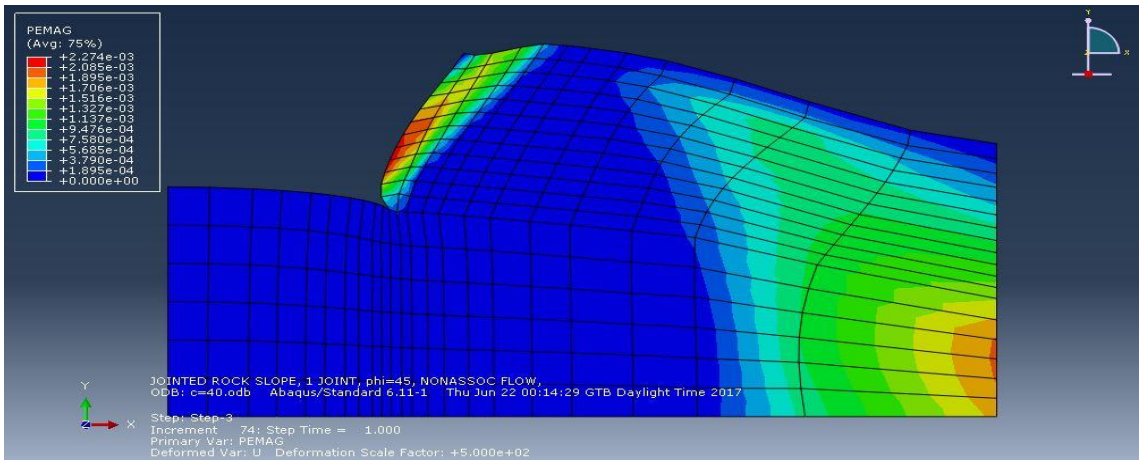

scale factor = 5e+02